

Title	Accuracy of computer-aided design/computer-assisted manufacture (CAD/CAM) fabricated dental restorations: a comparative study
Authors	Nasruddin, Mohd Faiz
Publication date	2015
Original Citation	Nasruddin, M.F. 2015. Accuracy of Computer-Aided Design/ Computer-Assisted Manufacture (CAD/CAM) Fabricated Dental Restorations: A comparative study. PhD Thesis, University College Cork.
Type of publication	Doctoral thesis
Rights	© 2015, Mohd F. Nasruddin. - http://creativecommons.org/licenses/by-nc-nd/3.0/
Download date	2024-04-25 14:14:27
Item downloaded from	https://hdl.handle.net/10468/2248

NATIONAL UNIVERSITY OF IRELAND, CORK

Accuracy of Computer-Aided Design/Computer-Aided Manufacture (CAD/CAM) Fabricated Dental Restorations

A comparative study

Dr Mohd Faiz Nasruddin (BDS, Mal)

A thesis for the degree of Doctor of Philosophy
(PhD) in University College Cork

(May, 2015)

Head of School: Prof Martin J Kinirons

Supervised by:

1. Dr Francis M Burke (BDentSc (Ire), MSc (UK), PhD (UK), FDSRCSEd, FFDRCSI, DipTLHE).
2. Dr Noel Ray (BSc Chemistry (Ire), MSc Chemistry (Ire), PhD Chemistry (Ire), H.Dip.in Ed. (Ire), PG.CertTLHE).
3. Dr Antonios Theocharopoulos (BSc Dent Tech (Gre), MSc Dent Mat (UK), PhD Dental Bioceramics (UK)).

Table of Contents

1	Literature Review	24
1.1	Computer-aided Design and Computer-aided Manufacturing	24
1.1.1	Definition	24
1.1.2	Historical Perspective	25
1.1.3	Examples of CAD/CAM's in Dentistry	30
1.1.4	Digitization	33
1.1.5	Manufacturing Processes	39
1.1.6	CAD/CAM Software.....	46
1.2	Accuracy	48
1.2.1	Definition of accuracy and precision	48
1.2.2	Volume measurements and superimpositions of CAD and CAM	50
1.2.3	Fit of CAD/CAM Fabricated Restorations	51
1.2.4	Methods of Measuring Fit	54
1.2.5	Analysis Software Utilised in This Study	66
2	Aim, Objectives and Null Hypothesis.....	71
2.1	Aim.....	71
2.2	Objectives.....	71
2.3	Null Hypotheses.....	71
3	Developing the Methods	74
3.1	Method Development.....	74

3.1.1	Initial Model Design and Processing.....	77
3.1.2	Preliminary Study.....	82
3.1.3	Validation of Methods	93
3.2	Method Development Results	102
3.2.1	Processed Trial Model	102
3.2.2	Preliminary Study.....	104
3.2.3	Validation of Methods	108
3.3	Discussion of Method Development	121
3.3.1	Repeatability of Method.....	122
3.3.2	Accuracy of method.....	122
3.3.3	Analysis Software.....	126
4	Definitive Method.....	128
4.1	Fabrication of Investigated Dental Copings.....	131
4.1.1	Master Model Design and Fabrication	131
4.1.2	Computer Aided Scans, Design and Processing.....	131
4.1.3	Micro Computed Tomography Scans (Micro CT).....	137
4.2	Volume analysis	139
4.3	Surface Mapping Analysis.....	140
4.4	Superimpositions	142
4.4.1	Coping Deviation Vs CAD	142
4.4.2	Coping Deviations Group Comparison.....	148
4.4.3	Localised Focussed Investigation.....	148

4.5	Alignment	150
4.5.1	Internal fit Analysis	150
5	Definitive Results.....	156
5.1	Fabricated dental copings from a single master CAD.....	156
5.2	Volume Analysis of Fabricated Coping	157
5.3	Colour Deviation Surface Mappings.....	158
5.3.1	Laser Sintered Cobalt Chrome Molybdenum Coping (LS) Deviations from CAD.....	159
5.3.2	5-Axis Milled Cobalt Chrome Molybdenum Coping (M-CoCrMo) Deviations from CAD.....	163
5.3.3	3-Axis Milled Zirconia Coping (ZAx3) Deviations from CAD.....	165
5.3.4	4-Axis Milled Zirconia Coping (ZAx4) Deviations from CAD.....	169
5.4	Superimpositions Analysis.....	172
5.4.1	Comparing Coping Deviation from CAD	172
5.4.2	Comparing Different CAM Methods of Coping Fabrication	174
5.4.3	Focussed analysis.....	175
5.5	Alignment Analysis.....	180
5.5.1	Comparison of Internal Fit of Different CAM Fabricated Copings.....	180
6	Discussion	189
6.1	Volume findings	189
6.2	Linear deviations from CAD-Surface mapping	189
6.2.1	LS Copings	190

6.2.2	M-CoCrMo Copings.....	191
6.2.3	ZAx3 Copings.....	192
6.2.4	ZAx4 Copings.....	194
6.3	Comparisons of Superimpositions	195
6.3.1	Comparison of Linear Deviations between fabricated copings with CAD.....	195
6.3.2	Comparison of Linear Deviations of CAD between Groups Investigated.....	197
6.3.3	Focussed Results	199
6.4	Internal Fit	201
6.4.1	Comparison of Internal Fit Results with Literature	202
6.5	Clinical implications	207
6.6	Limitations of Study	208
6.6.1	Universal Master Model Design for CAD/CAM studies	208
6.6.2	Design Limitations.....	209
6.6.3	Fabrication Limitations	211
6.6.4	Micro-CT Limitations.....	213
6.7	Recommendations	214
7	Conclusions	218
8	References	221
9	Appendix	232

List of Figures

Figure 1 Conventional method of lost-wax fixed dental prosthesis fabrication	27
Figure 2 History of dental CAD/CAM	29
Figure 3 Triangulation procedures of Optical Scanning.....	35
Figure 4 Mechanism of Structured Light scanning	36
Figure 5 CAM Milling Axes	43
Figure 6 Accuracy and Precision according to ISO 5725	49
Figure 7 Marginal Fit Definition	52
Figure 8 Principle of surface mapping measurement.....	62
Figure 9 Components of computerised micro-tomography	64
Figure 10 Flowchart of method development	76
Figure 11 Dimensions of Initial Design.....	78
Figure 12 EMCO lathe machinery	79
Figure 13 Parameter settings for trial model framework	81
Figure 14 Trial CAD construction	82
Figure 15 Models to be scanned with Incise.....	84
Figure 16 Importing STL files into GOM Inspect v7.5, SR2	87
Figure 17 Superimposition of micro-CT scanned coping and CAD showing that the exact design is different from the coping	88
Figure 18 Steps to display qualitative maps of coping to CAD deviations.....	88
Figure 19 Importing STL Files into Rhino v5	89
Figure 20 Steps to perform volume computation for CAD	90
Figure 21 Aligned master model and LS1 in Rhino 5	91
Figure 22 Fifty vertical radial cross sections in equidistance.....	92
Figure 23 Cross sectional view of aligned 3D models.....	93
Figure 24 NPL FreeForm Reference Standard.....	95
Figure 25 Example of Properties table in VG Studios	98
Figure 26 Density points of CAD	99
Figure 27 (a) Method to Thin Mesh of coping (LS1), (b) Changed points of (LS1) after Thin Mesh Procedure	101
Figure 28 Raw material turned and milled to fabricate the trial model.....	102

Figure 29 Finalized trial model after removal of sharp edges and separation from raw material	103
Figure 30 Original CAD created in InciseCAD, Renishaw	104
Figure 31 Imported STL formatted CAD in Rhino 5 and GOM Inspect	104
Figure 32 Exported surface models of the Incise scans	105
Figure 33 Voxel model created by VG Studios.....	106
Figure 34 Cast Fabricated Trial Coping.....	106
Figure 35 Overall Results table of deviations.....	107
Figure 36 3D view of surface comparisons	110
Figure 37 Variance distribution of deviations of surfaces micro-CT scanned LS1 to the CAD.....	111
Figure 38 Relationship of surface to deviation of LS1-CAD comparison	112
Figure 39 Surface mapping legend of Actual/nominal comparison of Multiple Scans of LS1 Vs Scan 1 (LS1)	113
Figure 40 Colour deviation mapping of Scan 2 to Scan 1	114
Figure 41 Variance distribution of deviations of surfaces micro-CT scanned LS1 (Scan 2) to Scan 1.....	115
Figure 42 Surface to surface comparison of NPL artefact with original NPL STEP file	116
Figure 43 Comparison of Surface Analysis of LS1 using VG Studios and GOM Inspect.	119
Figure 44 Box Plot of Median Volume with Confidence Interval readings of Laser Sintered Copings Via multiple Analysis Software and Resolutions.....	120
Figure 45 Cross section of micro-CT scanned NPL Freeform at Sphere 5 Region ...	123
Figure 46A Point to point measurement of surface of Sphere 5, Figure 78B Sphere diameter construction on Sphere 5 region	124
Figure 47 Surface mapping at Sphere 5 Region Selected	125
Figure 48 Flowchart of definitive method	130
Figure 49 Fabricated Master Aluminium Model.....	131
Figure 50 Framework Settings Determination.....	133
Figure 51 Selection of lowest (A) and highest point (B) of scan using the Incise scanner	133

Figure 52 CAD Master Design	134
Figure 53 Summary of Superimposition Analysis	142
Figure 54 Quantification of Mean Distance	144
Figure 55 Standardised sections of fabricated copings	145
Figure 56 Occlusal Surface mapping of copings (Comparison 2).....	147
Figure 57 Axial Surface Mapping of copings (Comparison 3)	147
Figure 58 Cervical Surface Mapping of copings (Comparison 4)	148
Figure 59 Focused Analyses on Occlusal Section of LS4	149
Figure 60 Aligned and cross sectioned coping scan and master aluminium model scan	152
Figure 61 Section 1 of Radial Cross Sections and Predetermined area of Fit Measurements	153
Figure 62 Fabricated copings using different techniques of CAM using the same CAD	156
Figure 63 Graph of Median Volume of Fabricated Copings utilising different methods of CAM.....	158
Figure 64 Surface Mapping Colour Legend of Actual Coping Deviations to CAD	159
Figure 65 Surface mapping of Laser Sintered Cobalt Chrome Molybdenum Coping (LS) deviation to CAD	161
Figure 66 Histogram of distribution deviations across the surface of LS fabricated copings	162
Figure 67 Surface mapping of Milled CoCrMo coping (M-CoCrMo) deviation to CAD,	164
Figure 68 Histogram of distribution deviations across the surface of M-CoCrMo fabricated coping	165
Figure 69 Surface Mapping Colour Legend of 3-Axis Milled Zirconia Coping Deviations to CAD	166
Figure 70 Cross-sectional Overlay of CAD and scanned 3-Axis Milled Zirconia coping in micro-CT	166
Figure 71 Surface mapping of 3-Axis milled zirconia coping (ZAx3) deviation to CAD, a.....	168

Figure 72 Histogram of distribution deviations across the surface of ZAx3 fabricated coping.....	169
Figure 73 Cross-sectional Overlay of CAD and scanned 4-Axis Milled Zirconia coping in micro-CT	170
Figure 74 Surface mapping of 4-Axis milled zirconia coping (Zax4) deviation to CAD,	171
Figure 75 Histogram of distribution deviations across the surface of ZAx4 fabricated coping.....	172
Figure 76 Focussed Sections on LS copings	176
Figure 77 Focussed Section on M-CoCrMo copings.....	178
Figure 78 Focussed Sections on ZAx3 copings	179
Figure 79 Focussed Sections on ZAx4 copings	180
Figure 80 Mean Vertical Marginal Adaptation across CAM fabricated copings.....	182
Figure 81 Mean Vertical Absolute Marginal Adaptation across CAM fabricated copings	183
Figure 82 Mean Axio-Margin Adaptation across CAM fabricated copings.....	184
Figure 83 Mean Axial Adaptation across CAM Fabricated Copings.....	185
Figure 84 Mean Occlusal Adaptation across CAM Fabricated Copings	186
Figure 85 Layered 20 micron deposition of material occlusally utilising laser sintering mechanism	191
Figure 86 Ballooning effect on machined dental copings.....	193
Figure 87 Micro-CT calibration Procedures	242

List of Tables

Table 1 Volume computation in Rhino 5	108
Table 2 Localised fit of fabricated coping (LS1)	108
Table 3 NPL freeform accuracy to CAD data results	117
Table 4 Composition of Direct Metal Laser Sintering of Cobalt Chrome Molybdenum copings	135
Table 5 Composition of Milled Cobalt Chrome Molybdenum copings.....	136
Table 6 Composition Table of Zirconia milled with 3-Axis apparatus.....	136
Table 7 Composition Table of Zirconia milled with 4 Axis apparatus	137
Table 8 Scan parameters for Cobalt Chrome Molybdenum coping Scan	138
Table 9 Scan parameters for Zirconia coping Scan	138
Table 10 Scan parameters of Master Model.....	139
Table 11 Sectional surface comparisons.....	146
Table 12 Mean Deviations of fabricated copings to CAD	173
Table 13 Comparison of sections Vs CAD	175
Table 14 Focused Results of LS sections	176
Table 15 Focused Results of M-CoCrMo sections.....	177
Table 16 Focused Results of ZAx3 sections.....	178
Table 17 Focused Results of ZAx4 sections.....	179
Table 18 Mean (SD) Internal Fit of Fabricated copings and CAD (n=250)	181
Table 19 Conditions for Calibration Rod VTX18CE000-013	243
Table 20 Scan Conditions for Master Model and Calibration Rod VTX18CE000-013	244
Table 21 Parameters of the NPL Reference Standard	245

Declaration

I Mohd Faiz Nasruddin (Student Number: 111220457) a student of University College Cork, Ireland hereby declare that the thesis submitted is my own work and has not been submitted for another degree, either at University College Cork or elsewhere.

.....

Mohd Faiz Nasruddin

May 2015

Abbreviations

Abbreviation	Meaning
CAD	Computer-aided Design
CAM	Computer-aided Manufacture
LS	Laser Sintered fabricated copings
M-CoCrMo	5-Axis Milled Cobalt Chrome Molybdenum fabricated copings
ZAx3	3-Axis Milled Zirconia fabricated copings
ZAx4	4-Axis Milled Zirconia fabricated copings
VLS	Volume of Laser Sintered fabricated copings
VM-CoCrMo	Volume of 5-Axis Milled Cobalt Chrome Molybdenum fabricated copings
VZax3	Volume of 3-Axis Milled Zirconia fabricated copings
VZax4	Volume of 4-Axis Milled Zirconia fabricated copings
VF	Vertical Marginal Fit
AM	Absolute Marginal Fit
AMF	Axio-margin Fit
AF	Axial Fit

OF

Occlusal Fit

Abstract:

**Accuracy of Computer-Aided Design/Computer-Assisted
Manufacture (CAD/CAM) Fabricated Dental Restorations:
A comparative study**

Introduction:

Computer-Aided-Design (CAD) and Computer-Aided-Manufacture (CAM) has been developed to fabricate fixed dental restorations accurately, faster and improve cost effectiveness of manufacture when compared to the conventional method. Two main methods exist in dental CAD/CAM technology: the subtractive and additive methods. While fitting accuracy of both methods has been explored, no study yet has compared the fabricated restoration (CAM output) to its CAD in terms of accuracy.

The aim of this present study was to compare the output of various dental CAM routes to a sole initial CAD and establish the accuracy of fabrication. The internal fit of the various CAM routes were also investigated. The null hypotheses tested were: 1) no significant differences observed between the CAM output to the CAD and 2) no significant differences observed between the various CAM routes.

Methods:

An aluminium master model of a standard premolar preparation was scanned with a contact dental scanner (Incise, Renishaw, UK). A single CAD was created on the scanned master model (InciseCAD software, V2.5.0.140, UK). Twenty copings were then fabricated by sending the single CAD to a multitude of CAM routes. The copings were grouped (n=5) as: Laser sintered CoCrMo (LS), 5-axis milled CoCrMo (M-CoCrMo), 3-axis milled zirconia (ZAx3) and 4-axis milled zirconia (ZAx4). All copings

were micro-CT scanned (Phoenix X-Ray, Nanotom-S, Germany, power: 155kV, current: 60µA, 3600 projections) to produce 3-Dimensional (3D) models. A novel methodology was created to superimpose the micro-CT scans with the CAD (GOM Inspect software, V7.5SR2, Germany) to indicate inaccuracies in manufacturing. The accuracy in terms of coping volume was explored. The distances from the surfaces of the micro-CT 3D models to the surfaces of the CAD model (CAD Deviation) were investigated after creating surface colour deviation maps. Localised digital sections of the deviations (Occlusal, Axial and Cervical) and selected focussed areas were then quantitatively measured using software (GOM Inspect software, Germany).

A novel methodology was also explored to digitally align (Rhino software, V5, USA) the micro-CT scans with the master model to investigate internal fit. Fifty digital cross sections of the aligned scans were created. Point-to-point distances were measured at 5 levels at each cross section. The five levels were: Vertical Marginal Fit (VF), Absolute Marginal Fit (AM), Axio-margin Fit (AMF), Axial Fit (AF) and Occlusal Fit (OF).

Results:

The results of the volume measurement were summarised as: VM-CoCrMo (62.8mm³) > VZax3 (59.4mm³) > VCAD (57mm³) > VZax4 (56.1mm³) > VLS (52.5mm³) and were all significantly different (p<0.05) from each other.

Qualitative 3D colour surface maps presenting inaccuracies in fabrication were created. The surface to surface distances between each coping and the CAD were

presented as areas with different colour. No significant differences were observed at the internal aspect of the cervical aspect between all groups of copings. Significant differences ($p < 0.05$) were however found at localised sections and focussed areas and are summarized below.

No	Comparison	Sections of coping
1	LS < M-CoCrMo	Internal Occlusal, Internal Axial and External Axial
2	ZAx3 > ZAx4	External Occlusal, External Cervical
3	ZAx3 < ZAx4	Internal Occlusal
4	M-CoCrMo > ZAx4	Internal Occlusal and Internal Axial

The mean values of AMF and AF were significantly ($p < 0.05$) different for all tested groups. AM and OF showed significant difference ($p < 0.05$) for all tested groups with the exception of M-CoCrMo and ZAx4. VF results were summarized as: LS and ZAx3 > M-CoCrMo and CAD > ZAx4. Only VF of M-CoCrMo was comparable with the CAD Internal Fit. All VF and AM values were within the clinically acceptable fit ($120\mu\text{m}$).

Conclusion:

The investigated CAM methods reproduced the CAD accurately at the internal cervical aspect of the copings. However, localised deviations at axial and occlusal aspects of the copings may suggest the need for modifications in these areas prior to fitting and veneering with porcelain. The CAM groups evaluated also showed different levels of Internal Fit thus rejecting the null hypotheses.

The novel non-destructive methodologies for CAD/CAM accuracy and internal fit testing presented in this thesis may be a useful evaluation tool for similar applications.

Proceedings associated with this work

- MF Nasruddin. Digital Dentistry: Are we there yet? Three minute Thesis, Doctoral Showcase University College Cork 2013, Aula Maxima UCC, 11 June 2013.
- MF Nasruddin, F Burke, N Ray, A Theocharopoulos. Novel method of volume measurement of CAD/CAM fabricated dental prostheses. 2nd Asia Pacific, CAD/CAM & Digital Dentistry International Conference 2013, Marina Bay Sands Hotel Convention Centre, Singapore, 4-5th October 2013.
- MF Nasruddin, F Burke, N Ray, A Theocharopoulos. Accuracy comparison of two dental CAD/CAM fabrication routes. International Association of Dental Research Annual Scientific Meeting 2013, IADR Irish Division, University College of Cork, 14-15th November 2013.
- MF Nasruddin, A Theocharopoulos, N Ray, F Burke. A Comparative Study on the Accuracy of Laser Sintered Vs Milled Fabricated Dental Restorations. 31st International Manufacturing Conference, Cork Institute of Technology, 4-5th September 2014.
- MF Nasruddin, A Theocharopoulos, N Ray, F Burke. Accuracy of Computer-Aided-Designed/Computer-Aided-Manufactured (CAD/CAM) dental copings. International Association of Dental Research Annual Scientific Meeting 2014, IADR Irish Division, Queen's University of Belfast, Malone Lodge Hotel, 13-14th November 2014.

Acknowledgements

It's no big secret that doing research requires tremendous amount of energy and time and this PhD journey is no exception. However there were a number of people that helped made this journey easier and were critically important to the success of this project.

Dr Francis M Burke has been my main supervisor and was greatly influential in determining together the concept and method implementation of the project. Without his support, this project would not been completed on time. Greatly appreciate all his efforts to encourage me throughout this whole process.

Dr Noel Ray has been my second supervisor and his help especially in statistical advice, analysis and project outlay was a major contributing factor to the success. Always a constant source of support are just example of words I could describe his dedication towards finalizing the project until completion.

Dr Antonios Theocharopoulos was my third supervisor and has worked closely beside me especially in the technical aspects of the project. He has always been generous with his time and his input throughout the planning process to the thesis write up was invaluable. My appreciation for research has improved tremendously under his guidance.

I would also like to thank a number of colleagues in the Dental School of University College Cork who have given me emotional support and advice throughout the project. If I could name them all, a large portion of this thesis will be filled with their names. However a special thank you is given to Dr Cristiane DaMata who recently completed her own PhD project and Dr Sayaka Tada who now works in Japan but did a year post-doctoral research in Ireland while I was here. I wish them the best of luck in their career development.

A token of appreciation also goes to my sponsors the Ministry of Education Malaysia and my employers Universiti Teknologi MARA, Malaysia for giving me the chance to complete my studies here in Ireland. A big thank you also goes to Renishaw, UK, South Eastern Applied Materials (SEAM), Waterford, National Physics Laboratory, UK and CybamanTech, UK in helping me out in various stages of the project.

Finally and most importantly, I owe gratitude of debt to my family. My wife Nurul Farhana Othman and my two daughters Nur Alisha Balqis and Amanda Qaisara who have helped me keep everything in perspective. I realise their effort in letting me have the freedom in completing my work while they sacrifice plenty. Not to forget my parents Nasruddin Jaafar and Norsidah Ismail for their invaluable advice and support back home.

Section 1

Literature Review

1 Literature Review

1.1 Computer-aided Design and Computer-aided Manufacturing

1.1.1 Definition

Computer-aided Design and Computer-aided Manufacturing (CAD/CAM) is a manufacturing process for designing and fabricating work pieces with the aid of computer software and computer controlled equipment. It consists of two components, the Computer-aided Design (CAD) and Computer-aided Manufacturing (CAM). Both elements are essential and linked together through electronic data exchange for an effective production system.

CAD is defined as the use of computers for the creation, analysis, modification and optimization of an engineering drawing or design (1). This design process is aided by dedicated CAD software. The design conveys specific information relating to choice of materials and dimensional settings used for fabricating the output. It also includes design tolerances information. This information can then be utilised for draft printing and analytical purposes prior to manufacturing. The finalised design can then be exported to CAM.

CAM is defined as the use of computer software for programming automation in manufacturing processes (1). CAM functions by incorporating planned strategies to fabricate work pieces using CAM software after receiving design specifications from the CAD software. Strategies are operational protocols used to drive the

manufacturing facility (Milling machine, 3D printer etc.) for work piece fabrication. Strategies of fabricating are dependent on CAM equipment capabilities and the CAM method utilized.

1.1.2 Historical Perspective

CAD was originally introduced as an engineering aid in schematic drawings and drafting procedures in the early 1960's by Dr Ivan E Sutherland (2). He developed the Sketchpad which introduced a light pen that could be utilised to draw directly on computer monitors screens (2). Earlier generations of CAD software overall were only capable of 2-dimensional (2D) drafting procedures and it was not until the late 1960's that 3-Dimensional (3D) CAD Software was developed by Casteljau and Beizier from Renault. Their work on 3D curves and surface geometry continues to be the foundation of 3D CAD software today (2015). In conjunction with development of CAD, CAM software was developed in 1957 but was only commercially available in the 1970's by Dr Patrick J. Hanratty (considered being the father of CAD/CAM) (2). Recent developments however in the technology have offered CAD integration of detailed three-dimensional (3D) design and CAM throughout the complete engineering process (Processes starting from the creation of the design to the fabrication of the product).

The CAD/CAM process was commercialized in the early 1970's (1) initially for automotive and aerospace industries. This was due to the high cost of computer

technologies which enabled only leading companies to own the technology. However the introduction of mini computers and enhanced software capabilities saw the use of CAD/CAM become more widespread. Conventionally CAD/CAM methods have been monopolized by a subtractive method in the form of milling strategies (1). However, advancements in the technology have seen an additive method (i.e. laser melting, laser sintering) being introduced for fabrication of work pieces. Currently, CAD/CAM utilisation includes use for such applications as industrial design, medical and dental prosthetics and computer animations.

1.1.2.1 Conventional methods of fabrication in Dentistry

Historically, the conventional method of fabrication of crowns and fixed prosthesis is the lost-wax technique. It has been developed through the introduction of different materials and methods (3). Figure 1 shows a summary of the conventional method of fabricating through lost-wax method. Initially a primary impression of the oral cavity is needed to produce a study model. A design is proposed on the study model but a secondary impression is required to capture the specific details of the teeth. This is followed by creation of working model which is used to incorporate a dental design by making a wax pattern. The wax pattern presents a model of the design required for final restoration. An investment mould is then made surrounding the wax pattern before it is heated to vaporize the wax and have it replaced with a suitable material such as molten metal alloy or ceramic through a channel via a wax sprue attached to the wax pattern (4). The fabrication method ends by smoothing the output by grinding with dental burs.

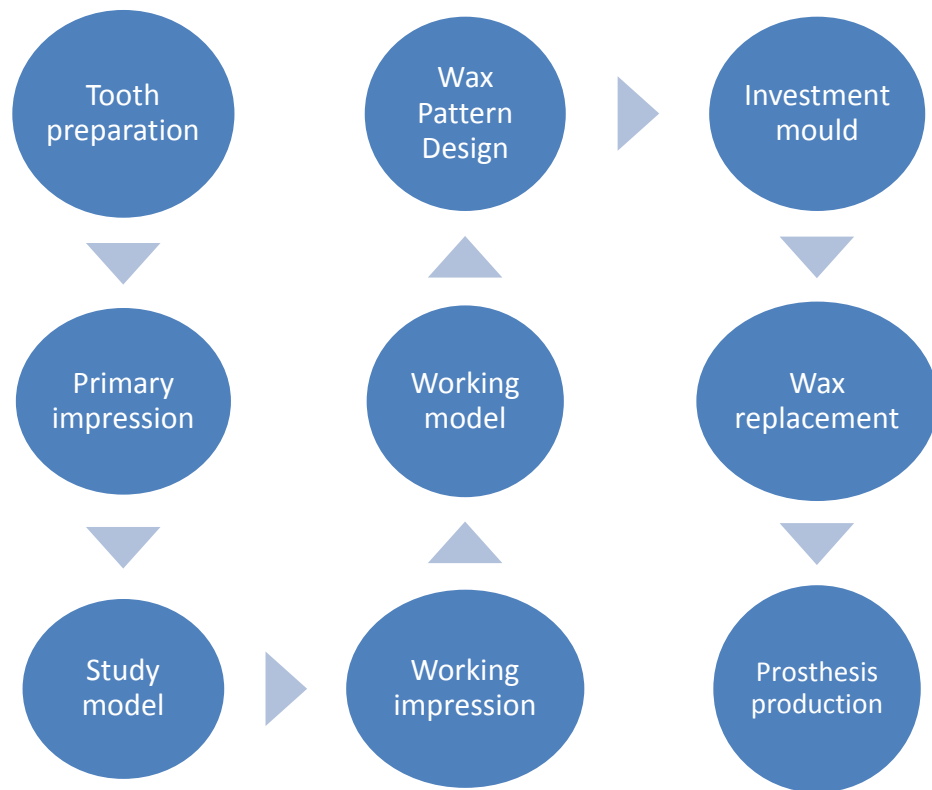


Figure 1 Conventional method of lost-wax fixed dental prosthesis fabrication

In addition to this, dental ceramic prostheses can also be fabricated by sintering. The method requires a ceramic material in slurry form to be brushed onto a refractory model/foil and then subjected to a heating protocol (firing/sintering). A shrinkage of up to 20% in volume may occur upon final firing procedures (5). To compensate this, the application of powder slurry is made in excess. Another dental ceramic fabrication method is the slip cast method which has been related to alumina based ceramic. It requires slurry of aluminium oxide (Al_2O_3) particles to be sintered (at 1120°C) on a refractory die for 10 hours. The result is a framework of alumina that has small pores which are then infiltrated with glass and fired again at 1100°C for 4 hours to close the pores and improve the material physical properties (6).

The conventional methods of fabrication of dental restorations have been utilised since the 19th century (7). However the dimensional accuracy of the fabricated restoration depends on dimensional changes relating to the wax pattern and the sintering process (8). [In practice, the conventional method of fabrication requires skill for restoration integrity, retention and fit (3)]. Accuracy is also important for luting agent space issues as the effect of increased space may cause looseness of restorations. A narrow space however may lead to improper seating of restorations due to inability of luting agents to spread evenly (8).

1.1.2.2 CAD/CAM in Dentistry

The previously mentioned rapid development of CAD/CAM in engineering was eventually introduced into the dental field. In the 1980's, Duret and colleagues pioneered the use of CAD/CAM in dentistry. The Duret system (regarded the 1st generation of dental CAD/CAM, Fig 1a) (9) was unpopular however due to complexity and cost (10). Morrman and Brandestini developed Chairside Economical Restoration of Esthetic Ceramics (CEREC). Its use of optical sensors (coupled charged devices or CCD) to digitize teeth (11) made the CEREC capable of producing inlays and onlays at the chair side (12). The disadvantage was that it could only fabricate single units (inlays, onlays or veneers).

While the concept stimulated considerable interest from researchers, most workers had difficulty in producing acceptable digital images of teeth (9) using the associated

scanner. This led to the 2nd generation of CAD/CAM in which a working model of the prepared cavity was created before data acquisition (Fig 1b). Recent developments in this field have seen improvements in the digitizing and manufacturing equipment. While earlier CAD/CAM systems could scan and produce only one dental prosthesis per episode of work, the latter have the ability to do multiple pieces simultaneously (9). Results have proven the 2nd generation of CAD/CAM systems ability to create dental restorations with clinical success (9, 13). The 3rd generation CAD/CAM present systems similar to the 2nd generation CAD/CAM systems but with reduced cost. Purchasing and maintaining CAM equipment is costly. Because of that, manufacturers have developed central manufacturing systems (9). CAD data (retrieved from users) could be sent electronically to the manufacturer for fabrication.

Fig 1a 1st generation of CAD/CAM

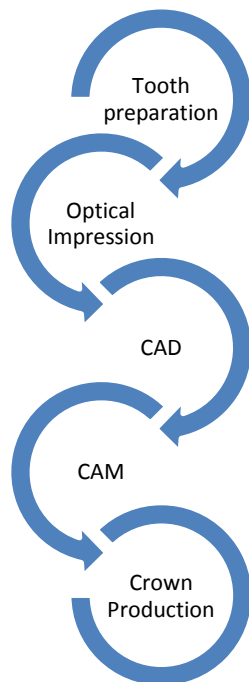


Fig 1b 2nd generation of CAD/CAM

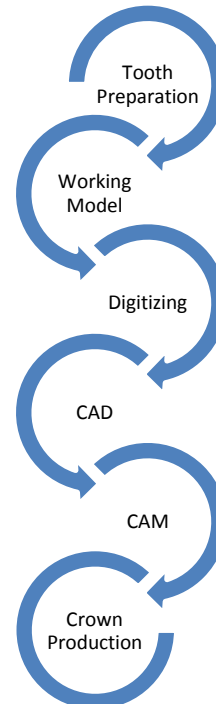


Figure 2 History of dental CAD/CAM, a: 1st Generation, b: 2nd Generation

Similar to utilization of CAD/CAM in other industries, fabrication strategies have primarily been focused on milling (subtractive method). Advancements in the area include use of 5 axis instrumentation, improved tooling equipment and material development (10, 14, 15). Clinical studies have shown favourable results in terms of fit (16). However milling strategies may produce waste and may involve high energy consumption. These limitations have resulted in the development of additive methods (17). Currently, only alloy construction exists for additive methods of CAD/CAM but initial attempts have been made to sinter zirconia via this method (11).

Continued developments have increased utilisation of CAD/CAM in orthodontics, maxillofacial prosthesis and fixed prosthesis (i.e. implants) (14). New techniques for collecting data (i.e. laser sensors, contact scanners) have emerged and future research is likely to be based on utilising the CAD/CAM systems in different contexts. Interestingly, CAD/CAM development has also increased material potential. Unlike before, high strength materials (e.g. Zirconia, CoCrMo) can presently be fabricated via the CAD/CAM methods thereby eliminating the need for technique sensitive methods.

1.1.3 Examples of CAD/CAM's in Dentistry

1.1.3.1 Incise

Incise is a dental CAD/CAM system developed by Renishaw (Wotton-under-Edge, Gloucestershire, UK). The company specializes in industrial metrology. Utilizing its

strengths in the field, they developed a touch probe scanner (DS10) for precision measurement and contact scanning of prepared teeth. The Incise system allows fabrication of major dental frameworks in suitable substrates such as Co-Cr-Mo, zirconia and dental resin. Dental alloys are fabricated by 3D printing (Laser melting machine, AM250, Renishaw, UK) with the use of high powered lasers to build intermittent layers. A 3-axis milling machine is utilised for fabrication of zirconia or dental resin frameworks.

There have been limited studies utilising the Incise system for research purposes. L Zhou *et al.* (2009) concluded that the contact scanner of the Incise system can be used to quantify tooth wear (18). Another study demonstrated the use of Incise to quantify the preparation angle of a tooth prepared for fixed partial dentures (19). Another study by KE Ahmed *et al* reported that the use of Incise contact scanner offers more precise measurement when compared to non-contact scanners(20). In conclusion, the limited studies available demonstrated the high accuracy of the Incise system due to its ability to quantify tooth wear, preparation angles and preciseness in direct comparison with non-contact scanners.

1.1.3.2 Procera

The Procera is a dental CAD/CAM system that utilizes the contact scanner. Enlarged alumina and zirconia copings can be fabricated and sintered at 2000°C to give maximum density. Upon completion of sintering procedure, the coping shrinks 25%

on cooling. In contrast to Incise CAD/CAM system, studies utilising Procera system are widely reported. The precision of fit has been reported to be less than 70µm (21). The Procera system has a niche area in fabrication of alumina and zirconia copings.

1.1.3.3 Cerec

Chairside Economical Restoration of Esthetic Ceramics or CEramic REConstruction (CEREC) is a dental CAD/CAM system from Sirona Dental Systems, Germany that was developed by Dr Mormann and Dr Brandestini during the 1980's. Currently the product is in its 3rd generation and has the advantage of making dental restorations at the chairside. The 3rd generation of CEREC also allows fabrication in the laboratory utilising CEREC inLab and uses 3D virtual models of teeth to design dental restorations. Previous versions utilised 2-dimensional data for fabrications. Earlier versions of CEREC utilised structured white light and reflective powder to scan teeth for visualisation in dental software. The introduction of short wave blue light increased the level of precision of the 3D camera and this then progressed to the Omnicam to facilitate powder-free scans.

Studies suggest that CEREC restorations have been generally successful (22, 23) but the recommendation is that these are confined to the anterior teeth. Ceramic chipping of dental restorations has been commonly reported to be a failure of CEREC based restoration however the amount has been deemed little as no functional loss

occurred. Although a variety of materials can be used, it does seem though that soft dental materials are more suited for CEREC.

1.1.3.4 CybaDent

CybaDent is a dental CAD/CAM system developed by Cybaman Technologies, a UK company specialising in hardware and software engineering development. Its niche area is the development of a 6 axis robotic manipulator for subtractive methods of CAD/CAM. It differs from other CAD/CAM systems in the market by moving the work piece while the cutter remains in a fixed position (24). The CybaDent is part of the development progress made of the Cybaman replicator. It comprises of a complete Computer Numerical Control (CNC) system that incorporates CAD and CAM into one machine. CybaDent allows importing of standard electronic files to its CAD software. It utilises DentalDesigner CAD Software (3Shape, Denmark) to design its dental restorations and HyperDent (Follow-Me, Germany) as its CAM software. The CAM software allows milling in a variety of dental materials including zirconia, titanium and CoCrMo. This is a distinct advantage over other commercially available dental CAD/CAM systems as the machine settings used (3kw with 50,000 rpm of water cooled spindle supported by an 18 station auto tool changer) for milling purposes allows it to mill fully dense materials (24).

1.1.4 Digitization

1.1.4.1 Scanners

Scanners collect data points over the surface of an object and project them in a coordinate system (called point clouds) to virtually reconstruct the surface scanned

in a 3D model. The process of data acquisition and 3D rendering is known as digitization (25). There are two types of commercially available scanners to perform this process; (a) contact and (b) non-contact scanners. Each has its own advantages and disadvantages.

Contact scanners; also referred as mechanical scanners are digitizing devices that utilise a touch probe to obtain data through physical contact. The scanner may consist of a touch ruby stylus tip, a 3-axis movable articulating arm structure and a data collection system. The method functions by recording point clouds when the stylus (attached to electronic spring) deflects on contact with the surface object. The stylus tip continuously drags along the object (spiral/zigzag motion) with low force (0.5kg/N) and record points at specified intervals. Coordinate points are then assigned on CAD software recording the movement of the stylus tip. As physical contact is required during the scanning process, modification or damage may occur on non-rigid specimens (26). In addition the process is time consuming. At the present time (2015) only the Procera and Renishaw CAD/CAM systems utilize this technology for fabrication of dental products.

Non-contact scanners (also known as optical scanners) utilize a source of electromagnetic energy to probe an object. Acquisition methods vary from source of light (i.e. laser, structured light). The most common approach involves a triangulation procedure that consists of a laser emitter and a camera sensor (CCD).

The emitted laser beam is reflected from the object and is captured by this sensor. With a determination of laser emitter-sensor distance and beam angle, the location of each point on a surface can be determined and assigned 3D coordinates. Distance (d) of reflected beam may then be calculated through geometrical considerations (Figure 3). The CEREC system makes use of non-contact scanning technology which makes it capable of creating digital impressions inside the mouth.

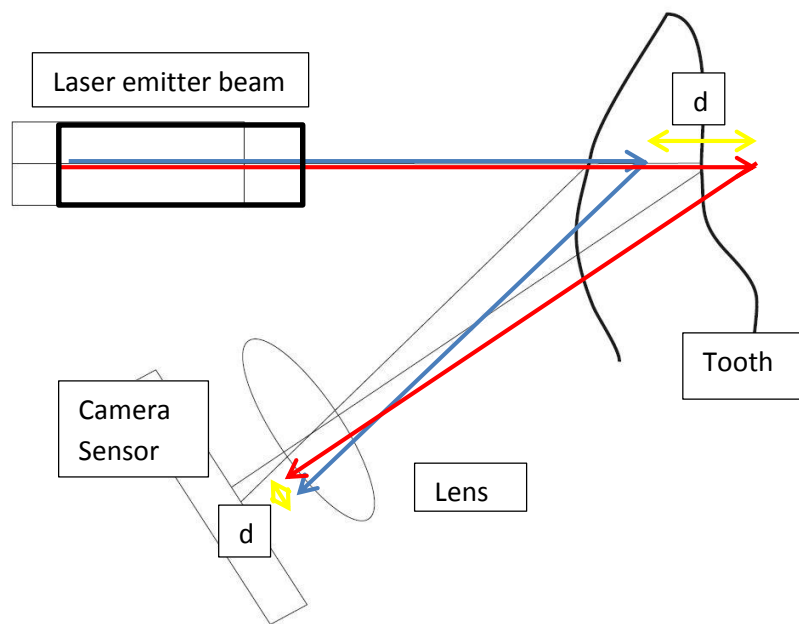


Figure 3 Triangulation procedures of Optical Scanning

The use of structured-light scanners operates by projecting a structured light pattern onto the object in investigation. As the pattern is projected on the object, its structure is distorted. The distorted pattern and the original structure pattern are then compared utilising a camera recorder and computer software and the offset distances (d) that vary from the original structured pattern are calculated. It is then translated into meaningful coordinate data (Figure 4). In contrast from laser point scanning, the method can scan multiple areas simultaneously thus improving speed

of scanning (27). Examples of manufacturers that utilise this method include the LAVA Scan, 3M ESPE and the Everest Scan, Kavo.

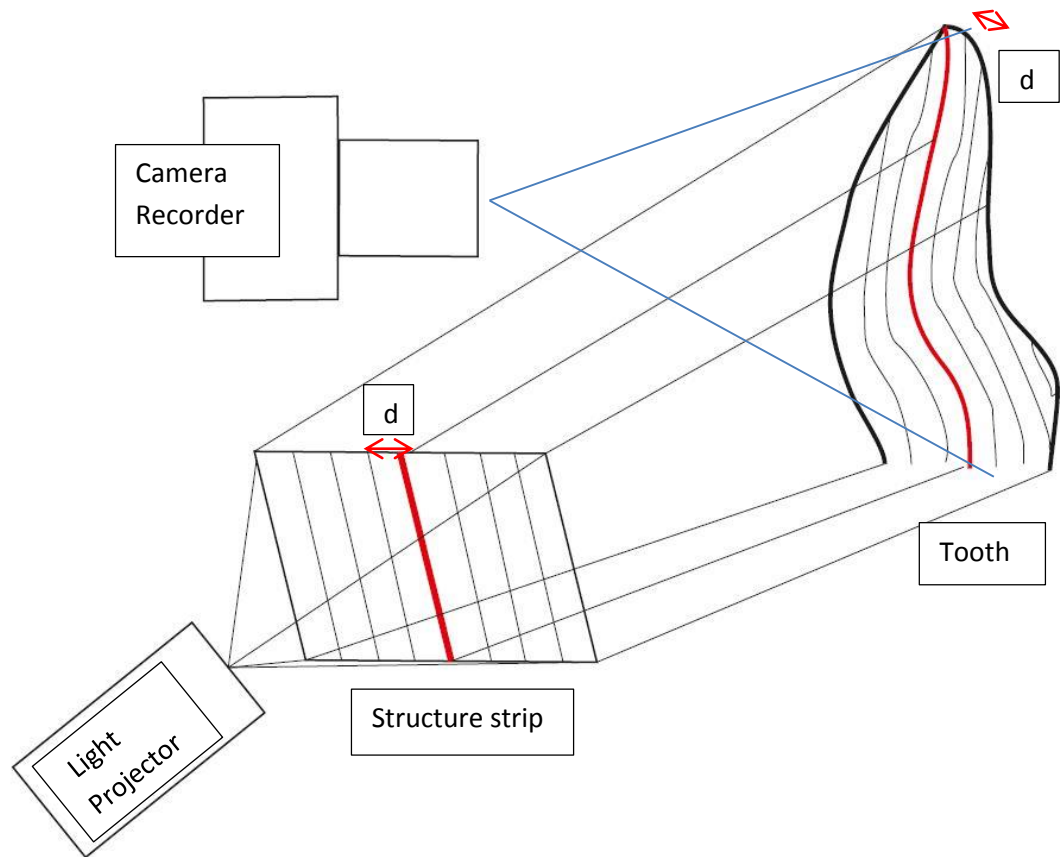


Figure 4 Mechanism of Structured Light scanning

Dental scanners are known to introduce some scanning inaccuracies (28). However, mechanical scanners are used as a standard in metrological inspection due to reduced inaccuracies when compared to non-contact scanners (26). For the purpose of this present study, a contact scanner was utilised in an attempt to minimize scanning introduced inaccuracies.

1.1.4.2 Electronic Exchange Files (STL, STEP, DICOM)

The digitisation process includes data acquisition and design processing. Data acquisition originates from the collection of data from the scanners while the design process is the drawing performed with computers in CAD software. In between these processes, transfer of files containing the design information is required. These information files are exchanged electronically. Electronic exchange files are computer files that are utilized data for transfer from a piece of software to another. Different exchange files exist each having its own advantages and disadvantages. The most common files are explained as follows.

Stereolithography or Standard Tessellation Language (STL) is a common format used for electronic exchange files within manufacturing, industrial and rapid prototyping applications (29). It consists of a collection of triangles that have inner and outer surface (Facets). Each triangle has 3 vertices (Lines) comprising of three data points that are connected to each other. Two adjacent triangles will always share only one vertex. This means that no overlap of triangles occur thus creating a surface model of a 3-Dimensional object (30). In order to achieve accurate surface detail, the STL format requires a high amount of data points, densely localised at areas of concern (Surfaces) to capture that particular surface geometry (30). The complexity of the design and ability of data acquisition are factors that affect the amount of data points required for 3D modelling. Although STL format is a standard file for data input of all manufacturing systems, mathematical errors of triangulation of data points may occur during construction of a 3D surface model (29).

Another file commonly used is the Standard for the Exchange of Product model data (STEP). It is also a standard file for exchange within Computer Aided Design applications. Similar to STL, it carries surface information of a 3D model. In addition, it may also display information of standard geometry (lines, dimensional data), texture and colour that may be utilized for metrological inspections making the file larger than STL (31). The STEP file is suitable for fabrication of items into many copies. A restoration however is a once off item. It has a complex design and no standard measurement in terms of geometry and dimensions thus always customised for the particular application. This makes the use of STEP data less suitable for electronic exchange between dental CAD/CAM appliances when compared to STL.

For radiographic devices, the standard file for electronic exchange is the Digital Imaging and Communications in Medicine (DICOM). DICOM are files that are produced when a scanned object is sliced digitally in a finite number of sections and stored as 2D images (32). These 2D images are then reconstructed into 3D objects by attaching the collection of 2D images in a bundle. Although DICOM files store a large number of these two-dimensional sectional data, the main disadvantage is the requirement of a dedicated viewing software for processing and analysis (32). The software usually comes with the digital x-ray machine. However, DICOM files are easily converted to multiple formats including STL files for 3D view manipulation. Micro-CT is an example of an appliance utilizing DICOM files for 3D simulation. Micro-CT generated data may require exportation to other software for analyses. Most

analysis software including software utilized for the present thesis is not capable of reading DICOM files hence exporting to a more common file (e.g. STL) becomes necessary.

All the files mentioned were common electronic exchange files. However STL files are more commonly used in applications where communication between different pieces of software is needed.

1.1.5 Manufacturing Processes

Manufacturing process is a process for fabricating a desired output following planned designs. Initially, information from the digitization and design processes is exported to CAM appliances. CAM software within the appliance then plans a strategy to fabricate the design. CAM is divided into two methods: - 1) the subtractive method and 2) the additive method. Strategies are dependent on the method utilized. A typical strategy would involve defining the material to use and the size of the material blank (billet) required. It also contains the order of specific coordinates in which the tools move to during the fabrication, the tool choice (e.g. sizes of burs) for each specific area of fabrication and the choice of rotation speed of the tools used at each step. Lastly the most effective route for fabrication of the product is selected during this strategy planning. The CAM software typically recommends a strategy for fabrication of a part however the software also allows a technician to modify the strategy used.

In general, the advantages of CAM when compared to the lost wax technique can be summarized as follows: 1) reduced work, 2) increased cost effectiveness and 3) improved quality and standardisation (33, 34). Due to the automated nature of CAM, the work required for fabrication mainly concentrates on creating strategies to utilize CAM machinery. This replaces the considerable effort required when conventionally fabricating restorations through the lost wax technique (33). In addition, time and effort from the dental technicians can be better spent on restoration finishing procedures including porcelain veneering. Utilisation of CAM increases cost effectiveness by increasing the speed of production and utilisation of cheaper material (e.g. mass produced blocks) (33). Quality of products can be better controlled as the conventional method has been too reliant on the dental technicians' expertise in contrast to CAM technology (33).

CAM can be utilized for a variety of dental restorations including monolithic crowns (e.g. Lithium disilicate and full contour zirconia), inlays/onlays (e.g. feldspathic porcelain, leucite and lithium disilicate glass-ceramics) and dental copings. The disadvantage however is that if copings are fabricated with CAM, the aesthetic component cannot be added via the same method (28). The aesthetic component may take the form of a glass, glass ceramic or porcelain and may be placed by pressing or layering on to the coping. However, the development of multi-layered translucent blocks may be a response for this in future. Currently dental fabrications are confined to single unit fabrication and anterior restorations however studies

looking at posterior and long span bridges look promising (35, 36). Lastly, a distinct disadvantage of CAD/CAM is the high capital cost to own and maintain CAM technology (28, 34).

1.1.5.1 Subtractive route

The subtractive route is basically a top-down approach of fabrication (37). It is the most common method of CAD/CAM in dentistry (37) and involves a variety of basic and complex strategies. In summary, the process is commonly controlled by computer numerically controlled (CNC) machine. The CNC machine receives electronic files of the design from designing software (usually dental CAD software) and the technician or dentist then plans and inputs strategies to fabricate it.

A common subtractive method strategy (38, 39) would include:

- 1) The use of large tools to remove a bulk of material (roughing)
- 2) The use of smaller tools to eliminate material to a small distance nearing the exact design (semi finishing)
- 3) The uses of even smaller tools to give a smooth surface finish for the design (finishing).
- 4) The outer surface of the design is milled first before the billet is rotated to mill the inner aspect of design.

Dental alloys, wax and resins are milled to the size required while most ceramic material (green [non-sintered] and white stage [pre-sintered]) are milled enlarged (28). The final sintering process shrinks the overall dimension to size. This is controlled by choice of ceramic whether it's pre-sintered or post-sintered each having advantages and disadvantages.

Dental CAM Processing is categorized by the number of milling axes (11). Three axis milling machines are CAM devices that utilize three defined tooling pathways; a) X-direction, b) Y-direction and c) Z-direction (Figure 5). Examples utilising this method is the inLab (Sirona), Lava (3M ESPE), Cercon brain (DeguDent) and the Incise (Renishaw). 5-axis milling machines have additional tooling pathways in the form of a rotating cutting tool (X-Plane) and a Y-Plane rotating object (Figure 5). Examples of these are the HSC Milling Device (Etkon), Everest Engine (KaVo) and the Cybaman Replicator (CybamanTech). While the use of a 3-axis device is simple and may save time in construction of items, complex designs may not be possible due to inaccessibility of cutting tools (10, 11). Beur *et al.* (2008) reported that the number of axes does not entirely improve quality of dental outcome (11). The quality is dependent on interaction of the full CAD/CAM process. However, utilisation of the 5-axis dental milling device is promising but investigation on the efficiency is lacking. There is also concern that the traditional tooth preparation are being altered to deal with limitations of CAD/CAM. This needs to be properly identified and investigated. Increasing the axes number in CAD/CAM machinery may aid the development of the CAD/CAM system.

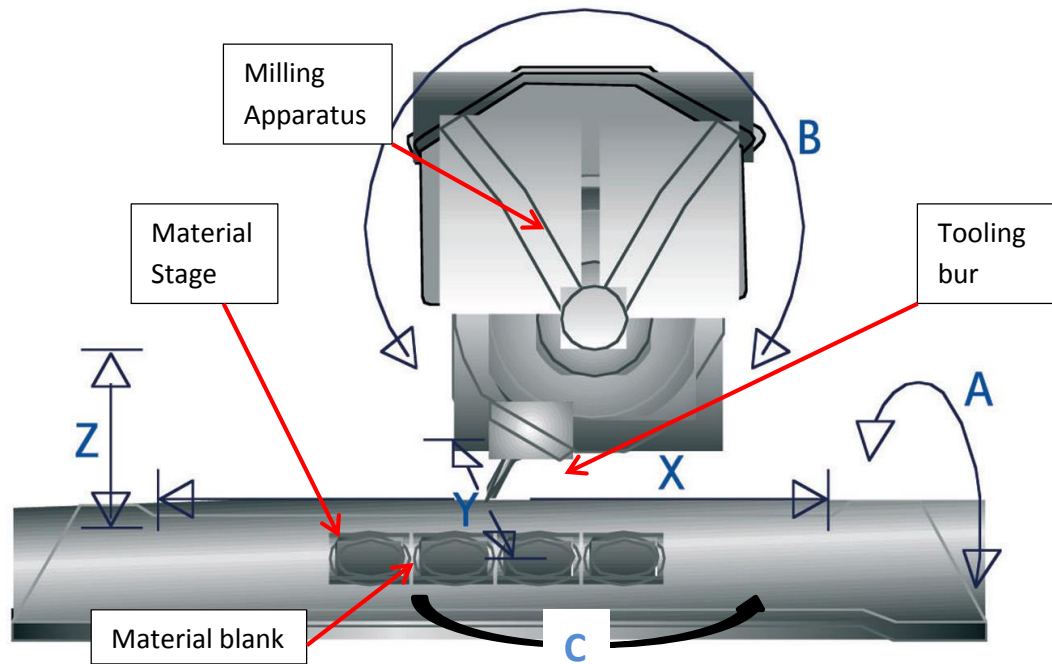


Figure 5 CAM Milling Axes: i) Directions X,Y and Z (3-axis); ii) Directions X,Y,Z and Stage rotation A (4-Axis); iii) Directions X, Y and Z, Stage rotation A and Apparatus Turn B (5-Axis); iv) Directions X, Y and Z, Stage rotation A, Apparatus Turn B and Stage rotation C (6-Axis) *diagram modified from Beur et al (2008) (11)

Advantages of using the subtractive method include improved accuracy, reduced fabrication time and the opportunity to create more standardised model when compared to the conventional method of fabrication (28, 37). However, the subtractive route may be wasteful of material (37), cause attrition to cutting tools thus leading to constant replacement of tools (40).

1.1.5.2 Additive route

The American Society for Testing and Materials (ASTM) defines the additive route as “The process of joining materials to make objects from 3D model data”(41). In contrast to the subtractive method of grinding large billets of raw material to the desired design, the additive method utilizes small particles of material and builds the

desired design by attaching the particles together in a bottom-up process. The additive route of CAD/CAM requires creating a 3D virtual design sliced into finite amount of layers all performed in CAM software. Each layer is then fabricated in sequence until the desired design is achieved. Additive methods of CAM include (42):

- stereolithography (SLA)
- fused deposition modelling (FDP)
- laser powder forming (SLS/SLM)
- electron beam melting (EBM)
- inkjet printing (IP).

SLA works by laying out a solution of photopolymer simulating a single layer of design. It is then polymerised by utilisation of ultraviolet light causing it to become hard before a second layer is made on top of it. The process continues until the design is completed. However, its accuracy of it depends on the layered material and this technique is reported to have a maximum of 10mm per layer (43). This accuracy is not suitable for dental restorations but might be applicable for other aspects of dentistry such as implant drill templates.

Similar to SLA in terms of layering techniques, the FDP method requires the use of a filament tube that holds thermoplastic material. Layering is done by heating the tube to aid flow. Upon exiting the filament, the material sets in air. The process is a cheaper alternative but has less manufacturing tolerance than SLA (0.25mm) making it less accurate and require finishing procedures (43).

In contrast to SLA and FDP the accuracy of laser powder forming methods is better.

It is divided into two:

- Selective Laser Melting (SLM) usually for metal alloys
- Selective Laser Sintering (SLS) for other materials.

The use of high powered laser is utilised to attach powder particles together by melting the highly refined powder particles in a controlled atmosphere making accuracy ranging from 10-20µm per layer. Upon cooling, the powder particles fuse together forming layers of material (a powder bed). Design is fabricated by repeated layering of formed powder bed until the desired design is complete. Similar to laser powder forming methods, EBM also melts metal powder together. However it utilizes electron beams. This makes the fabricated product stronger and clear of voids however its use is restricted to big applications such as metal plates as the accuracy is between 0.3-0.4mm per layer.

Another additive method of CAD/CAM is IP. It is currently the only method that allow colour to be added to the output, however its use is currently restricted to resin polymers. IP works by utilising liquid as monomer to polymerise powder particles. Colour may then be added to the liquid giving the final outcome a coloured appearance suitable for maxilla-facial prosthesis. Currently, only SLM technique provides dental restorations that are accurate enough for reproduction (42). For this reason only SLM was utilised for the present thesis.

Furthermore, an advantage of additive methods is ability to fabricate complex shapes (undercuts, planned voids, unique designs etc.) without the problems generated from the subtractive methods of fabrication (37, 42).

1.1.6 CAD/CAM Software

In general, all dental CAD/CAM systems have their dedicated proprietary programs and electronic file formats to operate their specific systems. This is called a closed system where data from one system cannot be readily exchanged with other systems. Most dental CAD/CAM systems adopt this closed system in which only their own dedicated data files can be utilised (28).

However open systems are also available. Open systems allow free access for data manipulation (Full capability of use from design to manufacture) (28). These systems utilize common formats of CAD/CAM such as the STL file. Renishaw Dental Studio and HyperDent are examples of softwares that use an Open System. Renishaw utilizes the Renishaw Dental Studio for the designing process while HyperDent is the software dedicated to drive CAM appliances for fabrication.

1.1.6.1 Renishaw Dental Studio

The dental scanner used in the present study is the Incise scanner from Renishaw (DS10, Renishaw, UK). The scanner is controlled by Renishaw's proprietary CAD

software (Renishaw Dental Studio, Renishaw, UK). It is an open CAD system that allows design of multiple dental restorations including crowns, fixed partial dentures and implants. Exchange within open systems requires the use of STL files. The software has a library of ready-made dental prostheses parts designs. The designs may then be applied on to the particular tooth and then modified as desired using appropriate software designing tools. This gives complete control of the design of the prosthesis to the user. Due to capability of the Incise system to export STL files, it was utilised for the present study.

1.1.6.2 HyperDent

HyperDent (Follow-Me dental Engineering, Germany) is a CAM software that allows milling a broad spectrum of dental restorations and materials. It is also an Open System which involves software which can be utilized with all types of scanners and CAD software. The software works by using predefined machining templates. However individualisation of procedures may be input if required. Initially the software starts with automation of steps that include margin identification, connector placement and connector direction. Connectors are pre-specified areas that remain un-milled and are utilised by the CAM appliances to hold the restoration connected to the billet while its fabrication occurs. This is followed by utilisation of basic strategies of milling (See 1.1.5 and 1.1.5.1). A step by step procedure with the tools available to mill the object is constructed. Speed of rotation is then determined suitable for different stages of milling strategy (1.1.5.1). Effectively this software

simulates the whole milling process virtually until the object is acquired and can also be used for inspection purposes.

1.2 Accuracy

1.2.1 Definition of accuracy and precision

ISO 5725 defines accuracy as “The closeness of a measurement to the true value” (44). Based on this definition in order to determine the accuracy of the measurement, the true value must be known. If a set of measurements were available, then the closeness of agreement between the average values from that set with the true value is what can be defined as ‘Trueness’ (44).

In contrast to accuracy and trueness, precision is defined as “The closeness of agreement between independent test results obtained under specified conditions” (44). These terms are different but inter-related. To aid understanding, the definitions are graphically explained in Figure 6 with the centre circle representing the true value and black dots as sampled data. Figure 6a shows data which are scattered around the centre of the circle which meant low precision. If a mean score was gathered from that data, result would be centralised at the middle of the circle which meant good trueness however low accuracy was evident due to the fact that the data was not at the centre of the circle but scattered. Figure 6b displayed data with good precision as the data were all grouped together but no accuracy (individual

data was not close to the centre) and trueness (mean result of individual data was not close to the centre) was evident.

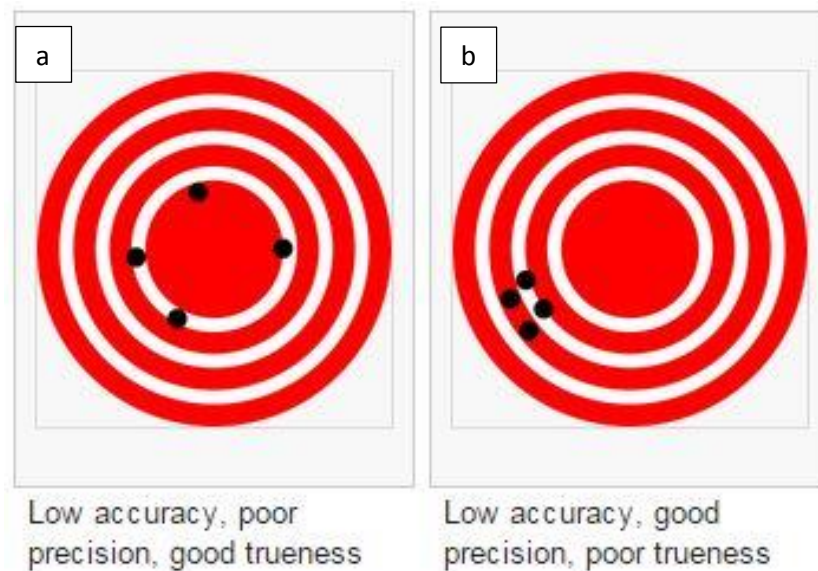


Figure 6 Accuracy and Precision according to ISO 5725, a: Good trueness, b: Poor trueness

In dentistry specifically in CAD/CAM, restoration accuracy is often determined by distance measurement of the restoration margins and internal fitting surface of the fabricated restorations with the die/tooth. Although few recommendations have been proposed for the size of this distance (See 1.2.3.3), there is yet to be a definite consensus.

CAD/CAM processes may involve systematic errors at various steps (45). Existing accuracy testing may neglect these individualised errors by only focussing on the final output. It may be useful to look at errors introduced at the various steps separately.

While studies reporting digitizing accuracy exist (45-47), no method has yet been proposed to investigate the accuracy of CAM fabrication according to its CAD.

1.2.2 Volume measurements and superimpositions of CAD and CAM

Volume is the amount of three-dimensional space enclosed by a boundary. Measuring the volume of the 3D design of a dental restoration (CAD) and that of the fabricated output (CAM) may provide useful accuracy information.

A volume of a simple geometrical (cube, cuboid, etc.) object can be measured by a simple mathematical equation (length x width x height). Dental restorations such as crowns/copings are however freeform objects and are difficult to measure volume. A method exists for volume measurement in the form of fluid displacement (48). This is performed by measuring the amount of fluid displaced when an object is immersed in that fluid. This method though cannot be utilized for determination of CAD volume as the design is in digital form. Fortunately computer software exists that is able to compute volume digitally by utilisation of computer algorithms.

In order to measure the volume of the fabricated output in the same way, a digital model of the output needs to be created. This can be achieved by micro-CT scanning of the output (Section 3.1.2.1.1). By measuring the CAD volume and that of the scanned fabricated restoration volume, a comparison of volume accuracy may be performed.

However on its own, the volume measurement will not give the location of differences. This is performed by digitally superimposing the scanned restoration and its CAD using appropriate software. The location of the differences in volume can then be displayed in the form of colour surface maps. The colour intensity in the maps is proportional to the distance between the superimposed surfaces.

Therefore superimpositions and volume measurement can be used in a complimentary manner for accuracy inspection between CAD and CAM of dental restorations.

1.2.3 Fit of CAD/CAM Fabricated Restorations

1.2.3.1 Definition

Fit definition has been published by Holmes *et al*/ 1989 (49) and is illustrated in Figure 7. This author defines analysis at the margin of restoration and the prepared tooth as marginal fit analysis. A “vertical marginal fit” is defined as the distance between the restoration and the preparation when measured parallel to the long axis of the tooth (49). A “horizontal marginal fit” is the distance between the restoration and the preparation when measured perpendicular to the long axis of the tooth (49). However, analysis in combination of vertical and horizontal discrepancy reflects more on the clinical aspect of marginal adaptation. Thus an “absolute marginal fit” is

defined as the linear distance from the finish line of the tooth preparation to the margin of the restoration (49).

The axial wall internal fit is defined as the perpendicular distance from the axial wall of the tooth to the internal surface of the restoration. Occlusal fit is the perpendicular distance from occlusal surface of the tooth to the interior occlusal surface of the restoration (49).

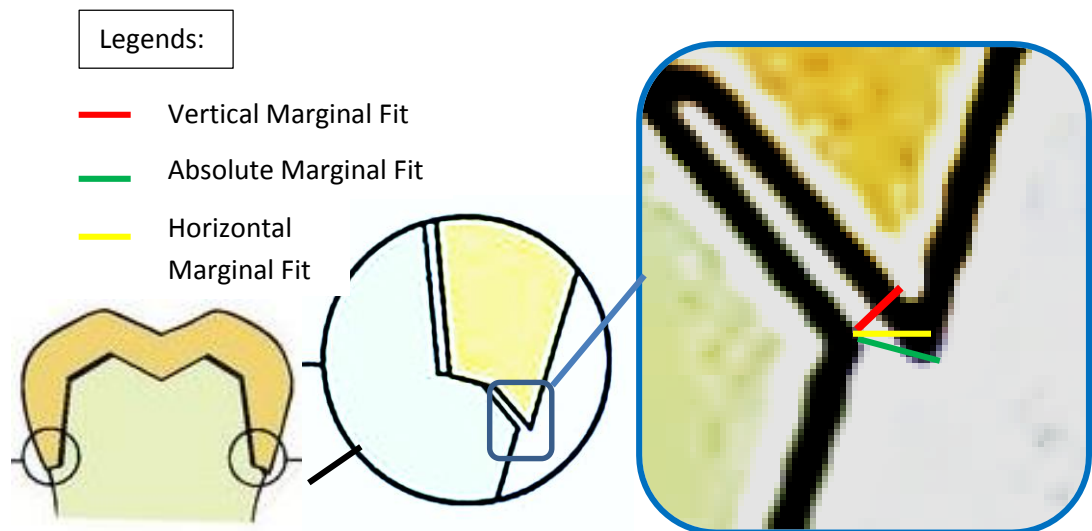


Figure 7 Marginal Fit Definition defined by Holmes *et al* 1989 (49) *pictured modified from pocketdentistry.com

1.2.3.2 Importance of Fit

The main goal of a fixed dental restoration i.e. crown, bridge is to replace missing teeth, restore function and aesthetics (50) without compromising oral health. In fabricating the crown, accuracy plays an important role into achieving this goal. Fitting accuracy of the prosthesis has been commonly researched (51) and complications due to misfit are appreciated.

Poorly fitting dental prostheses have been known to be associated with oral health diseases in patients. Misfit could lead to recurrent caries (52) via adherence of oral bacterial to its host and plaque accumulation (53). Coupled with interaction within the oral environment, progression of disease might trigger periodontal inflammation (54) and in exceptional circumstances initiate spread of pulpal pathology (52). In restorative dentistry, inadequate adaptation of prosthesis may lead to reduced strength, resistance and retention of restoration (55). This is mainly due to cement dissolution (53). Long term clinical success has also been reported (22, 56) to be affected. Aesthetic components of the dental prosthesis may also be jeopardized due to marginal discolouration (55).

1.2.3.3 Recommended Fit

There is disagreement about acceptable marginal and internal fit of fixed dental restorations (57). A cement lute in the range of 25-40 μ m has been recommended by the American Dental Association (ADA) if zinc phosphate cement is to be used for cementation (51, 53). However, this is seldom achieved in clinical practice. Consensus of several authors (21, 35, 57) suggests gaps of less than 120 μ m to be clinically acceptable due to satisfactory clinical performance. McLean and von Fraunhofer (57) reported that gaps of less than 80 μ m are difficult to detect clinically. Other reports of clinical acceptable fit vary from 50 to 150 μ m (55, 58). Optimum thickness of cement lute is almost certainly dependent on the cementing material (53). This study however uses 120 μ m as the benchmark for a clinically acceptable fit.

This topic has been widely reported (51). Ceramic systems fit analysis revealed diverse values of 3.7 to 206.3 μm (51, 53). Variations in alloy fit analysis are from 7.8 to 166 μm (36, 59). The variety of results may be due to the difference in methods of analysing, different testing parameters and different systems in prosthesis fabrication (51, 53). Some of the factors that affect the testing parameters include the type of cementation used, margin line configuration and the veneering process (53).

1.2.4 Methods of Measuring Fit

1.2.4.1 Direct measurement

Direct measurement of marginal fit relates to the presence of space between the crown margin and die. It is usually carried out using light microscopy (LM) or scanning electron microscopy (SEM) (51). The technique involves a master model or a tooth that has been prepared to receive a fixed dental restoration. The fixed prosthesis is then placed onto the master model/prepared tooth and stabilised. Specific points on the margin of specimens are chosen systematically and measurement procedures performed. On examination, vertical or horizontal distances between the prosthesis and master model at the defined points are recorded.

Microscopy is used for direct fit evaluation. While no significant difference between LM and SEM has been reported (60), margin line evaluation is suggested to be more

simple to apply with SEM (60). SEM is one of the most popular methods. It is accounted for 47.5% of 183 papers in one systematic review (51). It is simple, inexpensive and a relatively accurate method as it does not involve specimen sectioning or replicating cement space (61). However, this technique can only perform marginal analysis. Little emphasis has been given to the internal adaptation which may be of equal importance (55). As the prosthesis covers the die, the internal fit cannot be evaluated using this method.

1.2.4.2 Sectioning

Sectioning is widely used for fit analyses (51). As per direct measurement, the method allows uninterrupted visualisation and measurement of fit thus minimizing errors. Analysis of the internal fit of the dental prosthesis with respect to the master die could be achieved. The method involves a similar procedure as direct measurement but instead of directly measuring the marginal fit, the prosthesis is cemented onto the master model. The specimen i.e. the master model/prepared tooth and the fabricated prosthesis is then sectioned. Vertical discrepancies at predefined points between the model and prosthesis including the margins, axial wall and the occlusal surface of master model/tooth are analysed and recorded. Analysis is carried out by LM or SEM (62). Although the sectioning technique is applicable to the measurement of marginal and internal fit, the results obtained may not be a true reflection of overall accuracy (35) as data are confined to the sections obtained. Obviously, the method must be laboratory-based; the sections should be of minimal

thickness (63) and care must be taken to avoid damage (35) during the sectioning process.

1.2.4.3 Silicon Replica Method

The silicone replica method involves injecting a low viscosity silicone impression material inside the crown (or fixed partial denture) after fabrication. The crown is then placed on the master cast or prepared tooth to simulate cementation. This is usually done under finger pressure (64) mimicking the conventional technique of placement and seating a crown. One report (65) mentions the use of a dynamometer as a loading jig for the seating of crown to its abutment (65). A force of 20-50 N (64, 66); replicating finger pressure was applied to load the prosthesis axially with a cotton roll placed between the crown and lever. However, application of a mechanical force has been reported to be non-significant for fit evaluations (67). A thin lute of set silicone impression material will be present after polymerisation. On removal of the crown, the silicone lute will remain attached to the insides of the prosthesis. High viscosity silicone is then injected into the remaining crown space to stabilize the impression lute. Removal of the silicone replica from the prosthesis is carried out and the specimens are sectioned at regions of interest. A microscope is used to analyse the silicone impression lute at predefined points (68).

A modified version of this technique involves the use of silicone indicator paste for cement space replication. Stabilisation of the impression is done by applying acrylic

resin (66). The use of resin helps in the identification of the silicone indicator paste (Fit Checker) during measuring procedures as it is a different colour. Ability to differentiate (usually by colour) the low and high viscosity silicone impression might influence results. This may be due to operator fatigue during identification of layers in the measurement procedure (62).

This method can capture the cement space between crown and tooth or die without destroying the specimens(69). It tends to be valued by clinicians to measure the internal fit of dental prosthesis for the simplicity of the procedure (69). The method reflects clinical reality and can be carried out in either *in vitro* or *in vivo* experiments.

The silicone replica technique has its disadvantages when compared to 3D superimposition analysis. Internal fit analysis features three dimensions (3D). Measurement in different directions might satisfy this matter, but most studies evaluate only vertical gaps (65, 66, 70). Analysis of density and weight of silicone replica layer (71) could be done to record the space using a 3D technique. It should be noted however that weighing the silicone replica involves removing the silicone layer from the dental prosthesis. Dissecting/Removing the impression material from the prosthesis is a delicate procedure and time consuming (58, 65). In addition, defects in the silicone material might confound measurements (66).

When compared to the sectioning method, variances in results are apparent. Shearer *et. al* (72) indicated that the sectioning method is significantly different to the silicone replica technique with the sectioning method preferred. The author suggested that the use of silicone is not a true comparison of normal luting cement. In contrasts, reports showed that the silicone replica of cement layer acts similarly to zinc phosphate cement (68) for fit evaluations. Rahme *et. al* (61) did not report significant differences between methods utilising sectioning and the silicone replica method.

1.2.4.4 3-Dimensional Superimposition/Surface mapping)

Three-dimensional (3D) superimposition is generally placement of multiple digital 3D models on top of each other. It involves scanning an object with a dental scanner either of a contact or non-contact design. Point cloud data (set of data points in a coordinate system) are then recorded in x, y and z coordinates. This is followed by mapping of polygon meshes (collection of vertices, edges and faces) onto the point cloud data sets retrieve. The mapping procedure is performed by creating links within the data sets. Polygon meshes are usually composed of small triangles connected by three cloud data points to make up the surface area of a 3D scan (x, y and z coordinates). Finally a 3D model (rendered continuous surface) is produced by application of a surface layer onto the mesh utilising computer simulation software.

The 3D model is then utilized for superimpositions. Two or more 3D models may then be superimposed and analysed for differences through point (Surface of 1st 3D

model) to point (Surface of 2nd 3D model) measurement (73). In theory, if the 3D superimposition method was performed on a 3D model of a tooth and its restoration. The surface mapping result would reveal the distance from the surface of the tooth to the surface of the restoration. That would provide the thickness of restoration and the thickness of cement used. If the restoration thickness was known, the remaining distance would give the thickness of cement layer.

However a small disadvantage is that the rendered surfaces are not necessarily the true representation of the surfaces involved. The surfaces are dependent on the density of the data points. Resolution of the digital surface would be improved with more extensive data sets. Therefore a mesh with fewer points will not show up as smooth as the scanned object (73) making density of scanned data important. Shading is a procedure of rendering a surface mapping of the linked points to give a realistic appearance, hence what is presented in a final image may not be sufficiently resolved to represent the true surface geometry.

Advantages of 3D superimposition include its ability to digitally simulate measurement procedures of direct measuring, sectioning and silicone replication techniques as discussed earlier. Secondly because everything was performed digitally, the non-destructive measurement method makes it more versatile and advantageous over the destructive methods discussed. A digital sectioning tool within the computer software may be utilised to cut and measure at predefined

points. In addition, the main advantage of such superimposition procedure is the ability to analyse samples in three dimensions. Volumetric differences could be evaluated (63). Measurement investigations tend to be two dimensional (either vertical or horizontal) without taking into account the shape of the object investigated. Assessing distances in 3D over an area rather than pinpoint distances would provide more information.

3D superimposition methods have been previously utilised successfully for tooth wear evaluation (18, 74). However, only few studies have attempted fit evaluations using the 3D superimpositions method (58, 62). Schaefer *et al.* (2012) showed that the method could display results qualitatively giving a colour mapping of distances from two separate scans (62). Their methods in gaining quantitative data out of the colour maps produced were performed by calculating the overall quadratic deviation (root mean square or RMS). RMS served as an overall measure of the “goodness of fit” between their two separate scans with a score of zero being best fit.

Moldovan *et al.* (2011) showed that digitisation could be carried out on a silicone impression of the internal surface of copings and differences analysed by the 3D superimposition (75). The marginal discrepancy analysis however had to be done by a mechanical system i.e. coordinate measuring machines (CMM) as the silicone was damaged during removal from the copings. The use of a more rigid elastomeric material could potentially give better results of marginal and internal fit using the

proposed method. In another study, Schaefer *et al.* (2012) demonstrated a technique that incorporates internal scans of copings and external scans of master model (58). This study utilised computer software that incorporated best fit algorithm. However, during designing of the dental prosthesis, the CAD software utilized a pre-designed cement thickness which may affect the results. Thus, the method may not be a true representative of the internal fit through superimposition procedures.

Data collection for both studies (58, 75) utilizes triangulation measurement procedures. Triangulation is defined as a process of determining location of a point by measuring angles to it from known points at either end of a fixed baseline (Section 1.1.4.1). However, these procedures have been known to display inaccuracies during digitisation. This is due to the reflective surface of the material being scanned (47).

The use of a contact scanner might improve the results in terms of data collection. Although contact scanners may ignore features smaller than their resolution capacity limited by the probe radius, a study comparing laser scanners and contact scanners showed that the latter has increased data point collection (47). Analysis using the contact scanner provides dense cloud data giving opportunity for high resolution analysis (up to 5 microns) pixel by pixel at high precision (58, 62).

Resolutions are the distances between each point. However irrespective of density count, superimpositions and surface mapping measurement only utilize the surfaces

of two or more models for comparison. Measurements are performed on Mesh data point to the surface of CAD data (

Figure 8). The measurement method of 3D superimpositions does not exactly measure at point to point basis. In reality, the measurement procedure provides more of a point to surface measurement. Hence, higher amount of data points on Mesh model will provide more accurate measurements.

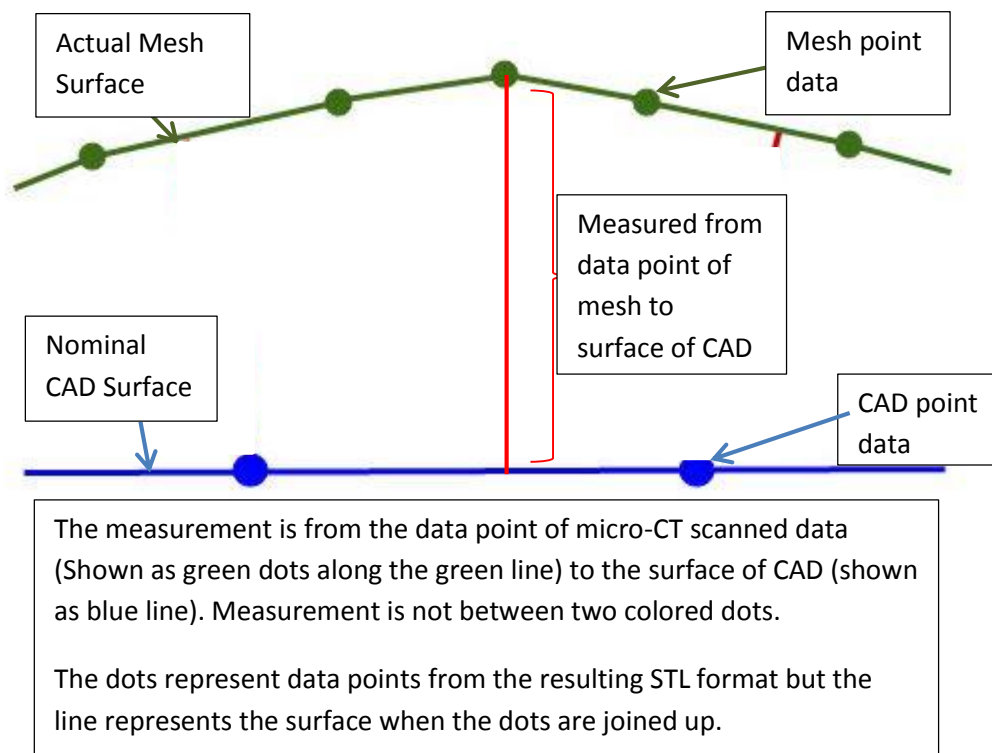


Figure 8 Principle of surface mapping measurement

1.2.4.5 Computerised micro tomography (Micro CT)

Computerised tomography (CT) is an x-ray imaging procedure in 3D. “Micro” indicates that the pixel sizes of the cross-sections are in the micrometre range. Micro-CT (also called industrial CT scanning) creates multiple digital cross sections within an

object. It utilizes a rotating x-ray projection of the fabricated prosthesis to be diagnosed. The x-ray projections are then collected by x-ray panel detectors and reconstructed in computer software to produce virtual 3-D models of the scanned object. Collection of data is affected by the x-ray absorption and scattering of the material. Hence a material that does not absorb x-rays will appear as radiolucent (darker appearance due to radiation easily passing through). The internal structures of the object are obtained by the x-ray projections that penetrate the object. Thin scan sections are produced and can be used for structural analysis depending on the x-ray settings utilised.

A normal medical computed tomography (CT scan) has the resolution in the range of 1.25 to 2mm that corresponds to 1-10 cubic voxel (voxel is a 3D analogue of a pixel) size. However, a micro CT scan has a spatial resolution of 5 μ m corresponding to a 1×10^{-7} cubic mm voxel size (76). The increase in resolution allows for a more detailed analysis when performed.

CT applications date back to the 1970's (77). Due to its non-destructive nature, materials analysis utilising CT scanning is becoming increasingly popular (77). Its ability to scan internal parts of a component without the need for dissection also makes it a competitor to other dimensional metrology either contact or non-contact methods. It should be noted however that for utilisation of the method for material and dimensional analysis, high resolution equipment has to be used. The use of it in

medical and dental imaging has limits in the specifications so as to not have effect on the patients (77). In this present study, a physical model was utilized for all scans hence the effects on patient is non-existent.



Figure 9 Components of computerised micro-tomography

Micro-CT scans in dentistry have been used in different applications. These include studies in dental material properties (78, 79), dental anatomy analysis (80) and fit analysis (51, 81). Studies utilizing micro-CT have used a variety of x-ray source voltage from 25 to 100 kV (80, 82, 83). This limitation may be due to precautions that were made to protect samples as x-ray projections produce heat. About 99% of x-ray spectrums are turned into x-ray when it hits the target sample(77). While this might be important in structures such as dentine (dentine collapses due to heat) it may or may not have effect on highly radiation absorbable material such as metal.

In addition to that limitation, scattering effects of x-ray projections may occur with source voltage of more than 250 kV (77). This could affect the sharpness on the resulting image being produced. The technology currently has advanced and a higher source of power may be utilised.

Another potential limitation is the high cost of maintaining the equipment and the time consuming methods it proposes (84). This however is expected to improve as the technology develops. Although these limitations exist with use of the micro-CT, most papers (76, 82, 83) agree that it is a useful tool in fit analysis.

Kakaboura *et al.* (2007) demonstrated the use of micro-CT scans to measure marginal adaptation of resin composite tooth restorative materials to teeth (81). The author concluded that sufficient contrast between the material and teeth must be present for analysis. Thus radiation absorption of material to be analysed must not be the same to ensure success of analysis.

Another study (82) showed that the method could allow the reconstruction of the cement space in 3-D software when evaluation was made between partial ceramic crowns and prepared teeth. However when analysis with zirconia based prosthesis and stainless steel models were performed, a 3D analysis could not be done due to

radiographic artefacts generated by the fixed partial denture (83). No cementation was used to establish the fitting space for the particular study and this was done to simplify measurement proceedings. Again, the same conclusion arises so as to have sufficient contrast of samples analysed for measurement to take place.

Another method (84) of quantifying cement space was demonstrated via scanning a silicone replica of the cementation space with micro CT. The original master die was replaced with a soft red boxing wax to act as a radiolucent support. Results could have been affected due to the dimensional properties of wax.

1.2.5 Analysis Software Utilised in This Study

This present study utilizes multiple pieces of software for different aspects of the investigations. The need for different software was evident as no single software could perform all the investigations. Rhinoceros software was mainly used for the creation of the model design and volume calculation. VG Studios was the software utilised with the micro-CT performing 3D superimpositions and surface mappings while the GOM Inspect was a 3rd party software that allows superimpositions and surface mapping without the need for the micro-CT to be present.

1.2.5.1 Rhinoceros (Rhino)

Rhinoceros Version 5 is a Three-Dimensional (3D) modelling software developed by Robert McNeel & Associates specialising in utilisation of free-form non-uniform

rational B-spline (NURBS) to create 3D models. NURBS are individual points that represent a curve or a surface. Rhino possess the ability to fabricate any 2-dimensional as well as 3-dimensional elements by manipulating these NURBS data by special tabs within the software.

A distinct advantage over other CAD packages is the ability of Rhino to export the fabricated design in different formats suitable for any CAM machines. It could also import most electronic exchange files to its software and use data to be manipulated or analysed. Its general ability to analyse includes distance and volume measurement, sectioning and Mesh Boolean Interactions. Other analyses such as finite element or thermal analysis may be performed with the aid of external plug-ins that is compatible with the software.

Distance measurement could be performed via a two point measuring tab. Measurements done within software have a tolerance of 0.001mm. This is great for distance measuring as the software also allows magnification of view to aid measurement procedures. Sectioning refers to cutting digital models to allow investigations on certain parts. This does give the advantage over a normal sectioning procedure where quite a lot of effort and special machinery are required. In addition, only few sections are feasible in the conventional way while a digital section product might include any amount of section procedures.

Another great feature of the Rhino is the ability to perform Mesh Boolean Interactions. Boolean Interactions are interactions made when two or more data sets interact (touch) with each other. In many circumstances the data sets could be either i) grouped together, ii) not grouped together or iii) shared in between. Boolean Interactions allows differentiation of the paired data and could remove the unwanted part by hiding or deleting it. Unfortunately, the accuracy produced by using this method has not been fully explored. This may be due to the difficulty of the procedure.

1.2.5.2 VG Studios

Volume Graphics (VG) was founded in 1997 in Heidelberg, Germany. It has been a dedicated member in industrial computer tomography and went on to create VG Studio. VG Studio is a visualisation software for the micro-CT. It allows reconstruction of voxel data by collecting image slices of the object scanned and creating a 3D virtual model to match. One main advantage over other CT software is that it allows direct import from the CT system itself. The images after importing procedures show a picture that has different grey scale values (Black and white). A mathematical algorithm is performed on the image to detect the edges of the model investigated. After virtually processing the images, basic procedures such as measurement distances and digitally sectioning could then be investigated. CAD data could also be imported into the software to perform comparisons with the original object. All results and CT-Reconstruction may then be exported as common exchange files within CAD/CAM applications.

1.2.5.3 GOM Inspect

Gesellschaft für Optische Messtechnik (GOM) or translated as Community of Optical Metrology was founded in 1990 and created the GOM Inspect. Currently in its 7th Version, the inspection software may perform a variety of 3-dimensional data analysis including superimpositions and surface mappings. It is also certified by the National Institute Standards and Technology (NIST), USA. Like most 3D analysis software, it also allows import of common exchange files of CAD data including STL. This makes it a useful 3rd party software as installation of it is free. The use of the free edition was sufficient as only its ability to superimpose and import STL files were required. For the present project, a 3D model was created by micro-CT but it required dedicated software that comes with the micro-CT to analyse it. GOM Inspect also allows the same inspection procedures without the need of the micro-CT close by.

Section 2

Aim, Objectives and Null Hypothesis

2 Aim, Objectives and Null Hypothesis

2.1 Aim

The aim of this present study was to compare the output of various dental CAM routes to a sole initial CAD and establish the accuracy of fabrication.

2.2 Objectives

- i. To develop a non-destructive method for detecting inaccuracies between the CAD of a dental coping and the CAM fabricated output.
- ii. To measure the volume of copings fabricated using different CAM methods and compare it to the volume of the initial CAD.
- iii. To quantify dimensional differences of copings fabricated using different CAM methods from the initial CAD.
- iv. To compare volume and dimensional differences between copings fabricated using different CAM methods.
- v. To perform measurements on the fit of copings fabricated using a variety of CAM routes on a master model using a novel non-destructive protocol.

2.3 Null Hypotheses

- i. Volumes of original CAD to volume of CAM fabricated copings do not exhibit significant differences.
- ii. No significant differences in dimensions and volume would be found between fabrication methods of CAD/CAM.

- iii. Fabrication methods of CAD/CAM would have no significant effect on internal fit of CAD/CAM fabricated copings.

Section 3

Developing the Methods

3 Developing the Methods

3.1 Method Development

Figure 10 shows a flowchart of the developmental aspect of the definitive method of the present study. A methodology was to be designed so that a virtual CAD of a dental coping could be compared with the actual CAM fabricated coping in terms of accuracy. In developing this method, several concepts had to be tested for feasibility before performing these tests on several CAM fabrication routes. The steps that were to be followed were:

- Firstly, a model of a prepared tooth was to be made (master model) and then digitised with a contact dental scanner (master model scan). A trial CAD of a dental coping that covers the prepared tooth master model was then to be created in a computer and stored as an STL file (CAD model)(Figure 10, Steps 1,2).
- A Co-Cr-Mo coping was to be made using conventional lost wax technique on the master model. The coping was then to be used as a trial for the creation of 3D scans using micro-CT. A successful micro-CT scan of this coping would be stored as an STL file and represent the trial digitised CAM output (Figure 10, Step 3).
- The STL files of the CAD model and the CAM output are imported into software for measuring their volume (Figure 10, Step 4a).
- The CAM output and the CAD model files are superimposed to check dimensional accuracy (Figure 10, Step 4b). Deviations between the CAD and

trial CAM output are displayed in the form of colour surface maps (Figure 10, Step 5a),

- The CAM output scan and the master model scan are aligned to check fit (Figure 10, Step 4c). A method of internal fit measurement was attempted via 2D calculations (Figure 10, Step 5b).
- The measurement methods were then validated. Repeatability of micro-CT was explored by scanning a coping multiple times and comparing the scans (Figure 10, Step 6a). Accuracy of the micro-CT was performed by scanning a standard artefact from the National Physics Laboratory with known dimensions (NPL Freeform) (Figure 10, Step 6b). The effect of using different pieces of software to measure volume was also investigated (Figure 10, Step 6c). Finally, the effect of different scanning resolutions on the measurement of volume was explored (Figure 10, Step 6d).

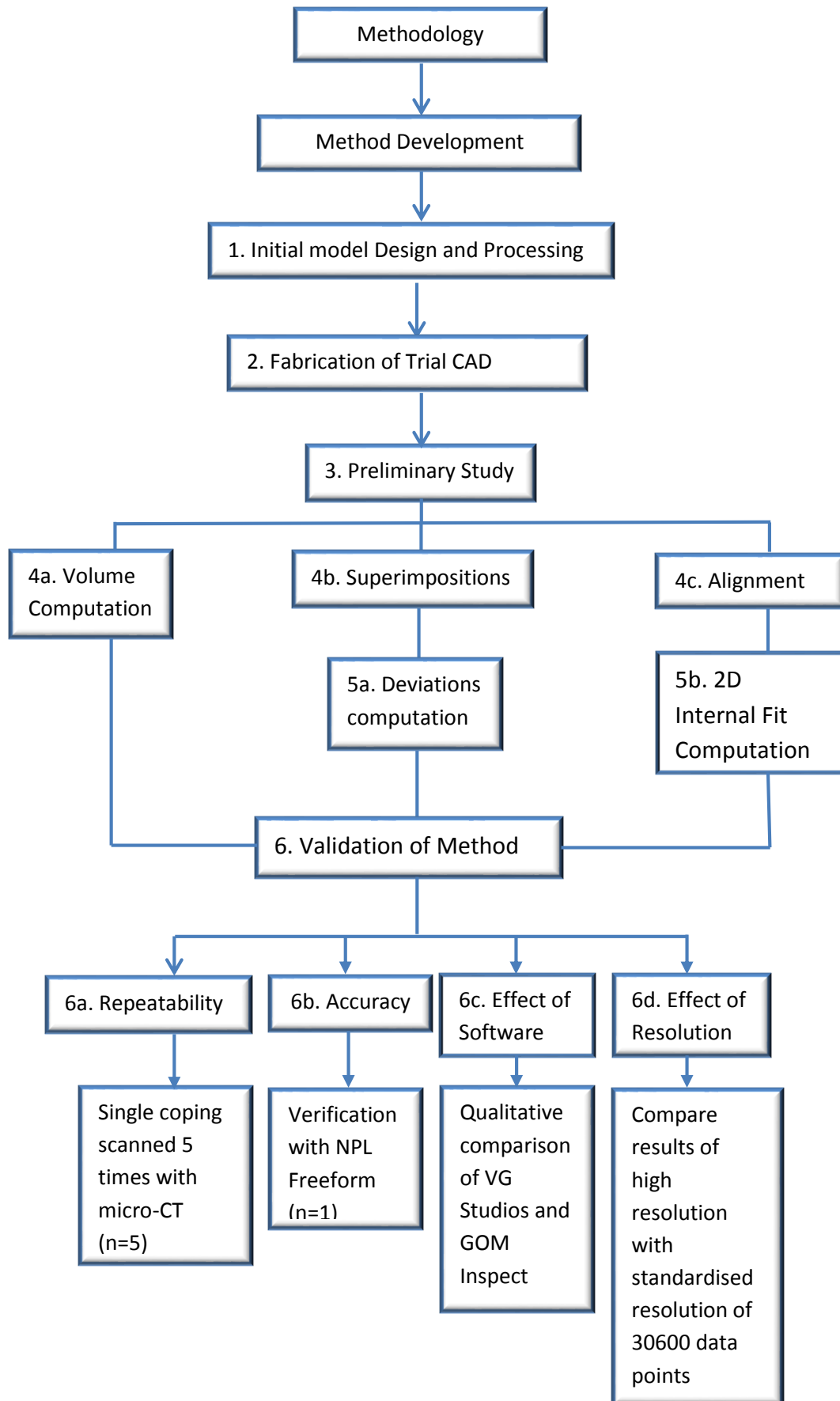


Figure 10 Flowchart of method development

3.1.1 Initial Model Design and Processing

A basic 2nd premolar design with a 360° shoulder margin was chosen. For simplicity, a uniform thickness preparation was chosen. The dimensions of the design are shown in Figure 11. The design was made with Rhinoceros (Rhino, Version 5, Seattle, USA). Three basic shapes (cylinder, cube and truncated cone) were designed using the “Solids” tool on the software (Solid>Cylinder/Box/Truncated Cone>type in dimensions). The cone was designed with a total occlusal convergence angle (TOC) of 12° and the three shapes were assembled (by ‘grouping’, ‘attaching’ and ‘welding’ commands) as displayed in Figure 11. Angles at joined surface areas with the exception of the margins were given a rounded edge of 0.6mm using the ‘fillet’ command. The prepared 1.5mm shoulder margins and the outer surface of the cylinder were given a sharp 90° angle to ease differentiation of the margin lines. The design then was saved (Nominal Data).

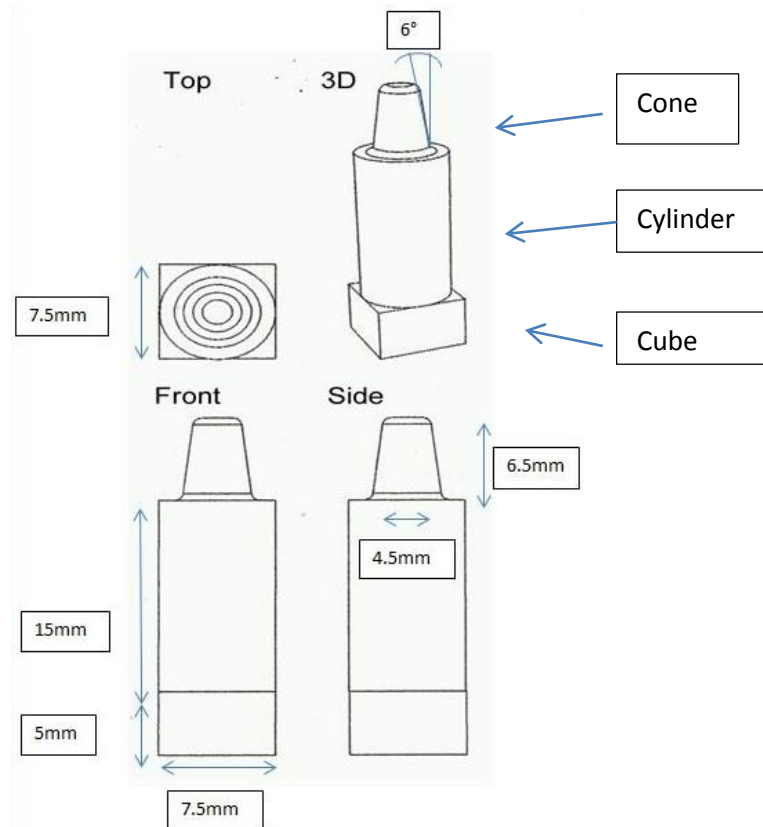


Figure 11 Dimensions of Initial Design

The saved design was processed in brass using a combination of lathe (Emcotronic T1, EMCO (Salzburg, Austria)) and mill methods. Fabricating the cylinder and cone aspect required the use of a lathe method where the brass material was turned and cut to its desired dimensions and design (Figure 11). A 5-axis milling machine (Bridgeport VMC 800xp (US) with a Heidenhain 424-430 controller (Germany) and a Nikken 120AX 5 axis attachment (Japan)) was utilised to fabricate the cube aspect of the design. In contrast to the lathe method, the milling burs move during the milling process and cut while the component milled was turned in a constant position (Figure 12). The cube aspect of the design was fabricated to make the model stand and for ease of handling for experimental procedures. The methodology concentrated on the accuracy of the coronal half.

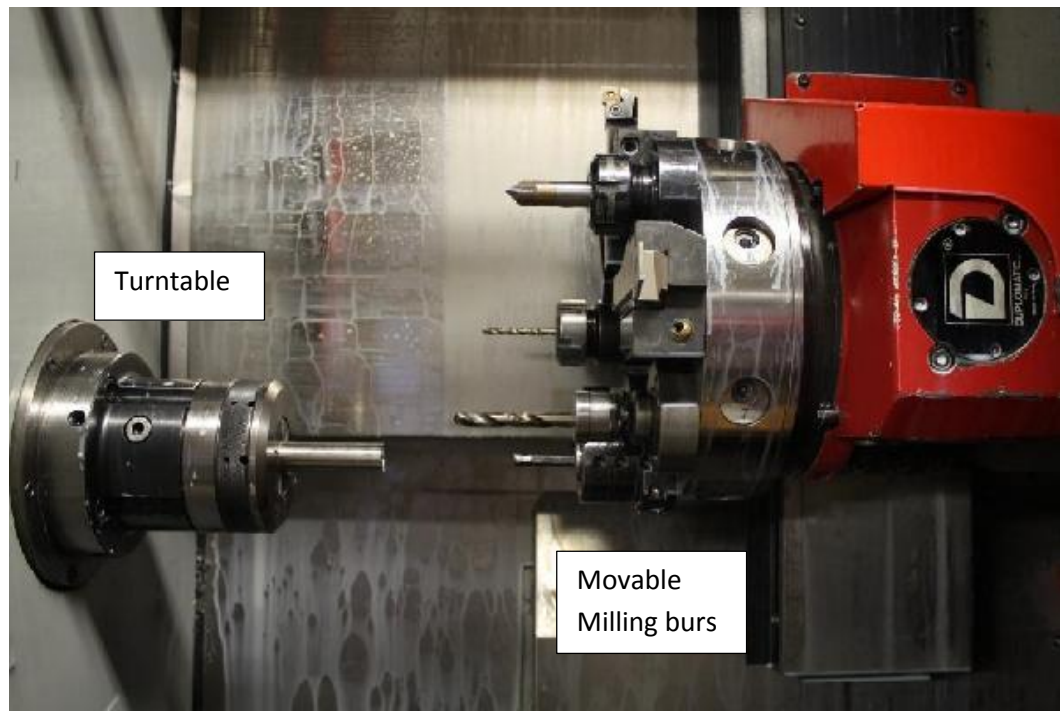


Figure 12 EMCO lathe machinery

3.1.1.1 Trial CAD

A contact dental scanner and the associated software were used to make the trial CAD for a basic coping on the brass model. Initially, calibration of the Incise scanner with a 6mm diameter calibration ball (A-5351-4157, Renishaw, Gloucestershire, UK) was performed following manufacturer instructions ("Utilities" tab, InciseCAD version 2.5.0.140, Renishaw, UK). The software accomplishes this by automatically storing reference points of the exact dimensions of the calibration ball when selected. Incise styli (A-5003-7785 & A-5003-7784, Renishaw, Gloucestershire, UK) keep in contact with the standard reference calibration ball. The following steps were then followed.

1. The brass model was secured on the holder of the Incise.

2. A prescription design form was completed. This allowed the machine to identify the trial model as a tooth. For this project, the framework was defined as a 'Basic Unit' of a Cobalt Chrome material coping on a lower right premolar (Tooth 45).
3. The cement space was set to be medium with the thickness of the coping set as thin (Figure 13).
4. The model was then scanned using the preferred settings by selection of the "Scan" tab.
5. Data was automatically captured and built on screen as a wireframe (Figure 14a) followed by a full surface rendering to resemble the initial model (Figure 14b).
6. The virtual model was then utilised for CAD by selection of the "CAD" tab.
7. CAD was initiated by defining the margin line. An automatic margin line is displayed by holding the control and clicking the left mouse button (Figure 14c). This line may then be manipulated by software tools such as "Nudge", "Partial Nudge" and the "Smooth" tool.
8. Upon determination of margin line successfully, the coping was then generated by selection of the "Generate Coping" tab (Figure 14d).
9. The resulting framework was then exported as an STL file.

Define Framework

Framework Definition	
Framework Type	<input type="text" value="Crown / Bridge"/>
Material	<input type="text" value="LaserPFM™ (Cobalt Chrome)"/>
Thickness	<input type="text" value="Thin"/>
Cement Space	<input type="text" value="Medium"/>

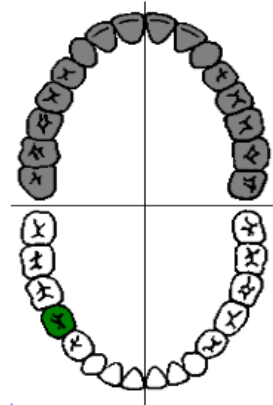


Figure 13 Parameter settings for trial model framework

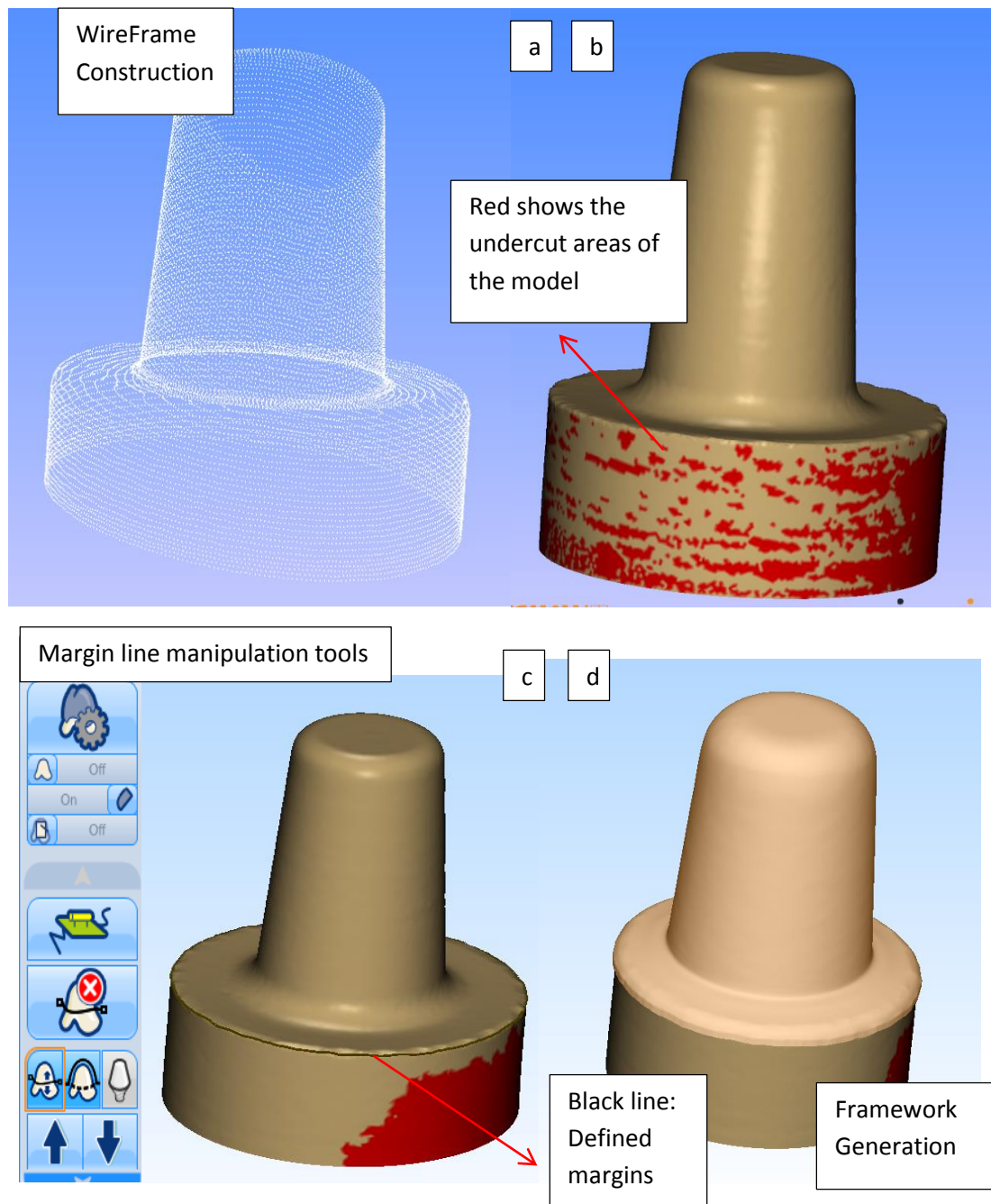


Figure 14 Trial CAD construction, a: Wireframe construction of scanned trial model, b: Fully surface rendered trial model, c: Determination of margin line, d: Generated CAD of coping

3.1.2 Preliminary Study

A cobalt chromium molybdenum (Co-Cr-Mo) coping was fabricated using the lost wax technique. The Incise dental contact scanner (Renishaw, UK) was used to digitise each step of the fabrication as follows (Figure 15):

1. The brass model was scanned utilising a 1mm ruby tip stylus (A-5003-7785) in continuous spiral motion starting from just below the margins to the top centre of the model. The start and finish of the scan had been determined earlier on the Incise software. Data was saved as Scan 1.
2. The brass model was then removed from the scanner and two layers of die spacer (P.D.Q. Die spacer Grey and Blue, Whip Mix, US) were applied onto the brass model to simulate the cement space. A second Incise scan was made and saved as Scan 2.
3. The brass model was removed again and a wax coping was manually fabricated and subsequently scanned with Incise as saved as Scan 3.
4. The waxed up model was then cast into metal (lost wax technique) using Co-Cr-Mo alloy. After removing the investment, the coping was processed to fit the brass model as per normal crown fitting process. The model and the coping in assembly was then placed back in the Incise and another scan was performed (Scan 4).
5. A total of four scans were then exported as STL files for analysis via alignment procedures.



Figure 15 Models to be scanned with Incise (a: Brass model, b: Die spacer applied, c: Waxed up model and d: Fitted coping)

3.1.2.1 Methods and Proof of Concept – deviation and volume computation

3.1.2.1.1 Microcomputed X-ray Tomography scan (micro-CT)

The fitted specimens (brass model & Co-Cr-Mo coping) were prepared for micro-CT scans to be performed (South Eastern Applied Materials Research Centre, Waterford Institute of Technology, Ireland - SEAM, WIT). The Phoenix X-Ray Nanotom-S (model XS180NF30F-144608, General Electric, Wunstorf, Germany) was utilized to perform the x-ray scans under source voltage of 168keV. Calibration of the micro-CT was initially performed. This was done by scanning and measuring a calibration device with known dimensions and making adjustments to measurements scanned to the exact measurements of the calibration device. A blank background scan was then scanned.

The models were then secured in the machine's stage at a small angle (77) using a jig. All scans made with the micro-CT utilised a slightly angled holder for standardisation of x-ray projections. A filter of 0.2mm Copper (Cu) and 0.5mm Tin (Sn) were utilised to avoid beam hardening during scan procedures. Beam hardening is a term used when low energy x-rays are absorbed by the material thus may have effect on edge detection as only high energy x-rays penetrate material and show. A continuous radially scanning method was performed in 360 degrees of the models in question. A total of 3600 x-ray projections from a step size of 10 projections per degree were computed on the micro-CT dedicated software (VG Studio 2.2, Heidelberg, Germany). The ability of x-ray source to penetrate the cobalt chrome coping made it possible to produce multiple slices of coping scans. Beam hardening

correction was then applied by reducing the intensity of the scans on software. Then using edge detection algorithms, a 3D image or a voxel model resembling the coping scanned was created, displayed and exported as STL file for analysis. The x-rays were not however capable of penetrating the brass model so at this stage only the coping was digitised.

As part of the development process, four micro-CT scans were made on the fabricated coping to investigate the penetration ability of the x-ray beam made followed by creation of the virtual model associated with it. The voltage power source was altered to assess parameters for enhanced utilisation of the micro-CT to scan the fabricated coping in terms of size and material. Power sources assessed were a) 100kV, b) 155kV, c) 160kV and d) 168kV. All scans utilised the same software for virtual voxel model construction. The models were then analysed visually and compared for optimum results in terms of resolution and capability of the micro-CT machinery to create virtual models without problems.

3.1.2.1.2 Method to Compute Differences of coping to CAD (Deviation Calculation)

The differences of fabricated coping to the CAD were investigated by performing deviation calculations. This was performed by importing appropriate STL files (Actual Data from micro-CT scan and Nominal Data from Incise, Renishaw CAD) to GOM Inspect, Version: V7.5 SR2, Germany for analysis (Figure 16). Procedure for the deviation calculation is outlined below.

1. Superimposition of the data sets was initiated by selecting the Pre-Alignment tab. The software automatically superimposes the two data sets and calculates the deviation between them (Figure 17).
2. The main alignment was then completed by selecting 'Local Best Fit' on entire Actual Data. The software automatically recalculates the deviation differences.
3. The superimposition process was then followed with a surface-to-surface comparison of CAD (Original coping design in Incise software) to Micro-CT scanned coping. This results in a colour mapping of deviations in three dimensional views for display.
4. Quantitative results were demonstrated by selecting the "I-Inspect" tab followed by "Visualisation" and "Results" (Figure 18). This displayed the Minimum, Maximum, Mean and Standard Deviations of the deviation distances between the CAD and the fabricated coping.

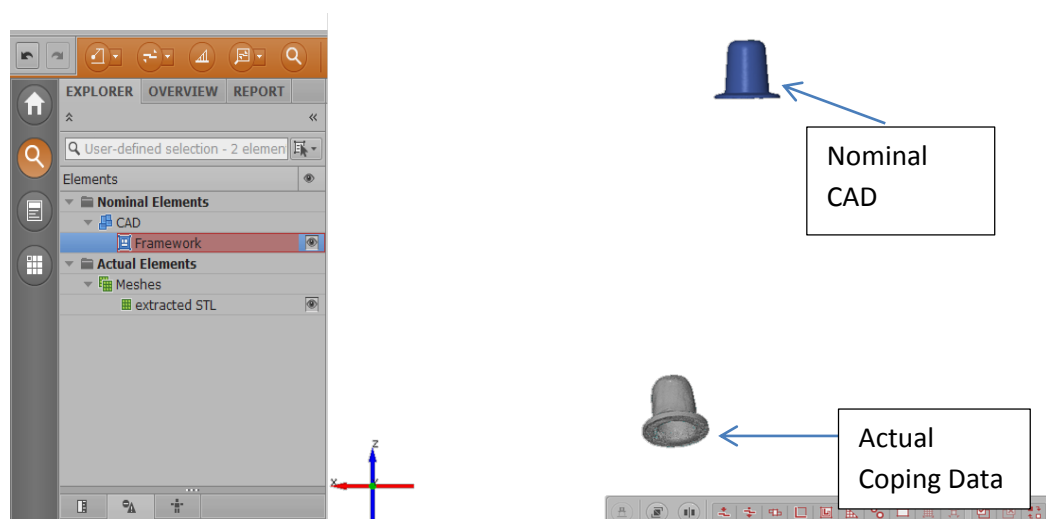


Figure 16 Importing STL files into GOM Inspect v7.5, SR2

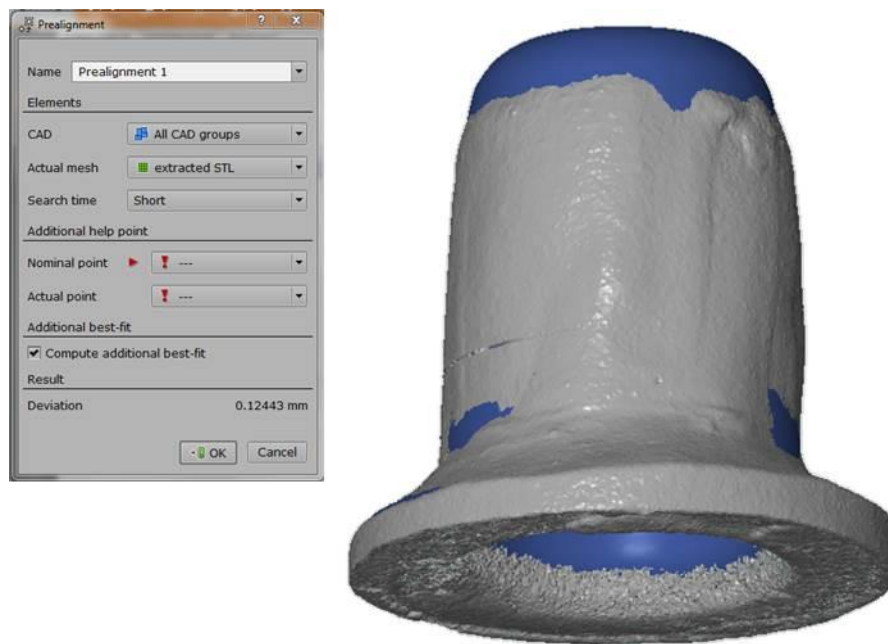


Figure 17 Superimposition of micro-CT scanned coping (grey) and CAD (blue) showing that the exact design is different from the coping

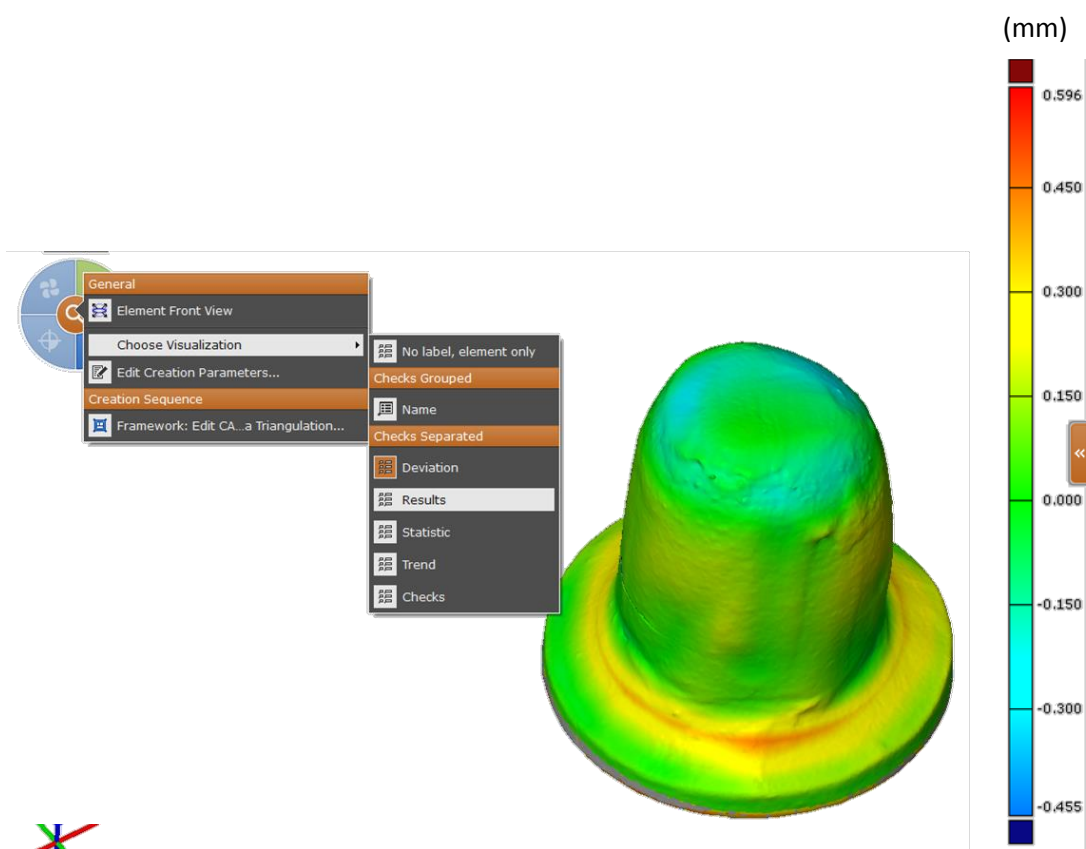


Figure 18 Steps to display qualitative maps of coping to CAD deviations

3.1.2.1.3 Method for CAD and fabricated coping Volume Calculation

The volume calculation was initiated by importing the STL files of CAD file and micro-CT scanned coping into the Rhinoceros software, (Version 5.0, Robert McNeel & Associates, Seattle, USA) (Figure 19). Upon successful import, Initial Design was selected and the volume of the Initial Design was computed by selecting the appropriate tabs in order: Analysis>Mass Properties>Volume. Result was displayed in mm³ and recorded (Figure 20). The process was repeated for the micro-CT scanned coping and the result was also recorded.

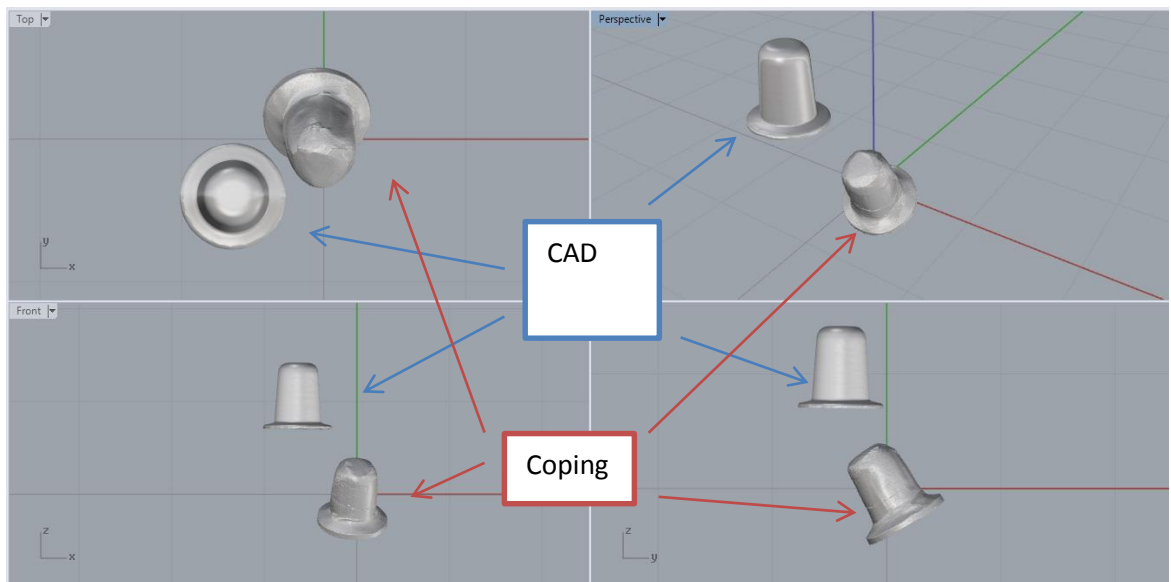


Figure 19 Importing STL Files into Rhino v5

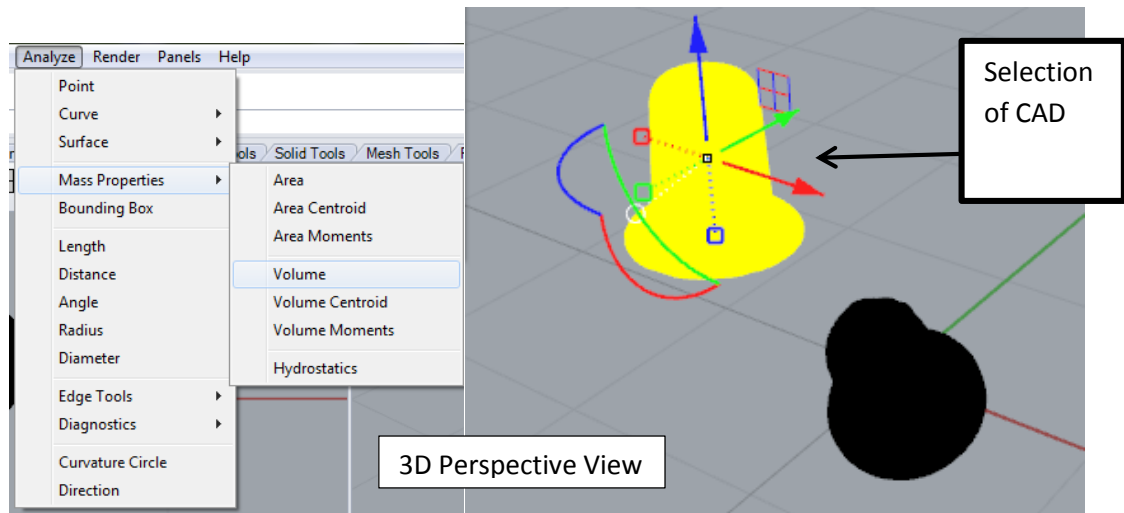


Figure 20 Steps to perform volume computation for CAD

3.1.2.2 Methods and Proof of Concept – Internal Fit

3.1.2.2.1 2-Dimensional calculation of Internal Fit

A method to derive 2-D quantitative data of internal fit was devised using imported scans of micro-CT (LS1) and CAD master model into Rhino 5 and aligning them together. As stated previously, alignment in this project was defined as placement of multiple 3-D models on top of each other at point of contact. An attempt to digitally measure the distance of contact between fabricated copings (LS1) to the master model was performed. In contrast to alignment done in GOM Inspect, the procedure in Rhino 5 was done completely manually utilising the margins as reference points (Figure 21). This was done by utilising the tabs “Translation” and “Rotation” for relative movement of the selected 3-D models in the software. The zoom-in and zoom-out capabilities of the software aided the alignment process.

This was followed by creating 50 radial cross sections (Curve>Curve from Objects>Section) along the vertical plane through the mid-centre of the digitally assembled model and coping. The 50 two-dimensional cross sections were spread out in standardised equidistant positions of 7.2 degrees from the centre of the coping (Figure 22). Selection of one cross-section is performed by application of “Lock Selected” while the rest is hidden from view with application of “Hide Selected”. This prevented unintentional change to all cross-sections while performing measurements.

A point-to-point measurement (Analyze>Distance) of selected points was then recorded. For this particular study, ten points that represent Vertical Marginal Height, Absolute Marginal Adaptation, Axio-Margin distance, Axial Distance and Occlusal Height were measured (Figure 23).

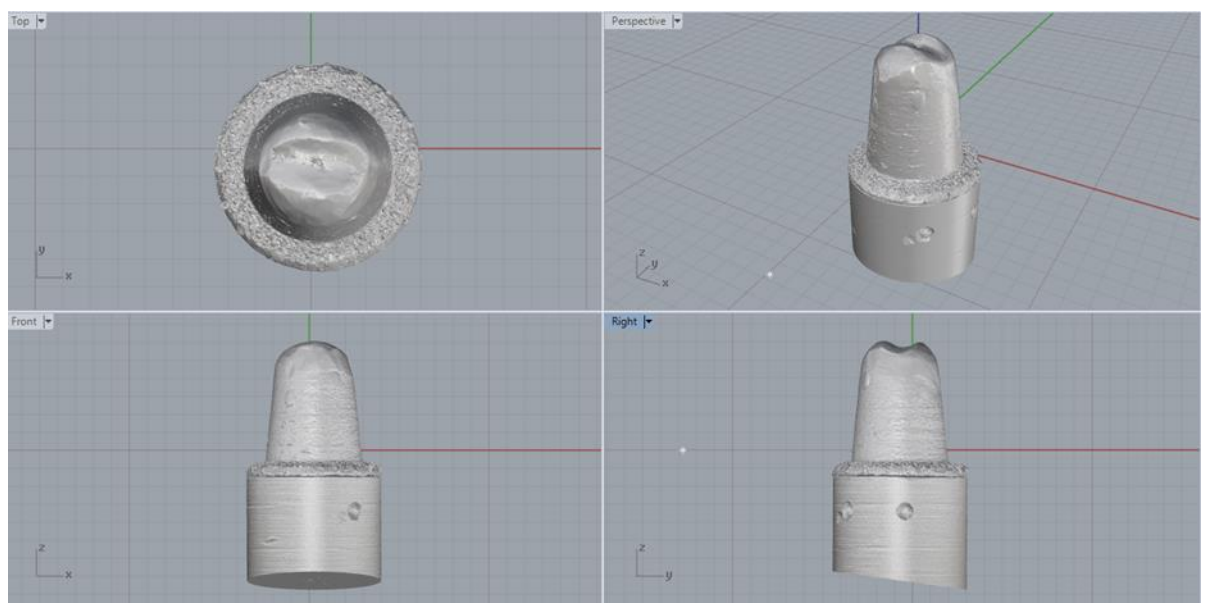


Figure 21 Aligned master model and LS1 in Rhino 5

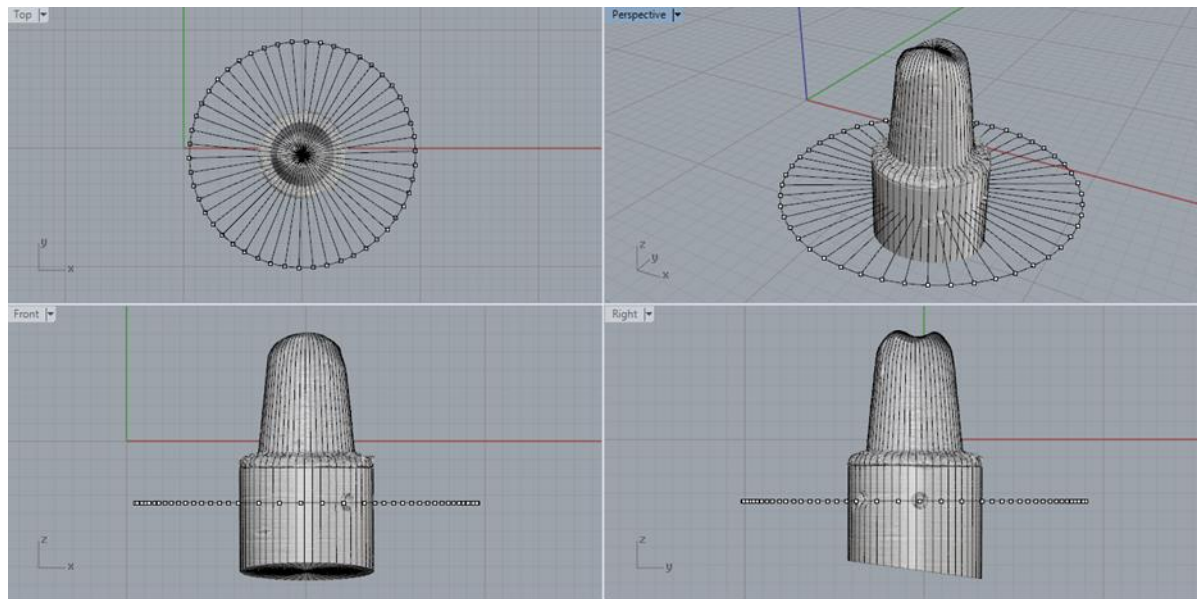


Figure 22 Fifty vertical radial cross sections in equidistance

The reference points used for measurements:

- Marginal adaptation was measured under **Vertical Marginal Height** which is distance of margin preparation to coping in 90 degrees (Figure 23, A) and **Absolute Marginal Adaptation** which is the distance measured from the marginal edge of the coping to the marginal edge of the master model preparation (Figure 23, B) defined similarly to Holmes (49).
- The **Axio-Margin Distance** is the distance from the outer surface of the model to the internal surface of the coping at the mid-junction between prepared margins and the axial wall of the model (Figure 23, C)
- The **Axial Distance** was defined as the distance between the outer surface of the model and the internal surface of the coping at the mid-point of the axial height ($6.5/2=3.25\text{mm}$) (Figure 23, D).

- The **Occlusal Height** was defined as the distance between the outer surface of the model to the internal surface of the coping at junction of the axial wall and the occlusal surface of the model (Figure 23, E).

In total 250 measurements were performed for a single coping. Measurements were analysed in SPSS (Version 21, IBM, New York, USA).

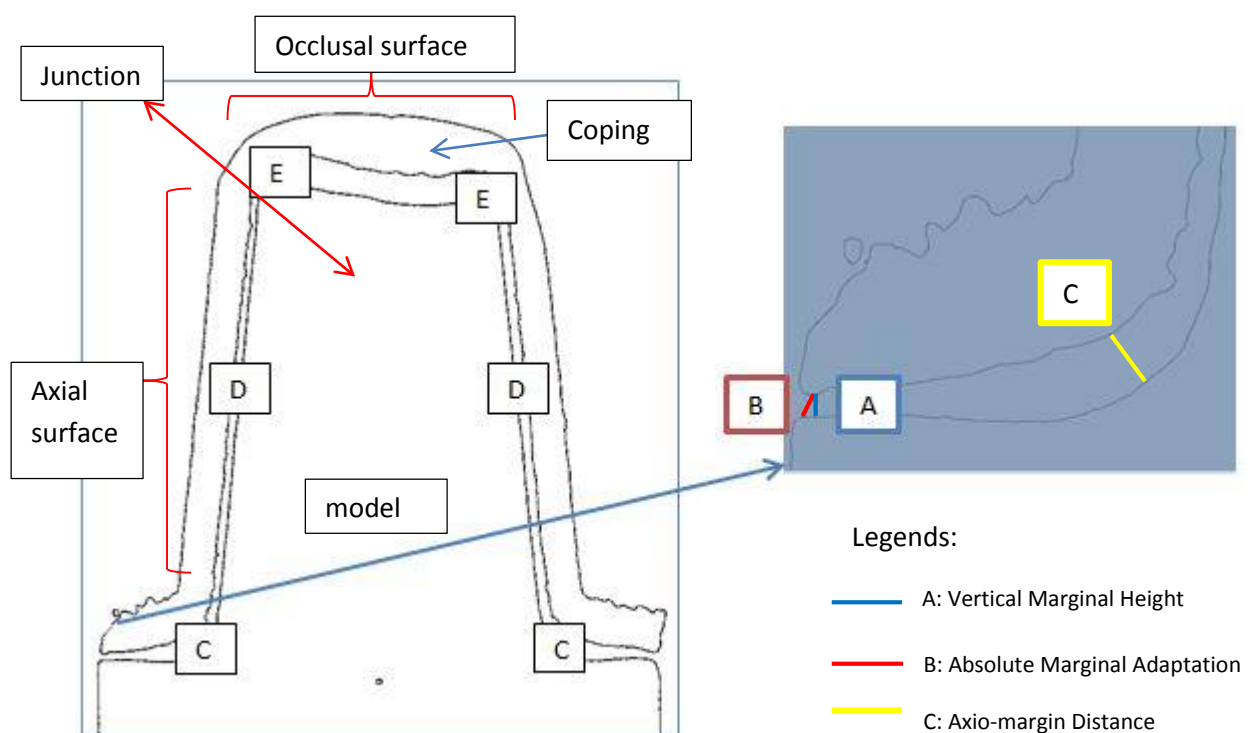


Figure 23 Cross sectional view of aligned 3D models. A: Vertical Marginal Height, B: Absolute Marginal Adaptation, C: Axio-margin Distance, D: Axial Distance, E: Occlusal Height

3.1.3 Validation of Methods

The validity of the measurement protocol relies heavily on the performance of the main measurement appliance which in this case is the micro-CT.

3.1.3.1 Repeatability of measurements

To test repeatability of data gained from the micro-CT, five standardised scans were made on one single coping. The procedure was performed on a laser sintered coping and given the name (LS1). A power source of 155keV with a current of 30 μ A was used and 3600 equal slices of projections were made per scan. Each scan was repeated under room temperature of 20°C. VG Studios (Version 2.2, Volume Graphics GmbH, Heidelberg, Germany) to create five virtual models.

The original CAD file (STL file created with Incise, Renishaw, UK) (Section 3.1.1.1) was imported into VG Studios. A surface-to-surface comparison was then performed on each of the models to the CAD separately. Each time, the CAD was assigned as the Nominal data and the micro-CT scanned models were assigned as the Actual data in the VG Studio software.

In addition, another surface-to-surface comparison was performed on the different scans retrieved from LS1. The following comparisons were made: Scan 1 to Scan 2, Scan 1 to Scan 3, Scan 1 to Scan 4 and Scan 1 to Scan 5. The results were in the form of colour deviation maps of distances between the surfaces of the investigated scans.

3.1.3.2 Accuracy of measurement

The accuracy of measurement was tested with aid of the NPL Freeform. The NPL Freeform is a model with known measurements supplied by the National Physical

Laboratory (NPL). Micro-CT scans of the high-grade aluminium standard model (Uncalibrated Standard NPL-WP-037) also known as the National Physical Laboratory-Freeform Reference Artefact (Figure 24) was then performed (SEAM, WIT). It utilized 140kV of voltage with a current of 70 μ A to suit the size and material used for this investigation. As a result 3000 projections were fabricated with a voxel resolution of 33.28 μ m. A virtual voxel model of the standards model was then created by the VG Studios software. The original CAD file of the standard reference was then imported into VG Studios and superimpositions and a comparison was performed.

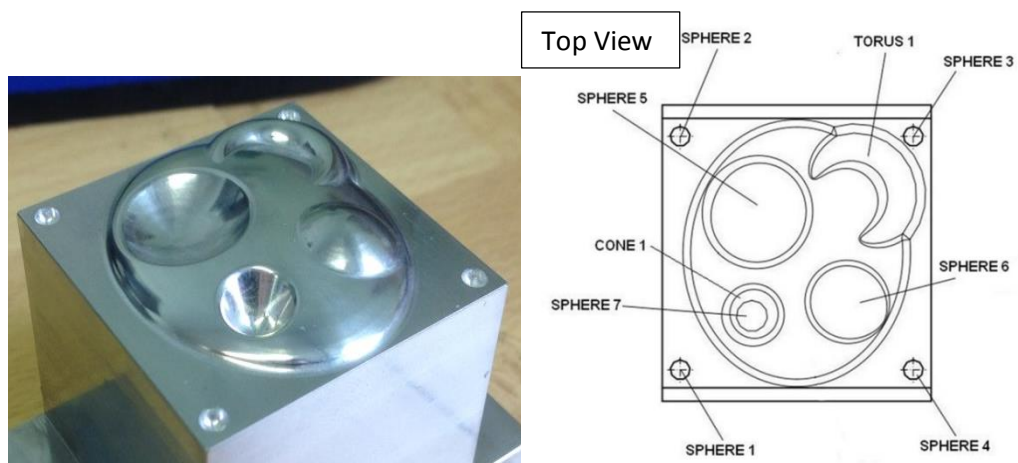


Figure 24 NPL Freeform Reference Standard (Uncalibrated Standard NPL-WP-037)

The uncertainty of the standard reference being built according to NPL was within 0.02mm. Hence any values outside the uncertainty value would be judged as a deviation from the nominal. The exact parameters of the reference are displayed in Table 21 (Appendix). Table 21 consists of x, y and z coordinates of the centre of features involved in testing.

In addition, the scanned standard reference was exported as an STL file to GOM Inspect. Superimpositions were again applied with the CAD of the reference model being imported accordingly. A surface comparison was then performed and localised surface mapping at designated features (Spheres, Cone and Torus) between NPL scan and the STEP file were investigated.

3.1.3.3 Effect of Software on measurements

3.1.3.3.1 GOM inspect vs VG studios for colour deviation maps

Both GOM inspect (freeware) and VG studios (micro-CT software) software was capable of displaying deviations of the fabricated copings to their CAD in the form of three dimension colour maps. In both cases, the CAD data and the coping data are in the form of STL files and are superimposed to give the colour deviation maps. It was of interest to see if there was any effect of the software in both the display of the colour deviation maps.

For this reason, a superimposition was carried out in both pieces of software after importing the relevant files (CAD data and coping data) in STL format. The colour deviation scales for the resultant qualitative maps were adjusted to the same range ($\pm 100\mu\text{m}$). The same colour effects set was also applied so that the resultant superimposition images could be qualitatively compared. The qualitative results are then displayed (Figure 43).

3.1.3.3.2 Rhino 5 vs VG studios for volume computation

The method for volume computation of the surface models (STL files) using GOM Inspect analysis was shown earlier (Section 3.1.2.1). VG Studios is however also capable of computing volume. It was of interest to compare the results of volume computation for our STL files using the two pieces of software. Upon successful scanning in micro-CT, VG Studios gives the option of selecting the model scanned and displaying a properties tab where volume and other information of the model can be extracted (Figure 25). The volume computation from the Rhino and VG Studios were recorded for repeated LS1 scans (see 3.1.3.1) and analysed (Kruskal-Wallis Test and Median Test) in SPSS version 21 (Version 21, IBM, New York, USA). All results were reported as Median Value of High Resolution Volume (Rhino), Micro-CT reported volume (VG Studios) in Figure 44.

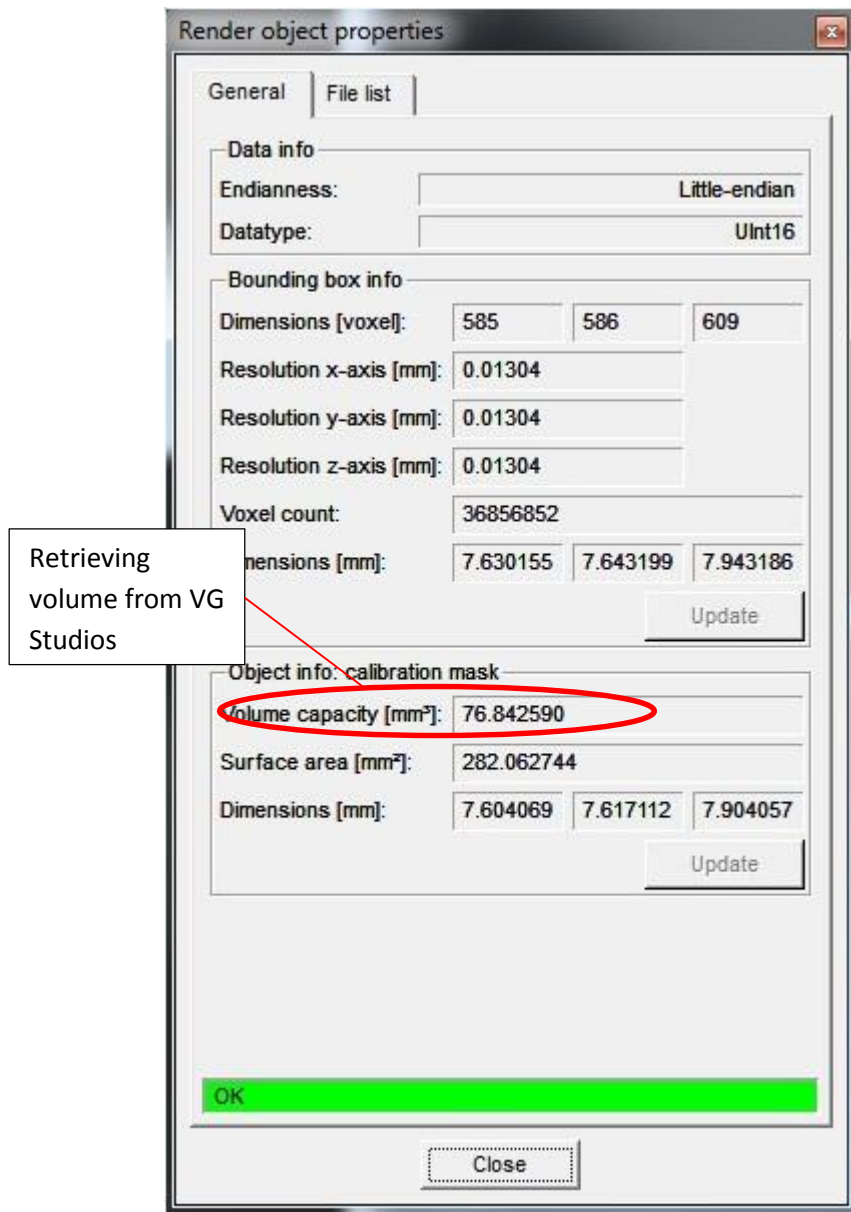


Figure 25 Example of Properties table in VG Studios

3.1.3.4 Effect of Resolution on volume measurements

The scanning point density of the CAD (created in the Renishaw Incise software) and of the micro-CT scans of the copings is quite different. This can be shown by importing the relevant STL files in the GOM inspect software and selecting the properties tab to display the number of points (Figure 26). The CAD has 30584 data

points while the LS scanned copings have 208236 data points. In order to identify the effect of this difference in resolution to the volume measurements, the following process was followed:

The density of data points of the micro-CT scanned copings needs to be reduced to a number that resembles the number of data points for the original CAD.

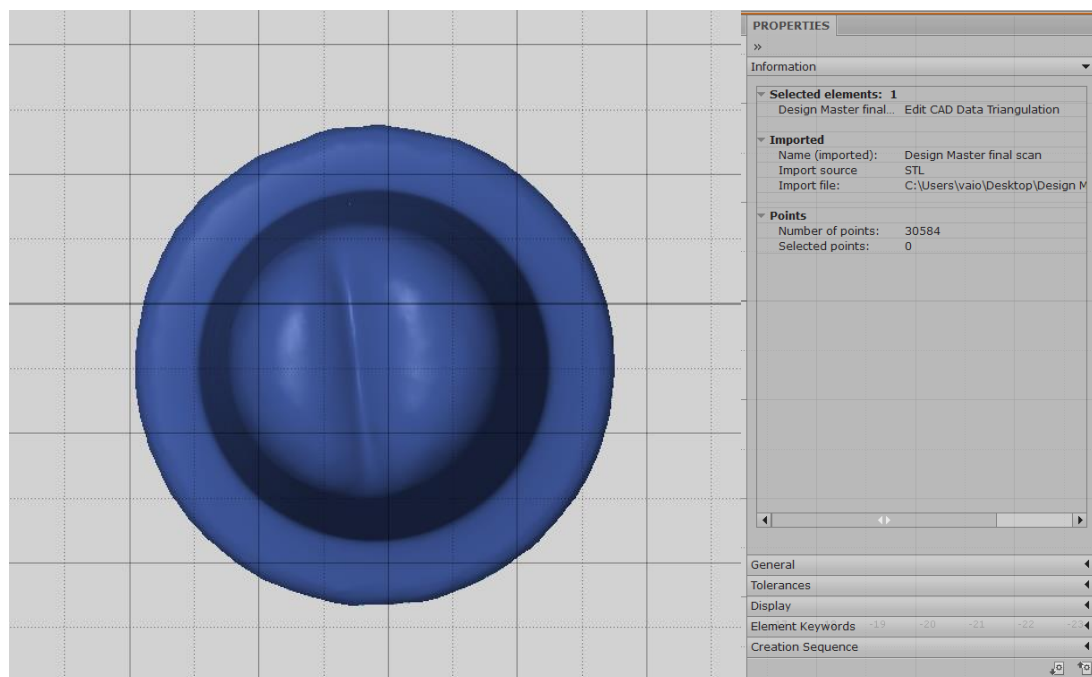


Figure 26 Density points of CAD

This was achieved by first selecting the fabricated coping (LS1) followed by the tab “Operations”. “Mesh” was then selected in the drop box followed by selection of the tab “Thin” (Figure 27). A box will then appear as Thin Mesh. The ‘Number of points’ tab was checked and edited by typing the number 30600 in the box provided (Figure 27b). The procedure was completed by selecting “Apply”.

This procedure was then replicated to all LS1 copings scanned five times (LS1 Scan1 –Scan 5). The density points of the scanned copings were automatically reduced to a number close to the CAD's density points, however each coping was verified by looking at the properties information again and recorded to ensure closeness of data points.

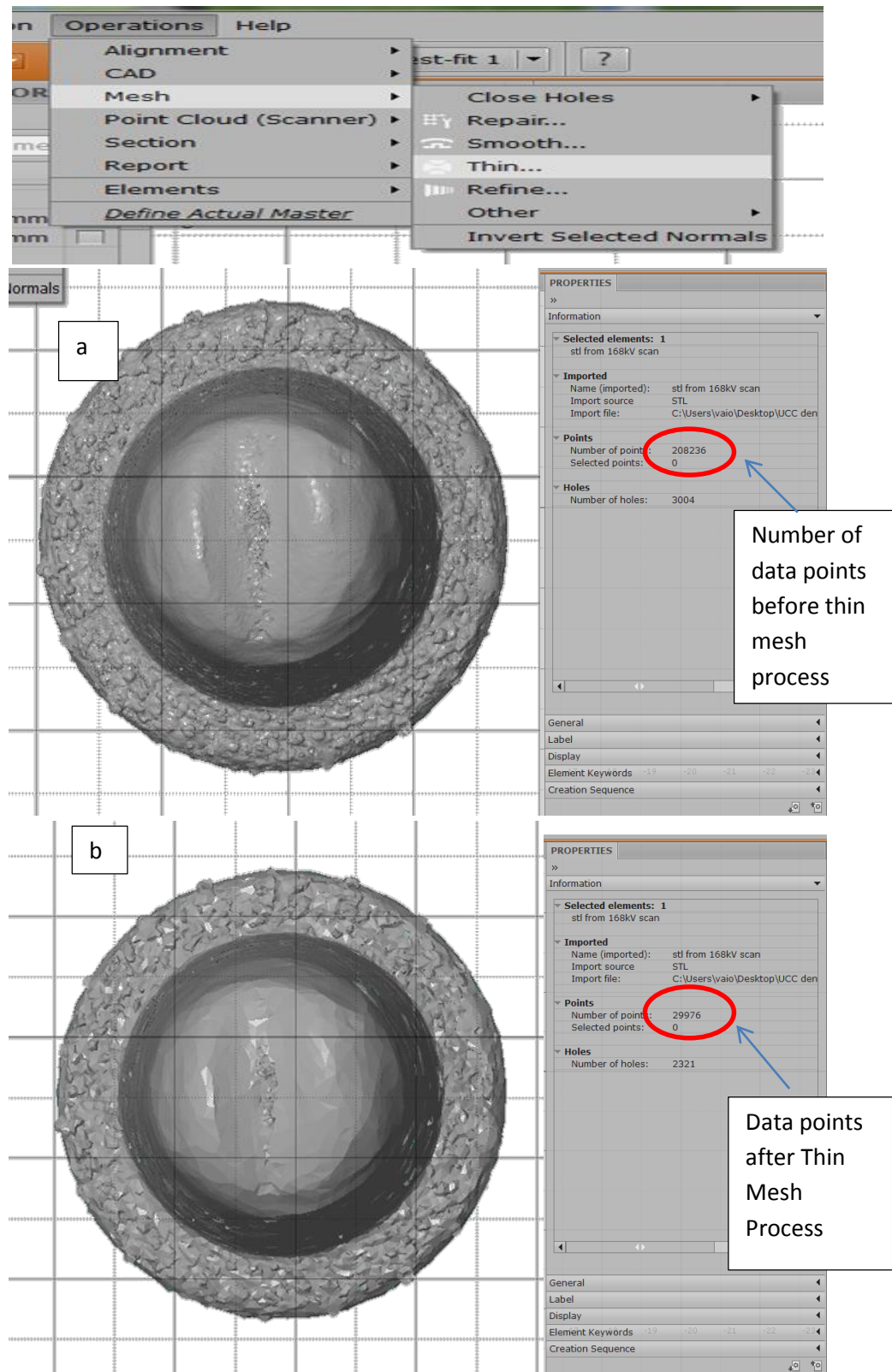


Figure 27 (a) Method to Thin Mesh of coping (LS1), (b) Changed points of (LS1) after Thin Mesh Procedure

The volume was then recorded using the relevant process in the Rhino software (See 3.1.3.1) both before and after the Thin Mesh procedure was applied. The results were displayed as “High Resolution” (Before procedure) and “Low Resolution” (After procedure) (Figure 44). All results were recorded and analysed in SPSS (Version 21, IBM, New York, USA). Median Volume was reported and an independent Kruskal Wallis Test and Median Test were then performed to compare whether Software and Resolution difference had any effect on Results of Volume.

3.2 Method Development Results

3.2.1 Processed Trial Model

The brass model created can be seen in (Figure 28-29).

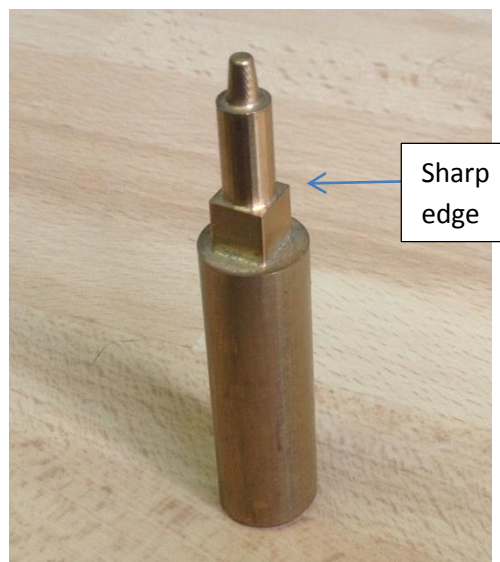


Figure 28 Raw material (brass) turned and milled to fabricate the trial model



Figure 29 Finalized trial model after removal of sharp edges and separation from raw material (brass)

3.2.1.1 Trial CAD

The original CAD created in Incise (InciseCAD version 2.5.0.140, Renishaw, UK) is presented in Figure 30. Design was made to be in cobalt chrome material. A surface model in STL format may then be created and exported to other softwares for use (Figure 31). The exported files of the CAD were identical to the original CAD created in Incise, Renishaw.

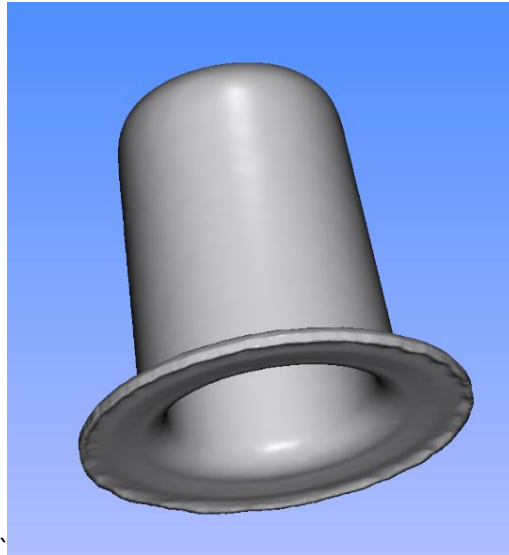


Figure 30 Original CAD created in InciseCAD, Renishaw

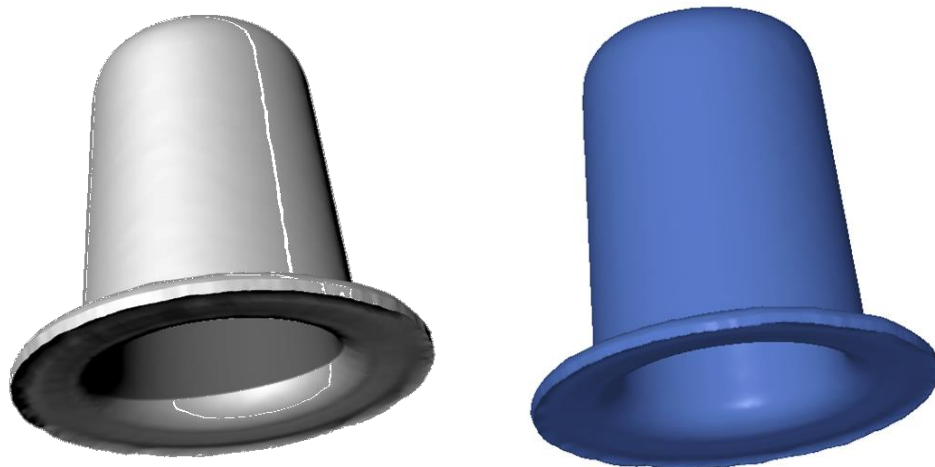


Figure 31 Imported STL formatted CAD in Rhino 5 (Rendered in Grey) and GOM Inspect (Blue)

3.2.2 Preliminary Study

Four surface models were created out of the four scans made with the Incise contact scanner. The first scan was the brass model scan, the second was the die spacer scan, the third was the waxed-up model scan and the fourth was the fitted cast trial model scan (Figure 32).

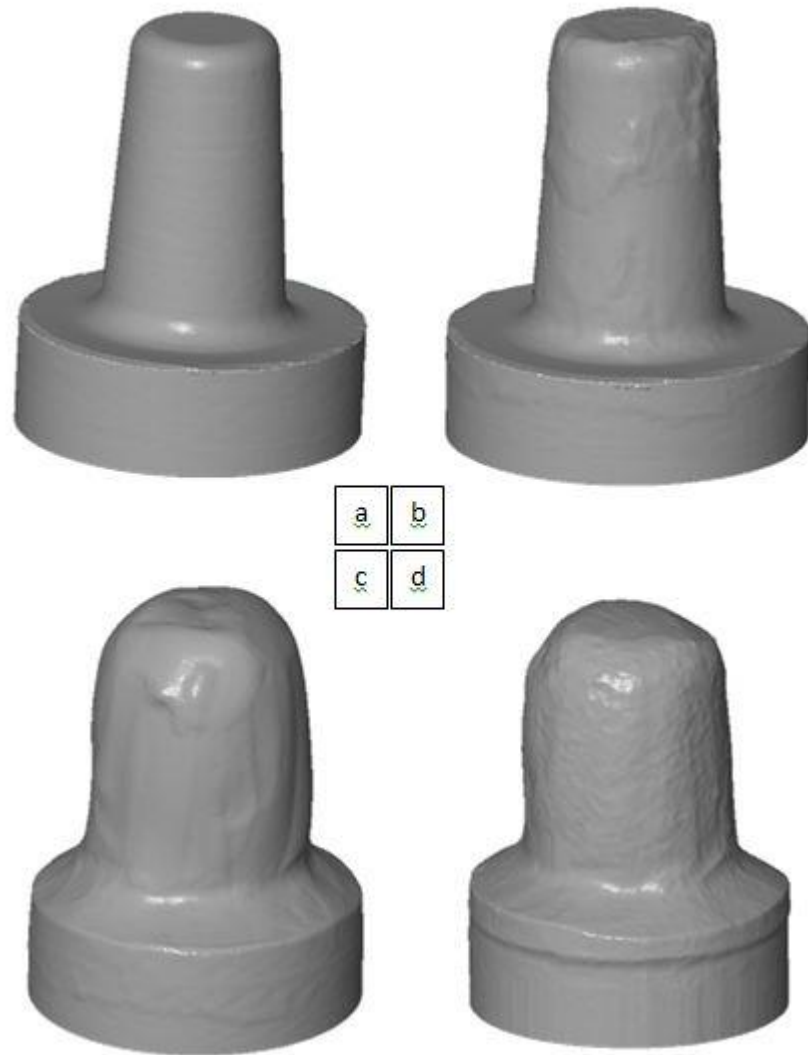


Figure 32 Exported surface models of the Incise scans a: brass model scan, b: spacer scan, c: waxed-up model scan, d: fitted cast coping scan

3.2.2.1 Methods and Proof of Concept – deviation and volume computation

3.2.2.1.1 Fabricated Virtual Models and Original Coping

The 3-dimensional voxel model created by VG Studio 2.2 (Heidelberg, Germany) from the scanned image of the cast coping with micro-CT is displayed next to actual photos (Figure 33-34).



Figure 33 Voxel model created by VG Studios (Bottom view and Side view)



Figure 34 Cast Fabricated Trial Coping (Bottom view and Side View)

This voxel model was then exported as a surface model to other analysing software (Figure 33). Then, four surface models in STL format utilising different parameters were created. The created digital models meant that micro-CT can be utilised in

different settings for penetration of copings using this design, thickness, size and material to create the surface model for analyses.

3.2.2.1.2 Deviation Calculation

The mean distances of Figure 35 show the overall deviation of coping to CAD. Results also show the minimum and maximum distance and the standard deviations. Associated legends may be utilised to qualitatively see localised deviations of three dimensional models.

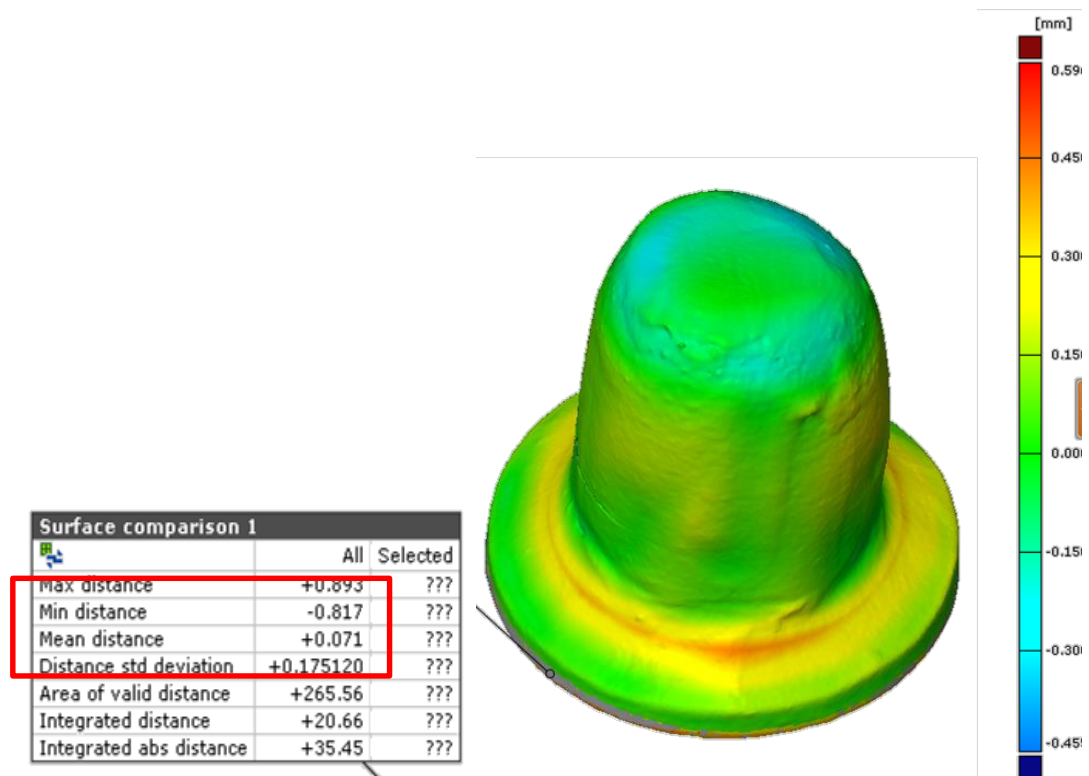


Figure 35 Overall Results table of deviations

3.2.2.1.3 CAD and Trial Model Volume

Volume results are shown in Table 1. The software was successful in giving a measurement of the 3D objects volume that could be used for comparisons.

Table 1 Volume computation in Rhino 5

Selected Mesh	Volume (mm3)
CAD	56.59 +/- 1e-08
Trial Coping	76.82 +/-1e-08

Table 1 showing the mesh of CAD and trial coping showing differences in terms of volume

3.2.2.2 Methods and Proof of Concept – Internal Fit

3.2.2.2.1 2-Dimensional calculation of Internal Fit

Table 2 shows the results on internal fit at the localised areas of LS1 calculated via 2D calculation. Results show increased distances of adaptation at the angles of the design 226(21) μm and 212(62) μm respectively. The highest adaptation of coping to the model was at the vertical marginal height (46(25) μm).

Table 2 Localised fit of fabricated coping (LS1)

Localised Fit	Mean(SD), n=50
Vertical Marginal Height	46(25)
Absolute Marginal Adaptation	64(28)
Axio-Margin distance	226(21)
Axial Distance	116(36)
Occlusal Height	212(62)

3.2.3 Validation of Methods

3.2.3.1 Measurement Repeatability of CAD to CAM Deviations utilising micro-CT

Figure 36 displays the different views of the 3D colour mapping of the deviations of LS1 to its CAD. Most of the copings were within 40 μm of the original design. However, increased deviations up to 0.2mm were found localised to outer surface at the axio-

occlusal angles of the coping and the occlusal side of the outer surface of coping at prepared margins (Figure 36A, B). Internal view showed negative deviations of about 200µm at the occlusal surface (Figure 36F).

Figure 37 shows the distribution of the deviations according to the surfaces involved. Most of the surfaces of the LS1 have little or no deviations from CAD however the histogram shows that positive and negative deviations of more than 100µm do exist. This suggests that alteration by trimming is needed to fit the coping to the master model or before proceeding for application of porcelain on the occlusal surface of the coping.

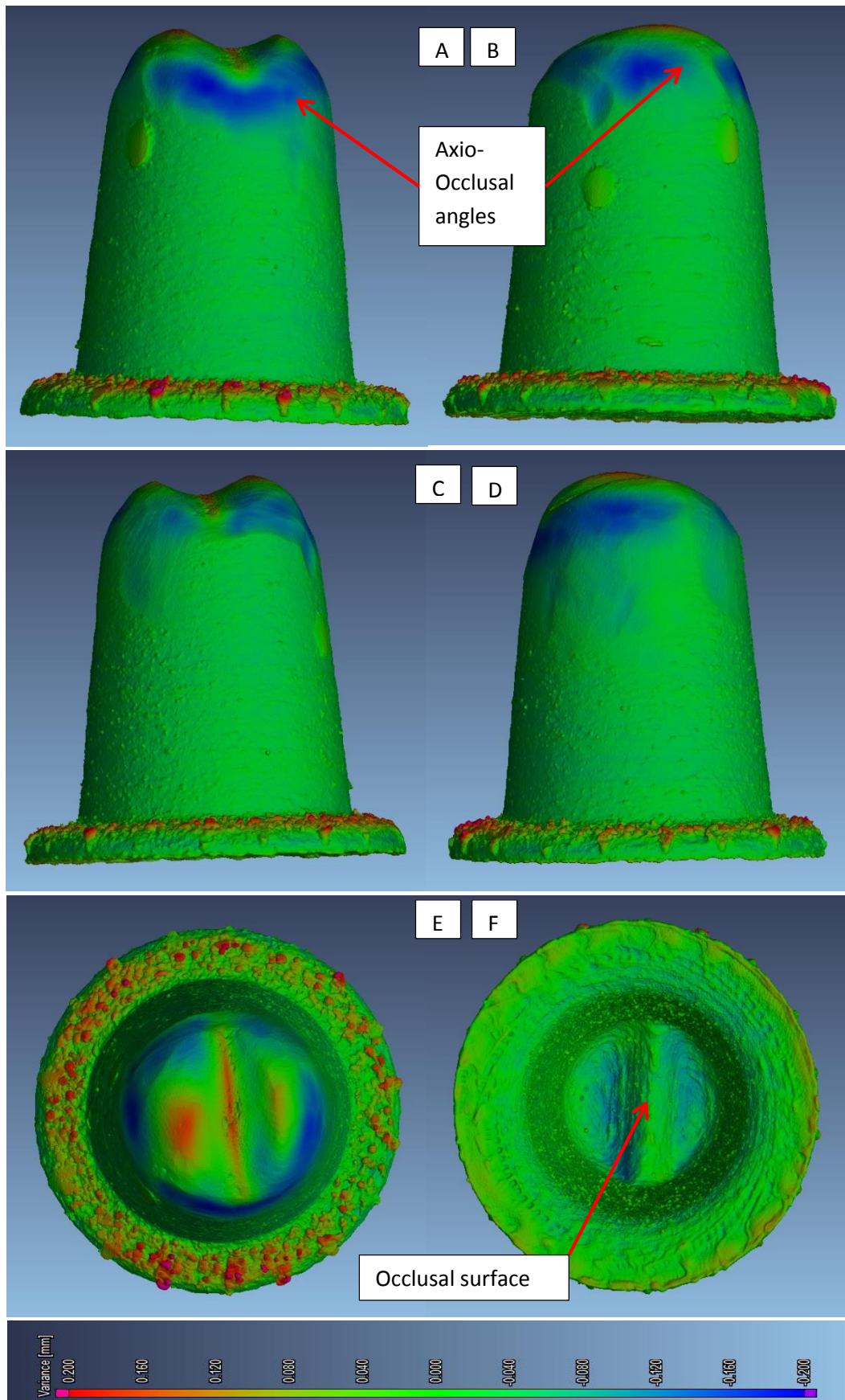


Figure 36 3D view of surface comparisons, A: side view, B: 90 degree view, C: 180 degree view, D: 270 degree view, E: Top view, F: Bottom view

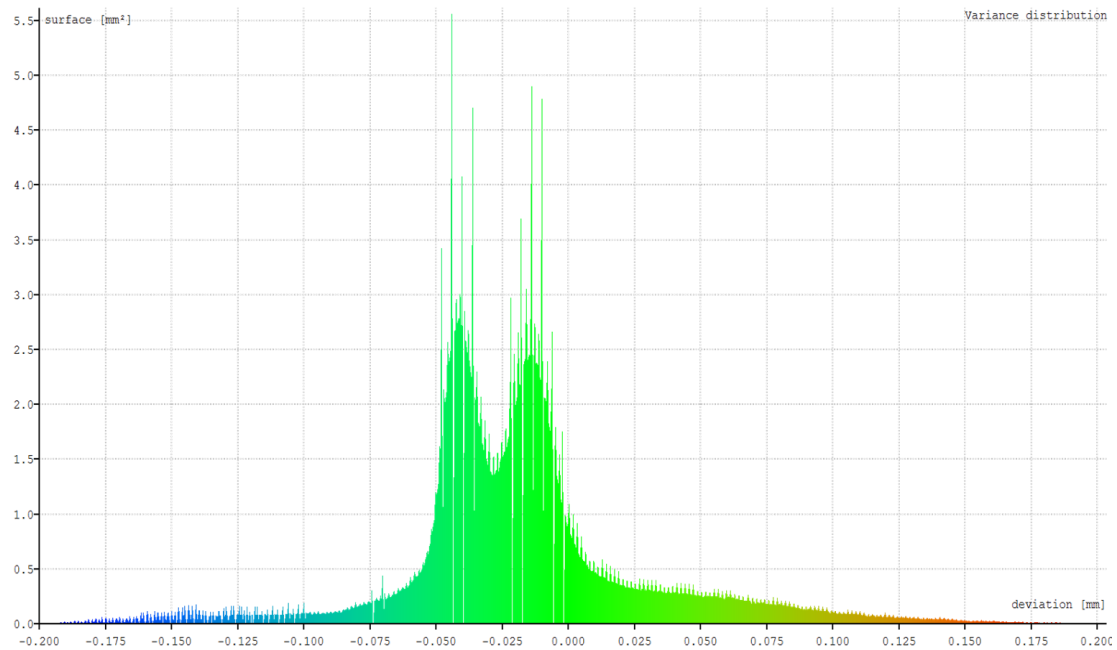


Figure 37 Variance distribution of deviations of surfaces micro-CT scanned LS1 to the CAD

3.2.3.1.1 LS1 (Actual) Versus CAD (Nominal) Comparison

Five histograms coming from five different scans of the same coping (LS1) vs CAD were available. The five histograms of LS1 copings display a similar pattern (Figure 38). The highest surface area involved in the surface mapping was 6 mm² (Figure 38), however deviations within that surface area value were minimal. The scans revealed that the most of the data (displayed in green) had deviations ($\pm 50\mu m$) when compared to the CAD. Scans also revealed slight differences for Scan 2 and 3 to the rest in which observed surface area (<1.5mm²) had a deviation of -25 μm while the rest had surface area (>2mm²) for that value. In total LS1 coping had 272mm² surface area but most surface areas showed deviations close to 0 (Shown in two peaks of histogram presented). The two peaks displayed in all histograms of LS1 scans ranged from 2.5-3mm² surface area having 40 μm and 10 μm negative deviations when

compared to the CAD. This shows that the superimpositions were close to CAD and only minimal localised areas were highly deviated.

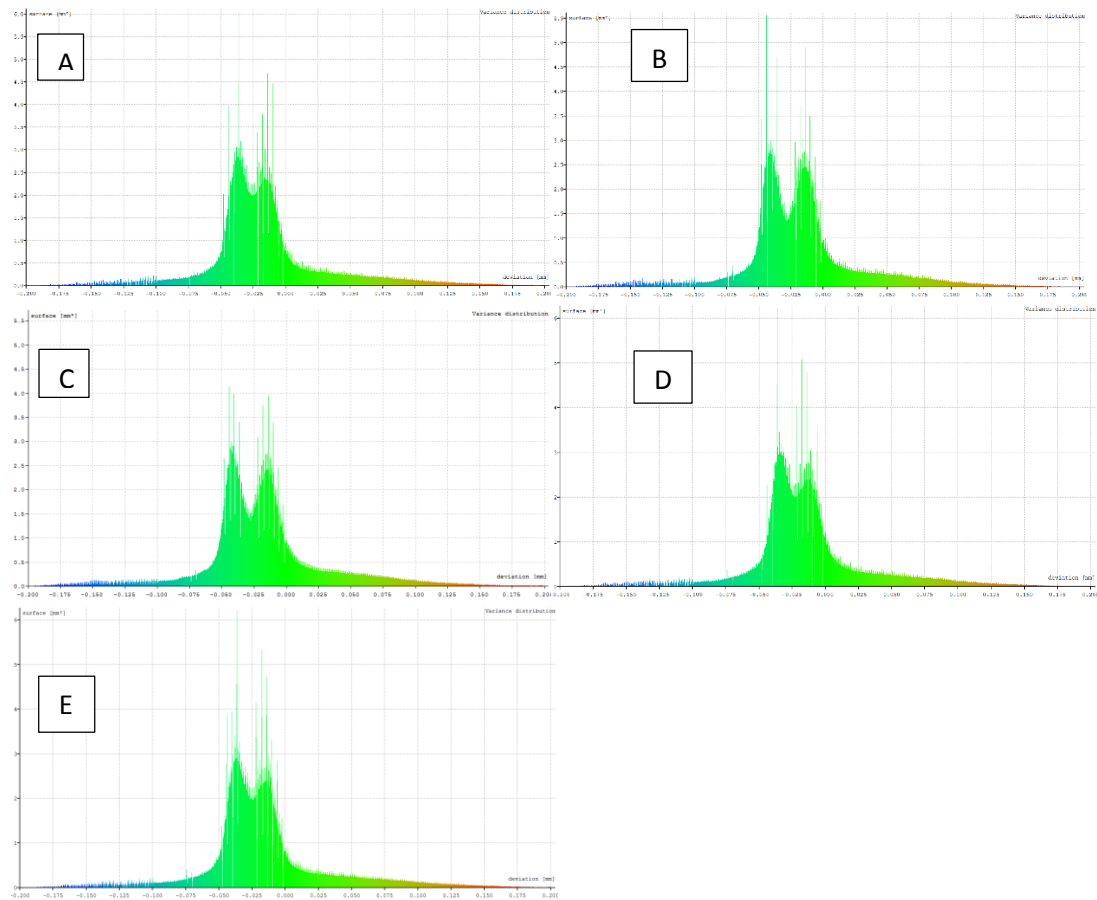


Figure 38 Relationship of surface to deviation of LS1-CAD comparison A: Scan 1, B: Scan 2, C: Scan 3, D: Scan 4, E: Scan 5

3.2.3.1.2 Multiple Scans of LS (Actual) Vs Scan 1 (Nominal)

Figure 40 shows the superimposed outcome of two micro-CT scans of the same coping (LS1), Scan 2 Vs Scan 1. Figure 39 reveals that superimposed scans (1&2) were similar or close ($\pm 4\mu m$). Maximum deviation between scans were $\pm 10\mu m$, however the amount of surface area within that value is minimal.



Figure 39 Surface mapping legend of Actual/nominal comparison of Multiple Scans of LS1 Vs Scan 1 (LS1)

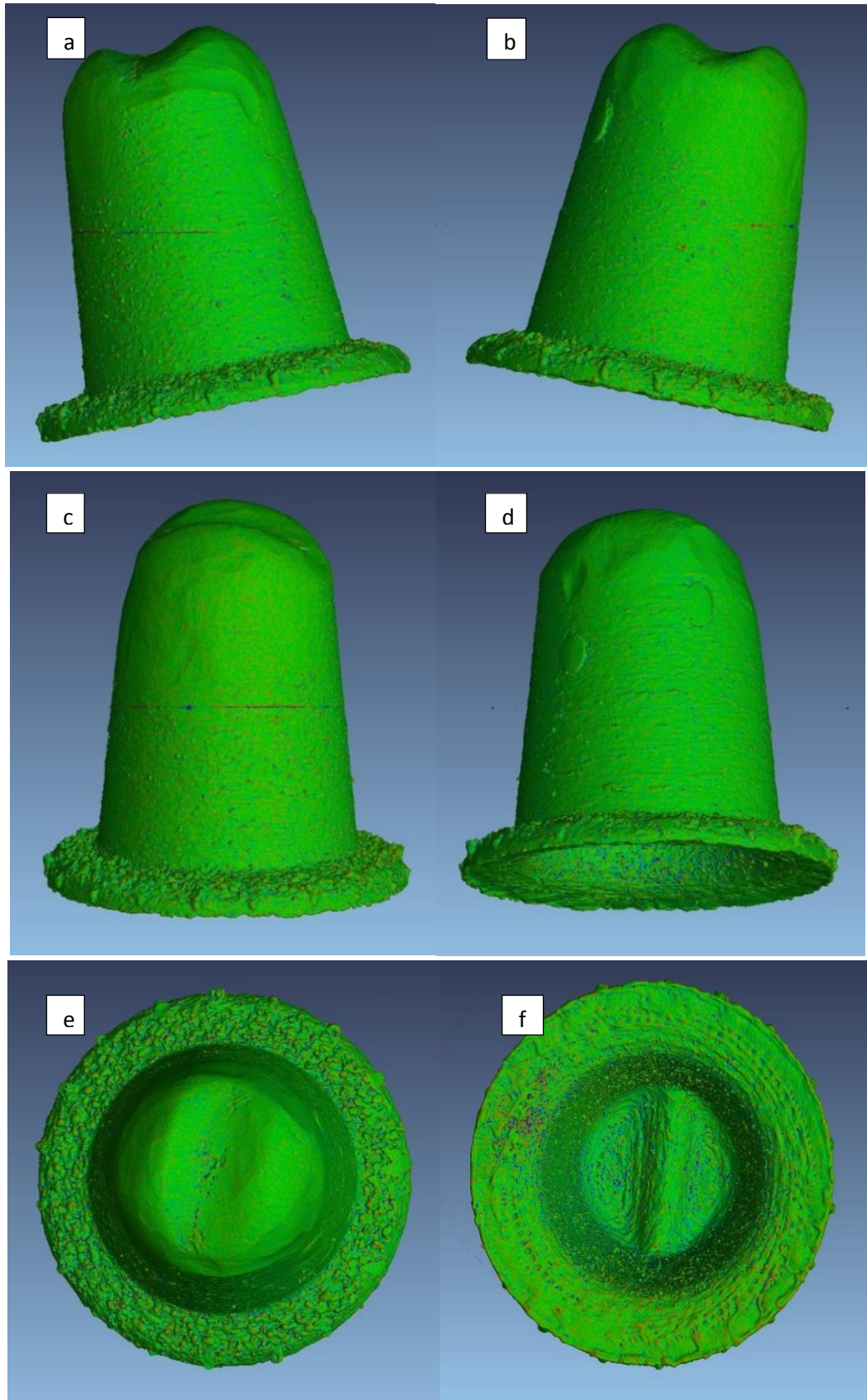


Figure 40 Colour deviation mapping of Scan 2 to Scan 1 a: side view, b: view rotated 72°, c: view rotated 144°, d: view rotated 216°, e: top view, f: bottom view

A histogram (Figure 41) comparing Scan 2 to Scan 1 showed similar results in terms of variance distribution. Scan 3, Scan 4 and Scan 5 were identical and displayed the same centre (1.25mm^2 showing no deviation) and had the same bell shaped curve.

The maximum deviation between the compared surfaces was $\pm 10\mu\text{m}$.

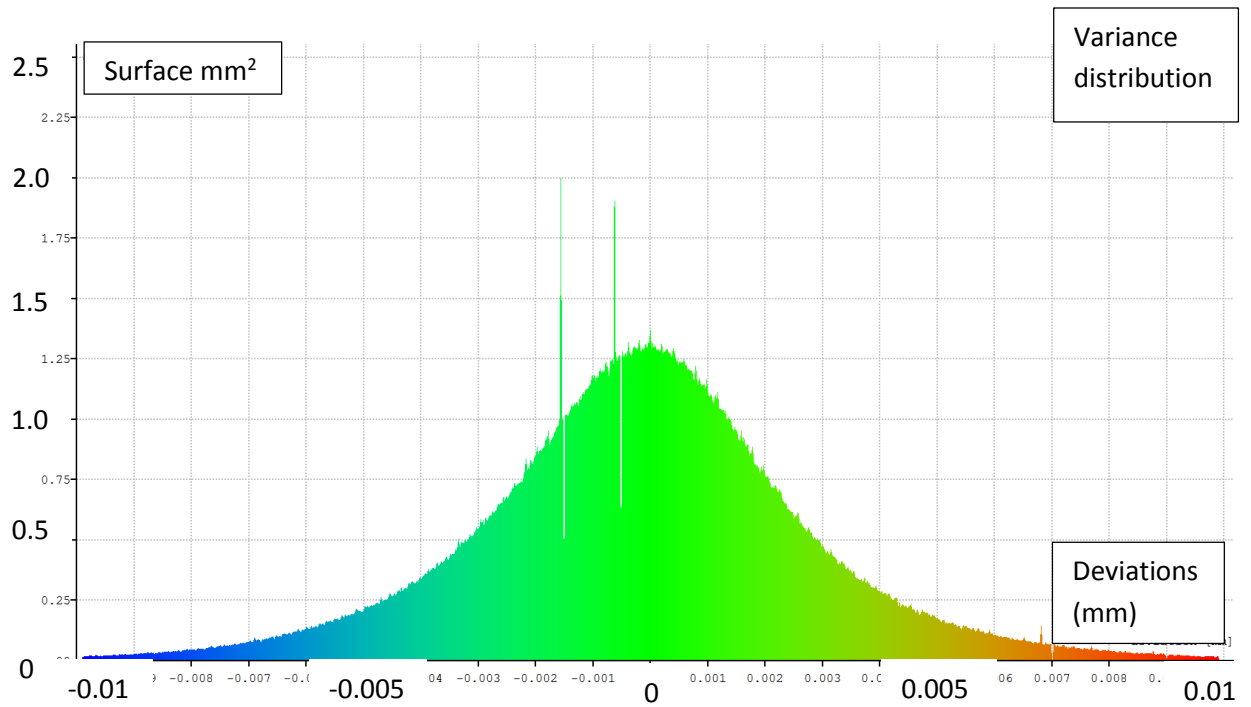


Figure 41 Variance distribution of deviations of surfaces micro-CT scanned LS1 (Scan 2) to Scan 1

3.2.3.2 Measurement Accuracy

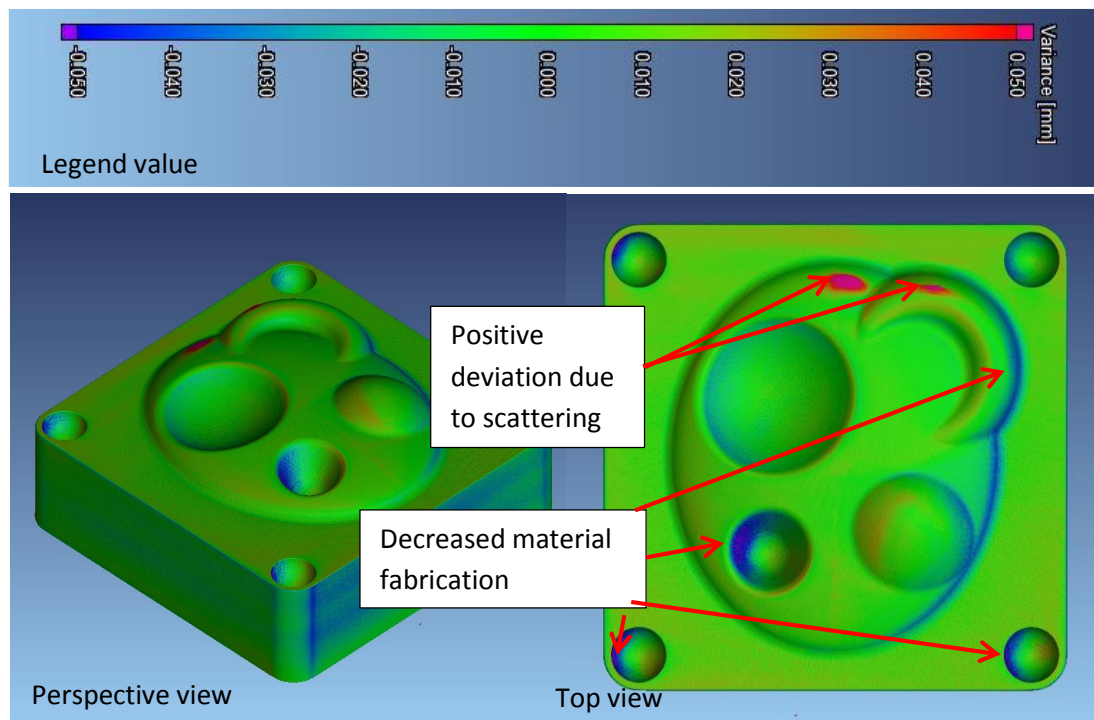


Figure 42 Surface to surface comparison of NPL artefact with original NPL STEP file

The results of the comparison of the scanned NPL reference model and its CAD File is shown in Figure 42. The actual nominal comparisons of the NPL reference model with the CAD file of the NPL model showed that most data were similar (Figure 42). Two areas on the top aspect of the model showed excess deposition of material between Torus 1 and Sphere 5 (Figure 42, Top View). Decrease in material appear to emerge at almost all spheres (Sphere 1, 2, 3, 4, 6 and 7) and cone (Figure 42, Top view).

Overall quantitative data showed that surface mapping was 53 μ m smaller than the overall dimensions of NPL CAD-Design. Results were summarized in

Table 3. The two excess material fabrication on the surface top of the NPL model were 48 and 68 μm respectively.

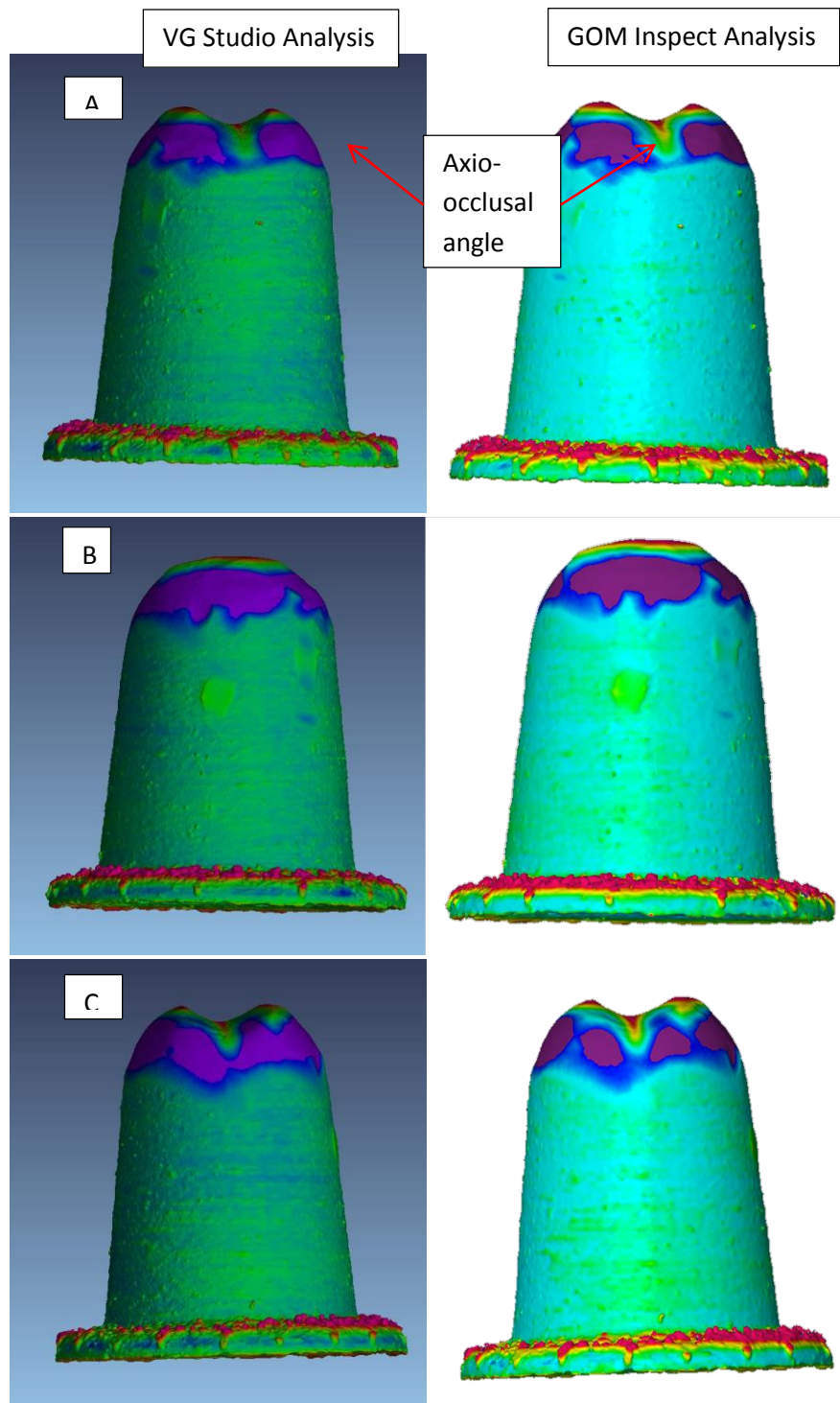
Table 3 NPL freeform accuracy to CAD data results

Feature	Surface mapping deviation
Sphere 1	-7 μm
Sphere 2	-1 μm
Sphere 3	0 μm
Sphere 4	-4 μm
Sphere 5	0 μm
Sphere 6	-1 μm
Sphere 7	-8 μm
Cone 1	-8 μm
Torus 1	4 μm

Table 3 showing small differences of distances between the NPL freeform to results of the CAD with highest and lowest data to be 8 μm and 0 μm respectively

3.2.3.3 Effect of Software on Surface Mapping and Volume Measurement

Figure 43 shows the deviations of a laser sintered coping (LS1) to the CAD. Two pieces of software were compared 1) VG Studio and 2) GOM Inspect performing the same analysis. Both software showed increased deviation (>100 μm) on the occlusal external surface and external surface of margins of coping (Figure 43E). The external surface of axio-occlusal angle (Figure 43A,B,C,D,E) of coping and internal surface (Figure 42F) of occlusal coping however exhibit less depositions of material (>100 μm smaller than design). This may well lead to a tight fit of the coping to the master model. Small or no deviations on the rest of the surfaces of the coping show similarities to the coping CAD.



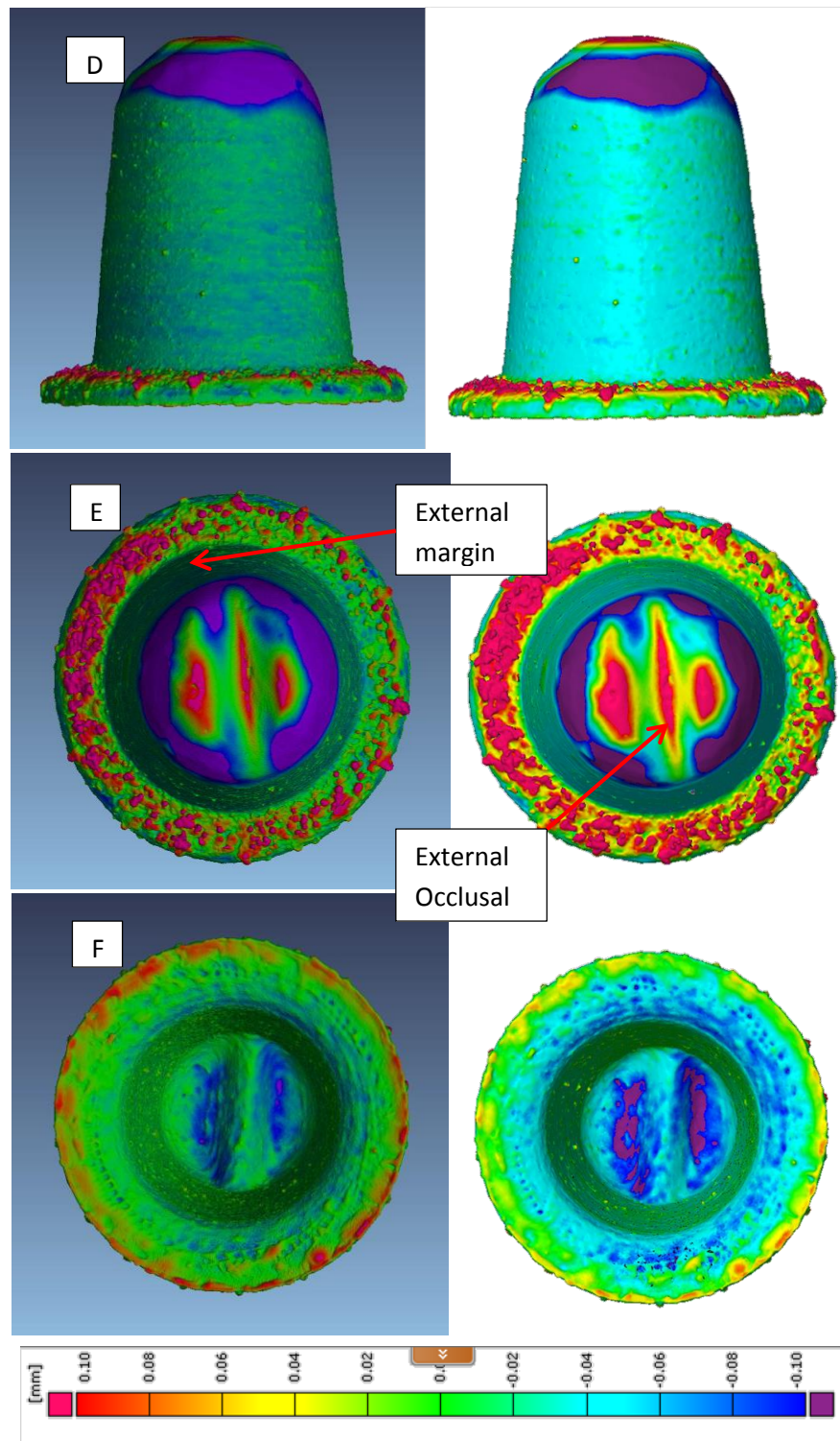


Figure 43 Comparison of Surface Analysis of LS1 using VG Studios and GOM Inspect. A: Side View, B: 90 degree view, C: 180 degree view, D: 270 degree view, E: Top view, F: Bottom view

Qualitatively, no significant visual difference was seen between VG Studios and GOM Inspect of surface mapping analysis of the same coping. Quantitatively, Figure 44 shows a box plot of volumes of Laser Sintered Copings with different pieces of software and Resolution used for analysis. Median values of volume analysis for High Resolution (Rhino), micro-CT (VG-Studios) and Low Resolution (Rhino) were 52.48mm^3 , 52.99mm^3 and 52.47mm^3 , respectively. A Kruskal-Wallis Test revealed no significant difference ($p>0.05$) between the three groups ($n=5$).

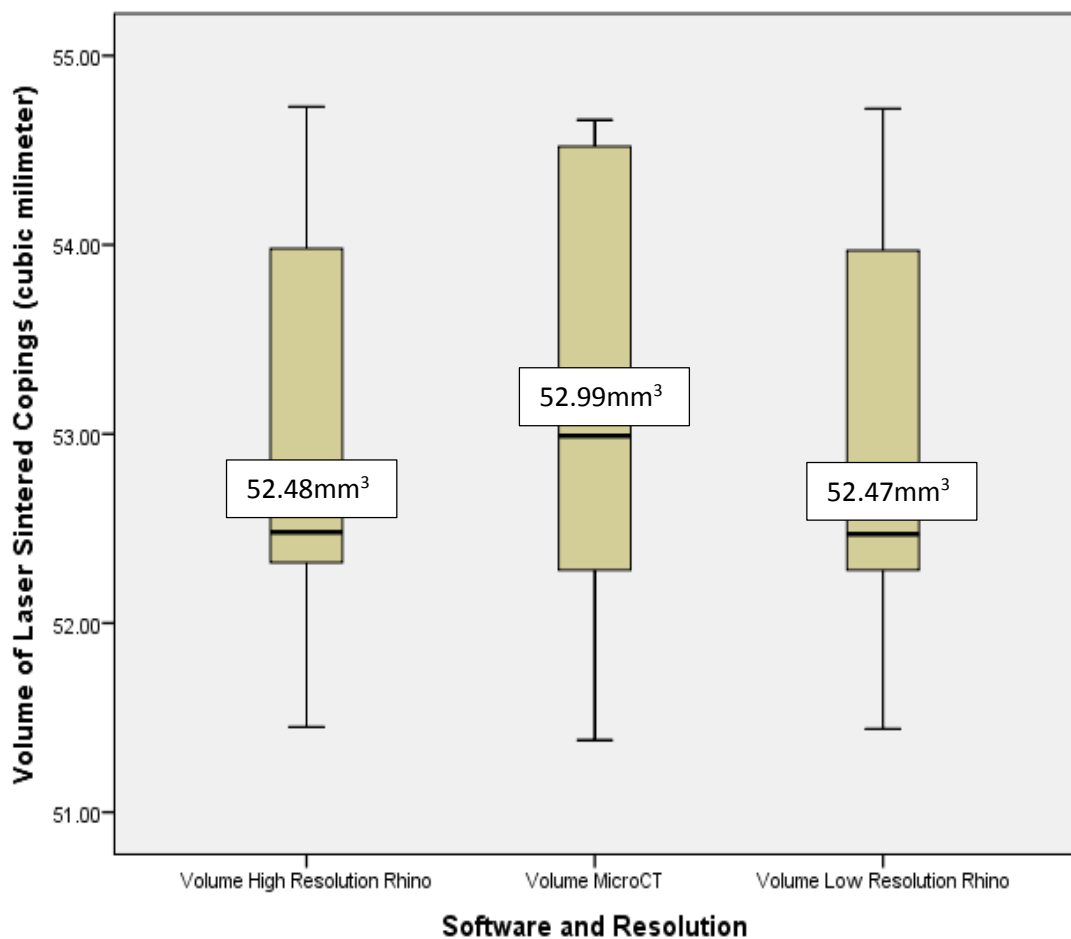


Figure 44 Box Plot of Median Volume with Confidence Interval readings of Laser Sintered Copings Via multiple Analysis Software and Resolutions

3.2.3.4 Effect of Resolution

No significant difference ($p>0.05$) was found when comparison (Kruskal Wallis Test) of the volume of LS copings using High Resolution (Rhino) and Low Resolution (Rhino) point density was performed (Figure 44).

3.3 Discussion of Method Development

Completion of method development meant that a definite method could be applied to the project. The main objective was to see whether there was any difference of fabricated coping to the CAD. Power sources of the micro-CT allowed penetration of x-ray through the coping, a minimum of 100kV and a maximum of 160kV was sufficient to perform this with no differences in quality throughout.

However, the use of a high power source burnt the filament of the micro-CT thus a 155kV power source was chosen. A higher power would also mean that more data points could be gathered from each resulting scan which would mean higher resolution, however development of the method to perform the deviation and volume computation show that there was no significance difference from analysis of two different sets of high resolution and low resolution analysis.

Internal fit was measured by the 2-Dimensional method of computing internal fit as the method could be performed digitally. This meant that the method was simple and easily performed and may be used for further investigations of Internal Fit

measurements between dental restorations. Accuracy and repeatability of the method measurements performed were also demonstrated.

3.3.1 Repeatability of Method

Five scans on a single coping were performed to test repeatability of the findings. No significant difference was found on volume results of the five scans. This demonstrated that the results could be repeated. Qualitatively, surface mapping showed similar display. When Scan 1 was used as nominal data for comparison of Scan 2-Scan 5, results were accurate to within 10 μm . Histogram of the Comparison of Scan2-Scan 5 revealed a similar bell shaped pattern (Figure 38 and Figure 41). This shows that the measurement method can be repeated.

3.3.2 Accuracy of method

The NPL Freeform was explained earlier in Section 3.1.3.2. The micro-CT scan of the NPL freeform is shown in Figure 45. The features imprinted on the surface of the NPL Freeform (various semi - spheres, a torus and part of a cone) are specifically defined as parts of larger objects of known dimensions in a co-ordinate system. For example the large semi-sphere depicted in Figure 45, is part of a known sphere with a diameter of 21.25mm and a centre at x, y and z of 11.75, 24.25, 10 (Parameters supplied with the NPL STEP file). Table 21 gives the relevant defined parameters for the rest of the shapes.

As all these shapes are only parts of the defined known shapes, the dimensions of these parts are unknown at any given location on the NPL freeform surface. Therefore a simple point to point measurement anywhere within these shapes (Figure 46A) is not enough to determine the accuracy of our scanning as we have no known dimension to compare this to. In order to circumvent this problem, after importing the NPL freeform scan STL file in Rhino, a sphere was modelled (Figure 46B) that would fit the imprint in the cross section taken from the micro-CT scan. The resultant diameter of that sphere was measured as 21.33mm, slightly larger than the given 21.25mm.

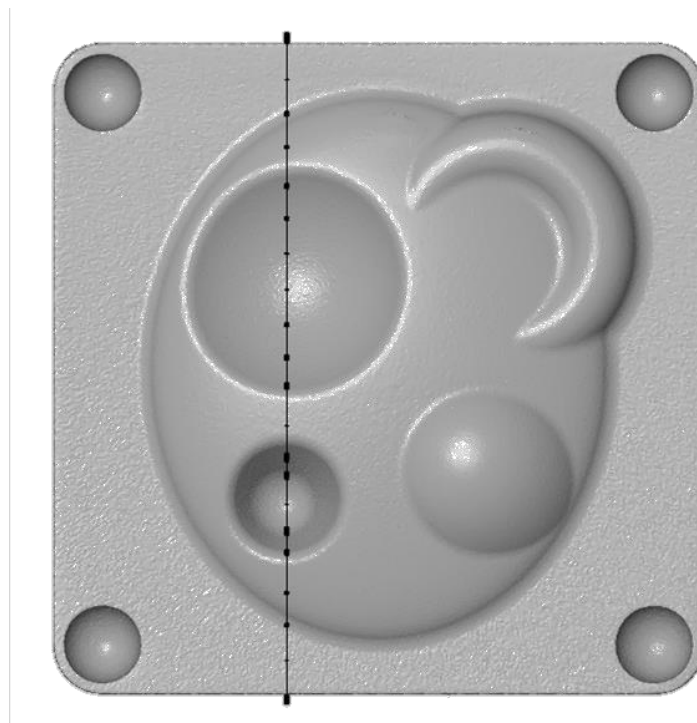


Figure 45 Cross section of micro-CT scanned NPL Freeform at Sphere 5 Region

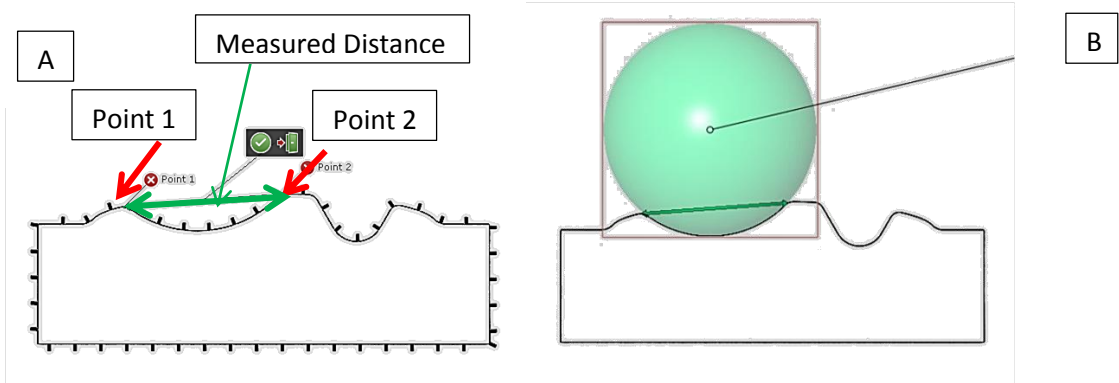


Figure 46A Point to point measurement of surface of Sphere 5, Figure 78B Sphere diameter construction on Sphere 5 region

Hence a surface mapping of the featured areas after superimposing the micro-CT scan and the NPL supplied STEP file of the NPL freeform, would give more insight on the measurement uncertainty (Figure 47). When this was performed, the result within that section was 0 (S.D 7) μm . This means that no deviations occurred on that particular selected section however a 7 μm standard deviation was evident. The manufacturer indicated that based on the manufacturing tolerance, the NPL freeform is expected to have an accuracy uncertainty of 0.02 mm/ 20 μm (Manufacturer data). This means that our method of measuring with micro-CT would be accurate and acceptable if data was lower than 20 μm . This particular section has 7 μm standard deviation and therefore was well within these limits on the manufacturer uncertainty.

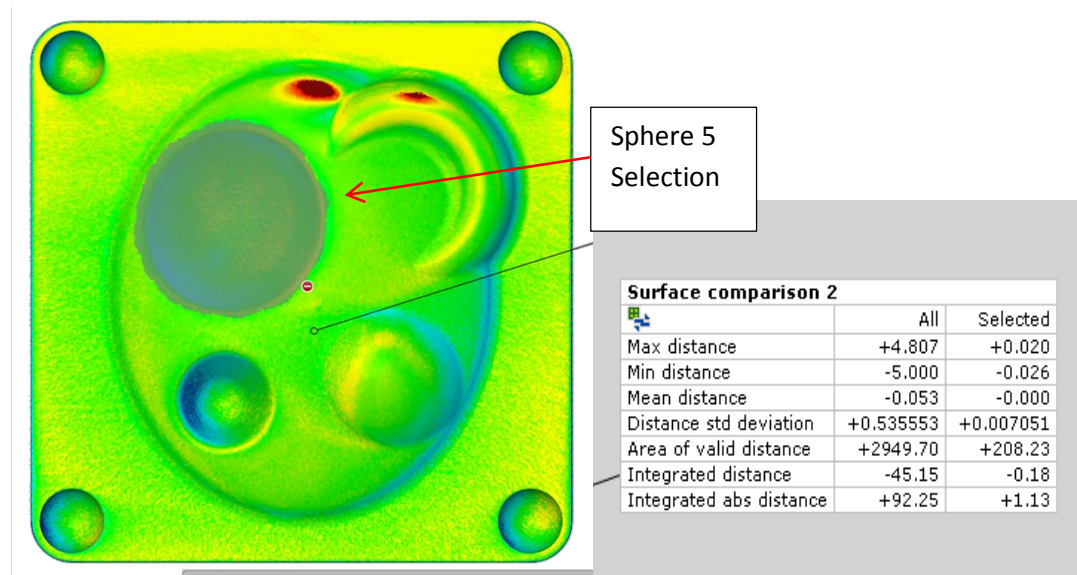


Figure 47 Surface mapping at Sphere 5 Region Selected

On the surface map of NPL freeform, the 3D model achieved close results to the CAD except at two areas on the top surface of the NPL model. These areas are probably due to noise and scattering effects of the micro-CT (77) and this should require further investigation. The overall data shows a -53 μ m difference, however this result is being affected by the two areas of noise and scatter (48 and 68 μ m).

The other featured area of results were below 8 μ m indicating an accurate representation of fabrication accuracy to its CAD-Design (STEP file). Nevertheless, the measurement method shows it was accurate if measurement was 8 μ m as the highest result of deviation from the NPL scan was retrieved (Table 3). Results were well within manufacturer tolerance of 20 μ m.

3.3.3 Analysis Software

As the design of the model was initially made by the Rhino 5, it seems logical to utilize the software for other purposes. The software also had the ability to compute volume. Hence volume readings were performed by this software (See 3.1.2.1.3). Reading was performed by a mathematical equation of a closed spline by calculation of amount of pixels used. Volume results conventionally can be made by measuring displacement of water (48). Measuring with a digital service is simpler and more reliable with predictable quality (85, 86).

Section 4

Definitive Method

4 Definitive Method

Figure 48 shows a flowchart of the definitive method of the present study. A methodology was to be implemented for comparison of CAD of a dental coping with the micro-CT scans of CAM fabricated coping in terms of accuracy. The developmental aspect of the method was described in Section 3. A definitive method was then determined from the results of the developmental aspect. The steps of the definitive method that were to be followed were:

- Firstly, a model of a prepared tooth was to be made (master model) and then digitised with a contact dental scanner (master model scan). A CAD of a dental coping that covers the prepared tooth master model was then to be created in a computer and stored as an STL file (CAD model) (Figure 48, Steps 1).
- A sample of five copings within each group of four CAM fabrication methods [Laser Sintered (LS), Milled CoCrMo (M-CoCrMo), 3-Axis milled zirconia (ZAx3) and 4-Axis milled zirconia (ZAx4)] was fabricated.
- The copings were then scanned with micro-CT creating a virtual 3D model of the fabricated restorations. The scans were then stored as STL file and represent the digitized fabricated CAM method (Figure 48, Step 2).
- The STL files of the CAD model and the CAM output were imported into software to measure volume (Figure 48, Step 3a).
- The CAM output and the CAD model files were superimposed to check dimensional accuracy (Figure 48, Step 3b). Deviations between the CAD and CAM output were displayed in the form of colour surface maps (Figure 48, Step 5a). In addition sectional results (Occlusal, axial and Cervical) of the

deviations of the copings from CAD were investigated (Figure 48, Step 4b). A more focussed result were then analysed at specific areas of interest (Figure 48, Step 5b). All deviations were then analysed.

- The CAM output scan and the master model scan were aligned to check fit (Figure 48, Step 3c). Internal fit measurement was attempted via 2D calculations (Figure 48, Step 5c).
- All results were analysed via IBM SPSS Version 21, (US) (Figure 48, Step 6).

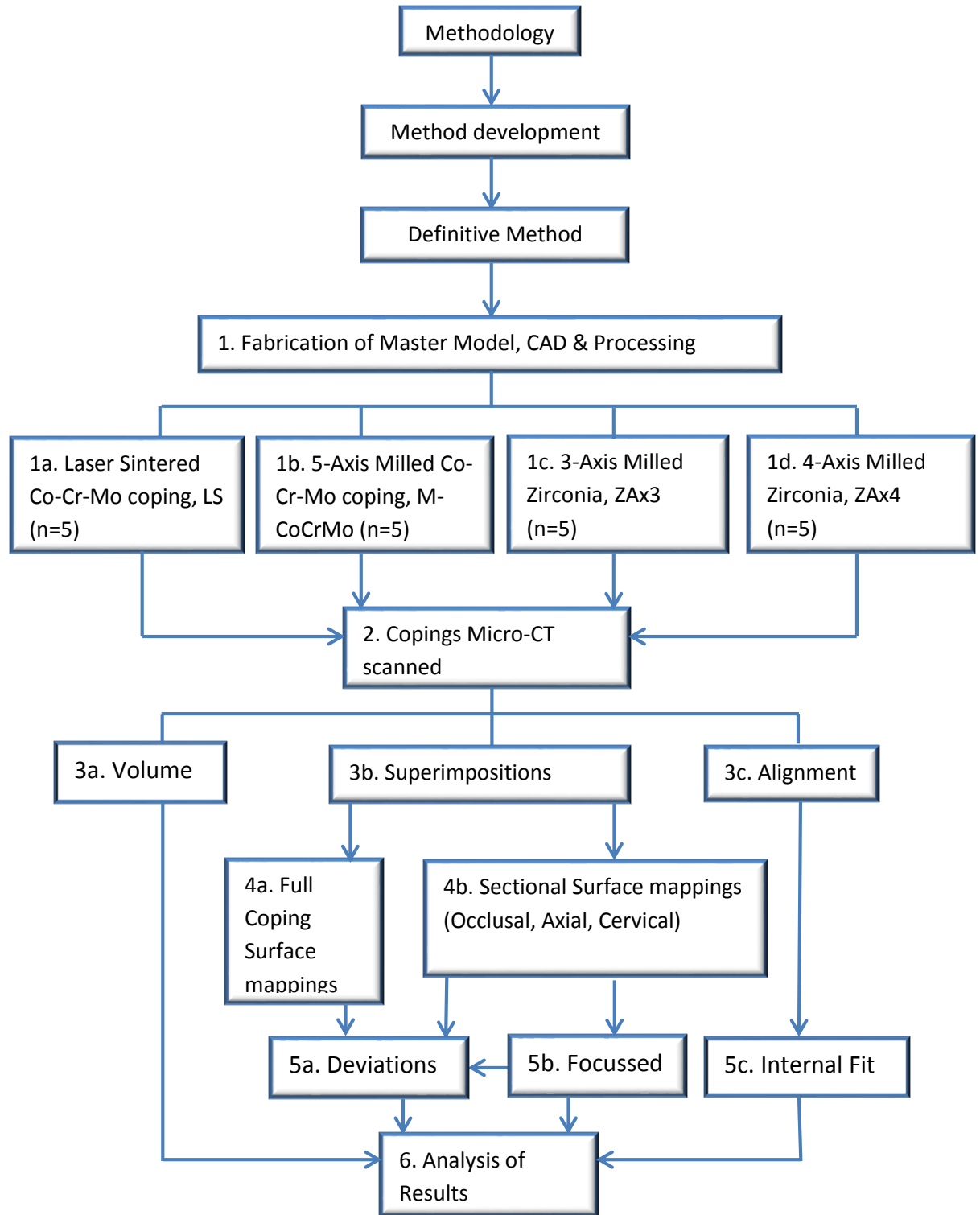


Figure 48 Flowchart of definitive method

4.1 Fabrication of Investigated Dental Copings

4.1.1 Master Model Design and Fabrication

The master model was fabricated as previously described (Section 3.1.1) in aluminium and is presented in Figure 49. A central groove was made manually with 1.2mm straight fissure bur with a depth of 0.6mm. Sharp angles were removed with a polishing bur. Three round marks serving as reference points were made using 1.2 mm round burs just below the margin line (Figure 49).

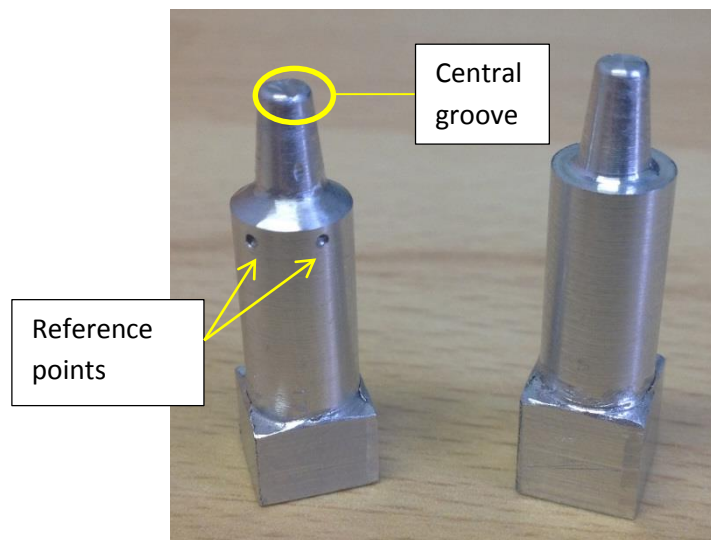


Figure 49 Fabricated Master Aluminium Model

4.1.2 Computer Aided Scans, Design and Processing

The master model was digitized using a contact scanner (Incise, Renishaw, UK). Design of the coping was performed by the Incise software. The following steps were performed.

1. The minimum thickness (0.3-0.5mm; data according to manufacturer) of the coping was determined (Figure 50).

2. Pre-cementation space was set at medium thickness (0.07-0.1mm; data according to manufacturer) (Figure 50).
3. LaserPFM (CoCrMo) was chosen for material of coping (Figure 50).
4. Manufacturer's instructions were carefully followed for scanning procedures. The master model was held in place by a die holder (Figure 51A) and the 1mm Stylus tip (A-5003-7785, Renishaw, UK) was utilised for scanning (Figure 51B).
5. Digitizing strategy included scanning from lowest point (below reference points, Figure 51A) to highest point (just above the model in centre, Figure 51B).
6. The scan was done in continuous spiral motions until completion (Figure 52a). Upon completion of digitization, a 3D image is created on the Incise software (Figure 52b).
7. Image is then brought to CAD function and margin line is determined (Figure 52b). Coping design is then automatically generated according to the pre-determined settings (Figure 52c).
8. The master design is then exported as STL file for use later on (Figure 52d).
The design is then sent to central manufacturing to be fabricated.

Define Framework

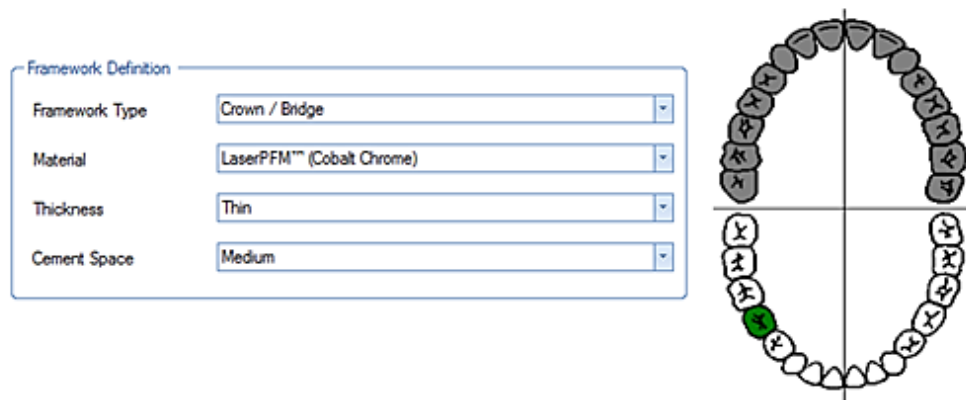


Figure 50 Framework Settings Determination

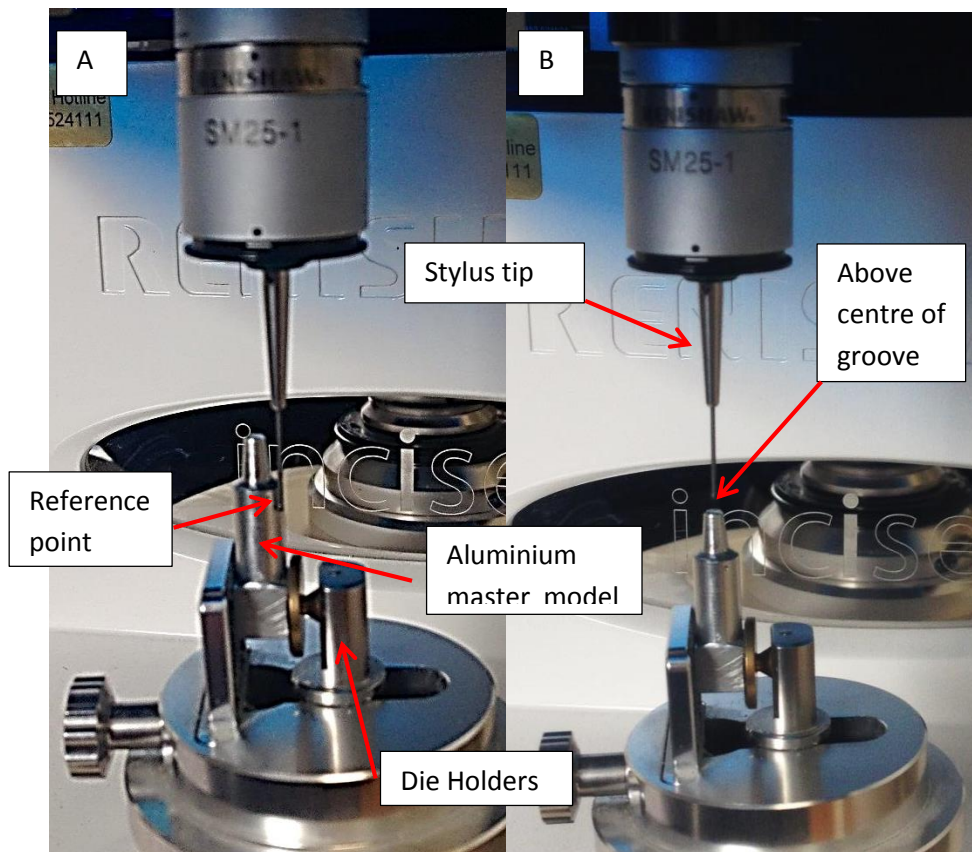


Figure 51 Selection of lowest (A) and highest point (B) of scan using the Incise scanner

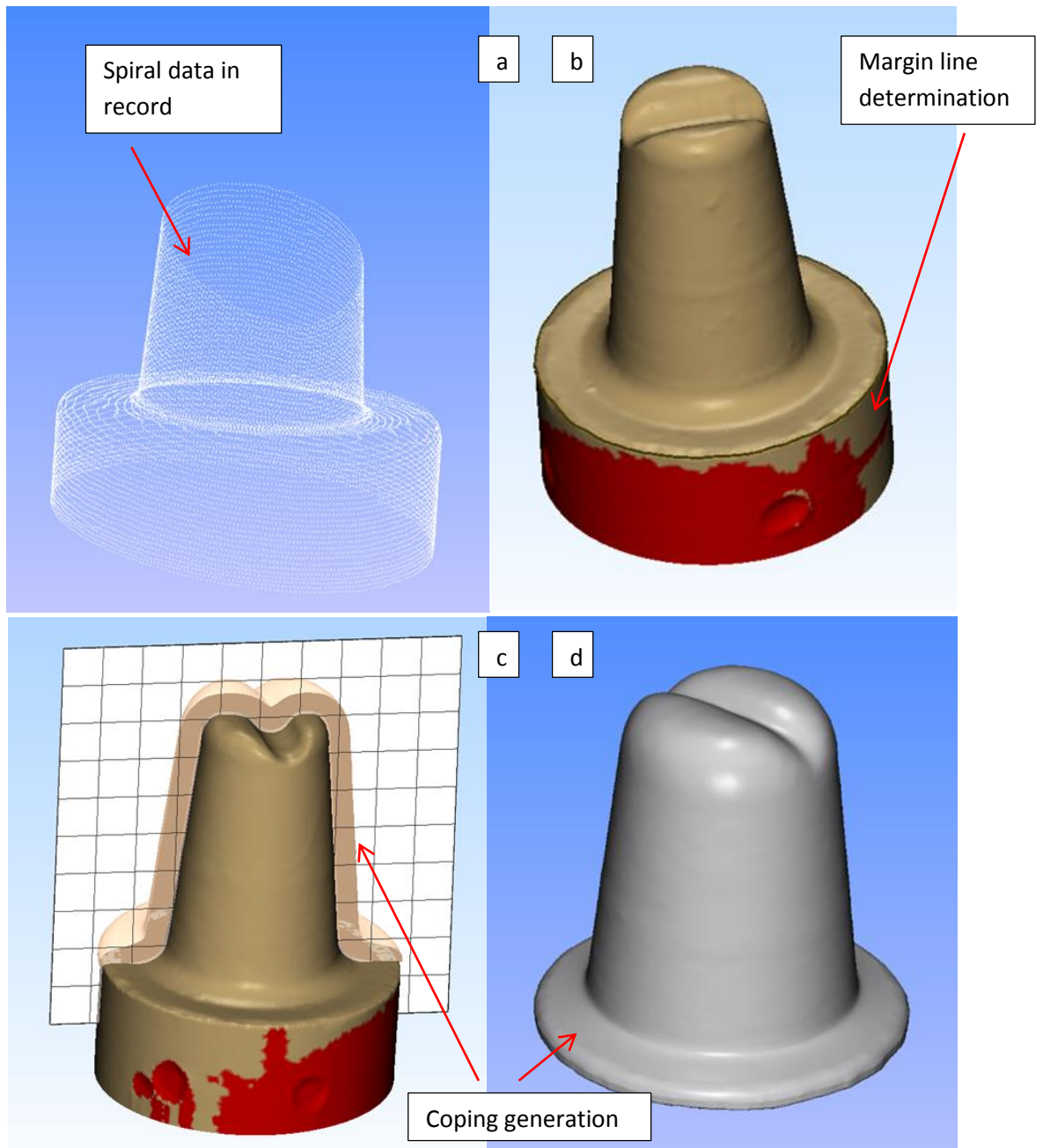


Figure 52 CAD Master Design, a: collection of spiral CAD data, b: simulation of model and margin line determination, c: Generation of coping, d: Completed surface model of coping (ready for export)

4.1.2.1 Laser melting Cobalt Chrome Molybdenum

CAD data was imported into the CAM (AM 125, Renishaw, UK) laser melting device.

Cobalt-chromium-molybdenum (CoCrMo) (EOS Cobalt Chrome SP2, Renishaw, UK,

Table 4) was utilized for fabrication of the master design. Five independent copings were made.

Table 4 Composition of Direct Metal Laser Sintering of Cobalt Chrome Molybdenum copings

Composition	Percentage (%)
Cobalt	61.8 - 65.8
Chromium	23.7 - 25.7
Tungsten	4.9 - 5.9
Molybdenum	4.6 - 5.6
Silica	0.8 - 1.2
Other (C, Fe, Mn, N)	0 - 0.6

4.1.2.2 Milling Cobalt Chromium Molybdenum

The original CAD made using the Incise (Renishaw, UK) was exported as STL files. It was imported into the Cybaman Replicator (UK) and milled according to the master design. CoCrMo (Table 5) copings were made utilising HyperDent, FollowMe (Germany) as the milling software. Burs used were from Franken Dental Range (Germany). Basic strategies of milling include milling the cavity and occlusal side with two different cycles. A 3mm torus, 3mm ball, 2mm and 1.5mm ball was utilised for a rough cycle followed by a finish cycle using selective use of 1 and 1.5mm ball. In total 12 minutes was used to fabricate per design. Five independent copings were made.

Table 5 Composition of Milled Cobalt Chrome Molybdenum copings

Composition	Percentage (%)
Cobalt	59
Chromium	25
Tungsten	9.5
Molybdenum	3.5
Silica	1
Other (C, Fe, Mn, N)	1.5

Table 4 and Table 5 showing differences in Tungsten content of the two investigated Cobalt Chrome Molybdenum copings investigated.

4.1.2.3 Milling Zirconia with 3 Axis CAM

For this purpose, the CAD was sent to central manufacturing (Renishaw , UK) for milling purposes. Setting of material was changed from Laser PFM to Zirconia. The other settings were maintained for fabrication of milled zirconia with 3-Axis CAM machinery (DM10, Renishaw, UK). Five zirconia (Zr100, Renishaw, UK) copings were fabricated. Compositions of the coping materials were as follow (Table 6).

Table 6 Composition Table of Zirconia milled with 3-Axis apparatus

Composition	Percentage (%)
ZrO ₂ , HfO ₂ , Y ₂ O ₃	>99
Al ₂ O ₃	<0.3
Fe ₂ O ₃	<0.1

4.1.2.4 Milling Zirconia with 4 Axis CAM

Similar to 3 Axis milling, the CAD was also sent to a centralised milling centre that utilizes 4 Axis Milling apparatus (iMes-iCore, Germany). Settings for milling were standardised as the 3-Axis apparatus. Five zirconia copings (CoriTech Zr Discs, Germany) were fabricated. Compositions of the copings were as follow (Table 7).

Table 7 Composition Table of Zirconia milled with 4 Axis apparatus

Composition	Percentage (%)
ZrO ₂ , HfO ₂ , Y ₂ O ₃	>99
Al ₂ O ₃	<0.5
Other oxides	<0.25

Table 6 and Table 7 showing relatively similar contents of investigated Zirconia fabricated copings.

4.1.3 Micro Computed Tomography Scans (Micro CT)

4.1.3.1 Fabricated Coping Scan

In total, 20 micro-CT scans (4x5) were carried out on the fabricated copings as previously discussed (Section 4.1.2). Calibration of the micro-CT was initially performed before all scans (See Appendix). The copings were individually placed on a holder with a slight angle for better data recording of x-ray projections (77). The 10 copings of the CoCrMo material were scanned separately using the Phoenix X-Ray Nanotom (model XS180NF30F-144608, General Electric, USA) using settings shown on Table 8. Filters utilised were 0.2mm Cu and 0.5mm Sn. All scans were computed in micro-CT software. All data were exported as STL files.

Table 8 Scan parameters for Cobalt Chrome Molybdenum coping Scan

Conditions	Parameters
Energy Source	155 keV
Current	42 μ A
Voxel Resolution	13.127453 μ m
Projections	3600

The 10 copings of zirconia material were scanned with the micro-CT (General Electric, USA) utilising different settings shown on Table 9. This system utilizes a micro focus tube that allows better penetration with lower source of energy. No filters were utilised for these scans. Similarly to the CoCrMo scans, all data were exported as STL files.

Table 9 Scan parameters for Zirconia coping Scan

Conditions	Parameters
Energy Source	155 keV
Current	60 μ A
Voxel Resolution	7.787092 μ m
Projections	3000

4.1.3.2 Master Model Scan

The master model was also scanned using the micro-CT. Settings utilised are displayed in Table 10.

Table 10 Scan parameters of Master Model

Conditions	Parameters
Energy Source	125 keV
Current	60 μ A
Voxel Resolution	9.975831 μ m
Projections	1440

Table 8, 9 and 10 showing specific settings of micro-CT to enable scans for Cobalt Chrome Molybdenum and Zirconia copings.

4.2 Volume analysis

Volume computation analysis was done by importing 3D models from micro-CT scans into Rhino 5. STL file of Master Design was first imported and selected within the software. “Analysis” tab was pressed and “Mass Properties” was selected followed by “Volume”. The software computes the volume in mm³ cube. Results were recorded. Volume determination for the actual copings was computed by repeating the same steps. STL files of the fabricated copings were retrieved from the micro-CT scans.

Appropriate statistical analyses were determined and as follow:

1. A median value of volume was determined from all groups of fabricated coping.
2. One sample Wilcoxon Signed Ranked Test was performed to compare the median values of coping volume to the volume of the CAD (56.96mm³).

3. Independent Kruskal-Wallis test was performed to investigate whether volume differences exist between all CAM methods.
4. Post-hoc pairwise comparisons of the Kruskal-Wallis test is performed to compare CAM methods in terms of volume:
 - a. Comparison of CAM methods: Additive Method (LS) Vs Subtractive Method (M-CoCrMo)
 - b. Comparison of CAM milling strategies axis utilisation: 3 Axis (ZAx3) Vs 4 Axis (ZAx4)
 - c. Comparison of material utilisation in CAD/CAM: CoCrMo (M-CoCrMo Vs Zirconia (ZAx4)

4.3 Surface Mapping Analysis

Surface mapping analysis is performed with VG Studios (Version 2.2, Volume Graphics GmbH, Heidelberg, Germany) analysis software similar to the method previously described (Section 3.1.2.1.2). It utilizes the voxel models of the CoCrMo and zirconia copings that were created by the micro-CT scans. The following steps were followed.

1. Initially the original CAD was imported into the software.
2. Voxel models of the copings were then superimposed individually with the CAD model. Superimposition (Section 3.1.2.1.2) of the CAD and fabricated coping were done automatically by the software's coordinate measuring module utilising proprietary algorithms.

3. This was followed by computation of best fit elements of the resulting superimpositions.
4. Final adjustments were then made by rotating the elements (coping voxel model and CAD) manually in software to give the exact fit for superimposition purposes.
5. The superimposition procedure was then followed by a nominal/actual comparison of the STL model of CAD with the voxel model of the cobalt chrome coping.
6. A colour coded surface map representing deviations from the actual coping to the CAD is then displayed with an associated legend. The legend links a range of distances that relates to the colour display.
7. Results of deviations of copings to CAD are appreciated in three dimensions on software. A “Zoom In” and “Zoom Out” tab may also be utilised to magnify view for analysis.
8. A summary of all analysis were then displayed in results (Section 5.3) and categorized as:
 - a. Deviations of Laser Sintered CoCrMo (LS) to CAD
 - b. Deviations of 5 Axis Milled CoCrMo (MCoCrMo) to CAD
 - c. Deviations of 3 Axis Milled Zirconia (ZAx3) to CAD
 - d. Deviations of 4 Axis Milled Zirconia (ZAx4) to CAD
9. A histogram of variance distribution of all categories was displayed (Section 5.3).

4.4 Superimpositions

A summary of the Superimposition analysis is shown on Figure 53. Three analysis softwares were utilised to perform different tasks.

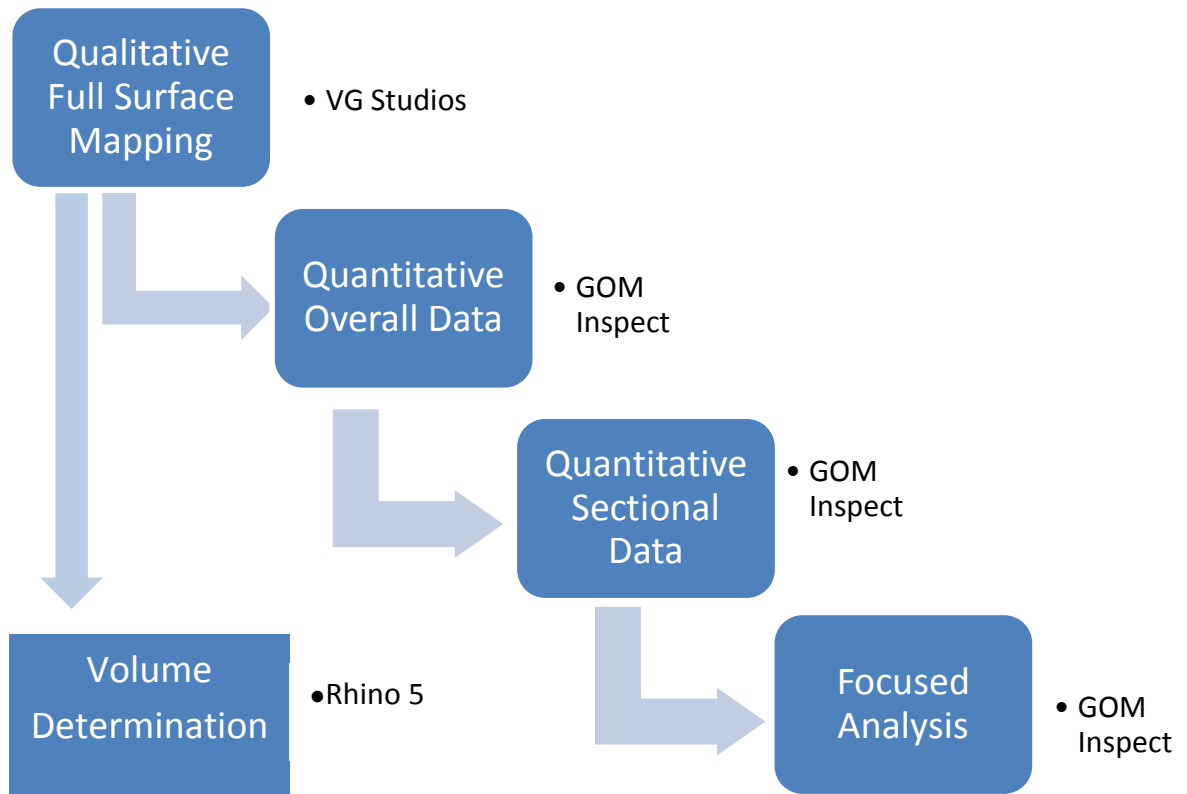


Figure 53 Summary of Superimposition Analysis

4.4.1 Coping Deviation Vs CAD

After superimpositions and overall surface mappings of all copings (Section 4.3), deviations seen qualitatively on the 3D models may be quantified (Figure 53). Initially, all voxel models created from utilisation of the micro-CT scans and VG Studios were exported into GOM Inspect (Version 7.5 SR1, Germany) as surface models (STL File). Upon importing, GOM requires some definition of the imported elements. The surface model of design was defined as CAD Body while the surface model of the scanned fabricated copings was defined as Mesh.

Similar to VG Studios, GOM Inspect requires superimpositions to be performed. This was completed by rough superimposition of CAD to Actual Mesh via selection of the “Pre-alignment” tab. The superimposition procedure was then enhanced by best fit algorithms of the software. After these procedures, surface mapping was achieved by selecting the “Surface Comparisons” tab and applying the comparisons on Actual Mesh. Similar to VG Studios, a colour map with associated colour legends representing the deviations of the copings (Actual Mesh) to CAD (CAD) could be displayed. Qualitative results were saved as “Surface comparison 1”.

Quantification of the results (Figure 54) was continued by selection of “Surface comparison 1” via checking the box in the inspection section of the software explorer. The “I-Inspect” tab was selected followed by the “Visualisation” and “Results” tab (I-Inspect>Visualization>Results). This procedure reveals a results table of the computed surface comparisons of CAD to Actual Mesh (Figure 54). Data was then recorded. To perform an analysis of the external surface of the fabricated coping, the software viewer was initially set in ‘Top View’. This is followed by selecting the “Select on Surface” tab and creating a box that covers the entire surface of the virtual model. Then by holding the right mouse button and releasing it on the ‘Add’ icon, the external surface of the virtual coping was selected and the software automatically computes the selected results (Figure 54). To perform the internal surface analysis, the “Select All” tab was selected followed by the “Select on Surface” tab. The box that covers the entire surface of the virtual coping was again reconstructed but in

contrast to the procedure before, the right mouse button was released on the 'Subtract' icon. This selects the internal surface of the coping and results are computed.

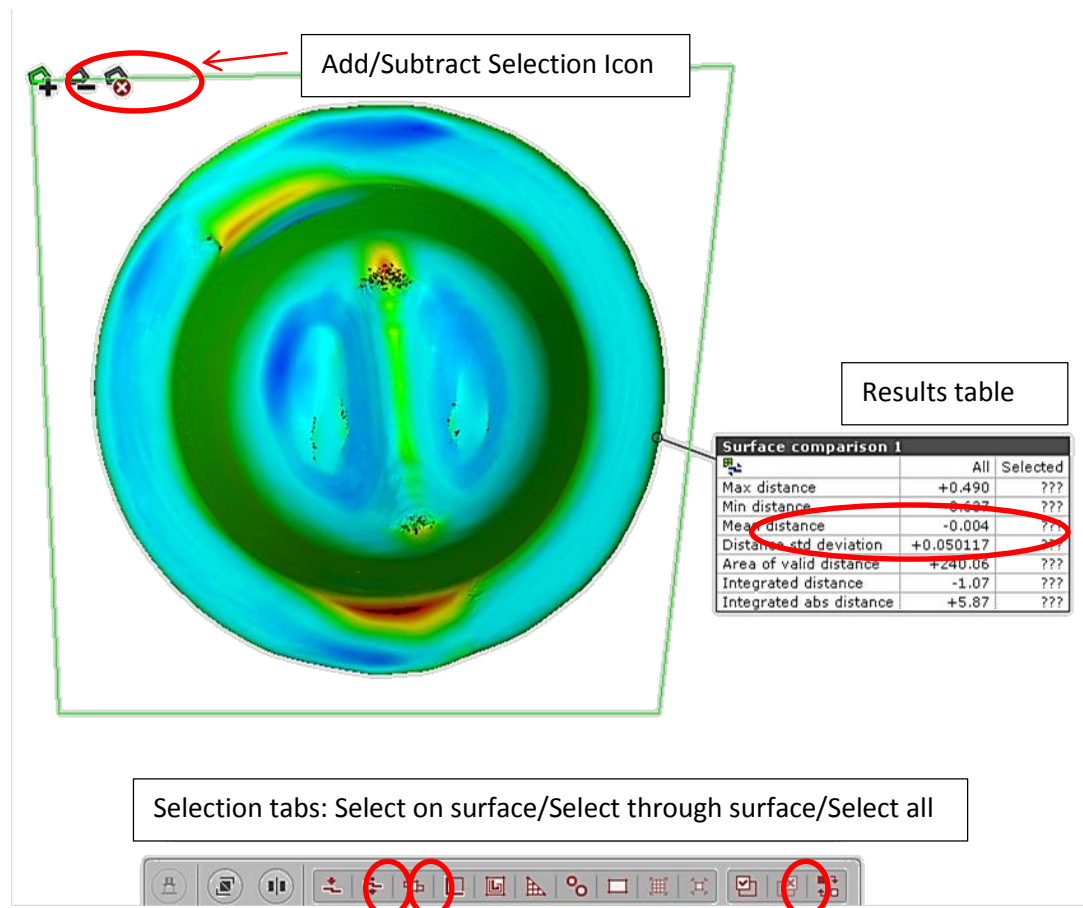


Figure 54 Quantification of Mean Distance (Top View)

Localised quantification of deviations was achieved by initially creating standardized sections of the copings. This was prepared by hiding all elements except CAD body in the software explorer. Then the "Inspection Section" tab was selected and two distinct planes across plane Z at +43.2mm and +48.2mm were added along the CAD body (Figure 55). The planes created will act as a guide for localised surface

comparisons. Then the CAD body was hidden from view and Surface Comparison 1 was checked in explorer and revealed. Viewer was then placed at side view.

Three standardised sections of all copings will then be created by selecting “Surface Comparison” tab and applying the comparisons on Actual Mesh. However in contrast to ‘Surface Comparison 1’ created before, only the required section of the coping was selected. This was performed by selecting the “Select Through Surface” tab to create a box with the aid of the guide curves that were fabricated earlier. Sections created represent different attributes of the surface comparisons of Actual copings to CAD and presented in Table 11.

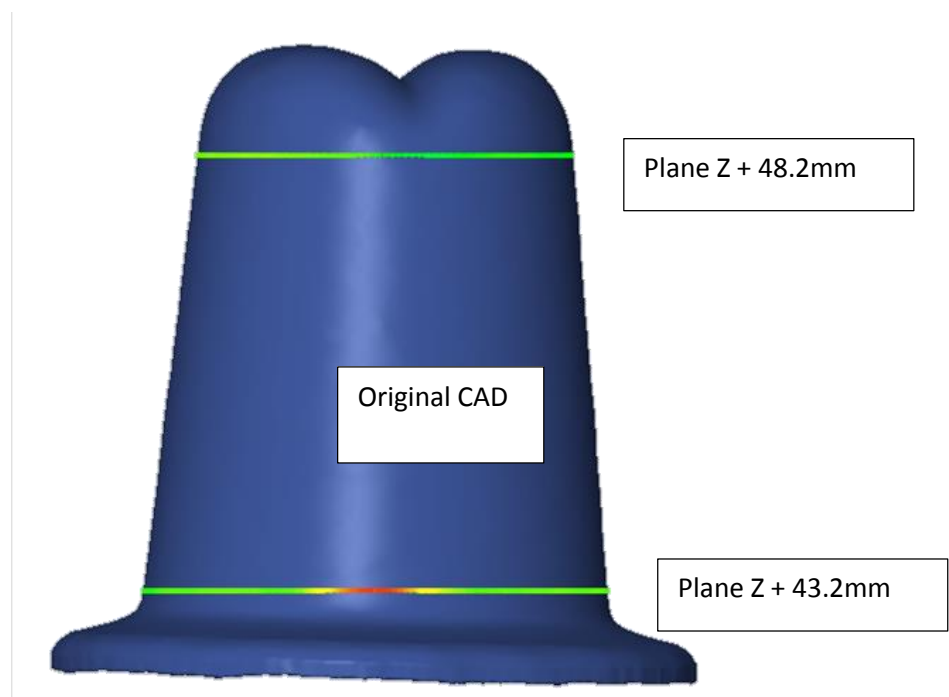


Figure 55 Standardised sections of fabricated copings

Table 11 Sectional surface comparisons

Surface Comparison of Actual Mesh to CAD	Position of sections	Representation
Comparison 1	Entire coping	Overall deviations of coping
Comparison 2	$X > Z + 48.2\text{mm}$ (Above Plane Z: 48.2mm)	Occlusal deviations of coping
Comparison 3	$43.2\text{mm} > X > 48.2\text{mm}$	Axial deviations of coping
Comparison 4	$X < Z + 43.2\text{mm}$ (Below Plane Z: 43.2mm)	Cervical deviations of coping

Table 11 shows position of line for sectioning purposes and the section representations.

Quantification of the results of localised, external and internal side of coping deviations were presented by performing deviation analysis as explained above. Selection of required localised comparisons (Figure 56-58) was performed via the “Toggle Visibility” tab in the explorer. Results demonstrating localised deviations of all the copings to CAD were recorded.

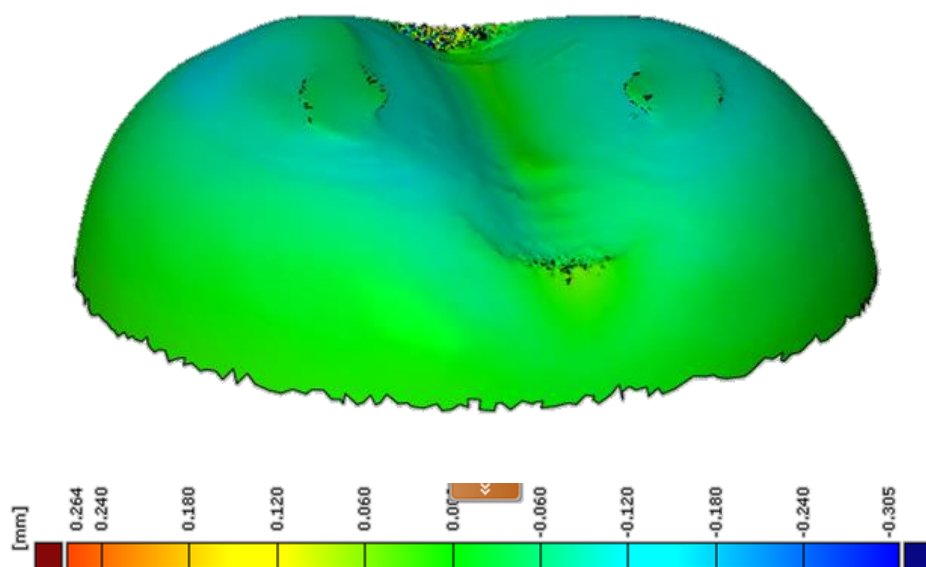


Figure 56 Occlusal Surface mapping of copings (Comparison 2)

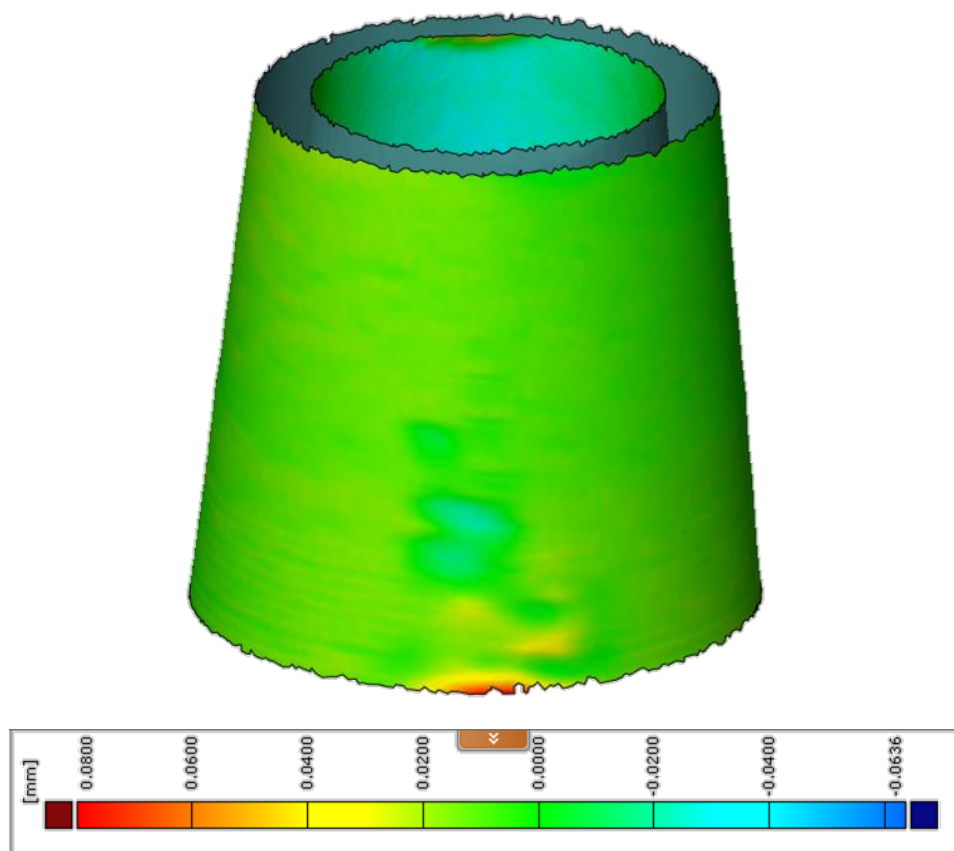


Figure 57 Axial Surface Mapping of copings (Comparison 3)

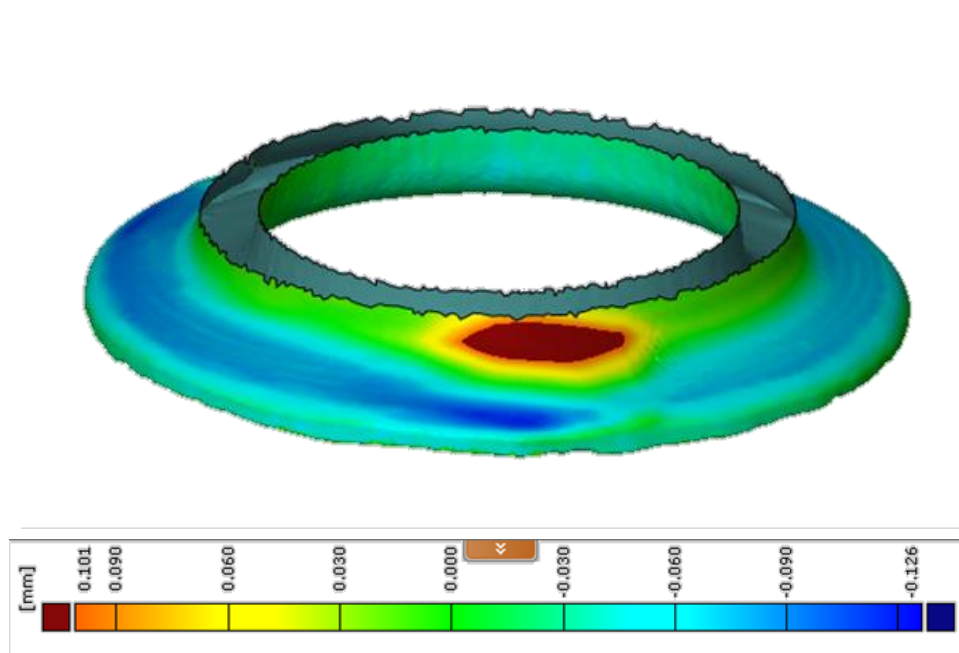


Figure 58 Cervical Surface Mapping of copings (Comparison 4)

4.4.2 Coping Deviations Group Comparison

Analysis of variance (ANOVA) with a post-hoc Tukeys test was performed to compare the different CAM methods. Results were summarized and additional comparisons were performed as follow:

- LS Vs M-CoCrMo: Compare deviations of Additive method to Subtractive method of CAM
- ZAx3 Vs Zax4: Compare deviations of CAM utilising 3 Axis milling to 4 Axis milling
- M-CoCrMo Vs ZAx4: Compare deviations of CAM utilising CoCrMo to Zirconia

4.4.3 Localised Focussed Investigation

Upon completion of localised sectional surface comparisons, the necessities for an in depth analysis at areas that may influence the sectional results arise. Thus focused analyses of surface comparison at specific areas were selected. Common areas

involved were excess material or reduced amount of material at occlusal section, axial and cervical of all four groups of copings. Example is given in Figure 59 where the external occlusal section deviation is computed as $-36\mu\text{m}$. However results which consisted of positive and negative findings were seen in the Qualitative Map. This might enlarge the variance in data.

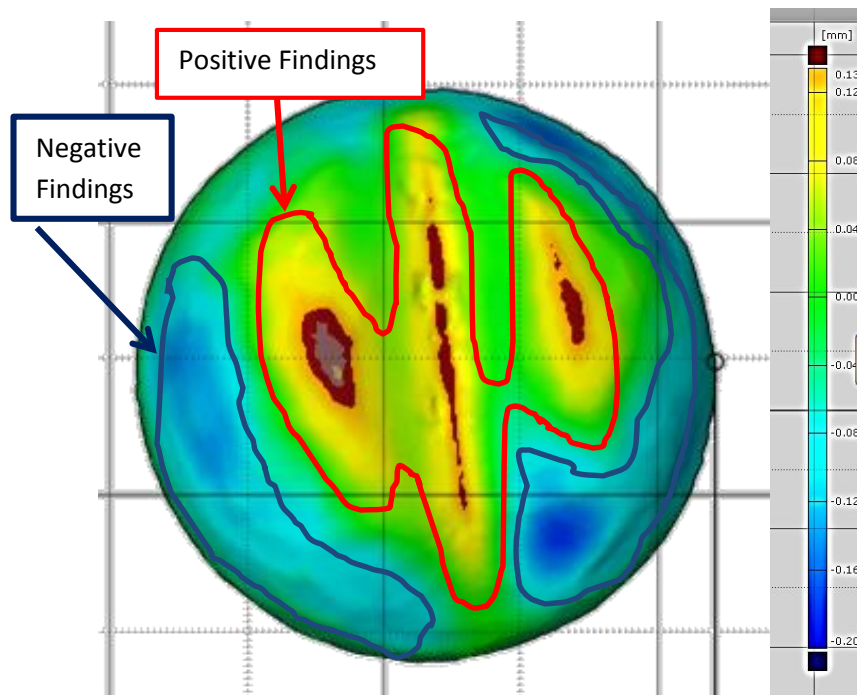


Figure 59 Focused Analyses on Occlusal Section of LS4

Focused analysis focuses on the exact change. In this case the positive (Shown in RED line, $117\mu\text{m}$) and negative areas (Shown in BLUE line, $-105\mu\text{m}$) were recorded. Data were then subjected to simple Mean calculations for all the 4 Groups in investigation. The methods for computation were as follows:

1. After performing superimpositions, sections and surface mappings (Section 4.4.1 and 4.4.2), selection of (Select/Deselect on surface) tab was performed.
2. Area of concern was then selected by clicking on the 'Add' button after carefully drawing a simulation line around the area of concern.

3. The software automatically computes the selected data of Results.
4. Results were saved and stored in SPSS version 21 and Descriptive statistics of Mean calculation were performed.

4.5 Alignment

Alignment was performed to calculate the Internal Fit of the CAM fabricated copings. Two-Dimensional Internal Fit Computation (3.1.2.2.1) was utilised for Internal Fit calculation as described below:

4.5.1 Internal fit Analysis

Internal fit computation was performed utilising Rhinoceros (Version 5, UK). The following steps were followed.

1. The master aluminium model scan and the coping scans from the micro-CT were imported into software. Alignment in this project was defined as placement of multiple 3D models on top of each other at point of contact (Figure 60).
2. The alignment procedure (coping on top) was done manually utilising the margins as reference points. Procedure was done by utilising tabs “Translation” and “Rotation” to move the 3D models in software for alignment purposes.
3. Upon alignment, 50 cross sections (Curve>Curve from Objects>Section) were made radially through the centre (Figure 60).

4. Centre was marked by the “Analyse” tab followed by “Mass Properties>Area centroid” on the Top View.
5. Section 1 utilizes the midpoint of 1 reference point below the margin area made earlier (Figure 49). Sections 2-50 are placed at equidistance of 7.2 degrees around the midpoint axis. This was to make all sections constant (Figure 60).
6. By grouping each section (Group 1-50); a 2D cross section was made (Figure 61).
7. The tab “Lock Selected” was utilized to lock Group 1 and the tab “Hide Selected” was utilized for Groups 2-50. Locking Group 1 prevents any change (i.e. translation, rotation) to the aligned 2D model while measurement was taken. By hiding groups 2-50, crowded superimposed 2D models could be hidden temporarily thus aiding measurement procedure.
8. Measurement was done by the “Analyze” tab followed by “Distance”. A point to point measurement could be made.
9. The procedure was repeated for groups 2-50 and measurements were recorded.

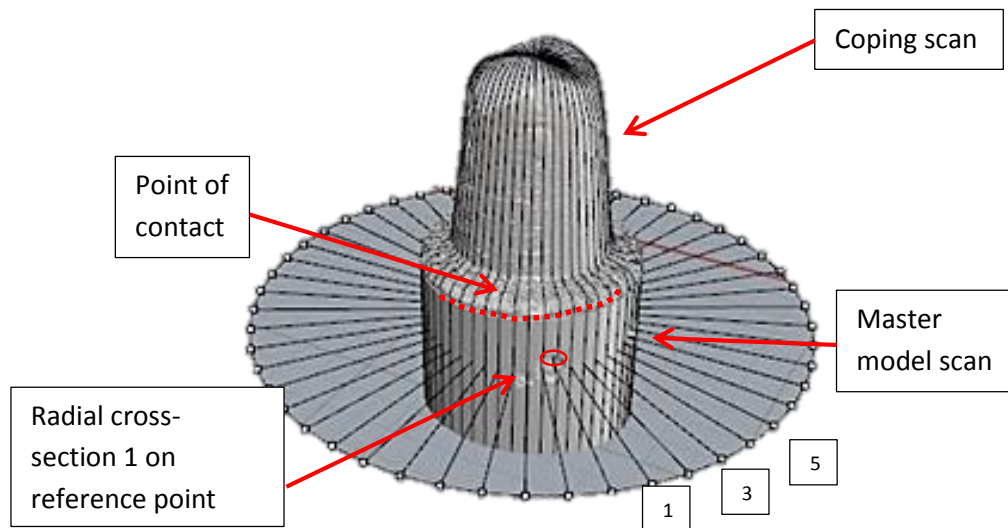


Figure 60 Aligned and cross sectioned coping scan and master aluminium model scan

Pre-determined points were measured (Figure 61). Definitions of points were explained in the Method Development/Reference points section (Section 3.1.2.2.1). In total, 5000 measurements were made for internal fit analysis of 20 copings. Each coping received 250 measurements. They included 50 measurements for Vertical Marginal Height (Figure 61, a), 50 measurements of Absolute Marginal Adaptation (Figure 61, b), 50 measurements of Axio-Margin Distance (Figure 61, c), 50 measurements of Axial Distance (Figure 61, d) and 50 measurements of Occlusal Height (Figure 61, e) for each group. In addition, measurements were also performed on the CAD alignment to the master aluminium model scan utilising the same measurement methods.

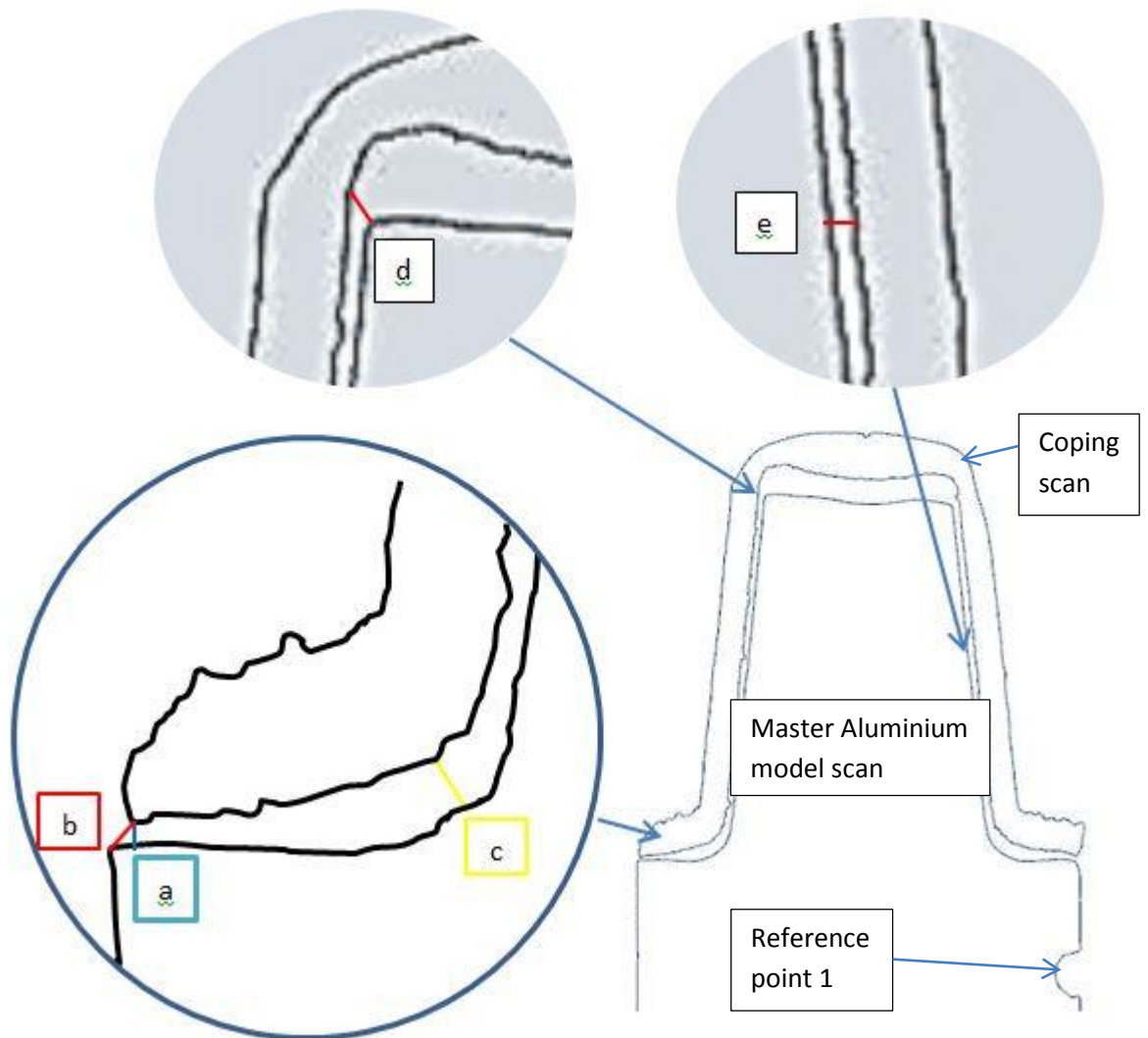


Figure 61 Section 1 of Radial Cross Sections and Predetermined area of Fit

Measurements

All measurements were recorded in SPSS Version 21 (IBM, New York, USA). Summary of analysis were performed as follow:

- Mean and Standard Deviation computation of all measurements of each group were recorded.
- ANOVA analyses to compare all the CAM method groups were performed for all measurement points.

- Post-hoc Tukeys's Test was performed to know which sections at all measurement points were significantly different.
- One-sample t-test was performed to compare between specific group measurements with original CAD measurements.

Section 5

Definitive Results

5 Definitive Results

5.1 Fabricated dental copings from a single master CAD

One coping per fabrication route is displayed in Figure 62. Laser Sintered (LS) copings feature visually an external rough surface finish when compared to the other methods of CAM. 5-Axis Milled CoCrMo (M-CoCrMo) visually has the smoothest surface finish among the milled copings. The 3-Axis Milled Zirconia coping (ZAx3) was slightly different occlusally when compared to the CAD (Figure 52). The CAD had a central groove on the occlusal surface which in the ZAx3 coping did not replicate accurately. The coping showed an occlusal surface with four cusps as opposed to the central groove of the CAD.

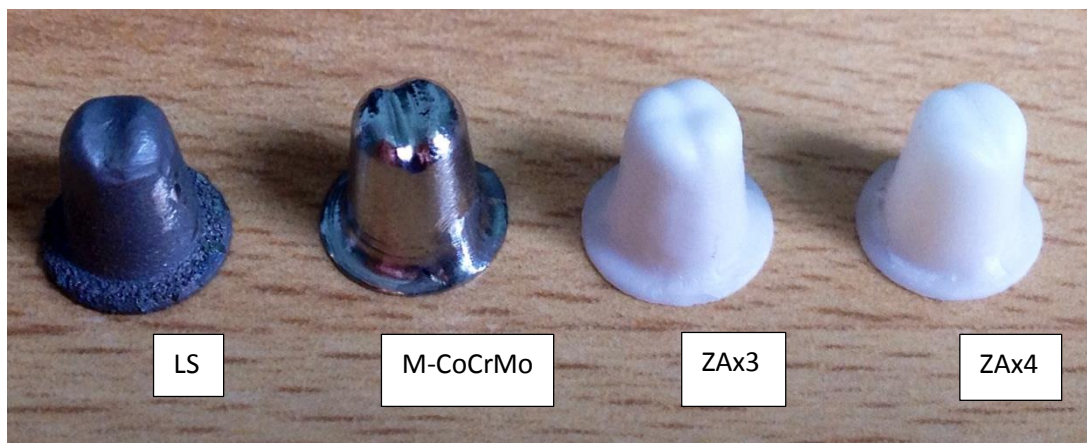


Figure 62 Fabricated copings using different techniques of CAM using the same CAD [Laser Sintered CoCrMo coping (LS), 5-Axis Milled Cobalt Chrome Molybdenum coping (M-CoCrMo), 3-Axis Milled Zirconia coping (ZAx3), 4-Axis Milled Zirconia coping (ZAx4)]

5.2 Volume Analysis of Fabricated Coping

Figure 63 shows a graph of the Median Volume of the copings fabricated utilising different methods of CAM. The original CAD had a volume of 56.96 cubic millimetres (mm^3) (Red Line in Figure 63). One-Sample Wilcoxon Signed Ranked Test revealed that LS and ZAx4 fabricated copings were fabricated significantly smaller than the CAD ($p < 0.05$). Median values of LS and ZAx4 were 52.48mm^3 and 56.08mm^3 respectively. In contrast to the LS and the ZAx4, the M-CoCrMo and the ZAx3 were fabricated bigger ($p < 0.05$) than the CAD with values of 62.8mm^3 and 59.39mm^3 respectively. An Independent Kruskal-Wallis test between the four methods of CAM revealed significant differences ($p < 0.01$). A summary of Pairwise comparisons of the Kruskal-Wallis test results comparing the groups are displayed below:

- All pairwise comparisons are not statistically significant apart from the following:
 - a. LS < M-CoCrMo ($p < 0.001$)
 - b. LS < ZAx3 ($p < 0.05$)

Pairwise comparison of Kruskal-Wallis test revealed no significant difference available ($p > 0.05$) between zirconia fabricated with 3-Axis CAM and 4-Axis CAM (ZAx3 Vs ZAx4) in terms of coping volume. Pairwise comparison of Kruskal-Wallis test also revealed no significant difference ($p > 0.05$) between CAM fabrication with materials of zirconia and CoCrMo (ZAx4 Vs M-CoCrMo) in terms of coping volume.

No significant difference ($p>0.05$) exists in terms of coping volume between groups (M-CoCrMo, ZAx3, ZAx4) utilising the subtractive method of CAM fabrication.

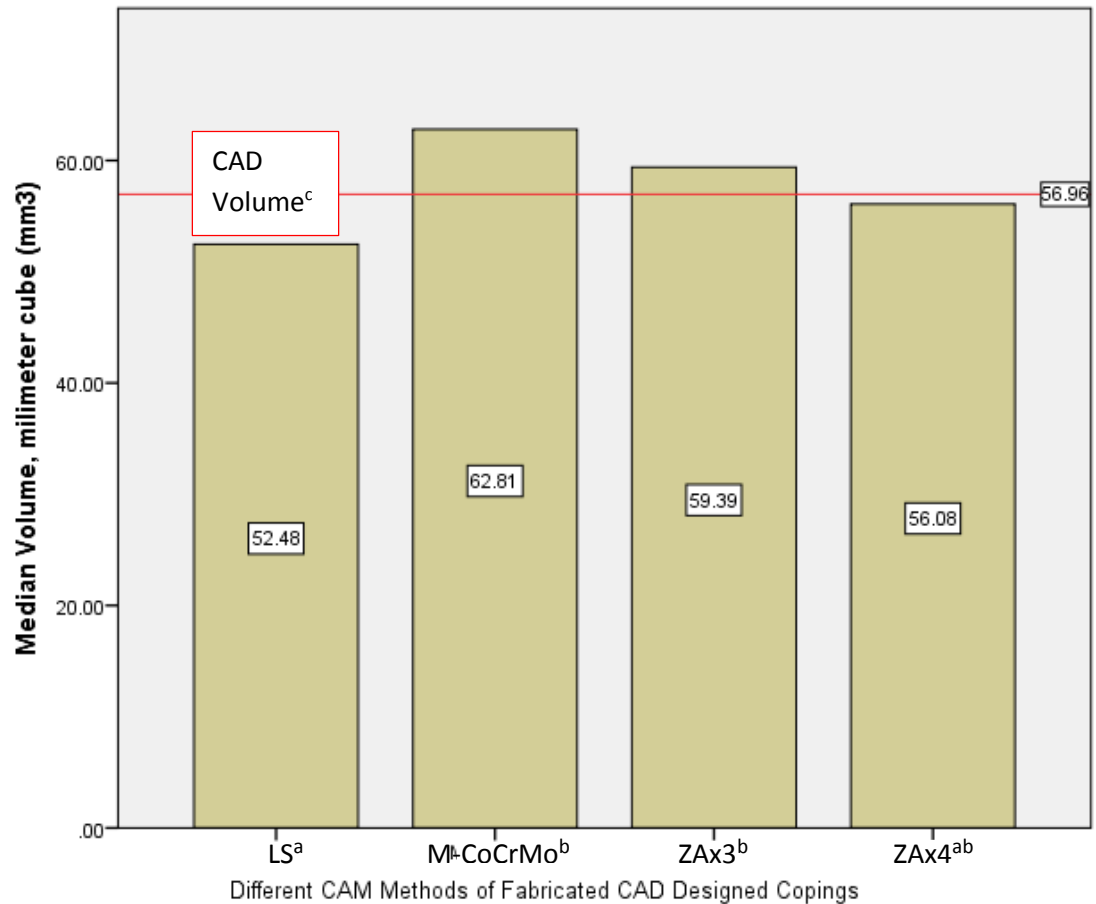


Figure 63 Graph of Median Volume of Fabricated Copings utilising different methods of CAM (Different superscript letters show significant difference ($p<0.05$) when comparison was made)

5.3 Colour Deviation Surface Mappings

The qualitative differences of CAD to CAM are displayed in the form of colour deviation maps (Figure 64). The red indicates a positive divergence from the nominal CAD. In contrast, the blue colour indicates a negative divergence. The positive and negative divergences have a maximum reading of 200 μ m (Figure 64).

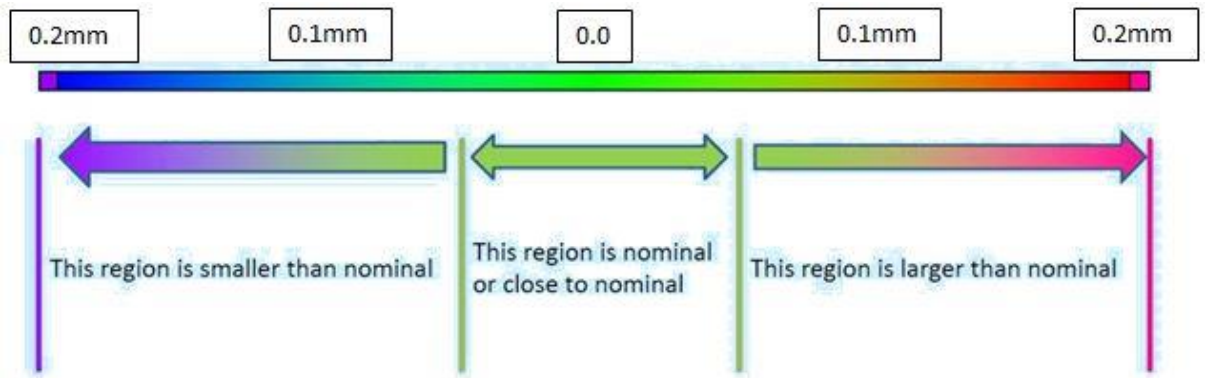


Figure 64 Surface Mapping Colour Legend of Actual Coping Deviations to CAD

5.3.1 Laser Sintered Cobalt Chrome Molybdenum Coping (LS) Deviations from CAD

Micro-CT scanned LS copings revealed rough surface patterns on the outer surface of the copings (Figure 65). The actual marginal edge (Figure 65a) and the axial surface (Figure 65c, d) of the external coping were similar or close ($\pm 20\mu\text{m}$) to the original CAD. Small nodules up to $200\mu\text{m}$ are seen projecting onto the axial-cervical external (Figure 65c) surface of copings (Red areas, Figure 65a, b, c, d, e). The external axio-occlusal surface (Figure 65a, b) shows less material fabrication ($<200\mu\text{m}$) when compared to the CAD (Blue areas, Figure 65).

An occlusal view of copings revealed increased material deposition on the reference groove and the highest point of the occlusal surface (Red areas, Figure 65e). The bottom view displays that the inside of the cusps is smaller than the CAD (Blue areas, Figure 65f). The rest of the internal surfaces appear to be similar or close to the CAD

($\pm 20\mu\text{m}$) except for some localised areas at the margins that displayed positive overlaps of less than $200\mu\text{m}$ (Figure 65f).

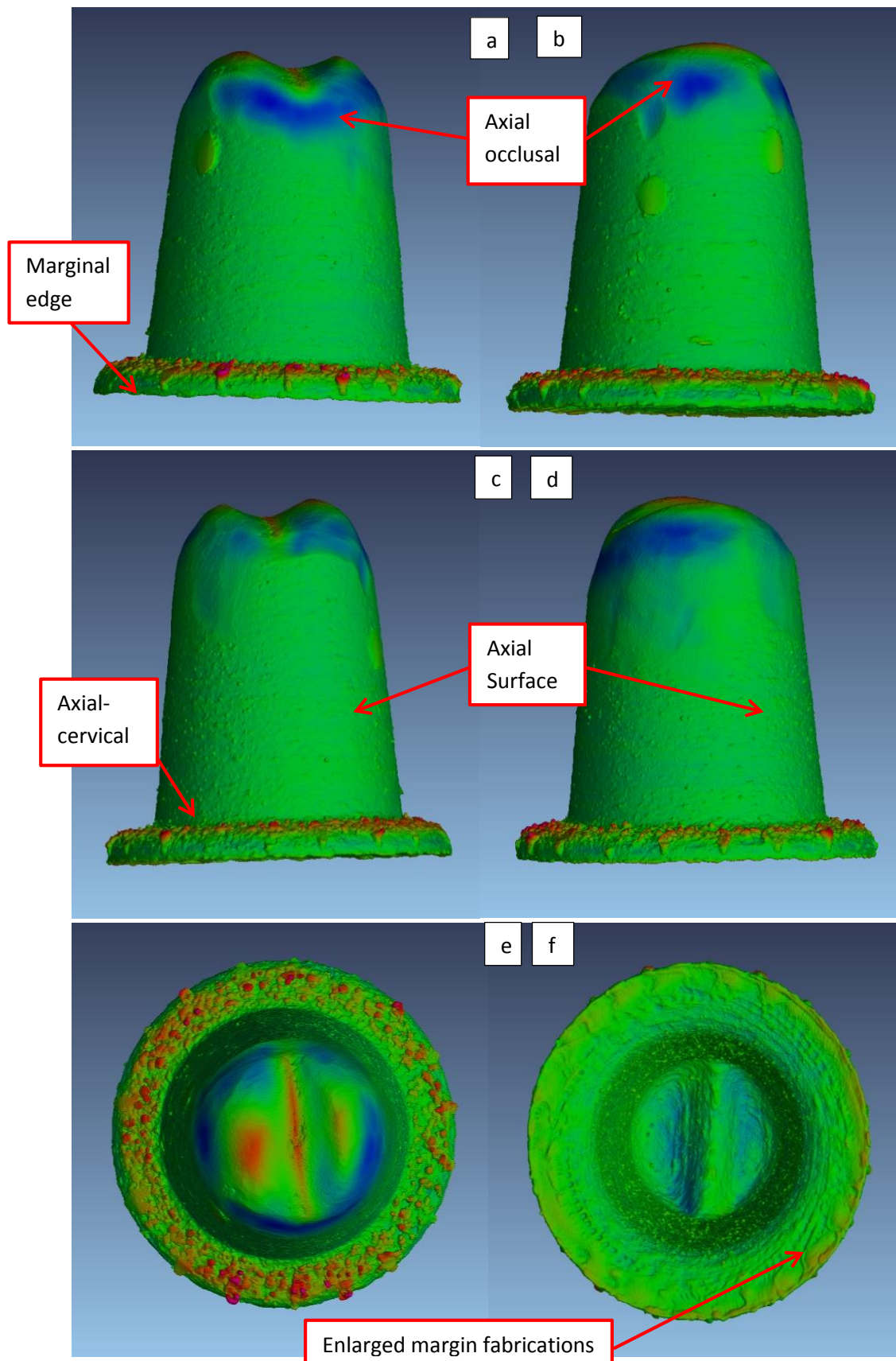


Figure 65 Surface mapping of Laser Sintered Cobalt Chrome Molybdenum Coping (LS) deviation to CAD, a: side view, b: view rotated 90°, c: view rotated 180°, d: view rotated 270°, e: vertex view, f: bottom view

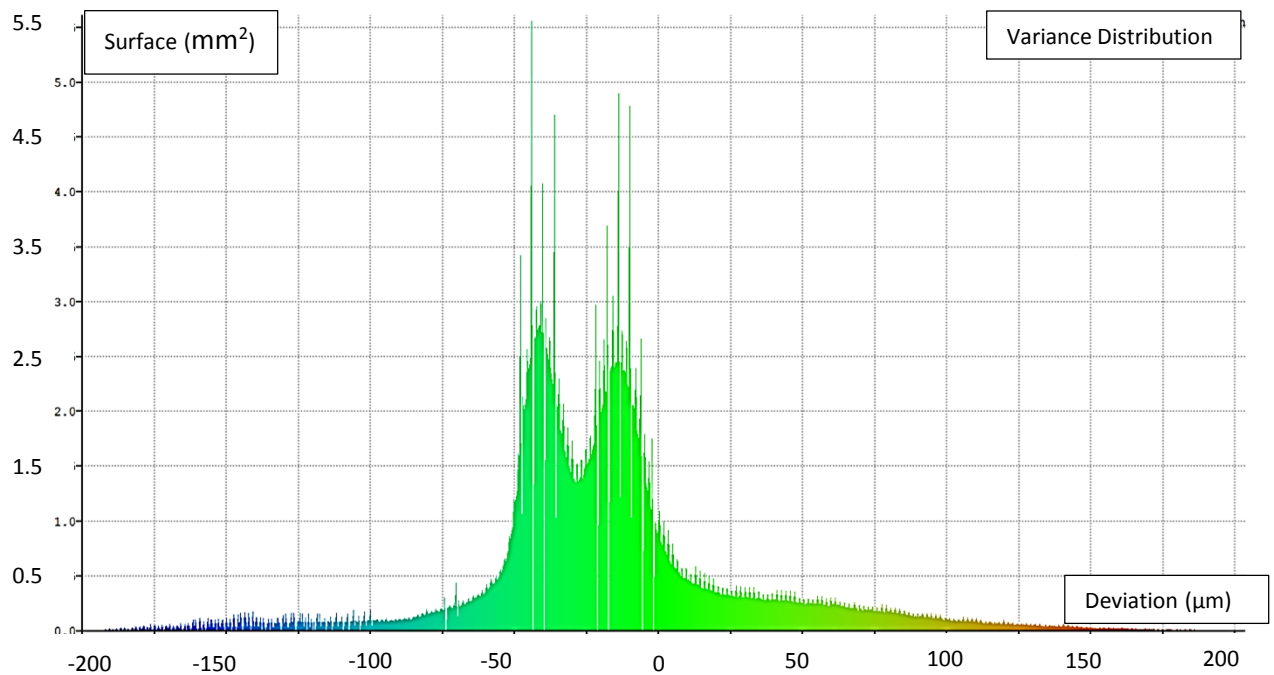


Figure 66 Histogram of distribution deviations across the surface of LS fabricated copings

A distribution of deviations histogram across the surface of LS fabricated copings is shown in Figure 66. Positive deviations mean an enlargement of coping fabrication while negative deviations mean a smaller fabrication. A large amount of coping surface area close to 0mm deviation would indicate an accurately fabricated CAD. This graph however is shifted to the left indicating a smaller coping being fabricated compared to the original CAD.

5.3.2 5-Axis Milled Cobalt Chrome Molybdenum Coping (M-CoCrMo)

Deviations from CAD

Overall, milled copings were slightly enlarged compared to the CAD in the external axial aspects and internal cervical aspects of coping (Green Reddish areas, Figure 67). However three large areas of excess material ($>200\mu\text{m}$) were noted (Pink areas, Figure 67a) on the external surface of the axial wall. Smaller fabrications were seen on the axial-cervical external (Purple areas, Figure 67c, d) surface and the external occlusal surface (Purple areas, Figure 67c, d, e). Occlusal view showed localised areas (Groove area) having less material ($>200\mu\text{m}$) when compared to the CAD (Figure 67e). Scans of the internal aspect of milled copings reveal localised excess material ($>200\mu\text{m}$) on the occlusal and axial walls (Figure 67f).

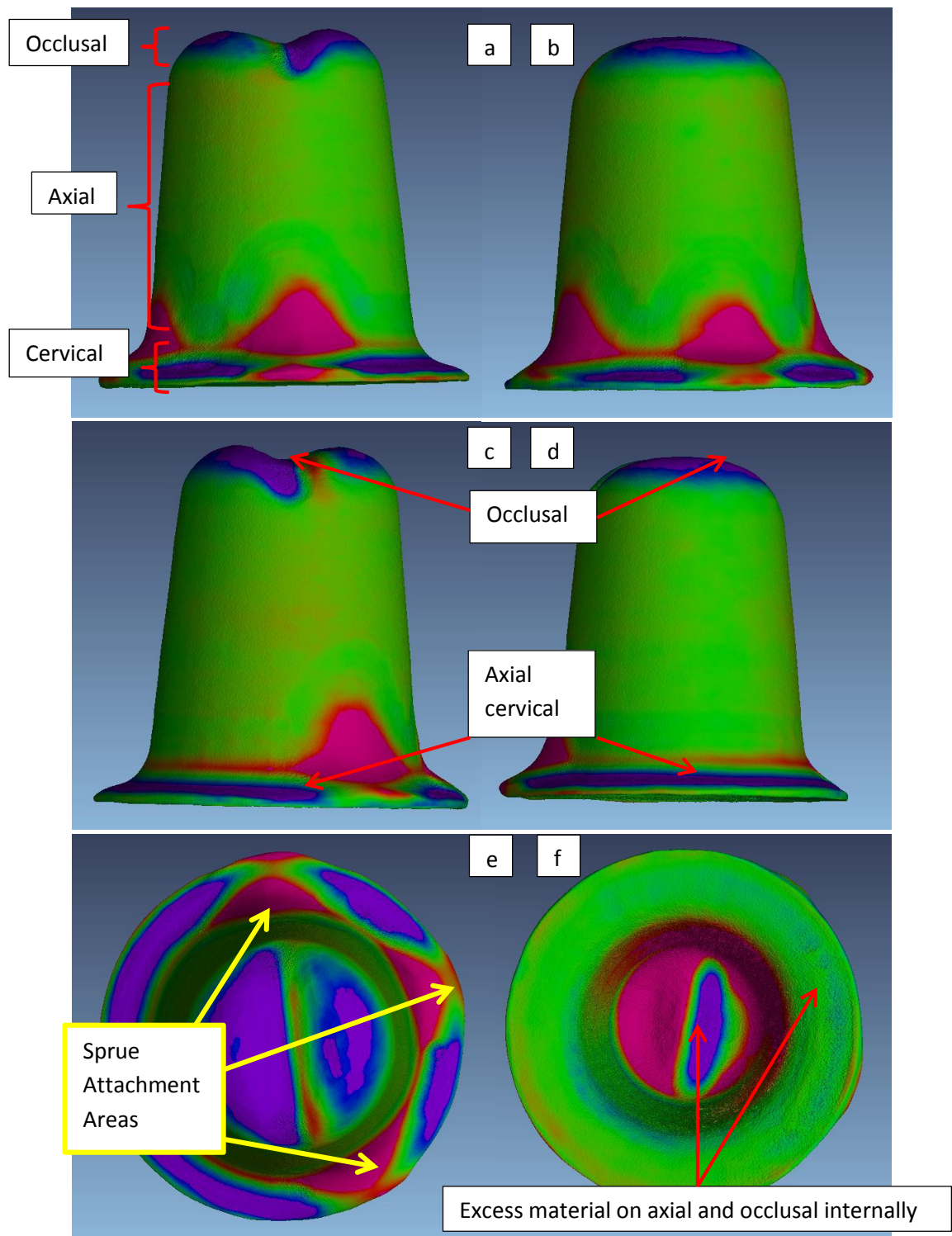


Figure 67 Surface mapping of Milled CoCrMo coping (M-CoCrMo) deviation to CAD, a: side view, b: view rotated 90°, c: view rotated 180°, d: view rotated 270°, e: vertex view, f: bottom view

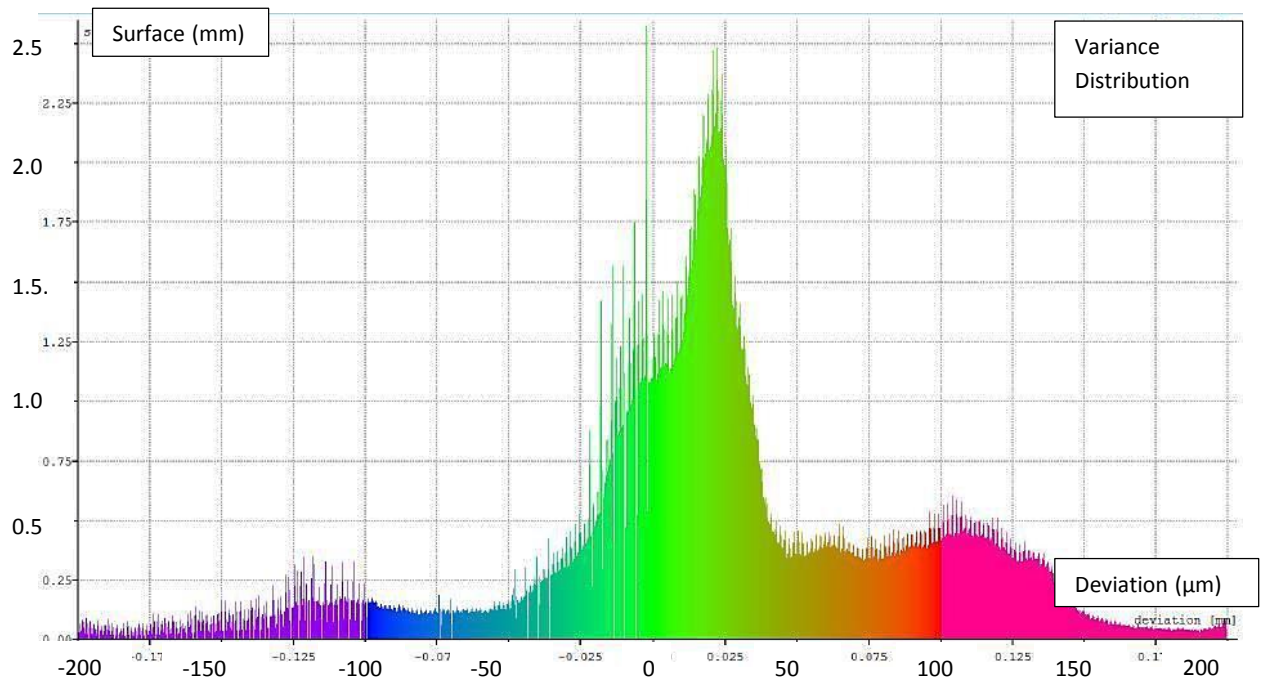


Figure 68 Histogram of distribution deviations across the surface of M-CoCrMo

fabricated coping

The distribution of deviations histogram (Figure 68) was shifted to the right indicating a coping that is larger than the original CAD. The large amount of data above 100 μ m largely reflects the sprue attachment areas that were left after its fabrication (Figure 67e).

5.3.3 3-Axis Milled Zirconia Coping (ZAx3) Deviations from CAD

The qualitative differences of milled zirconia copings utilising 3-axis CAM to CAD require the use of a high value legend (Figure 69). Readings up to a maximum of 0.5mm (Figure 69) were observed. The CAD overlay of the original CAD with a micro-CT scanned zirconia coping in cross-sections is referred in Figure 70. The axial aspects of the coping look similar to the CAD. However, enlargement in fabrication was noted

on the occlusal and cervical aspects of the fabricated coping (Figure 70). In addition, the margins of the copings appear to be wider when compared to the CAD. Quantification of this margin area is displayed in Section 5.5.



Figure 69 Surface Mapping Colour Legend of 3-Axis Milled Zirconia Coping Deviations to CAD

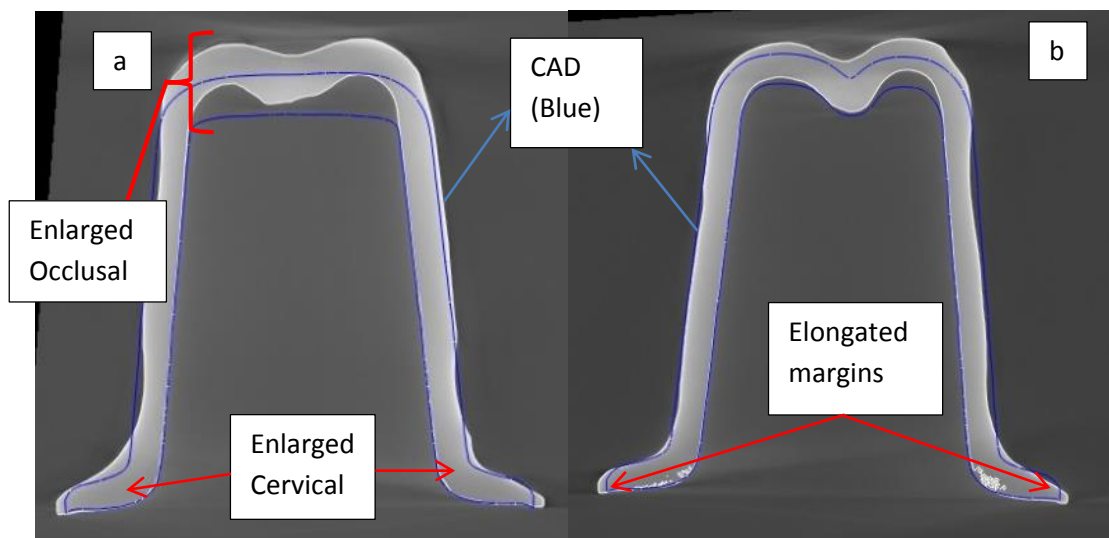


Figure 70 Cross-sectional Overlay of CAD (Blue) and scanned 3-Axis Milled Zirconia coping in micro-CT, a: side view, b: view rotated 90°

Figure 71 shows a coloured surface mapping comparison of the zirconia scans to the CAD. It shows that zirconia fabricated millings present a fine stripe appearance on the surface of the copings (Figure 71c, d). Increased material (<0.5mm) was also noted on the occlusal external surface of the coping (Red areas, Figure 71e). The Internal view also showed smaller fabrication in localised areas on the occlusal aspect

of the coping (Blue areas, Figure 71f). The four occlusal cusps observed visually (Figure 62) were also evident in this surface mapping comparison (Figure 71e).

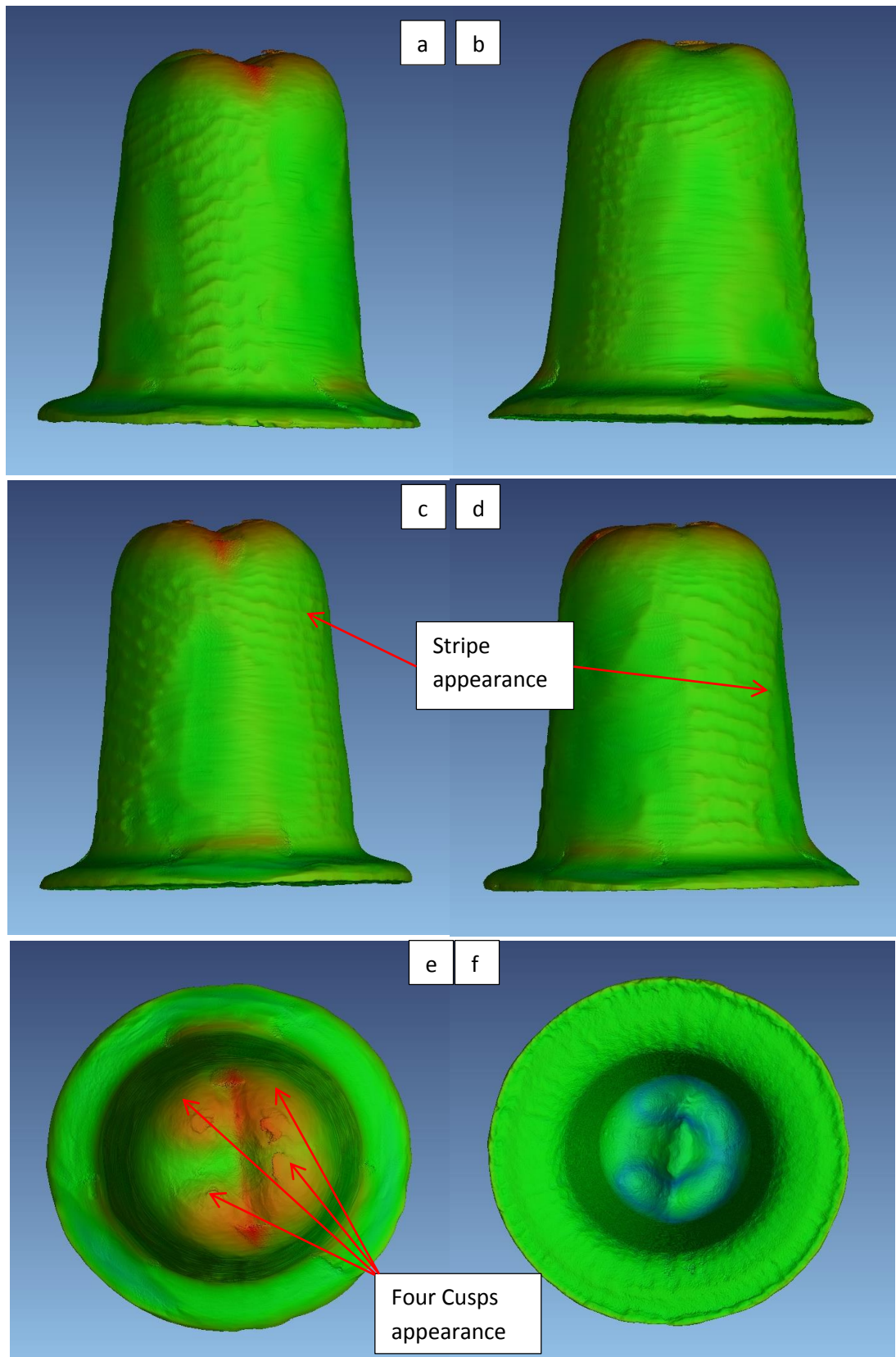


Figure 71 Surface mapping of 3-Axis milled zirconia coping (ZAx3) deviation to CAD, a: side view, b: view rotated 90°, c: view rotated 180°, d: view rotated 270°, e: vertex view, f: bottom view

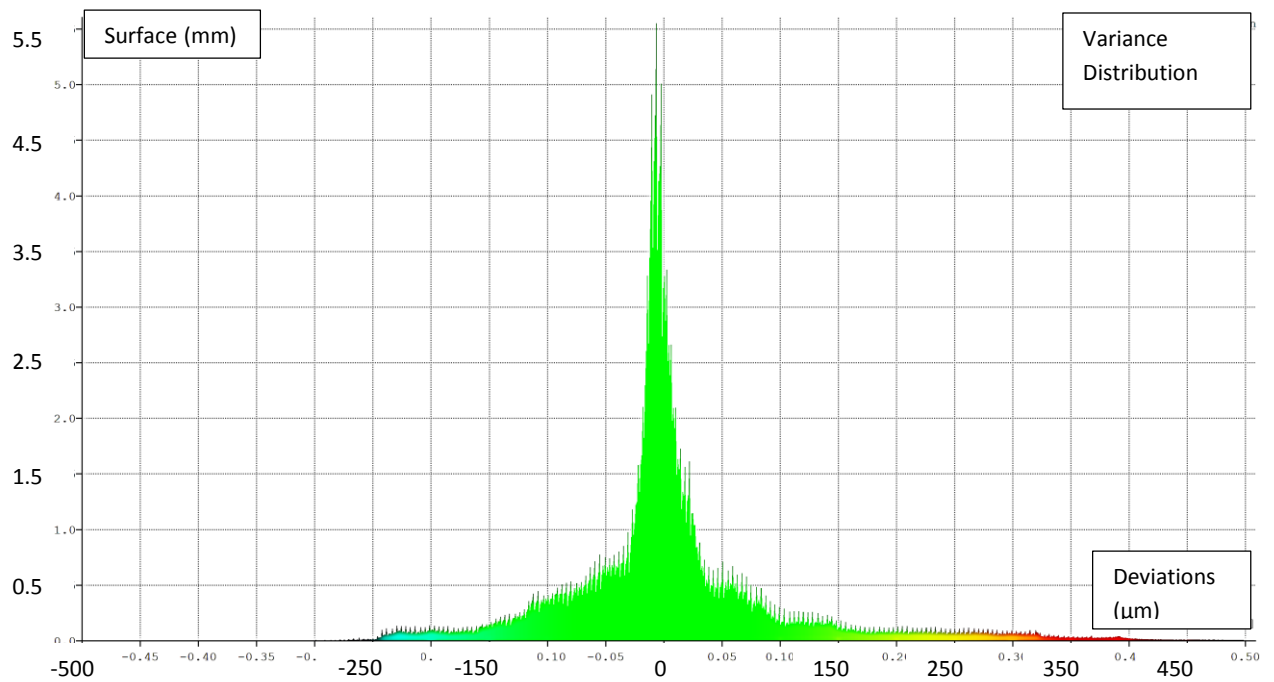


Figure 72 Histogram of distribution deviations across the surface of ZAx3 fabricated coping

A distribution of deviations histogram (Figure 72) across the coping surfaces shows a single peak at the centre (0mm deviation). This suggests a coping that is largely similar to the CAD although localised high deviations of more than 200μm are also present.

5.3.4 4-Axis Milled Zirconia Coping (ZAx4) Deviations from CAD

4-Axis milled zirconia was evaluated to a maximum reading of 200μm (Figure 64). In general, a cross-sectional overlay of the CAD and the scanned zirconia coping showed similarities apart from some localised areas (Figure 73). The axial aspect of the coping looks thicker in certain areas when compared to the CAD (Figure 73a). At the line angle occlusally, excess material is evident both internally and externally (Figure 73a, b).

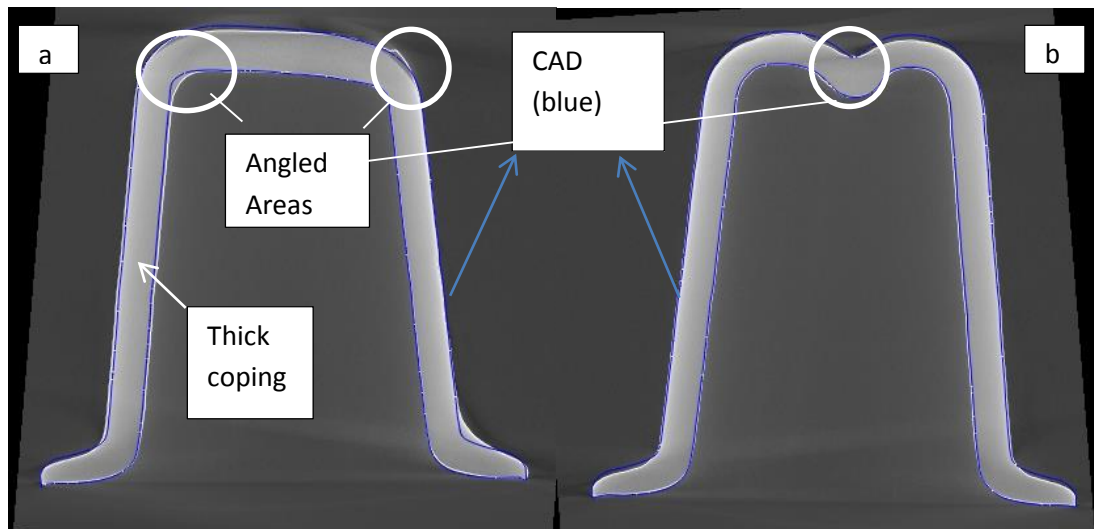


Figure 73 Cross-sectional Overlay of CAD (Blue) and scanned 4-Axis Milled Zirconia coping in micro-CT, a: side view, b: view rotated 90°

Figure 74 shows surface mapping of deviations between CAD and ZAx4. A fine stripe appearance on the surface of the coping was evident. Overall, the coping was fabricated similar to the CAD with deviations of less than 50µm. However, less material (<100µm) was noted on the external surface of the coping occlusally and cervically (Figure 74e). Excess material (Red areas, Figure 74a, c, d, e) was found locally on the external surface of the coping axially (Figure 74a) and internal surface at angles of the occlusal (Figure 74f).

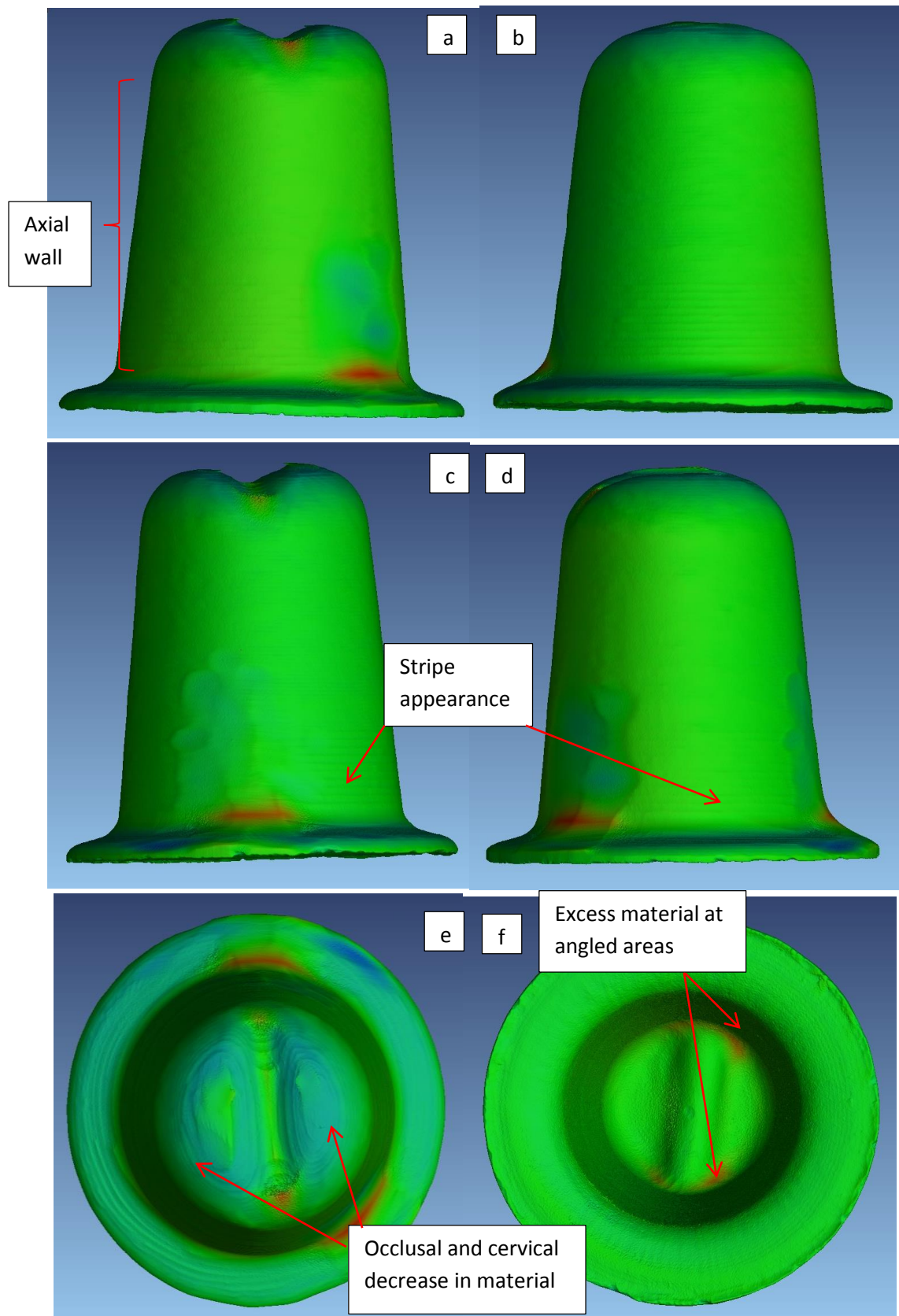


Figure 74 Surface mapping of 4-Axis milled zirconia coping (Zax4) deviation to CAD, a: side view, b: view rotated 90°, c: view rotated 180°, d: view rotated 270°, e: vertex view, f: bottom view

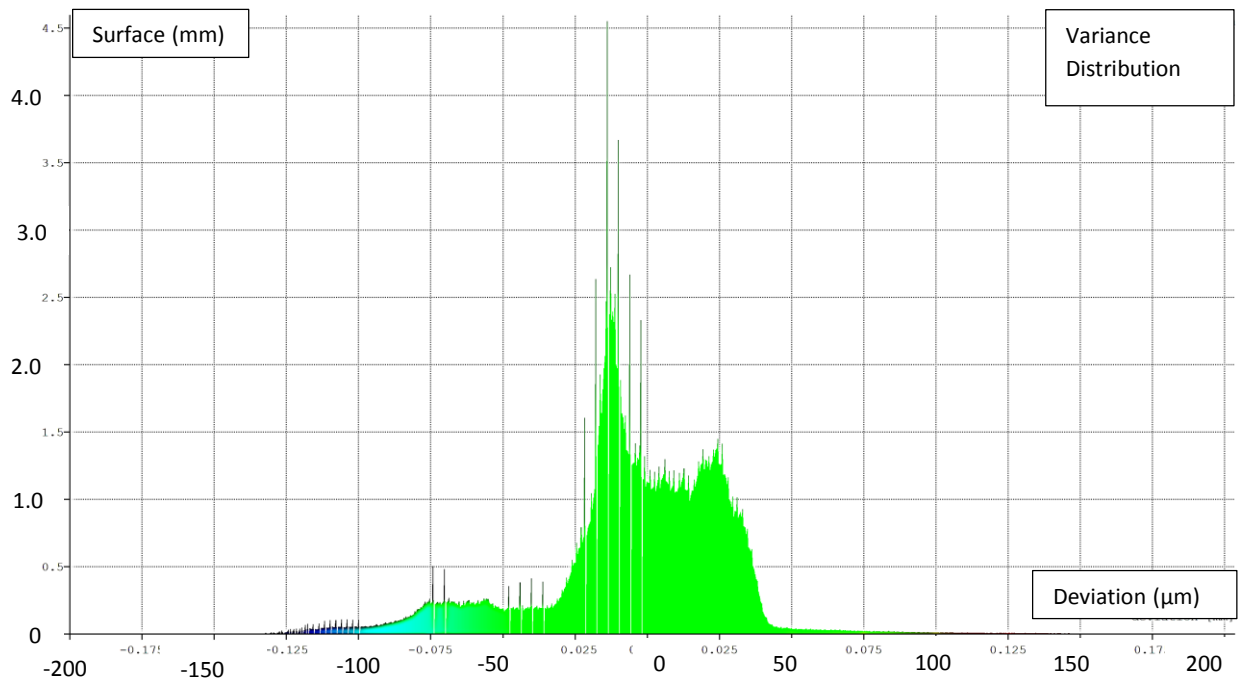


Figure 75 Histogram of distribution deviations across the surface of ZAx4 fabricated coping

A distribution of deviations histogram (Figure 72 and Figure 75) across the coping surfaces shows a single peak near the centre. Most of the data were within a 50μm deviation to the CAD however a negative tail distribution was also noted. This suggests that some parts were made smaller than the CAD.

5.4 Superimpositions Analysis

5.4.1 Comparing Coping Deviation from CAD

The deviations between the CAD and the micro-CT scans of the copings at the various investigated sections (Figure 55-58) are shown in Table 12. Positive values indicate an enlarged fabricated component and negative values indicate a reduced fabricated component at the respective section.

Table 12 Mean Deviations of fabricated copings to CAD

Mean (SD) Deviations, µm (n=5)	Laser Sintered CoCrMo (LS)	Milled 5-Axis CoCrMo (M- CoCrMo)	Milled 3-Axis Zirconia (ZAx3)	Milled 4-Axis Zirconia (ZAx4)
Internal Occlusal	-52(20) ^a	54(9) ^b	-136(29) ^c	-3(28) ^d
External occlusal	-26(16) ^a	-6(15) ^a	130(65) ^b	-30(31) ^a
Internal Axial	-14(6) ^a	37(15) ^b	-7(6) ^{ac}	7(5) ^c
External Axial	-30(6) ^a	39(6) ^b	-3(42) ^{ac}	10(7) ^{bc}
Internal Cervical	-46(47) ^a	-18(5) ^a	-44(66) ^a	-26(31) ^a
External Cervical	34(4) ^a	15(3) ^{ab}	21(10) ^a	-13(31) ^b

*Different superscript letters across the table rows show a significant difference (p<0.05).

Table 12 shows deviations of copings to CAD at specific sections. Only Internal Cervical section (Highlighted) were comparable across all investigated groups. The rest of the findings significantly different for certain aspects of sections and were summarized in text and Table 13.

Large discrepancies (<136µm) were found on the occlusal aspect of ZAx3 (Internally and externally). ZAx3 was also the only group that produced positive deviations on the External Occlusal Section. In terms of Internal Occlusal Sections, only M-CoCrMo was enlarged when compared to the other methods of CAM.

The Internal Cervical Sections of all groups were smaller when compared to the CAD but not significantly (p>0.05) different from each other (highlighted in Table 12). At

the External Cervical Section, all groups exhibited an enlarged fabrication with the exception of ZAx4.

The LS copings were fabricated smaller than the CAD on all sections investigated except the External surface of the cervical. The M-CoCrMo copings were fabricated larger than the CAD with the exception of External Occlusal and Internal Cervical Sections. The ZAx3 copings were fabricated smaller than the CAD with the exception of the External Occlusal and External Cervical sections. ZAx4 copings were also fabricated smaller than the CAD except for the Axial Sections (Internal and External).

5.4.2 Comparing Different CAM Methods of Coping Fabrication

A series of ANOVA tests across the rows of indicated that the results were significantly different ($p < 0.05$) with the exception of the Internal Cervical row ($p > 0.05$). When additive and subtractive CAM methods of fabricating CoCrMo copings were compared (LS Vs M-CoCrMo), results were highly significant ($p < 0.01$) on the Internal Occlusal, Internal Axial and External Axial sections of copings. Significant differences ($p < 0.05$) were also observed between the External and Internal Occlusal and External Cervical sections of Zax3 and Zax4. CoCrMo coping (M-CoCrMo) versus zirconia coping (Zax4) material comparison revealed a significant difference ($p < 0.05$) on the Internal Occlusal sections of the copings. In addition, the Internal Axial sections of the latter copings displayed a highly significant difference ($p < 0.01$).

A summary of these results is displayed below (Table 13):

Table 13 Comparison of sections Vs CAD

No	Comparison	Sections
1	LS < M-CoCrMo	Internal Occlusal, Internal Axial and External Axial
2	ZAx3 > ZAx4	External Occlusal, External Cervical
3	ZAx3 < ZAx4	Internal Occlusal
4	M-CoCrMo > ZAx4	Internal Occlusal and Internal Axial

Table 13 summarizes the deviations (Distances) that were significantly different when compared to CAD.

5.4.3 Focussed analysis

Results of the localised sections were analysed more in depth and tabulated (Table 14-18). These included areas that displayed intense deviations (Shown in Figure 76-79).

5.4.3.1 Laser Sintered Focussed Deviations

Figure 76 shows a maximum of 111µm positive deviation and 108µm negative deviation on LS copings. External nodules at the cervical aspect are observed to have deviations of 90µm positively to CAD [Figure 76 (E)]. Other focussed areas of interest on LS copings are shown in Table 14.

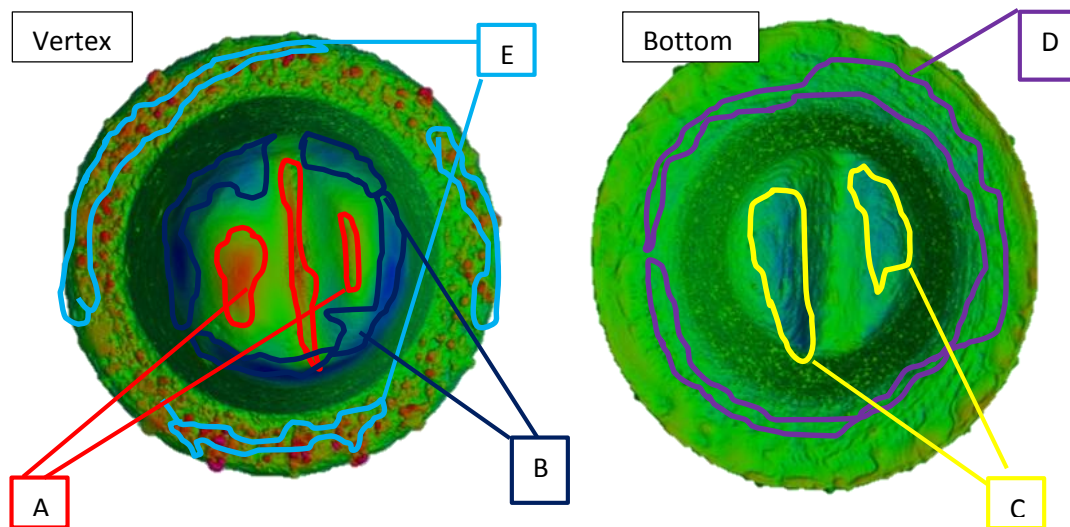


Figure 76 Focused Sections on LS copings; Left picture Vertex View, Right picture Bottom View

Table 14 Focused Results of LS sections

LS	Mean (SD), μm (n=5)
Focussed Occlusal External (A)	111(4)
Focussed Angled Areas of Occlusal External (B)	-108(4)
Focussed Occlusal Internal (C)	-88(11)
Focussed Cervical Internal (D)	-60(22)
Focussed Cervical External (E)	90(34)

Table 14 shows localized areas of laser sintered copings that were investigated in depth.

5.4.3.2 M-CoCrMo Focussed Sections

Focussed areas of M-CoCrMo sections are shown in Table 15. Positive and negative deviations were evident on the internal aspect of M-CoCrMo occlusally [Figure 77 (B, C)]. M-CoCrMo copings exhibit a maximum positive deviation of 121µm at the focussed occlusal aspect internally [Figure 77, (C)]. The highest negative deviations were found at Focussed Cervical Sections externally [Figure 77, (E)]. Sections that need modification by removal of material also included the Internal Axial [Figure 77, (D)].

Table 15 Focused Results of M-CoCrMo sections

M-CoCrMo	Mean (SD), µm (n=5)
Focussed Occlusal External (A)	-49(17)
Focussed Occlusal Internal (negative) (B)	-77(9)
Focussed Occlusal Internal (positive)(C)	121(71)
Focussed Axial Internal (D)	82(18)
Focussed Cervical External (E)	-86(4)
Focussed Cervical Internal (F)	-54(11)

Table 15 shows localized areas of milled CoCrMo copings that were investigated in depth.

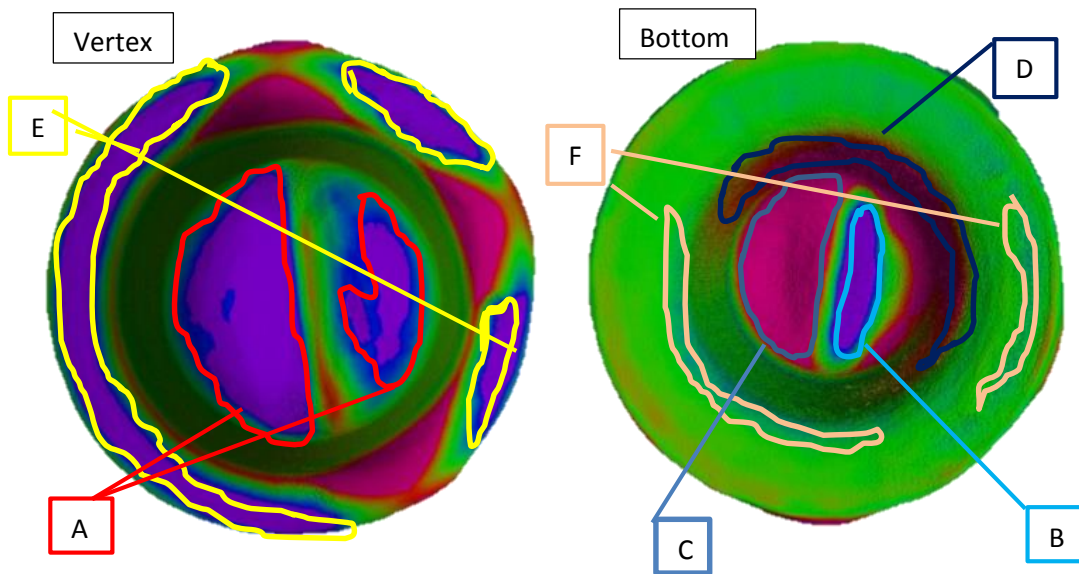


Figure 77 Focused Section on M-CoCrMo copings; Left Vertex View, Right Bottom View

5.4.3.3 ZAx3 Focussed Sections

All focussed area results of interest are listed in Table 16. For ZAx3 copings, the groove area was analysed because of it being an area occlusally that was not modified during fabrication. The four cusps seen internally and externally [Figure 78, (C, D)] gave results of 260 μ m and -292 μ m respectively (Table 16). Modification though can only be carried out externally at the focussed groove section [Figure 78, (A)] and focussed occlusal cusps external [Figure 78, (C)] as only that was positively deviated.

Table 16 Focused Results of ZAx3 sections

ZAx3	Mean (SD), μ m (n=5)
Focussed Groove External (A)	284(46)
Focussed Groove Internal (B)	-227(39)
Focussed Occlusal Cusps External (C)	260(36)
Focussed Occlusal Cusps Internal (D)	-292(30)
Focussed Axial External (E)	-11(5)
Focussed Cervical Internal (F)	-40(18)

Table 16 shows localized areas of milled zirconia copings utilizing 3 axis CAM machine that were investigated in depth.

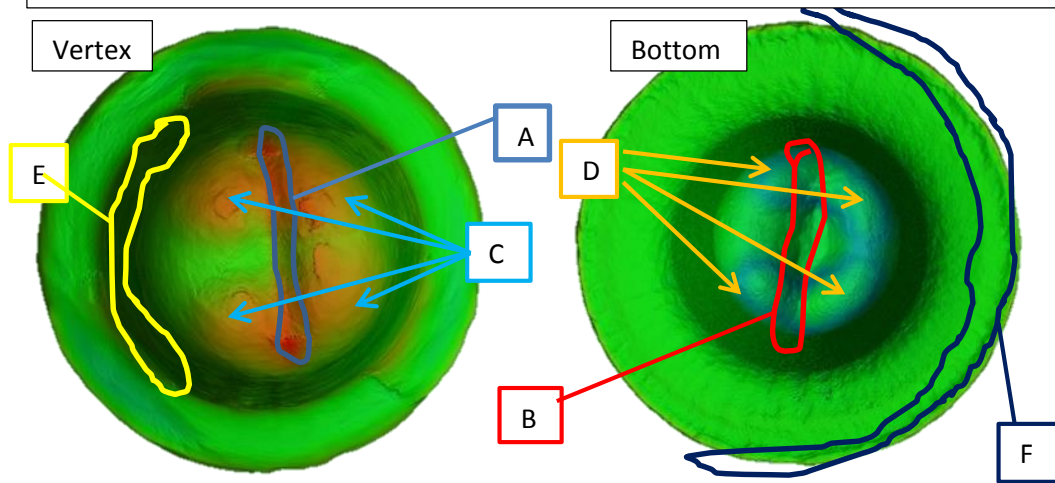


Figure 78 Focussed Sections on ZAx3 copings; Left Vertex View, Right Bottom View

5.4.3.4 ZAx4 Focussed Section

Results of Focussed areas of ZAx4 are shown in Table 17. ZAx4 copings have the smallest deviations to CAD when compared to the other groups, however the localised areas that do need attention remained highly deviated to CAD. Modification though can only be done at focussed internal section (Just lateral to the groove area) on occlusal shown in Figure 79, (B). At least 87 μ m removal is needed before fitting procedures were performed (Table 17).

Table 17 Focused Results of ZAx4 sections

ZAx5	Mean (SD), μ m (n=5)
Focussed Occlusal External (A)	-71(33)
Focussed Occlusal Internal (B)	87(15)
Focussed Cervical External (C)	-62(24)
Focussed Cervical Internal (D)	-31(20)

Table 17 shows localized areas of milled zirconia copings utilizing 4-axis CAM machine that were investigated in depth.

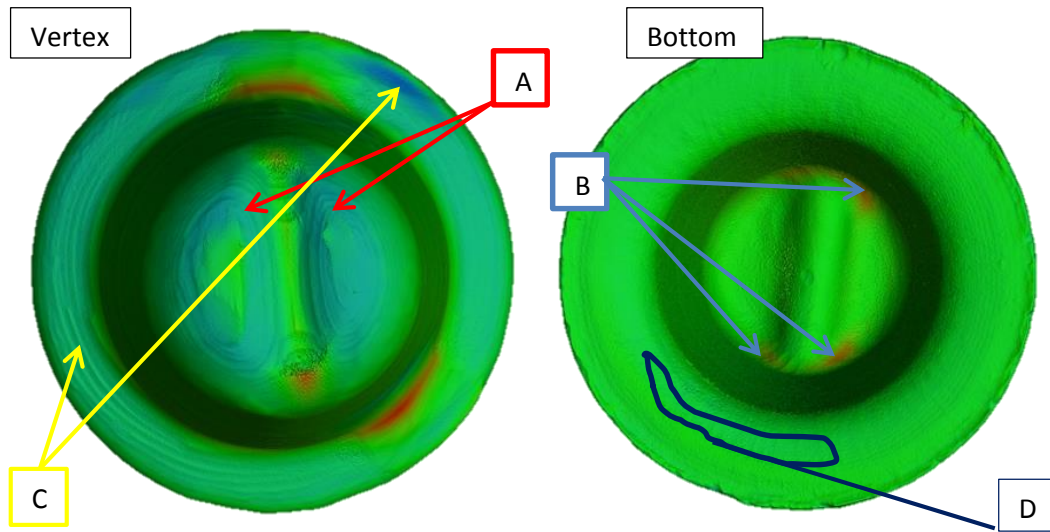


Figure 79 Focused Sections on ZAx4 copings; Left Vertex View, Right Bottom View

5.5 Alignment Analysis

5.5.1 Comparison of Internal Fit of Different CAM Fabricated Copings

Table 18 shows the mean results (n=250) of internal fit measurement from all copings made by different methods of CAM. ANOVA revealed significant differences ($p > 0.05$) of measurement points investigated between each group. A Post – hoc Tukey’s test ($\alpha = 0.05$) showed exactly where the differences lie within each group (shown with different superscript letter across the table). Only Vertical Marginal measurement of M-CoCrMo was found not to be significantly different ($p > 0.05$) from the CAD measurement.

The highest discrepancy readings were found at the Axio-Margin junction of all groups with the lowest findings found on the Vertical Marginal aspect of all group copings.

Table 18 Mean (SD) Internal Fit of Fabricated copings and CAD (n=250)

Mean (SD) Internal Fit, (μm)	LS	M-CoCrMo	ZAx3	ZAx4	CAD
Vertical Marginal	39(21) ^a	32(17) ^b	41(37) ^a	26(13) ^c	31(11) ^b
Absolute Marginal	66(22) ^a	48(19) ^b	98(26) ^c	46(21) ^{bd}	42(12) ^e
Axio-Margin	206(24) ^a	135(24) ^b	158(25) ^c	126(10) ^d	144(12) ^e
Axial	90(28) ^a	40(25) ^b	80(29) ^c	60(15) ^d	75(25) ^e
Occlusal	161(48) ^a	68(52) ^b	183(46) ^c	67(32) ^{bd}	111(23) ^e

*different superscript letters across the table show significant difference when compared ($\alpha=0.05$)

Table 18 shows the Internal Fit of all investigated copings. Note that only Laser Sintered Vertical Marginal fit of M-CoCrMo was comparable to the CAD.

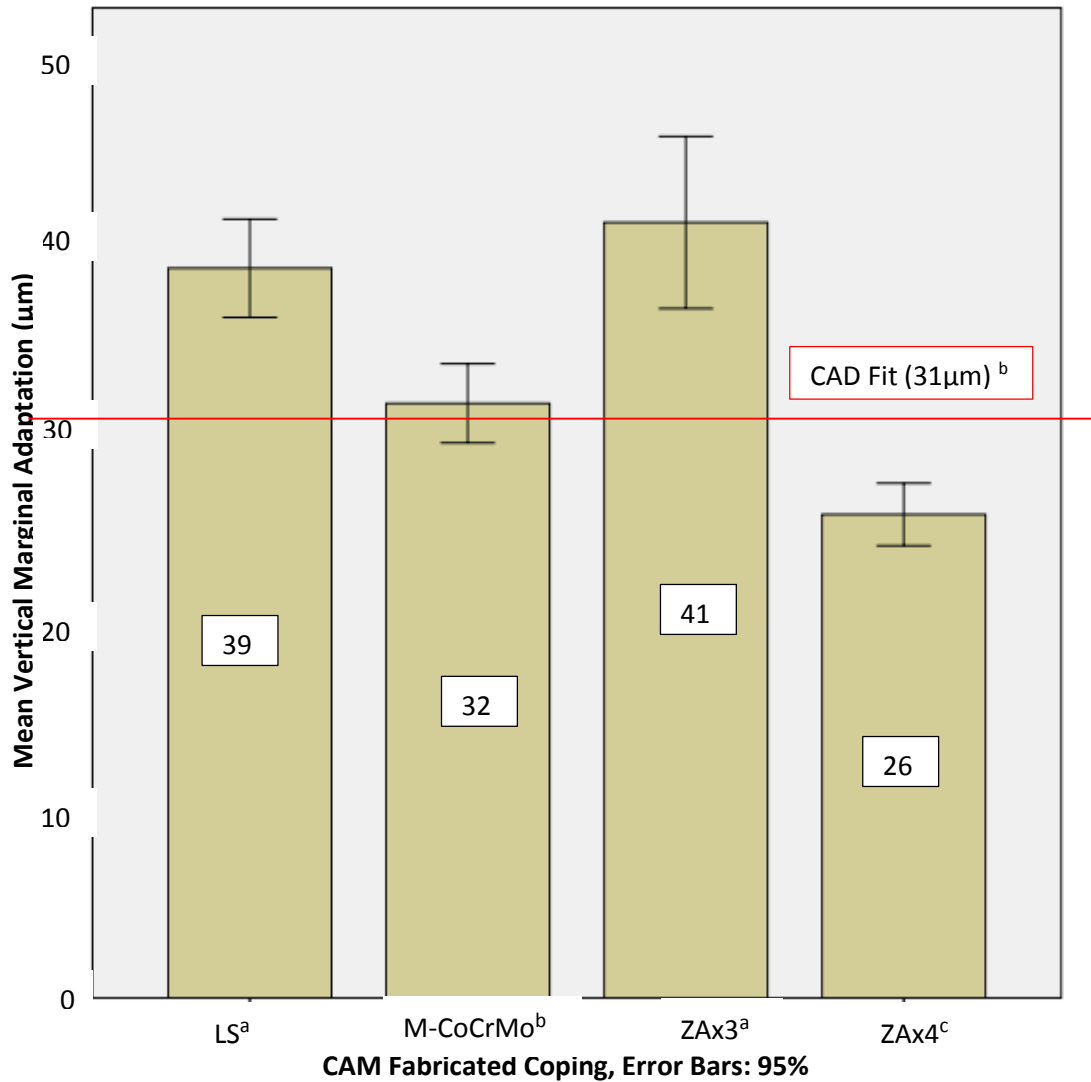


Figure 80 Mean Vertical Marginal Adaptation across CAM fabricated copings (Different superscript letters across graph show significant difference ($\alpha=0.05$), no comparison was made with groups with no superscript letters)

Figure 80 shows the mean results of Vertical Marginal Adaptations across different methods of CAM fabrication. ANOVA results ($\alpha=0.05$) between all the groups revealed statistically highly a significant difference ($p<0.01$). A post-hoc Tukey's analysis shows the LS to be comparable to ZAx3 at the marginal vertical adaptation.

In summary, the lowest Vertical Marginal Adaptation in order are ZAx4<M-CoCrMo<LS and ZAx3. One sample t-test showed that CAD fit to be comparable with M-CoCrMo. LS and ZAx3 Mean Vertical Marginal discrepancy was higher than CAD Fit while ZAx4 was lower.

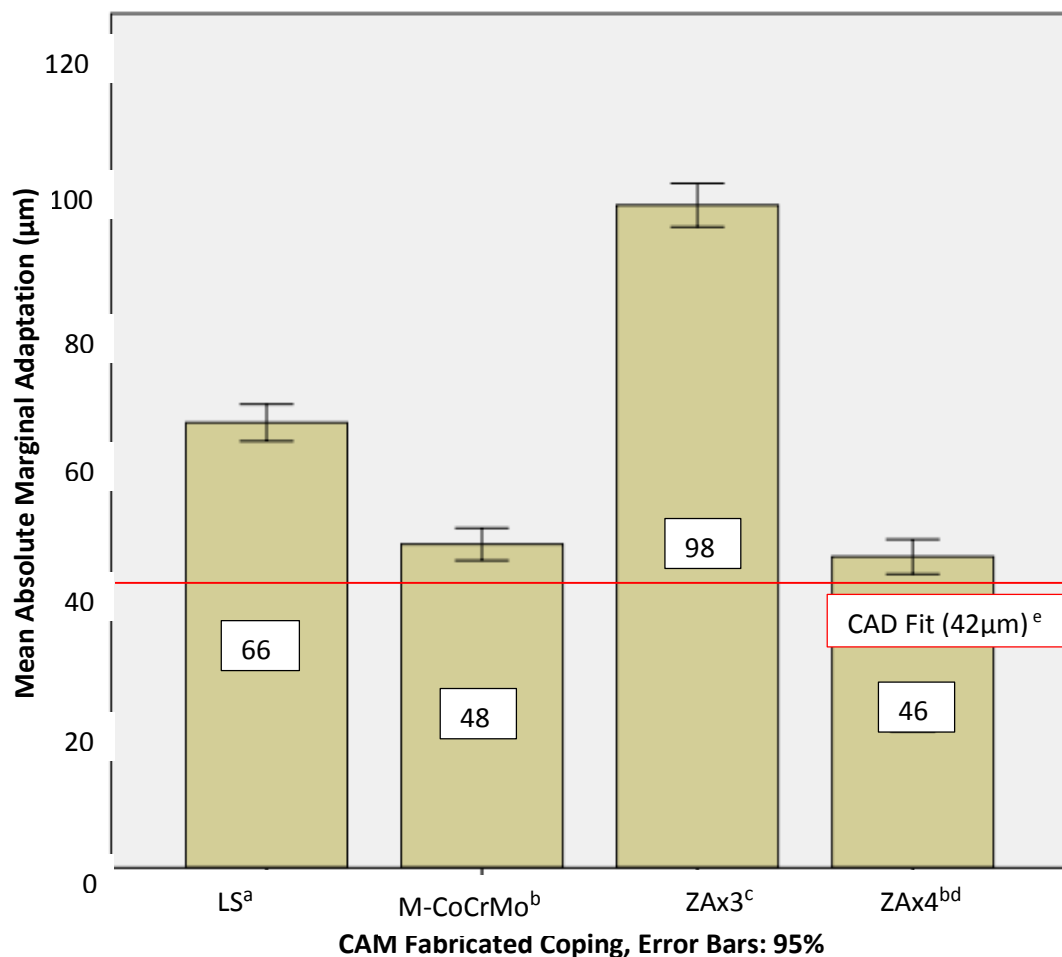


Figure 81 Mean Vertical Absolute Marginal Adaptation across CAM fabricated copings (Different superscript letters across graph show significant difference ($\alpha=0.05$), no comparison was made with groups with no superscript letters)

Figure 81 shows the Mean Absolute Marginal Adaptation across different methods of CAM fabrication. ANOVA shows a comparison difference between investigated groups ($\alpha=0.05$). A post-hoc Tukey's test shows that all group comparison were highly significantly different ($p<0.01$) with each other apart from comparisons of M-CoCrMo and ZAx4.

A summary of the lowest Absolute Marginal Discrepancy in order are ZAx4 and M-CoCrMo<LS<ZAx3. All groups of absolute marginal measurements discrepancy were higher than the CAD fit measurement.

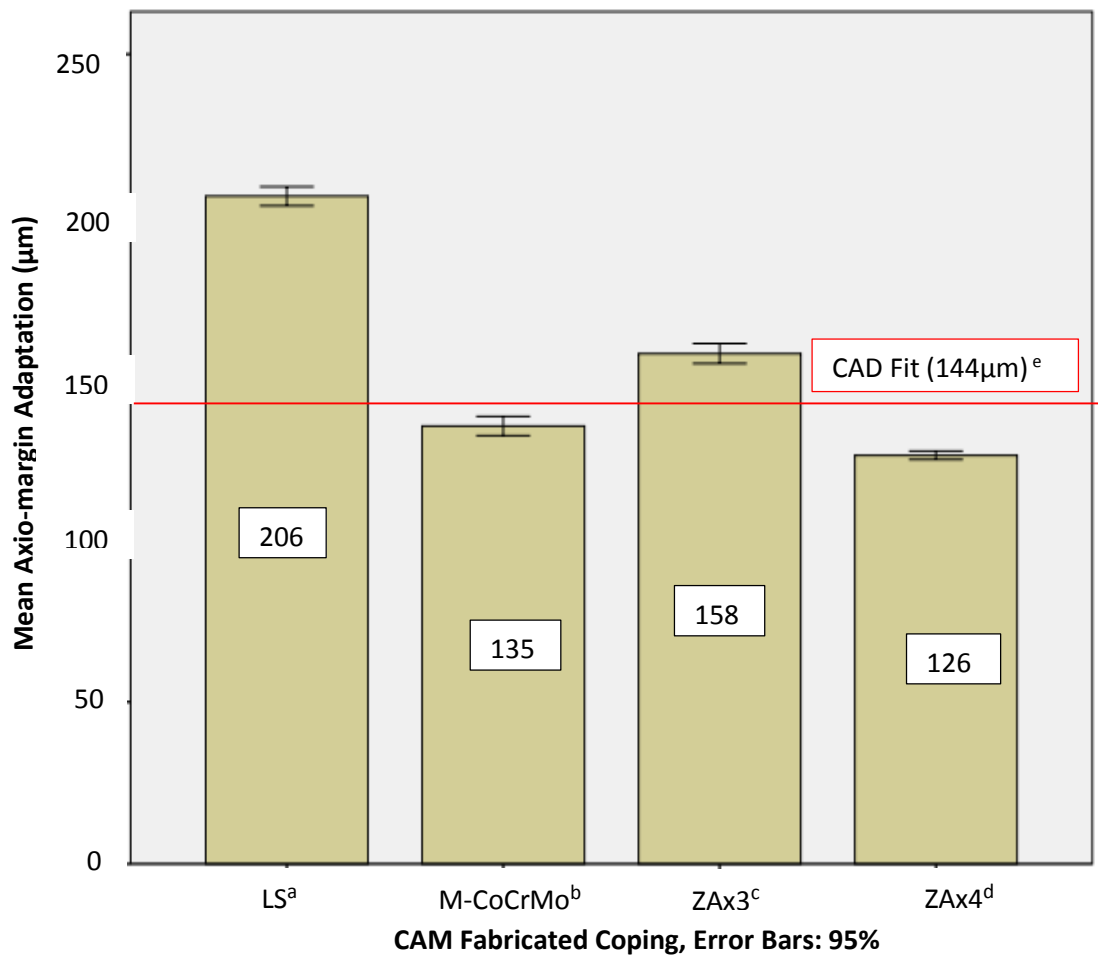


Figure 82 Mean Axio-Margin Adaptation across CAM fabricated copings (Different superscript letters across graph show significant difference ($\alpha=0.05$), no comparison was made with groups with no superscript letters)

Figure 82 shows the Mean Axio-Margin Adaptation across different methods of CAM fabrication. ANOVA gives evidence of a comparison difference between investigated groups ($\alpha=0.05$). A post-hoc Tukey's test shows that all group comparisons were highly significantly different ($p<0.01$) with each other.

A summary of the lowest Axio-Margin discrepancy in order are ZAx4<M-CoCrMo<ZAx3<LS. The Mean Axio-Margin Fit discrepancy of LS and ZAx3 was higher than CAD Fit while the M-CoCrMo and the ZAx4 was lower.

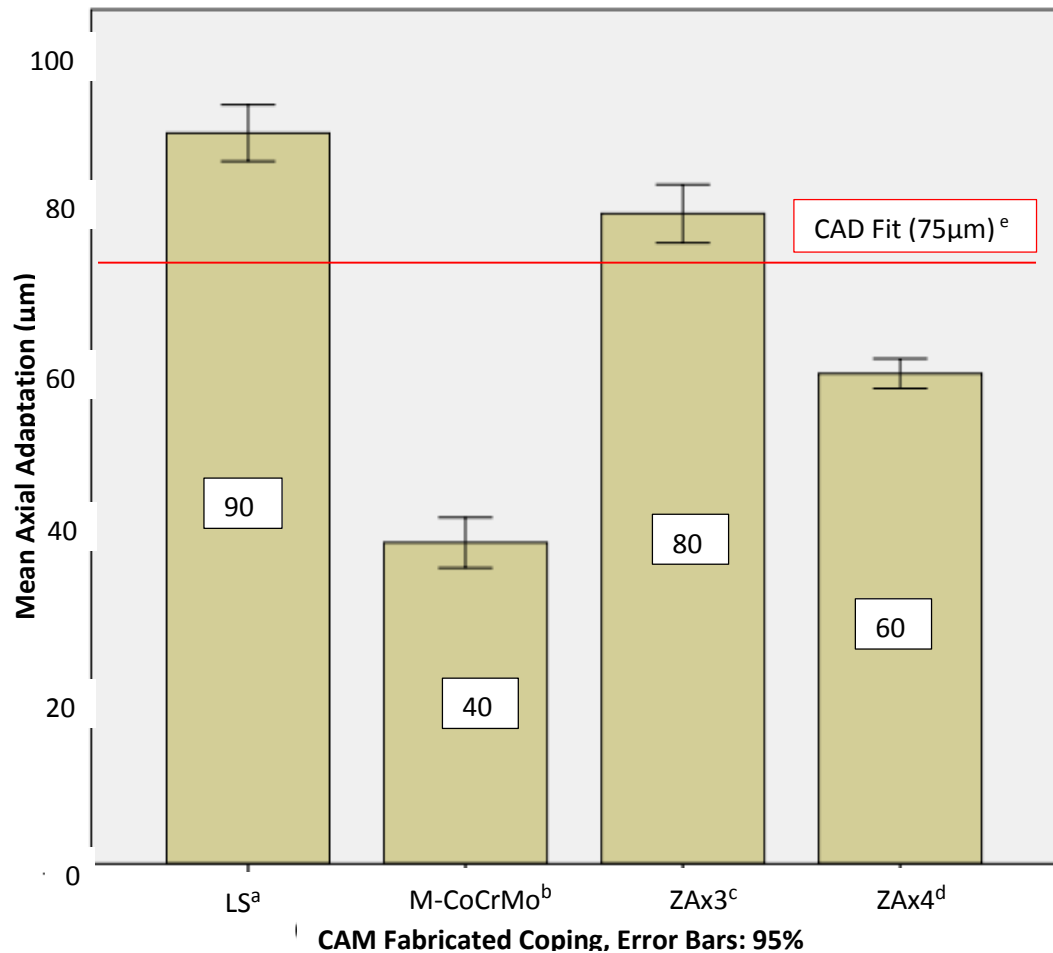


Figure 83 Mean Axial Adaptation across CAM Fabricated Copings (Different superscript letters across graph show significant difference ($p < 0.05$), no comparison was made with groups with no superscript letters)

Figure 83 shows the Mean Axial Adaptation across different methods of CAM fabrication. ANOVA gives evidence of a comparison difference between investigated groups ($\alpha = 0.05$). A post-hoc Tukey's test shows that all group comparisons were highly significantly different ($p < 0.01$) with each other.

A summary of the lowest axial discrepancy in order are M-CoCrMo< ZAx4<ZAx3< LS.

The Mean Axial Fit discrepancy was higher than CAD fit for LS and ZAx3 while the M-CoCrMo and the ZAx4 was lower.

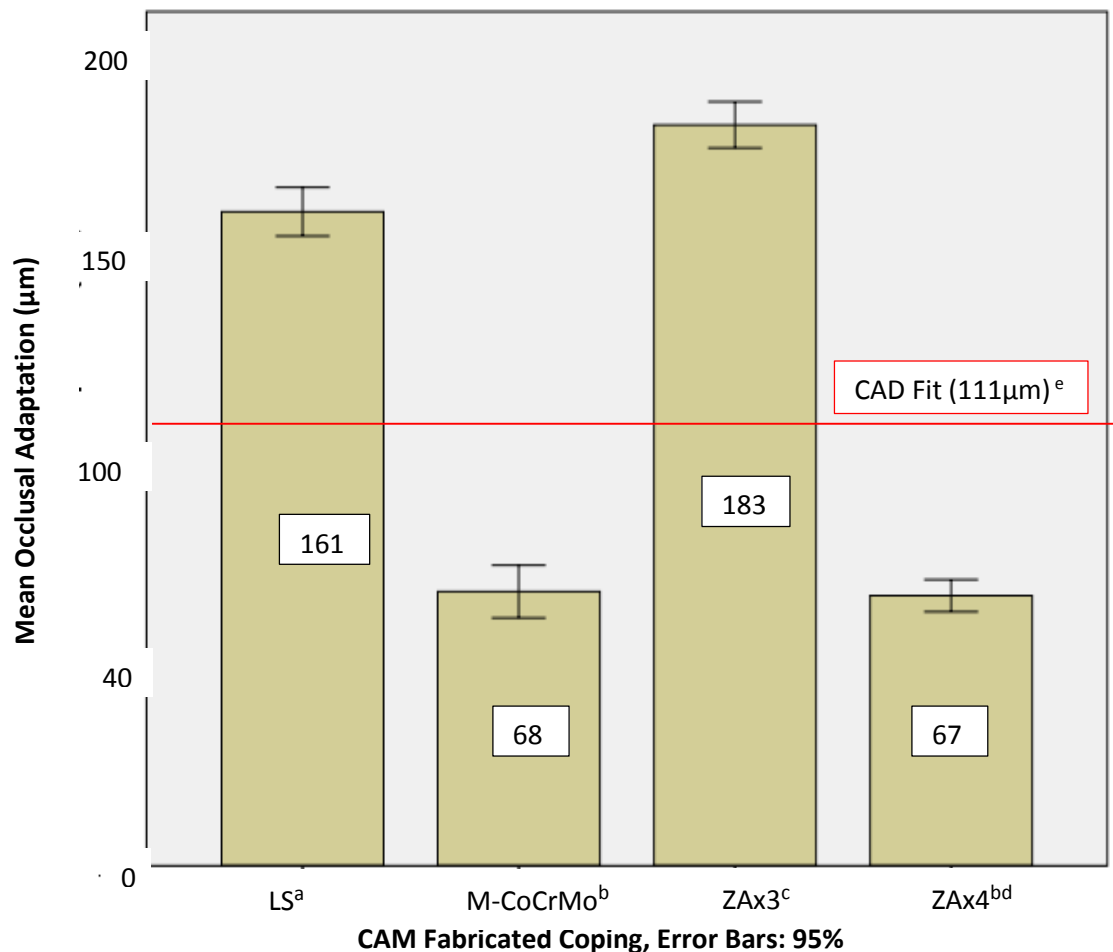


Figure 84 Mean Occlusal Adaptation across CAM Fabricated Copings (Different superscript letters across graph show significant difference ($p < 0.05$), no comparison was made with groups with no superscript letters)

Figure 84 shows the Mean Occlusal Adaptation across different methods of CAM fabrication. ANOVA gives evidence of a comparison difference between investigated groups ($\alpha = 0.05$). A post-hoc Tukey's test shows that all group comparisons were highly significantly different ($p < 0.01$) with each other apart from comparisons of M-CoCrMo and ZAx4.

A summary of the lowest occlusal discrepancy in order are ZAx4 and M-CoCrMo < LS < ZAx3. Comparison with CAD fit shows the LS and ZAx3 have higher discrepancy readings at Occlusal Fitting surface while the M-CoCrMo and the ZAx4 had lower reading than the CAD Fit.

Section 6

Discussion

6 Discussion

6.1 Volume findings

The original CAD volume was statistically different from all the groups of fabricated coping ($p < 0.05$). Interestingly, although evidence of surface roughness from LS copings was seen (Figure 62), an increase in volume when compared to the CAD was expected. However, a smaller volume when compared to the milling technologies group and the CAD was found (Figure 63). This meant that use of additive methods of CAM utilize less material for fabrication and is in accordance to findings that utilization of it produces less waste (11, 25).

The present finding of volume compliments the surface mappings tools to exhibit accuracy testing between CAD and CAM. The method for volume calculation and comparison proposed in the present study may be used for assessments of CAD/CAM accuracy in the development of dental CAD/CAM systems.

6.2 Linear deviations from CAD-Surface mapping

In addition to the importance of volume comparison in fabrication of accurate CAD/CAM copings, surface mapping of the distance from coping to the CAD is useful. This method displays the exact location of the excess or under fabricated coping areas. It will also indicate where modifications may be required before ceramic overlay or fitting procedures are performed.

6.2.1 LS Copings

In general, reports indicate that the surface layers on the occlusal part of laser sintered products are fabricated in excess due to surface roughness (71, 87). However, limited studies have been reported for dentistry (87, 88). This present study confirms this increased deposition on the occlusal aspect of the coping (Figure 65, Table 14). The excess deposition is more extreme on the external surface of the coping particularly towards the base exhibiting nodule like surfaces.

This is probably due to the mechanism of laser sintering in utilising multiple holders at the external surface of the base for fabrication purposes (89, 90). Further research is therefore needed to clarify this issue.

The angled areas on the external surfaces however show less deposition (Figure 65). Terrace like features are known to be present at angled areas (Figure 85) of items fabricated via additive methods of CAM (89) and this could potentially cause the deficiencies found (Figure 65). However this needs further investigations. The histogram that shows that most surface area of the LS copings is smaller in respect to the CAD (Figure 66) also support the volumetric comparison of the coping (Figure 63).

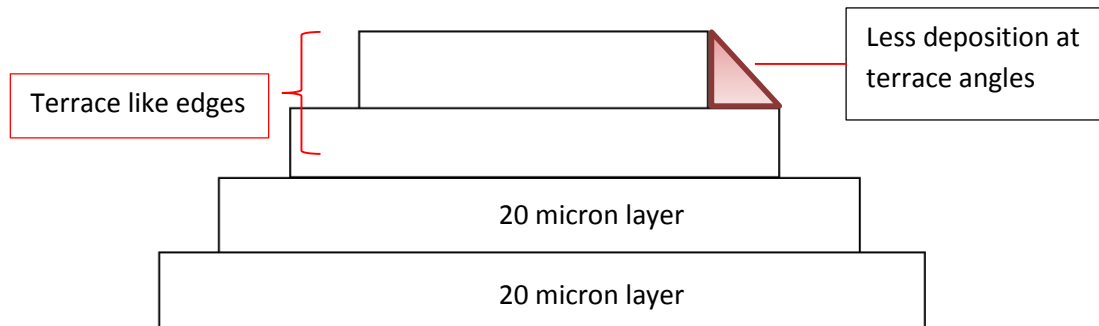


Figure 85 Layered 20 micron deposition of material occlusally utilising laser sintering mechanism

6.2.2 M-CoCrMo Copings

Milled cobalt chrome copings display areas on the axial external aspect that show increased thickness of material (Figure 67). These areas were utilised as holders of the coping during milling. The holders were ground off on completion of the milling procedure. Any excess grinding would alter the wall thickness of the coping wall thus a small amount of material was left to avoid over grinding. The external surface mapping (Figure 67) showed that the occlusal surface of the copings was made smaller than the CAD. The results (Figure 67) suggest that excess milling was performed especially on the occlusal surface. The angled areas of the copings though were similar to the CAD. This is probably due to the master design (fillet angles of 0.6mm) and ability of the smallest bur (0.6mm) in accessing that section of the design to remove material.

A histogram (Figure 68) of milled copings showed data that were skewed to the right indicating enlargement of the copings. This was in contrast to the laser sintered copings where it was skewed to the left (Figure 66). This also supports the volume

findings (Figure 63) where the M-CoCrMo copings were found to be larger than the CAD.

6.2.3 ZAx3 Copings

The 3-Axis milled zirconia copings exhibited a striation-like appearance on the external surface of the coping. This was most likely due the use of small round burs to mill the design. In contrast to cobalt chrome which is hard, zirconia in its pre-sintered form is soft. The bur shape is seen on the external surface as the material was easily penetrated. However, results relating to the occlusal aspect of this coping must be treated with caution. The Incise CAM was used to mill this design and the system initiated its own software correction causing a ballooning effect on the output. This was also evident on the micro-CT results thus explaining why high readings were established (Figure 69).

Ballooning is a CAM compensation where the CAM software locally modifies the CAD in an attempt to maintain minimum coping thickness. The modification occurs at sharp corner points where the smallest available tool due to its radius will still result in removing more material from the internal surface than the design dictates. A balloon is therefore created on the respective external surface to compensate for the minimum thickness at that point (Figure 86).

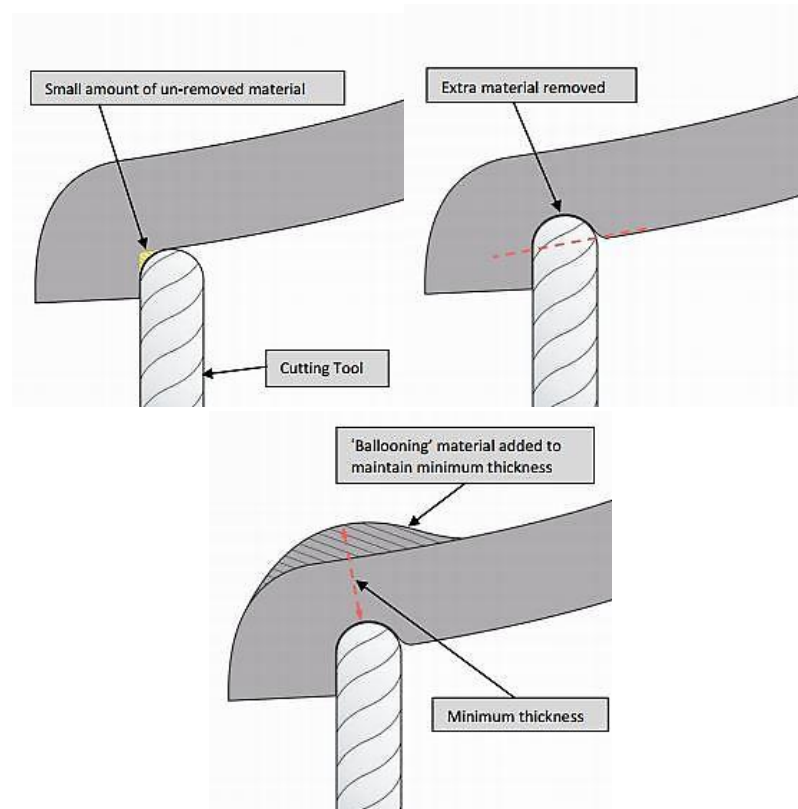


Figure 86 Ballooning effect on machined dental copings (Figure from Renishaw)

Nevertheless, it does reveal the CAD/CAM limitations on receiving a complex design for milling. The smallest bur diameter utilised was 1mm which resulted in the CAM aspect to mill a 0.5mm radius angle. Our design incorporated a 0.6mm radius angle on the occlusal groove. This means that Incise CAM via millings does not follow closely the existing design if fabrication of it was performed. However, results (Figure 69) on the simple areas of design (i.e. axial and cervical) were relatively similar when compared to the original design (<45µm deviation).

With respect to 3 axis-milling in zirconia, a histogram (Figure 72) of the deviation results shows that most of the data were close to zero deviation from the CAD. This

represents closeness to original design. However, a lot of repairs and modification was needed especially at the occlusal sections where 280µm needed to be removed externally (Table 16) to maintain thickness of ceramic layer. Volume results which showed zirconia copings that were made larger than the CAD (Figure 63) and may be explained by the ballooning effect occurring.

6.2.4 ZAx4 Copings

Zirconia copings milled with the 4-axis CAM were closer to the designed data as opposed to other fabrication methods. The extra axis seem to allow the bur to reach more complex areas of the design (e.g. occlusal grooves) (91). Similar to 3-Axis milling, fine striations were evident in surface mapping results of the micro-CT on both internal and external aspect of the coping (Figure 74). The excess material on the axial aspect of the external surface should again be neglected due to it being where the holder was located for the milling procedure to occur. The occlusal aspect showed a localised deviation from CAD (200µm). Similarly to 3-axis milled zirconia, the histogram (Figure 75) showed closeness to the original data. However the volume results (Figure 63) of the ZAx4 which was closer to the original CAD file, means that this was more accurate.

6.3 Comparisons of Superimpositions

6.3.1 Comparison of Linear Deviations between fabricated copings with CAD

The LS coping fabrication component (AM250, Renishaw, UK) has reported a manufacturing tolerance of 20µm (90). The micro-CT uncertainty (measurement by pixel/2) was 8µm and was better than the manufacturing tolerance provided. This provides an accurate high resolution analysis when measurements were made with micro-CT. Any results above 20µm deviation however should be investigated as that would mean that the restoration was fabricated outside the manufacturing tolerance of the manufacturer.

Sectioned areas of results (Table 12) were performed to obtain a more fundamental understanding of fabricated copings. Negative results (Table 12) suggest that LS copings need to be fabricated larger to maintain the wall thickness and conformity with the CAD before cementation of the restoration were performed. The internal aspects of LS copings (axial and occlusal) were also negative with respect to CAD which results in a passive fit (Without alteration of the inner coping). If the CAD fitting surface has already had a 70-100µm micron relief, the negative readings of the internal gap would add to the relief given.

In contrast to LS, the internal aspect axially and occlusally of the M-CoCrMo coping was larger (<54µm) than the CAD (Table 12). With a predetermined cement space of

70-100µm, a perfect case scenario would suggest a cement space of 24µm to be present on the internal axial aspect (70-54µm). This suggests a very tight fit axially. Cement space recommendation is dependent upon material use for cementation (92). ADA Standards recommend a type I luting agent (Zinc Phosphate) for a cement space of lower than 25µm (92). Results of this present study suggest the use of type II (Resin Based Cement) luting agents be utilised. If 100µm cement space was simulated, the anticipated cement space would be 54µm. However, a type II luting agent requires cement space of a maximum of 40µm and possible excess may result in loss of cement physical property (93). Another possible method is to alter our CAD or strategy to get a better result in terms of space for luting cement layer.

As for ZAx3, a good fitting accuracy may be suggested if the occlusal aspect was ignored. If results of the occlusal analysis were taken into consideration (Table 16), 280µm would have to be removed externally for any ceramic material to be applied on the coping. If not a heavy occlusion could occur or perforation of ceramic material could happen upon finishing restoration excess removal procedures. Thinning of the occlusal part of zirconia also would influence zirconia physical properties as the minimal recommendation thickness of zirconia is 0.5mm (94). In addition, increased thickness of cement will affect retention of the restoration (93). It is therefore suggested that use of a 4-axis milling apparatus may be more beneficial if the design of the restoration was similar to our design.

ZAx4 sectioned results (Table 12) showed less material fabrication on all sections except the axial. However the minimum and maximum results had a wide range indicating some areas with large deviations from the CAD. A more focussed analysis was thus deemed necessary.

6.3.2 Comparison of Linear Deviations of CAD between Groups Investigated

A comparison between additive and subtractive method of CAD/CAM can be done by comparing LS and M-CoCrMo. LS copings however showed smaller fabrications when compared to M-CoCrMo copings ($p < 0.05$) at all aspects of the fabricated coping except for the internal cervical.

A comparison could be made with regards to the milled 4-axis zirconia (ZAx4) with milled 5-axis CoCrMo (M-CoCrMo). Although the same master design was utilised, the CAM method was different due to unavailability of the same system to mill both materials. Milled zirconia copings were made bigger to accommodate the 25% shrinkage that happens when final sintering procedures are performed. In terms of volume, milled CoCrMo was larger when compared to zirconia.

A comparison of CAM milling with different axes could be performed with two groups of zirconia copings (3-Axis and 4-Axis). The 3-Axis milled copings were summarised as being bigger externally however smaller internally on the occlusal aspect.

However, the relevant results have to be treated with caution as the ballooning effect on the occlusal aspect with the 3-Axis copings may have biased the findings (Table 13). The original central groove which mimics a 2 cusp premolar was seen as a 4-cusp premolar because of this effect although procedures (Making a 0.6mm rounded edge on all edges of the design) were taken to avoid this.

In terms of volume, the focused analysis of the occlusal section may have also influenced the results of a higher volume when compared to copings of 4-Axis milled origin (Figure 63). Comparison was only meaningful at the groove aspect of occlusal section as it was the only place with a constant design. A significant difference was found at that section ($p < 0.05$) concluding that a 4-Axis milled zirconia had a better accuracy to its design.

In general, the 4-Axis CAM displayed a better overall comparison with the CAD (Table 12, Figure 63) when compared to the 3-Axis technique. Although the two methods utilize the same strategy of first making the external aspect followed by milling the internal aspect, the extra axis enabled the coping to be rotated and fabricated more specifically at the angled areas of the design. If the master design had no angles, looking like a rounded coping with no angles and no grooves, the 3-Axis CAM would have been sufficient to reproduce the desired design. The coping could be rotated once (180 degrees) to fabricate the area with no concerns of undercuts or angle.

However due to the relative complexity of the master design, a 4/5-Axis CAM was more suitable. The extra shift in angle could thereby help reach the areas of concern (angled and undercut) and mill it. Nevertheless, both methods displayed smooth surfaces on copings after full sintering procedures. Due to milling burs being round, striations were observed on the surfaces (Figure 71, Figure 74). Smaller burs were utilised to surface finish the coping, however the striation appearance was still evident on the micro-CT images.

Some dental CAD/CAM manufacturers (10, 11) utilize 3-Axis CAM machine. In the present study, need for repairs and modification was observed with such a system. With that in mind, the use of a 4/5-Axis milling machine is suggested when a complex design is sought i.e. occlusal groove, proximal groove or implant brackets (91).

6.3.3 Focussed Results

A more detailed analysis was performed on LS copings especially at the areas with a higher deviation from the CAD. This included the angles especially on the external surface of the coping (Table 14).

For the LS copings, the results were greater in an absolute sense than the cumulative results (Table 14). Studies have shown that a gap of 120µm in marginal fitting is clinically acceptable (57). However a gap less than 100µm is hard to detect clinically

thus any differences of $>100\mu\text{m}$ will have to be investigated. Nevertheless, a deviation of more than $\pm 120\mu\text{m}$ is alarming which in this case is in abundance (Figure 66). A maximum of $110\mu\text{m}$ is thereby suggested to be removed occlusally before application of ceramic layer is performed on LS copings (Table 14). This is to prevent a high occlusion and to maintain enough space for ceramic overlay.

For M-CoCrMo copings sectional and focussed analysis of the excess material fabrication internally (Shown as positive results in Table 12 and Table 15) showed that the coping needs to be adjusted by grinding before fitting the coping to the master model/tooth was completed. Data (Table 15) of results showed that the inner axial aspect is the location for adjustments by grinding. The recommended thickness of copings within dental alloys were 0.22mm (95). Due to thickness of 0.5mm which was predetermined earlier, results (Table 12) showed that only small removal ($<60\mu\text{m}$) of sectioned areas of the coping was needed to resemble the original CAD. Thus material removal on the occlusal or external aspect may be performed.

For ZAx3, the main difference that needs modification (Table 16) by grinding was found to be on the occlusal aspect as explained earlier (See 6.2.3, 6.3.1, 6.3.2).

ZAx4 was the closest to the CAD; however the internal aspect of the Occlusal surface would still require modification through grinding (Table 14 and Table 17). Qualitative maps reveal that the only place that needs to be modified was essentially lateral to

the grooves made on the occlusal section. This suggests that repairs are needed only at complex areas (groove areas) within this design if a 4-Axis dental CAM was utilized.

Table 14-18 displayed results that showed positive and negative deviations. Clinically the positive deviations can be ground away. However no modifications can be done on the negative deviations. Therefore the results of the present study may aid in development of the CAD/CAM. Knowledge of the location of the differences may be used to aid this development. In addition, the negative results mean that fitting of copings to the master model will be passive however if results of negative aspects were evident, the restoration might be loose.

6.4 Internal Fit

Internal fit was measured digitally by placing the micro-CT scan fabricated coping on top of the micro-CT scan of the master aluminium model of the die. Placement was performed manually with the aid of zooming tools and by utilising the central groove for referencing. Alignment was defined as visual on contact of both models. However, the procedure might introduce inaccuracies during the alignment procedure. Therefore, five measurements of the same coping were made to determine repeatability of the method (See 3.1.3.1.) No significant differences were found between each measurement (See 3.2.3.1).

Other studies actually removed sections of the internal aspect of the coping first before placing it on top of a model and measuring fit (53, 96). This study presented a novel method of internal fit measurement by placing the scanned fabricated coping on top of the master model digitally. Studies within dental CAD/CAM applications have reported an occlusal and axial internal fit for fixed dental restoration of less than 300µm and 80µm respectively (36, 83) and the findings of this present study report similar tolerances (Table 18).

It was suggested by Groten *et al.* (2000) that the minimum measurement required for a marginal fit in vitro testing was 50 measurements (97). This present study is in accordance to their use of a minimum of 50 measurements for a meaningful result.

6.4.1 Comparison of Internal Fit Results with Literature

The lowest gaps reported for all groups were at the vertical marginal aspect (Table 18). The CAD fit at the Vertical Marginal aspect was only comparable to the M-CoCrMo although the lowest reading came from the ZAx4 group [26(13) µm].

The highest mean reading though came from the Axio-Margin aspects of all groups with the highest reported for LS (206µm) and lowest ZAx4 (126µm). Either way both of these results were more than the recommended internal fit of 120µm (57).

No studies were found to compare internal fit of dental alloys fabricated by Incise, Renishaw and CybaDent, CybamanTech dental systems. Very few studies have investigated fit of cobalt chrome fabricated by use of CAD/CAM. Ucar *et al.* (2009) reported a mean gap of 58.21µm for laser sintered cobalt chrome on a PHENIX CAD/CAM system (71). However the author did not specify area of fit. Nevertheless, the LS result in this present study (Table 18) is in concordance to their findings in terms of absolute marginal adaptation (66µm).

The results in this present study (Table 18) however, are in contrast to Ortorp *et al.* (2011) with regards to findings of a milled cobalt chrome vertical marginal height (88). This study reported a 32µm gap where as their study reported 185µm and 220µm. The difference could be due to use of a 3-unit framework (premolar-molar) in their study while this present study used a standard premolar design. Selection of measurement points may also affects results. The mean internal fit of milled CoCrMo though was reported higher (163µm) than all of this present study milled CoCrMo internal fit results (max: 135µm) .However their LS results (36) were comparable to this work (Table 18). Nevertheless a direct comparison could not be completed due to different parameters being utilized. This present study is also in accordance to results of Quante *et al* (2008) where they report a laser sintered cobalt chrome marginal gap of 73µm (66).

Attempts to measure marginal fit of ceramic copings utilizing micro-CT have been limited (16). Pelekanos *et al* (2009) reported that In-Ceram alumina ceramic coping mean vertical marginal adaptation using micro-CT value was 55µm (76). The difference to this present study was that the authors utilized a new design for each fabrication of a restoration while this study only utilizes a single master design. The results however was in accordance to the 3-Axis (Incise, Renishaw system) and 4-Axis (CORiTECH, Imes-Icore system) milled zirconia results of the present study which were 41µm and 26µm respectively. Results of mean absolute marginal discrepancy of the present study though was 46µm less when compared to the CEREC inLab system of 179µm (76) for the ZAx4 (Figure 81). This may be due to the use of a 3 Axis CAM machine that was utilised at that particular time for CEREC in Lab system. The results of this study of 3-Axis milled zirconia also showed high discrepancy (98µm) which was similar to their study (76) supporting information that the use of a 3 axis-milling machine produces high marginal discrepancies.

Borba *et al* (2011) reported pre-sintered and fully sintered In-CERAM zirconia copings of 79µm and 99µm respectively but both displayed higher readings when compared to this present study (Figure 80) (83). This could be due to the use of bridge framework for analysis but reported the abutment as individual data.

The report of a single abutment result to display mean data of the fabricated copings were investigated. The results may have achieved results with good fit due to the use

of a single unit for investigations. This was in accordance to findings that single crown results having better fit than fit of framework (98). Procera single zirconia copings were reported to have mean axial fit of 106 μ m, mean vertical marginal height of 51 μ m and mean absolute marginal height of 86 μ m (99). The result of mean vertical height from their study was comparable to mean vertical marginal adaptation results (Figure 80) of the 3-Axis and 4-Axis fabricated zirconia 41 μ m and 26 μ m of this present study. However, the results of mean absolute marginal adaptations of this study for ZAx4 (46 μ m) and ZAx3 were in contrast to the mean absolute marginal adaptations results of Grenade et al. (2011) study. The results of ZAx3 (98 μ m) though were similar to their respective study. Results (Figure 83) of mean axial of both 3 and 4 Axis milled zirconia were better than the Procera report (80 μ m and 60 μ m respectively) (100). This could be due to the methodology of not grinding the internal aspect before fitting procedures as in this present study method relied on digital placement.

A comparison between milling in different materials of cobalt chrome (M-CoCrMo) to zirconia (ZAx4) can be performed. All sections of results of ZAx4 were significantly different from other groups with the exception of Absolute Marginal Adaptation and Occlusal Adaptation with M-CoCrMo (Figure 80). The comparisons showed that milling with Zirconia (ZAx4) have less discrepancy when compared to milling with Cobalt chrome (M-CoCrMo).

Fabrication technique comparison can also be performed with additive method of cobalt chrome molybdenum coping (LS) and milled cobalt chrome molybdenum (M-CoCrMo). Results (Figure 80) of M-CoCrMo copings having a better marginal fit than the LS copings would agree with a study (88) of the additive method of having higher occlusal readings. All other sections also favour the M-CoCrMo when compared to the LS with less discrepancy in Internal Fit measurements. However results (Table 12, Table 14, Table 15) of CAD deviations showed that internal aspect of CoCrMo copings need to be trimmed first before fitting can occur. The LS copings would provide a passive fit.

The comparison of axis usage may be performed by comparing internal fit 3-Axis and 5-Axis milled zirconia. On all of sections of measurements, the ZAx4 significantly has less gap discrepancy from the master model ($p < 0.05$) than the ZAx3 (Table 18, Figure 80-95). The results showed that (Table 18) that 4-axis milling improves Internal fit of copings including the margin areas, in contrast to Ortorp *et al.* 2011 (11). However, utilisation of 4-Axis CAM exhibited a tight fit with milled zirconia and is also similar with 5-axis milled cobalt chrome (Figure 70 and Figure 73). This translates to focused areas internally needing removal through manual adjustment procedures before fitting of copings can be performed. It may also explain why results were similar in two sections of measurements between M-CoCrMo and ZAx4.

No studies were found to compare data of the Renishaw and Imes-Icore fabricated zirconia copings. Nevertheless, this present study results (Figure 80-92 and Figure 83-95) showed that both systems fabricate acceptable coping comparable to other systems in dentistry in terms of marginal fitting accuracy.

6.5 Clinical implications

Studies showing marginal fit of CAD/CAM fabricated copings are well documented. Most studies however alter the internal aspect of the copings before fitting procedures and analysis (53). The present study showed how much that internal aspect needs to be modified and where the locations are for all groups of copings.

If internal aspects of coping were adjusted, the present study revealed that vertical and absolute marginal fit would be acceptable due to good fitting accuracy (<100micron). If vertical marginal adaptation was measured, all results (Figure 80) suggest the use of zinc phosphate for cementation procedures following American Dental Association (ADA) guidelines for cementation procedures (92). However, more clinically relevant results would be the absolute marginal discrepancy in which readings were from 46-66µm. ADA recommends the use of resin based cements for cementation procedures can be carried out for results of this present study. Only one group was reported a marginal discrepancy of 96µm which was the 3-Axis milled zirconia. This was still below the acceptable marginal fit threshold of 120 microns (49). LS reports were similar to related studies in terms of occlusal findings but may

aid in passive fitting due increased gaps on the internal fitting surface for dental restorations (42).

6.6 Limitations of Study

6.6.1 Universal Master Model Design for CAD/CAM studies

The present project utilised a design with deep 1.5mm shoulder margins on a model with dimensions of a suggested lower premolar for fabrication of the master model. Currently an ISO standard is under construction in dental CAD/CAM: ISO/CD 18845 (Dentistry-CAD/CAM systems - Accuracy of machined indirect restorations -Test methods and marking) (101). This standard may allow accuracy testing of CAM and may not match the standard used in this present study. The design was not a standard preparation for ceramic restorations, hence future development of the technique might include the use of a heavy chamfer design. Emphasis must be given to a design that could accept a universal material in terms of crown preparation.

However, the only available standard related to dental CAD/CAM at the moment is ISO 12836:2012 which is a standard specifying test methods for the assessment of accuracy of digitizing devices for CAD/CAM systems for indirect dental restorations (102). This document can be utilized for testing accuracy of the digitizing device but does not specify use for CAM accuracy testing. Nevertheless, the model design respects the standard design the available in the above said document and was utilized for this present study.

A 0.6mm fillet (rounded edge) was fabricated on all edges of the design. This was to ensure that effects of ballooning are avoided from all manufacturing tolerances. The 0.6mm fillet would allow a possible use of a 1.2mm bur diameter as the largest bur for machining purposes. However the present study demonstrated that this compensation was still not sufficient to avoid ballooning effects by milling procedures.

The design for laser sintering methods of CAM does not feature this effect due to its additive method of fabrication (103). It fabricates the coping layers without using cutting tools. Sharp corners can therefore be accommodated in the design and no ballooning compensation needs to be applied. Thus this will allow any complex design to be fabricated. In addition, the universal model design adopted can allow different materials to be tested including zirconia and polymers. Hence this may be used as a standard design for CAD/CAM prosthesis investigations.

6.6.2 Design Limitations

The Master Design was created by using the InciseCAD (Version 2.5.0.140, Renishaw, UK). InciseCAD utilised a 1mm ruby ball contact scanner to record the surfaces of the master model and simulate it on software. Due to the accuracy of mechanical digitizers, Persson and colleagues utilised the scanner for creation of reference models to compare scanners and study models (47, 104).

However, contact scanners exhibit a 0.5 kg/N force on the scanned model which may lead to deformation of soft materials (26). In the present study, the master model was fabricated in solid aluminium so this effect was expected to be negligible. It would therefore appear reasonable that use of contact scanners would be preferred over non-contact scanners for creation of a Master CAD due to the accuracy it provides. The accuracy of the Incise scanner was also in accordance with international standards for Coordinate Measuring Machine (CMM) Accuracy Testing and Performance Verification (ISO 10360-4) and is accurate to within 20 μm (According to manufacturer).

The CAD that was fabricated was saved as surface models in Stereolithography (STL) format. STL format is a collection of triangular faces that are joined together along the edges. The scanner utilizes data points gathered from the digitisation process to create these triangles by connecting the points together. An increase in sampling points improves construction quality of the original 3D model (105).

However, automatic point distribution may have irrelevant or missing points due to smoothing constraints (105). An increase in density would not be beneficial if the increase was not localised to areas of interest (e.g. margins). STL is a common format for exchange between CAD/CAM applications (106). The increased data point does not affect the method of measurement utilising the micro-CT (See Sections 3.1.3.4

and 3.2.3.4). Although the procedure attempted to standardize data points to 60 000, no data points were deleted or reconstructed from the original 120 000. A thinning mesh procedure was performed which essentially hid points. This then makes the creation of triangles for triangulation procedures larger. Little or no difference would occur due to reason that only original points were being utilised (107).

6.6.3 Fabrication Limitations

The present study utilized one master CAD. It was then fabricated with different materials and techniques. Comparisons of fitting accuracy of CAD/CAM appliances are thoroughly investigated. However, most studies utilized their own digitization process and created a CAD using their own specific CAD software (88, 108). Variability in the digitization process and CAD is evident (106). The present study attempts to control this variation that may have effect on results.

Comparison between the subtractive and additive method of CAM were performed by comparison of fabricated cobalt chrome copings. Utilisation of the subtractive method may decrease in cost effectiveness of CAM in fabrication because the wear life of milling burs utilised was reduced (83, 109). As a result, constant replacement of milling burs was required. The Cybaman Replicator was one of the few CAM systems (etc. Origin Pro, Ceramill) that allowed milling of a dental alloy including cobalt chrome.

Milled copings utilising the 3-Axis versus the 4-Axis machinery was investigated. A paper by Beuer *et al.* (2008) concluded that no quality difference was evident when the two CAM systems were compared (11). However the paper related more to the fitting accuracy of fabricated restorations. The fitting of the fabrication to the original CAD were not mentioned. No direct comparison was available in the literature.

However, complex design (undercut areas, small grooves) was better replicated with a 4-Axis CAM when compared to a 3-Axis CAM (91). Use of 3-Axis CAM was sufficient for simple (No grooves, undercuts and proximal box) dental restorations (91). CAM accuracy was dependent on the strategy used for fabrication of the coping. Only companies with dental background were utilized for the present study. This was to mimic a real setting of a dentist-technician scenario where the teeth were scanned, the coping designed and saved as an STL file before physical copings were manufactured and returned for clinical fitting procedures. This suggests that common strategies for fabrication of dental copings/restorations can be utilised (See 1.1.5.1).

As for zirconia, final sintering procedures of the copings were performed by the respective manufacturers. The original design was made specifically for laser sintered cobalt chrome copings and saved as STL format. Dimensional change could not occur due to the format being utilised. Because of this the design had to be enlarged (performed by manufacturer Renishaw and Imes I-Core) 25% in the software to

compensate for the firing shrinkage upon sintering. This is a common procedure within Zirconia CAD/CAM fabricated restorations. Milling after the sintering stage is not cost effective (108), but reports have shown to provide better fitting accuracy (108). Nevertheless, in the present study, it was attempted to mimic the most common fabrication of zirconia milled copings which is in the pre-sintered form.

6.6.4 Micro-CT Limitations

Micro-computed tomography was utilised in the present study as a dimensional analysis tool to test the inconsistencies between CAD and CAM. Very few attempts have been made in the literature to utilize micro-CT in restorative dentistry (80, 81). Restorative dental studies that utilize micro-CT have looked into cementation space of partial crowns (82, 84) and volume of composite fillings (78). In another study, it was found that glass-ceramic could not be scanned with micro-CT as it produces artefacts (83). Attempts to scan cobalt chrome were lacking probably due to the fact that the material was dense in nature and the unavailability of a micro-CT powerful enough to penetrate such dense objects.

The limited number of studies that utilised micro-CT in general used a machine with power voltage capability of up to a maximum of 100 kV (80). The micro-CT used for the present study (Nanotom-S, Germany) had the power voltage capability of a maximum of 300 kV. Sufficient radiographic contrasts were needed to carry out measurement analysis using this micro-CT. However the during trial studies, it was

established that zirconia and cobalt chrome coping scans could be performed by use of power between 100 and 160 kV (Section 3.2.2.1.1). The trial study found that volume and deviation differences were not significantly different with the different settings used (Section 3.2.3.4).

A definitive setting of 155kV was finally utilized because when power of 160 kV was used, the bulb filament burnt out repeatedly. This required repeated changes when repeated scans were performed. Applying the 155kV power voltage, the scan resolution was 16 μ m per pixel and uncertainty was 8 μ m. Excessive use of power voltage might penetrate the coping too easily and cause findings to be perceived as air radiographs. Absorbing x-ray beam displays itself as radio-opacity on radiograph.

Unfortunately, no method is currently available to give exact settings for a particular object to receive maximum effects of micro-CT scans (77). The literature suggests the need for trial and error procedures for an acceptable result (77). Therefore, the settings displayed in the Methods section may be used as a guide for future dental restoration studies involving the use of micro-CT on zirconia and cobalt-chrome-molybdenum (CoCrMo).

6.7 Recommendations

It would be of interest to check accuracy of the two systems combined, which is the laser sintering methods and the milling methods in one system. Currently in its

development stage, Cybaman Technologies is pioneering a method to incorporate both techniques into one system (110). Developing one for the dental system may be beneficial. The method demonstrated may be utilised to check the accuracy of any systems or modifications made.

Secondly, a method to measure internal fit by utilising Boolean operators within the Rhino software may be recommended. Boolean operators are functions in most CAD software that allows subtraction between superimposed 3D models. The concept is to subtract two scans utilising the micro-CT. Scan 1 is a scan of a coping and a tooth in assembly. Scan 2 is a scan of a coping on its own. This is followed by superimposition of the two scans. By subtracting the scan of the assembly (Scan 2) to the scan of the coping (Scan 1), we hope to be left with the 3D model of the free space (cement space) between the two (Space Scan). If a scan of just the tooth (Scan 3) was made available, superimpositions of the tooth scan (Scan 3) and the Space Scan with the Boolean operators function may display a virtual cement space. However, a full investigation of the concept is required and this may lead to possible research studies. A scan (Scan 1) also has to be performed in assembly and this meant that physical modification of the internal aspect of the restoration was required to fit the restoration to the tooth.

Thirdly, this thesis utilizes 5 test subjects for four groups investigated as sample sizes ($n=5$). No standard point prevalence estimates could be used to determine sample

size. This was probably because the particular field is a relatively new approach to determine accuracy of CAD/CAM. Each measurement produced approximately 200 000 data points, so it is highly unlikely there was a sample size problem for a qualitative research. However progress in this field of research may benefit with increased sample sizes for a quantitative research protocol.

Finally, another manufacturing method worth mentioning is a new method to mill cobalt chrome in a pre-sintered stage. Milling in a soft stage might be cost effective, however further investigations is required in terms of accuracy. The method proposed in the present study may be used to test accuracy of the new system. Any developments in the CAD/CAM field all would benefit in use of this proposed method to guide the development process. The potential use of this method for measuring accuracy of CAM may possibly be used as industry standard in future.

Section 7

Conclusions

7 Conclusions

The following conclusions could be made from the present study:

1. The dental CAD/CAM process involves two main processes in fabrication of dental restorations which are the CAD and the CAM. Accuracy of both processes is important to achieve a successful fabrication of dental restorations. Accuracy testing of CAD exists in the form of ISO 12836:2012. Currently CAM accuracy testing is not available. The method proposed in this study may be utilised for accuracy testing of CAM fabricated component according to its CAD.
2. The Volume of CAD/CAM fabricated copings using different materials (CoCrMo/Zirconia) and methods (Laser Sintering and Milling) differ from the volume of original CAD. This means that fabrication of LS, M-CoCrMo, ZAx3 and ZAx4 copings does not follow the existing CAD in terms of volume. LS and ZAx3 were bigger than CAD while M-CoCrMo and ZAx4 were smaller.
3. The surface mapping results of LS, M-CoCrMo, ZAx3 and ZAx4 show dimensional differences in localised areas when compared to CAD. The internal cervical aspects of all groups of coping were comparable whereas other sections of the copings in the investigation varied. LS and ZAx3 showed differences at the occlusal section. The Zax4 was the coping that closely resembled the CAD compared to the other types of fabrication.
4. The volume of LS, M-CoCrMo, ZAx3 and ZAx4 fabricated copings were significantly different from each other. The dimensional differences of LS, M-CoCrMo, ZAx3 and ZAx4 fabricated copings were also different from each

other except at the Internal Cervical aspect. The External Cervical aspect was similar between LS and ZAx3, while the ZAx4 was similar to M-CoCrMo.

5. The Internal Fit is a measure of the coping adaptation from the internal side of the coping to the external side of the master model. It represents the cement space required for fixation of the investigated copings to the tooth. Only M-CoCrMo was comparable to the CAD Internal Fit at the Vertical Marginal Internal Fit section. All other groups other measurements between the groups to the CAD at various areas were significantly different.
6. The Internal fit of LS, M-CoCrMo, ZAx3 and ZAx4 fabricated copings differ from each other at the Axio-Margin Internal Fit and the Axial Internal Fit. LS and ZAx3 were comparable at the Vertical Marginal Internal fit while the M-CoCrMo and the ZAx4 were comparable at two sections, the Absolute Marginal Internal Fit and the Occlusal Internal Fit.
7. In general, all investigated fabricated copings produced clinically acceptable internal fit however improvements to the system was required to achieve more accurate CAM fabrication according to the CAD.

Section 8

References

8 References

1. Groover MP, Zimmers EW. CAD/CAM: Computer Aided Design and Manufacturing. New Jersey: PTR Prentice Hall Prentice-Hall, Inc; 1984. pp 83-11132.
2. Higgins A. The CAD/CAM Hall of Fame. Machine Design. 1999;71(20):52.
3. Denry I, Hooloway JA. Ceramics for Dental Applications: A Review. Materials. 2010;3:351-68.
4. Rosenstiel SF, Land MF, Fujimoto J. Investing and Casting. Contemporary Fixed Prosthesis. St. Louis, Missouri: Mosby Elsevier; 2006. pp. 681-708.
5. Venkatachalam B, Goldstein GR, Pines MS, Hittelman EL. Ceramic pressed to metal versus feldspathic porcelain fused to metal: a comparative study of bond strength. The International Journal of Prosthodontics. 2009;22(1):94-100.
6. Conrad HJ, Seong WJ, Pesun IJ. Current ceramic materials and systems with clinical recommendations: a systematic review. The Journal of Prosthetic Dentistry. 2007;98(5):389-404.
7. Asgar K. Casting metals in dentistry: past--present--future. Advances in Dental Research. 1988;2(1):33-43.
8. Rosenstiel SF, Land MF, Fujimoto J. Wax Patterns. Contemporary Fixed Prosthesis. ST. Louis, Missouri: Mosby Elsevier; 2006. pp. 555-88.
9. Miyazaki T, Hotta Y. CAD/CAM systems available for the fabrication of crown and bridge restorations. Australian Dental Journal. 2011;56 Suppl 1:97-106.
10. Liu PR. A panorama of dental CAD/CAM restorative systems. Compendium of Continuing Education in Dentistry (Jamesburg, NJ : 1995). 2005;26(7):507-8, 10, 12 passim; quiz 17, 27.
11. Beuer F, Schweiger J, Edelhoff D. Digital dentistry: an overview of recent developments for CAD/CAM generated restorations. British Dental Journal. 2008;204(9):505-11.
12. Mormann WH. The evolution of the CEREC system. Journal of the American Dental Association. 2006;137 Suppl:7S-13S.
13. Bindl A, Mormann WH. Marginal and internal fit of all-ceramic CAD/CAM crown-copings on chamfer preparations. Journal Oral Rehabilitation. 2005;32(6):441-7.

14. Davidowitz G, Kotick PG. The use of CAD/CAM in dentistry. *Dental Clinics of North America*. 2011;55(3):559-570.
15. Giordano R. Materials for chairside CAD/CAM-produced restorations. *Journal of the American Dental Association*. 2006;137 Suppl:14S-21S.
16. Demir N, Ozturk AN, Malkoc MA. Evaluation of the marginal fit of full ceramic crowns by the microcomputed tomography (micro-CT) technique. *European Journal of Dentistry*. 2014;8(4):437-444.
17. Silva NR, Witek L, Coelho PG, Thompson VP, Rekow ED, Smay J. Additive CAD/CAM process for dental prostheses. *Journal of Prosthodontics*. 2011;20(2):93-96.
18. Zou L, Cherukara G, Hao P, Seymour K, Samarawickrama D. Geometrics of tooth wear. *Wear*. 2009;266:605-8.
19. Rafeek R, Seymour K, Zou L. Dimensional Measurement for Dentistry. In: Cocco DL. *Modern Metrology Concerns: InTech*; 2012. p. 458.
20. KE A, Ju X, Whitters CJaP, MacLeod Sa, Norman C. Calibration of 3D Scanners for Quantification of Tooth Wear. *Continental European Division of the International Association for Dental Research*; 2013 2013-09-04 - 2013-09-07; Florence.
21. May KB, Russell MM, Razzoog ME, Lang BR. Precision of fit: the Procera AllCeram crown. *The Journal of Prosthetic Dentistry*. 1998;80(4):394-404.
22. Wittneben JG, Wright RF, Weber HP, Gallucci GO. A systematic review of the clinical performance of CAD/CAM single-tooth restorations. *The International Journal of Prosthodontics*. 2009;22(5):466-71.
23. Martin N, Jedynakiewicz NM. Clinical performance of CEREC ceramic inlays: a systematic review. *Dental Materials*. 1999;15(1):54-61.
24. Connolly C. Innovations and applications of the Cybaman replicator from Traki-iski Ltd. *Assembly Automation*. 2009;29(3):209-13.
25. Hodolic J, Puskar T, Besic I. Current status and future trends in dental CAM restorative systems. *34th International Conference on Production Engineering*; 28-30; Nis, Serbia 2011.

26. Quaas S, Rudolph H, Luthardt RG. Direct mechanical data acquisition of dental impressions for the manufacturing of CAD/CAM restorations. *Journal of Dentistry*. 2007;35:903-908.
27. Salvi J, Pagès J, Batlle J. Pattern codification strategies in structured light systems. *Pattern Recognition*. 2004;37(4):827-49.
28. Uzun G. An Overview of Dental CAD/CAM Systems. *Biotechnology & Biotechnological Equipment* 2008. pp. 530-5.
29. Szilvsi-Nagy M, Mátyási G. Analysis of STL files. *Mathematical and Computer Modelling*. 2003;38(7–9):945-60.
30. Chen YH, Ng CT, Wang YZ. Generation of an STL File from 3D Measurement Data with User-Controlled Data Reduction. *International Journal Advanced Manufacturing Technology*. 1999;15(2):127-31.
31. Hardwick M, Loffredo D, Fritz J, Hedlind M. Enabling the Crowd Sourcing of Very Large Product Models. In: Kovács G, Kochan D, editors. *Digital Product and Process Development Systems*: Springer Berlin Heidelberg; 2013. pp. 254-72.
32. Graham RNJ, Perriss RW, Scarsbrook AF. DICOM demystified: A review of digital file formats and their use in radiological practice. *Clinical Radiology*. 2005;60(11):1133-40.
33. Miyazaki T, Hotta Y, Kunii J, Kuriyama S, Tamaki Y. A review of dental CAD/CAM: current status and future perspectives from 20 years of experience. *Dental Materials Journal*. 2009;28(1):44-56.
34. Bidra AS, Taylor TD, Agar JR. Computer-aided technology for fabricating complete dentures: Systematic review of historical background, current status, and future perspectives. *The Journal of Prosthetic Dentistry*. 2013;109(6):361-6.
35. Beuer F, Naumann M, Gernet W, Sorensen JA. Precision of fit: zirconia three-unit fixed dental prostheses. *Clinical Oral Investigations*. 2009;13(3):343-9.
36. Ortorp A, Jonsson D, Mouhsen A, Vult von Steyern P. The fit of cobalt-chromium three-unit fixed dental prostheses fabricated with four different techniques: a comparative in vitro study. *Dental Materials*. 2011;27(4):356-63.
37. van Noort R. The future of dental devices is digital. *Dental materials*. 2012;28(1):3-12.

38. Samet N, Resheff B, Gelbard S, Stern N. A CAD/CAM system for the production of metal copings for porcelain-fused-to-metal restorations. *The Journal of Prosthetic Dentistry*. 1995;73(5):457-63.
39. Willer J, Rossbach A, Weber H-P. Computer-assisted milling of dental restorations using a new CAD/CAM data acquisition system. *The Journal of Prosthetic Dentistry*. 1998;80(3):346-53.
40. Kohorst P, Junghanns J, Dittmer M, Borchers L, Stiesch M. Different CAD/CAM-processing routes for zirconia restorations: influence on fitting accuracy. *Clinical Oral Investigations*. 2011;15(4):527-36.
41. International A. Standard Terminology for Additive Manufacturing Technologies. ASTM F2792-12a. West Conshohocken, PA: ASTM International; 2012.
42. Azari A, Nikzad S. The evolution of rapid prototyping in dentistry: a review. *Rapid Prototyping Journal*. 2009;15(3):216-25.
43. Tanvi D, Dhaman G, Naveen S, Sandeep P. Advent or Advancement: CAD/CAM-A Review. *International Journal of Medical and Applied Sciences*. 2014;3(2):168-75.
44. ISO. Accuracy (Trueness and Precision) of measurement methods and results. Part 1: General principles and definitions: ISO/TC 69/SC 6; 1994.
45. Persson M, Andersson M, Bergman B. The accuracy of a high-precision digitizer for CAD/CAM of crowns. *The Journal of Prosthetic Dentistry*. 1995;74(3):223-9.
46. Vlaar ST, van der Zel JM. Accuracy of dental digitizers. *International dental Journal*. 2006;56(5):301-9.
47. Persson A, Andersson M, Oden A, Sandborgh-Englund G. A three-dimensional evaluation of a laser scanner and a touch-probe scanner. *The Journal of Prosthetic Dentistry*. 2006;95(3):194-200.
48. Oberholzer TG, Grobler SR, Pameijer CH, Rossouw RJ. A modified dilatometer for determining volumetric polymerization shrinkage of dental materials. *Measurement Science and Technology*. 2002;13(1):78.
49. Holmes JR, Bayne SC, Holland GA, Sulik WD. Considerations in measurement of marginal fit. *The Journal of Prosthetic Dentistry*. 1989;62(4):405-8.

50. Shillingburg HT. Fundamentals of Fixed Prosthodontics. 3rd ed. Carol Stream, Illinois; 1997.
51. Nawafleh NA, Mack F, Evans J, Mackay J, Hatamleh MM. Accuracy and Reliability of Methods to Measure Marginal Adaptation of Crowns and FDPs: A Literature Review. *Journal of Prosthodontics*. 2013.
52. Goodacre CJ, Bernal G, Rungcharassaeng K, Kan JY. Clinical complications in fixed prosthodontics. *The Journal of Prosthetic Dentistry*. 2003;90(1):31-41.
53. Contrepois M, Soenen A, Bartala M, Laviole O. Marginal adaptation of ceramic crowns: A systematic review. *The Journal of Prosthetic Dentistry*. 2013;110(6):447-54.e10.
54. Felton DA, Kanoy BE, Bayne SC, Wirthman GP. Effect of in vivo crown margin discrepancies on periodontal health. *The Journal of Prosthetic Dentistry*. 1991;65(3):357-64.
55. Abduo J, Lyons K, Swain M. Fit of zirconia fixed partial denture: a systematic review. *Journal of Oral Rehabilitation*. 2010;37(11):866-76.
56. Roggendorf MJ, Kunzi B, Ebert J, Roggendorf HC, Frankenberger R, Reich SM. Seven-year clinical performance of CEREC-2 all-ceramic CAD/CAM restorations placed within deeply destroyed teeth. *Clinical Oral Investigations*. 2011.
57. McLean JW, von Fraunhofer JA. The estimation of cement film thickness by an in vivo technique. *British Dental Journal*. 1971;131(3):107-11.
58. Schaefer O, Kuepper H, Sigusch BW, Thompson GA, Hefti AF, Guentsch A. Three-dimensional fit of lithium disilicate partial crowns in vitro. *Journal of Dentistry*. 2012.
59. Witkowski S, Komine F, Gerds T. Marginal accuracy of titanium copings fabricated by casting and CAD/CAM techniques. *The Journal of Prosthetic Dentistry*. 2006;96(1):47-52.
60. Groten M, Girthofer S, PrÖBster L. Marginal fit consistency of copy-milled all-ceramic crowns during fabrication by light and scanning electron microscopic analysis in vitro. *Journal of Oral Rehabilitation*. 1997;24(12):871-81.
61. Rahme HY, Tehini GE, Adib SM, Ardo AS, Rifai KT. In vitro evaluation of the "replica technique" in the measurement of the fit of Procera crowns. *The Journal of Contemporary Dental Practice*. 2008;9(2):25-32.

62. Schaefer O, Watts DC, Sigusch BW, Kuepper H, Guentsch A. Marginal and internal fit of pressed lithium disilicate partial crowns in vitro: a three-dimensional analysis of accuracy and reproducibility. *Dental Materials*. 2012;28(3):320-6.
63. Shah S, Sundaram G, Bartlett D, Sherriff M. The use of a 3D laser scanner using superimpositional software to assess the accuracy of impression techniques. *Journal of Dentistry*. 2004;32(8):653-8.
64. Molin M, Karlsson S. The fit of gold inlays and three ceramic inlay systems: A clinical and in vitro study. *Acta Odontologica Scandinavica*. 1993;51(4):201-6.
65. Boening KW, Wolf BH, Schmidt AE, Kastner K, Walter MH. Clinical fit of Procera AllCeram crowns. *The Journal of Prosthetic Dentistry*. 2000;84(4):419-24.
66. Quante K, Ludwig K, Kern M. Marginal and internal fit of metal-ceramic crowns fabricated with a new laser melting technology. *Dental Materials*. 2008;24(10):1311-5.
67. Weaver JD, Johnson GH, Bales DJ. Marginal adaptation of castable ceramic crowns. *The Journal of Prosthetic Dentistry*. 1991;66(6):747-53.
68. Davis SH, Kelly JR, Campbell SD. Use of an elastomeric material to improve the occlusal seat and marginal seal of cast restorations. *The Journal of Prosthetic Dentistry*. 1989;62(3):288-91.
69. Laurent M, Scheer P, Dejou J, Laborde G. Clinical evaluation of the marginal fit of cast crowns--validation of the silicone replica method. *Journal of Oral Rehabilitation*. 2008;35(2):116-22.
70. Vigolo P, Fonzi F. An in vitro evaluation of fit of zirconium-oxide-based ceramic four-unit fixed partial dentures, generated with three different CAD/CAM systems, before and after porcelain firing cycles and after glaze cycles. *Journal of Prosthodontics*. 2008;17(8):621-6.
71. Ucar Y, Akova T, Akyil MS, Brantley WA. Internal fit evaluation of crowns prepared using a new dental crown fabrication technique: laser-sintered Co-Cr crowns. *The Journal of Prosthetic Dentistry*. 2009;102(4):253-9.
72. Shearer B, Gough MB, Setchell DJ. Influence of marginal configuration and porcelain addition on the fit of In-Ceram crowns. *Biomaterials*. 1996;17(19):1891-5.

73. Ireland AJ, McNamara C, Clover MJ, House K, Wenger N, Barbour ME, et al. 3D surface imaging in dentistry - what we are looking at. *British Dental Journal*. 2008;205(7):387-92.
74. Mehl A, Gloger W, Kunzelmann KH, Hickel R. A new optical 3-D device for the detection of wear. *Journal of Dental Research*. 1997;76(11):1799-807.
75. Moldovan O, Luthardt RG, Corcodel N, Rudolph H. Three-dimensional fit of CAD/CAM-made zirconia copings. *Dental Materials*. 2011;27(12):1273-8.
76. Pelekanos S, Koumanou M, Koutayas SO, Zinelis S, Eliades G. Micro-CT evaluation of the marginal fit of different In-Ceram alumina copings. *The European Journal of Esthetic Dentistry*. 2009;4(3):278-92.
77. Kruth JP, Bartscher M, Carmignato S, Schmitt R, De Chiffre L, Weckenmann A. Computed tomography for dimensional metrology. *CIRP Annals - Manufacturing Technology*. 2011;60(2):821-42.
78. Sun J, Lin-Gibson S. X-ray microcomputed tomography for measuring polymerization shrinkage of polymeric dental composites. *Dental Materials*. 2008;24(2):228-34.
79. Nomoto R, Komoriyama M, McCabe JF, Hirano S. Effect of mixing method on the porosity of encapsulated glass ionomer cement. *Dental Materials*. 2004;20(10):972-8.
80. Parkinson CR, Sasov A. High-resolution non-destructive 3D interrogation of dentin using X-ray nanotomography. *Dental Materials*. 2008;24(6):773-7.
81. Kakaboura A, Rahiotis C, Watts D, Silikas N, Eliades G. 3D-marginal adaptation versus setting shrinkage in light-cured microhybrid resin composites. *Dental Materials*. 2007;23(3):272-8.
82. Seo D, Yi Y, Roh B. The effect of preparation designs on the marginal and internal gaps in Cerec3 partial ceramic crowns. *Journal of Dentistry*. 2009;37(5):374-82.
83. Borba M, Cesar PF, Griggs JA, Della Bona A. Adaptation of all-ceramic fixed partial dentures. *Dental Materials*. 2011;27(11):1119-26.
84. Rungruanganunt P, Kelly JR, Adams DJ. Two imaging techniques for 3D quantification of pre-cementation space for CAD/CAM crowns. *Journal of Dentistry*. 2010;38(12):995-1000.

85. Zapassky E, Finkelstein I, Benenson I. Ancient standards of volume: negevite Iron Age pottery (Israel) as a case study in 3D modeling. *Journal of Archaeological Science*. 2006;33(12):1734-43.
86. Pinsky HM, Dyda S, Pinsky RW, Misch KA, Sarment DP. Accuracy of three-dimensional measurements using cone-beam CT. *Dento Maxillo Facial Radiology*. 2006;35(6):410-6.
87. Traini T, Mangano C, Sammons RL, Mangano F, Macchi A, Piattelli A. Direct laser metal sintering as a new approach to fabrication of an isoelastic functionally graded material for manufacture of porous titanium dental implants. *Dental Materials*. 2008;24(11):1525-33.
88. Örtorp A, Jönsson D, Mouhsen A, Vult von Steyern P. The fit of cobalt–chromium three-unit fixed dental prostheses fabricated with four different techniques: A comparative in vitro study. *Dental Materials*. 2011;27(4):356-63.
89. Yadroitsev I, Smurov I. Surface Morphology in Selective Laser Melting of Metal Powders. *Physics Procedia*. 2011;12, Part A(0):264-70.
90. Krol M, Dobzanski LA, Reimann L, Czaja I. Surface quality in selective laser melting of metal powders. *International Scientific Journal of Materials Science and Engineering*. 2013;60(2):87-92.
91. Leeson D. 4-Axis Vs 5-Axis Milling Machines: The numbers game. *Lab Perspective; Vol 1(1)* .
92. Association AD. ANSI/ADA Standard N0.96 Dental Water-based Cements. American Dental Association; 2012.
93. Tuntiprawon M, Wilson PR. The effect of cement thickness on the fracture strength of all-ceramic crowns. *Australian Dental Journal*. 1995;40(1):17-21.
94. Dendry IL. All-Ceramic Restorations. *Contemporary Fixed Prosthodontics*. St, Louis, Missouri: Mosby Elsevier; 2006. pp. 774-804.
95. Rosenstiel SF, Land MF, Fujimoto J. Framework Design and Metal Selection for Metal-ceramic Restorations. *Contemporary Fixed Prosthodontics*. St. Louis, Missouri: Mosby Elsevier; 2006. pp. 589-615.
96. Abduo J, Lyons K, Swain M. Fit of zirconia fixed partial denture: a systematic review. *Journal of Oral Rehabilitation*. 2010;37(11):866-76.

97. Groten M, Axmann D, Probster L, Weber H. Determination of the minimum number of marginal gap measurements required for practical in-vitro testing. *The Journal of Prosthetic Dentistry*. 2000;83(1):40-9.
98. Sachs C, Groesser J, Stadelmann M, Schweiger J, Erdelt K, Beuer F. Full-arch prostheses from translucent zirconia: Accuracy of fit. *Dental Materials*. 2014;30(8):817-23.
99. Grenade C, Mainjot A, Vanheusden A. Fit of single tooth zirconia copings: comparison between various manufacturing processes. *The Journal of Prosthetic Dentistry*. 2011;105(4):249-55.
100. Grenade C, Mainjot A, Vanheusden A. Fit of single tooth zirconia copings: comparison between various manufacturing processes. *Journal of Prosthetic Dentistry*. 2011;105(4):249-55.
101. 9 ITS. Dentistry-CAD/CAM systems-Accuracy of machined indirect restoration-Test methods and marking.
102. 9 ITS. Dentistry-Digitizing devices for CAD/CAM systems for indirect dental restoration-Test methods for assessing accuracy. 2012.
103. <http://www.renishaw.com/en/renishaw-enhancing-efficiency-in-manufacturing-and-healthcare--1030>.
104. Persson AS, Andersson M, Oden A, Sandborgh-Englund G. Computer aided analysis of digitized dental stone replicas by dental CAD/CAM technology. *Dental Materials*. 2008;24(8):1123-30.
105. Fabio R. From Point Cloud To Surface: The Modeling And Visualization Problem. *International Workshop on Visualization and Animation of Reality-based 3D Models*; Tarasp-Vulpera, Switzerland 2003.
106. Rudolph H, Luthardt RG, Walter MH. Computer-aided analysis of the influence of digitizing and surfacing on the accuracy in dental CAD/CAM technology. *Computers in Biology and Medicine*. 2007;37(5):579-87.
107. mbH G. Inspection V7.5 SR1 Manual - Basic: GOM mbH; 2010.
108. Kohorst P, Brinkmann H, Li J, Borchers L, Stiesch M. Marginal accuracy of four-unit zirconia fixed dental prostheses fabricated using different computer-aided design/computer-aided manufacturing systems. *European Journal of Oral Sciences*. 2009;117(3):319-25.

109. Strub JR, Rekow ED, Witkowski S. Computer-aided design and fabrication of dental restorations: current systems and future possibilities. *Journal of the American Dental Association* (1939). 2006;137(9):1289-96.
110. Limited T-i. Cybaman Intelligent Robotic Manufacturing. UK, 2015 Available from: <http://www.cybamantech.co.uk>.

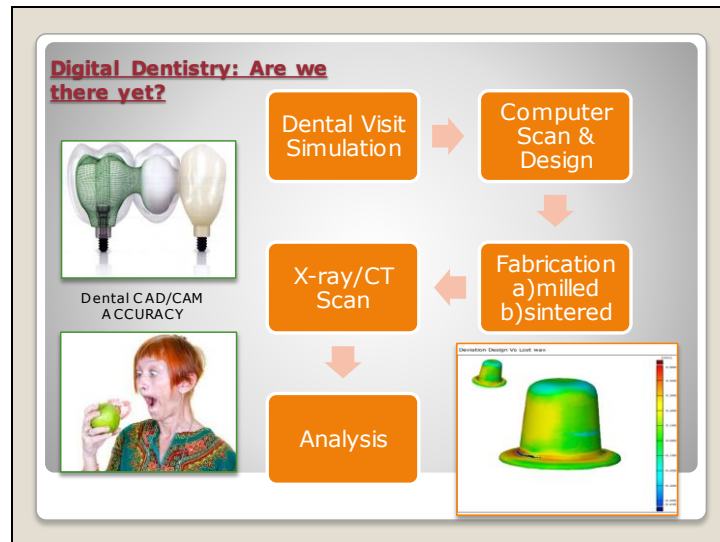
Section 9

Appendices

9 Appendix

University College Cork, Doctoral Showcase 2013 Oral Presentation

A three minute presentation in a single slide of the thesis undertaken was presented.





2nd Asia – Pacific Edition
CAD/CAM & Digital Dentistry International Conference
4-5 October 2013, Marina Bay Sands Hotel, Convention Center, SINGAPORE



Novel method of volume measurement of CAD/CAM fabricated dental prosthesis

Nasruddin MF^{1, 2}, Burke F¹, Ray N¹ and Theocharopoulos A¹

1. Restorative Department, Dental School and Hospital, University College Cork, Cork, Ireland

2. Centre of Studies for Restorative Dentistry, Universiti Teknologi MARA, Shah Alam, Selangor, Malaysia



Introduction

Computer Aided Design (CAD) and Computer Aided Manufacturing (CAM) of dental prostheses can save both time and effort for dental technicians. While improvements in fitting accuracy have been achieved, inaccuracies arising from the transition of a virtual digital model to an actual fabricated component are still evident.

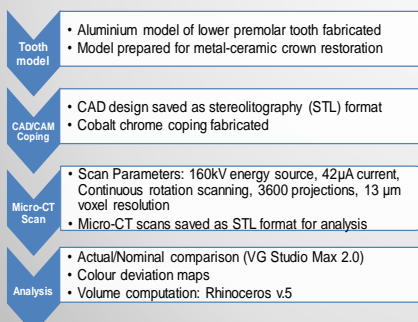
Objective

To introduce a novel method that examines the ability of CAM systems to fabricate CAD designed prostheses accurately using micro computed tomography (micro-CT).

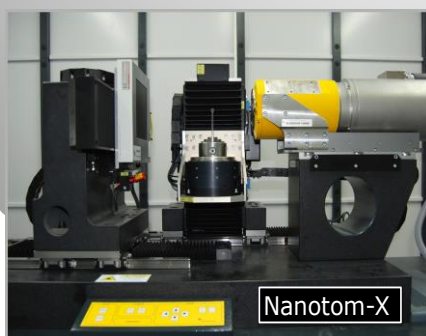


Picture from Nobel Biocare

Methods



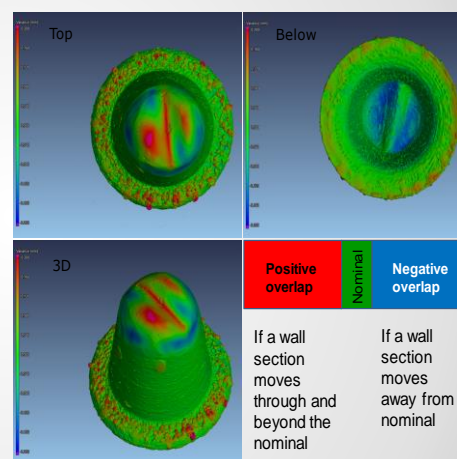
Detector Manipulator X-Ray Gun



Results

Sample	Volume (SE)
Original CAD Design	56.96 (1x10 ⁻⁹)mm ³
Fabricated coping	54.73 (1x10 ⁻⁹)mm ³

Actual/Nominal Comparison	Mean Deviation	Min Deviation	Max Deviation
CAD vs Coping	0.026mm	0.26mm	0.43mm



Discussion

Method Advantages

- Provide non-destructive high resolution method of analysis
- 3D reconstruction could be done quick
- Alignment and mean statistics could be done automatically

Method Disadvantages

- Sufficient radiographic contrast has to exist for micro-CT scans.
- Require instrument availability and training

Conclusion

The presented method was able to express the differences between the Selective Laser Sintered fabricated coping to its original CAD design in terms of total volume and colour thickness maps. This holds promise as a non-destructive method for manufacture accuracy testing.

References

1. J.P. Kruth et. al/ Computed tomography for dimensional metrology. CIRP Annals – Manufacturing Technology 60 (2011) 821-842
2. P. Rungtuanant et. al/ Two imaging techniques for 3D quantification of pre-cementation space for CAD/CAM crowns. Journal of Dentistry 38 (2010) 995-1000

Accuracy comparison of two dental CAD/CAM fabrication routes

Presented By:

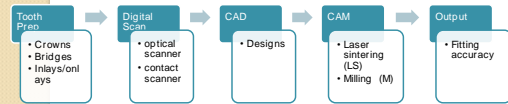
Dr Mohd Faiz Nasruddin ^(1,2),

Dr Frank Burke ⁽¹⁾, Dr Noel Ray ⁽¹⁾, Dr Antonios Theodoropoulos ⁽¹⁾

(1) University College Cork, Cork, IRELAND. (2) Universiti Teknologi MARA, Shah Alam, MALAYSIA.

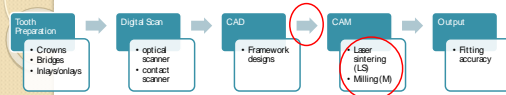
Background

- Computer-Aided-Design (CAD) and Computer-Aided-Manufacturing (CAM) of dental prostheses saves time & effort for dental technicians thus reducing cost of manufacture.



• Miyazaki T. et al. CAD/CAM systems available for the fabrication of crown and bridge restorations. Australian dental journal. 2011;56 Suppl 1:97-106.
• Liu P.R.A. panorama of dental CAD/CAM restorative systems. Compendium of continuing education in dentistry (Jamesburg, NJ : 1995). 2005;26(7):507-8, 10, 12 passim; quiz 17, 27.

Literature Review



Ortorp *et al.* found laser sintering (LS) to produce significantly ($p < 0.05$) better vertical and marginal fit when compared to milling (M)

- B Roh *et al.* The effect of preparation designs on the marginal and internal gaps in Cerec3 partial ceramic crowns. *Journal of Dentistry* 37(2009):374-382
- F Bauer *et al.* Effect of preparation angles on the precision of zirconia crown copings fabricated by CAD/CAM system. *Dental Materials* 2008; 27(6):814-820
- Persson A *et al.* A three-dimensional evaluation of a laser scanner and a touch-probe scanner. *The Journal of prosthetic dentistry* 2006;95(3):194-200.
- Han HSYang HSLim HRPark YJ Marginal accuracy and internal fit of machine-milled and cast titanium crowns. *The Journal of Prosthetic Dentistry* 2011; 106(3):191-7.
- Witkowski S, Komine F, Gerds T. Marginal accuracy of titanium copings fabricated by casting and CAD/CAM techniques. *The Journal of Prosthetic Dentistry* 2006;96(1):47-52

Objectives

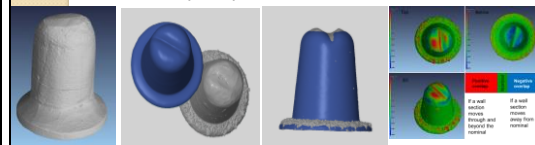
1. To introduce a novel method utilising micro-computed tomography (micro-CT) that examines the CAD to CAM transition introduced inaccuracies.
2. To compare volume between LS and M fabricated copings.
3. To compare accuracy of LS and M copings to the original CAD design.

Methods

1. An aluminium model of a prepared lower premolar tooth for a metal-ceramic crown was made.
2. A virtual cobalt chrome coping was then designed (InciseCAD, Renishaw, UK) and saved as stereolithography (STL) format.
3. 2 groups of 5 copings were fabricated via LS (AM125, Renishaw, UK) and M (Cybaman Replicator, Cybaman-Tech UK) methods of CAD/CAM.

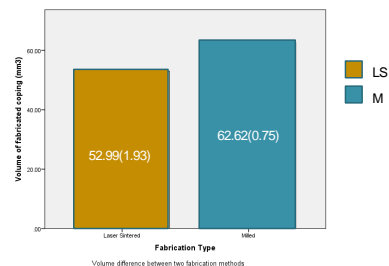


4. All copings were then scanned and saved as STL format with micro-CT (Nanotom-X) to produce three-dimensional digital models.
5. Actual/Nominal comparisons were then performed utilising multiple modelling/inspection software.
6. Coloured deviation maps and volume differences were computed and statistically analysed.

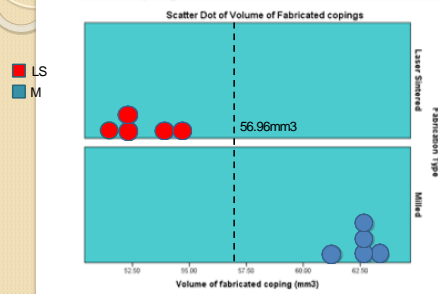


Results

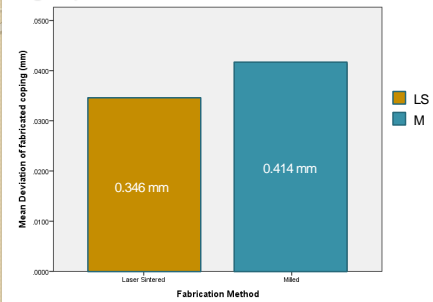
1. Volume of LS copings differentiated significantly ($p < 0.01$) to M



2. Volume of CAD design (56.96 mm^3) was significantly different ($p < 0.01$) to volume of LS and M copings.

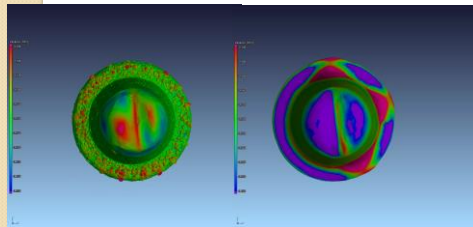


3. The mean deviations from CAD design were significantly different ($p < 0.05$) for LSVs M groups.



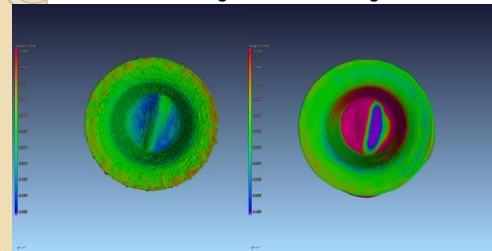
4. Coloured distance mapping of both groups revealed different surface patterns.

- Laser sintering
- Milling



Internal view

- Laser Sintering
- Milling



Discussion

- Volume and surface pattern difference may be due to how the copings were fabricated:
 - LS: additive method, multiple holders on occlusal surface
 - M: subtractive method, 3 holders on side
- Advantages
 - Provide non-destructive high resolution method of analysis
 - Alignment and mean statistics done automatically
- Limitations
 - Sufficient radiographic contrast has to exist for micro-CT scans.
 - Mean deviations from CAD design too generalized

Conclusion

- The CAD design significantly differed from the actual fabricated components.
- Observed differences may partly negate time, labour and cost saving benefits of CAD/CAM, however may also facilitate improvements.
- The presented method holds promise as a non-destructive method for manufacture accuracy testing.

Thank you for your attention

International Manufacturing Conference 2014 Oral Presentation

A Comparative Study on the Accuracy of Laser Sintered Vs Milled Fabricated Dental Restorations

M.F. Nasruddin^{1,2}, A. Theodoropoulos¹, N. Ray¹ and F. Burke¹

1. Department of Restorative Dentistry, Dental School and Hospital, University College of Cork, Ireland.
2. Centre for Restorative Dentistry Studies, Faculty of Dentistry, Universiti Teknologi MARA, Shah Alam, Malaysia.

* Author correspondence email: 111220857@umail.ucc.ie



Background

“The Engineer in the Innovation Ecosystem”

2013 GMCI report identified ‘Talent Driven Innovation’ as the most important global driver of a nation’s competitiveness for the manufacturing industry

www.cit.ie/imc311 assessed on 21/6/2014

CORK UNIVERSITY DENTAL SCHOOL AND HOSPITAL



Innovations in Dentistry

- Development of dental Computer-Aided-Design (CAD) and Computer-Aided-Manufacturing (CAM)
- Saves time & effort for dental technicians thus reducing cost of manufacture.



- Miyazaki T et al. 2011. CAD/CAM systems available for the fabrication of crown and bridge restorations.
- Liu PR 2005. A panorama of dental CAD/CAM restorative systems.

CORK UNIVERSITY DENTAL SCHOOL AND HOSPITAL



Objectives

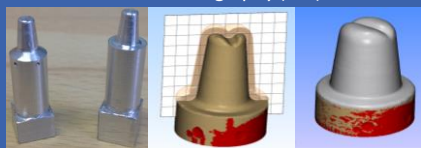
1. To introduce a method for measurement of the CAD to CAM transition inaccuracies.
2. To compare accuracy of fabricated copings by milling (M) and laser sintering (LS) methods of CAM to its original CAD Design in terms of deviation.

CORK UNIVERSITY DENTAL SCHOOL AND HOSPITAL



Methods

1. An aluminium model of a prepared lower premolar tooth for a metal-ceramic crown was made.
2. A virtual cobalt chrome coping was then designed (InciseCAD, Renishaw, UK) and saved as stereolithography (STL) format.

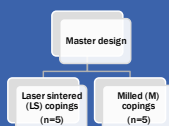


CORK UNIVERSITY DENTAL SCHOOL AND HOSPITAL



Methods

3. 2 groups of 5 copings were fabricated via LS (AM125, Renishaw, UK) and M (Cybaman Replicator, Cybaman-Tech, UK) methods of CAD/CAM.



Detector Manipulator X-Ray Gun

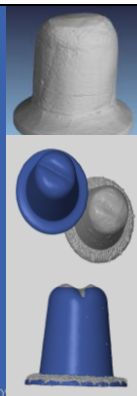


CORK UNIVERSITY DENTAL SCHOOL AND HOSPITAL



Methods

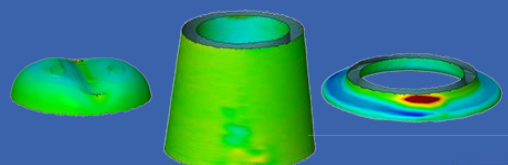
4. All copings were then scanned and saved as STL format with micro-CT (Nanotom-X) to produce three-dimensional digital models.
5. Actual/Nominal comparisons were then performed utilising multiple modelling/inspection software.



CORK UNIVERSITY DENTAL SCHOOL AND HOSPITAL

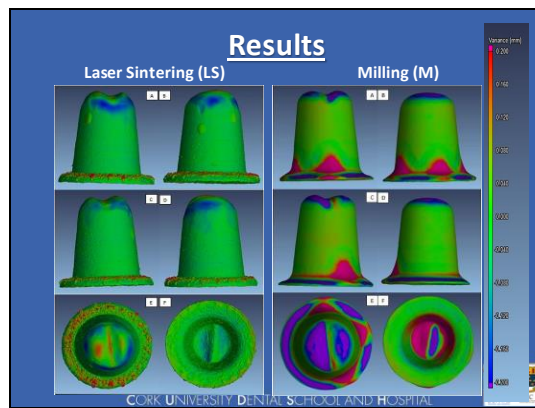
Methods

6. Full and sectional surface mappings were computed and statistically analysed including external and internal aspects.



CORK UNIVERSITY DENTAL SCHOOL AND HOSPITAL





Results of Mean Deviations

Laser Sintering (LS)				Milled (M)			
LS Coping Analysis	External $\mu\text{m}(\text{SD})$	Internal $\mu\text{m}(\text{SD})$	Overall $\mu\text{m}(\text{SD})$	M Coping Analysis	External $\mu\text{m}(\text{SD})$	Internal $\mu\text{m}(\text{SD})$	Overall $\mu\text{m}(\text{SD})$
Full	-6(5)	-32(36)	-21(20)	Full	25(6)	17(10)	21(4)
Occlusal	-26(16)	-52(20)	-38(12)	Occlusal	-6(15)	54(9)	16(8)
Axial	-30(6)	-14(6)	-21(3)	Axial	39(6)	37(15)	39(6)
Base	34(4)	-46(47)	-10(40)	Base	15(3)	-18(5)	-6(3)

- Negative findings mean smaller fabrication to CAD
- Positive findings mean enlarged fabrication to CAD

CORK UNIVERSITY DENTAL SCHOOL AND HOSPITAL

Discussion

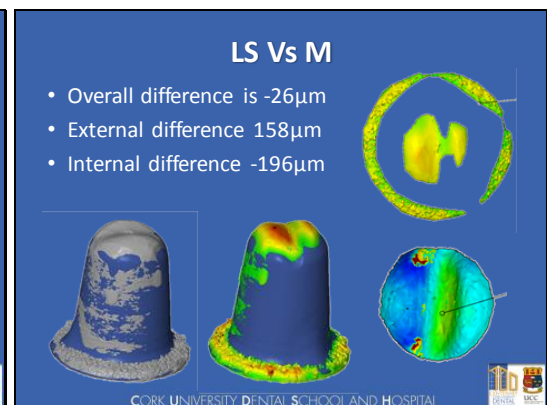
Laser Sintering

- LS give external rough surfaces
- Easily adapted to teeth
- Localised external areas need trimming: might lead to perforations

Milled

- M gives a more smoother surface
- Tighter fit

CORK UNIVERSITY DENTAL SCHOOL AND HOSPITAL



Micro-Computed Tomography

Advantages

- Provide non-destructive high resolution method of analysis
- Alignment and mean statistics could be done quick and precise

Disadvantages

- Sufficient radiographic contrast has to exist for micro-CT scans.
- Cost of scans expensive

CORK UNIVERSITY DENTAL SCHOOL AND HOSPITAL

Conclusion

- Accuracy of LS and M fabrication methods according to its CAD Design were similar.
- However further improvement could be done to develop the dental CAD/CAM system in terms of milling and laser sintering strategies for CAM utilisation
- Method proposed can allow analysis of the CAD to CAM transition and may be used as a guide for the development.

CORK UNIVERSITY DENTAL SCHOOL AND HOSPITAL

Thank you for your attention


M.F. Nasruddin^{1,2}, A. Theocharopoulos¹, N. Ray¹ and F. Burke¹

- Department of Restorative Dentistry, Dental School and Hospital, University College of Cork, Ireland.
- Centre for Restorative Dentistry Studies, Faculty of Dentistry, Universiti Teknologi MARA, Shah Alam, Malaysia.

* Author correspondence email: 111220457@umail.ucc.ie

CORK UNIVERSITY DENTAL SCHOOL AND HOSPITAL

IADR Ireland 2014 Oral Presentation



Accuracy of Computer-Aided-Designed/Computer-Aided-Manufactured (CAD/CAM) dental copings

M.F. Nasrudin^{1,2}, A. Theodoropoulos¹, N. Ray¹ and F. Burke¹

1. Department of Restorative Dentistry, Dental School and Hospital, University College of Cork, Ireland.
2. Centre for Restorative Dentistry Studies, Faculty of Dentistry, Universiti Teknologi MARA, Shah Alam, Malaysia.

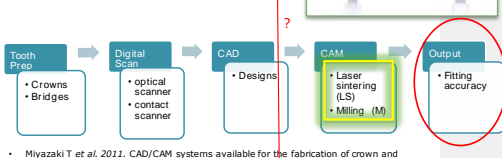
* Author correspondence email: 11.1220957@gmail.com

A TRADITION OF INDEPENDENT THINKING

UCC
University College Cork, Ireland
Cúlaíste na hOllscoile Corcaigh

Dental CAD/CAM

- Development since 1980's until date.
- Promotes time efficiency & improves cost benefit of manufacture.



- Miyazaki T et al. 2011. CAD/CAM systems available for the fabrication of crown and bridge restorations. Aust Dent J
- H. Rudolph et al 2006. Computer-aided analysis of the influence of digitizing and surfacing on the accuracy in dental CAD/CAM technology. Comp Bio and Med.

UCC
University College Cork, Ireland
Cúlaíste na hOllscoile Corcaigh

Objectives

- This study attempts to compare a single coping CAD design to its output form after various CAD/CAM fabrication methods:

- Volume
- Linear Dimensional Effects (Shape)

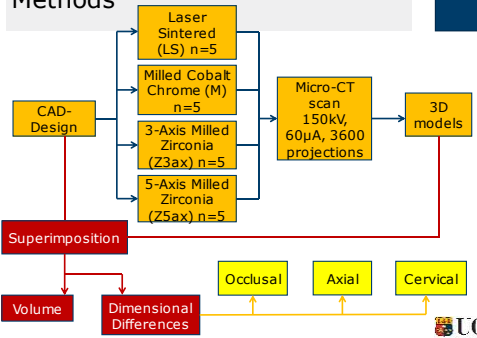
UCC
University College Cork, Ireland
Cúlaíste na hOllscoile Corcaigh

Null Hypothesis

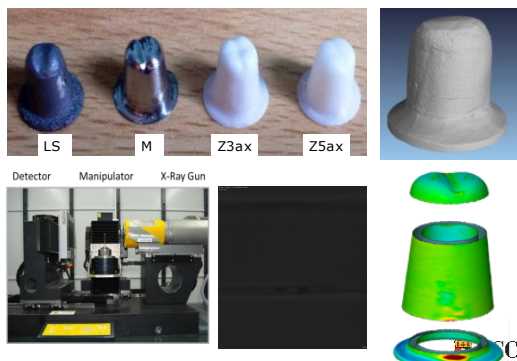
- No difference in accuracy is found between investigated CAD/CAM fabrication methods to its CAD Design.

UCC
University College Cork, Ireland
Cúlaíste na hOllscoile Corcaigh

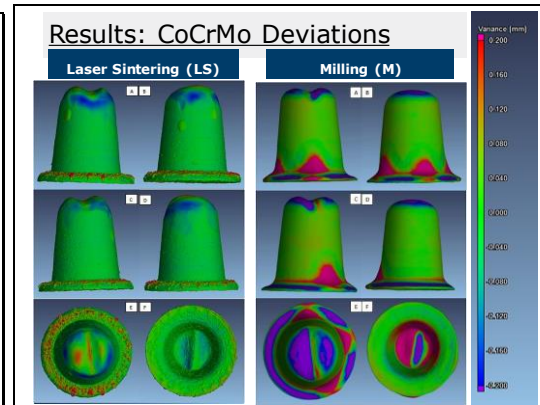
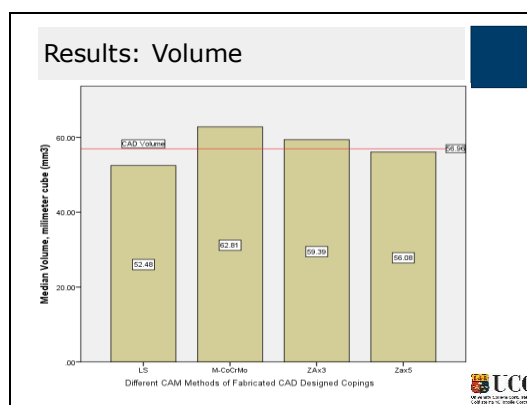
Methods

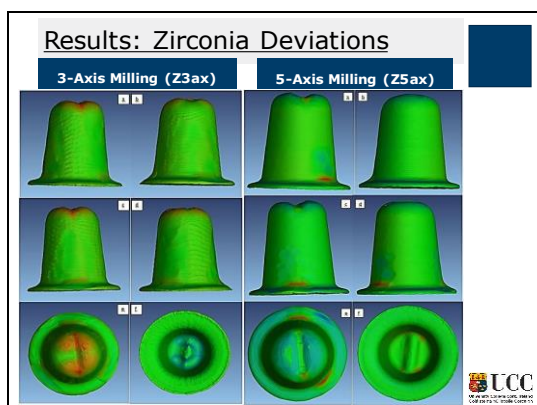


UCC
University College Cork, Ireland
Cúlaíste na hOllscoile Corcaigh



UCC
University College Cork, Ireland
Cúlaíste na hOllscoile Corcaigh

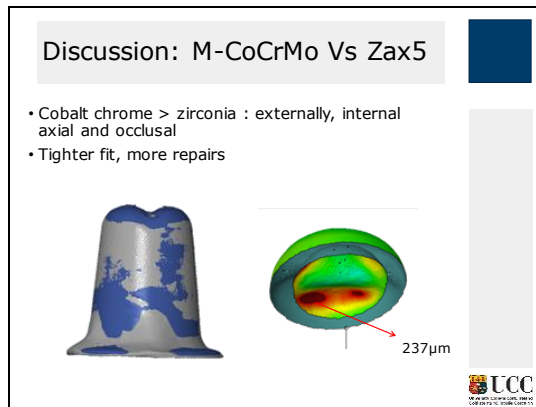
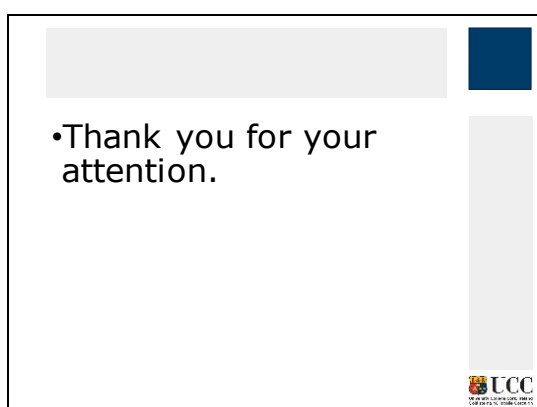
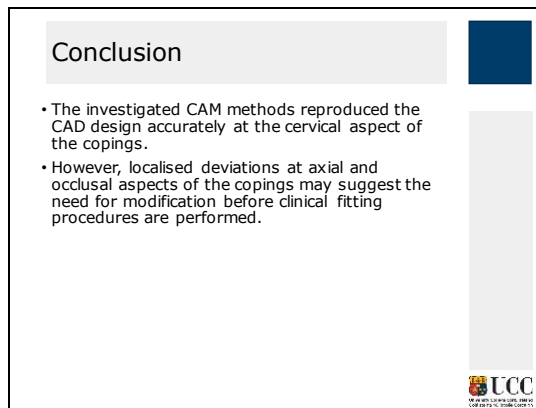
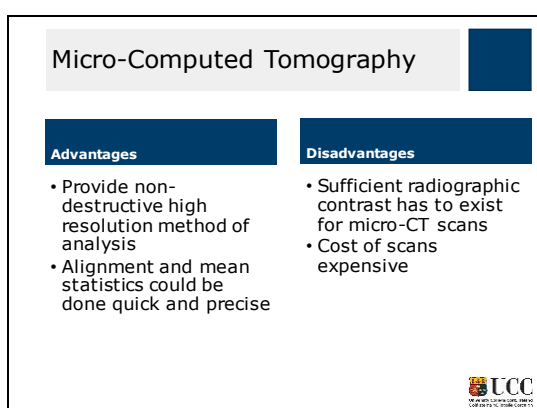
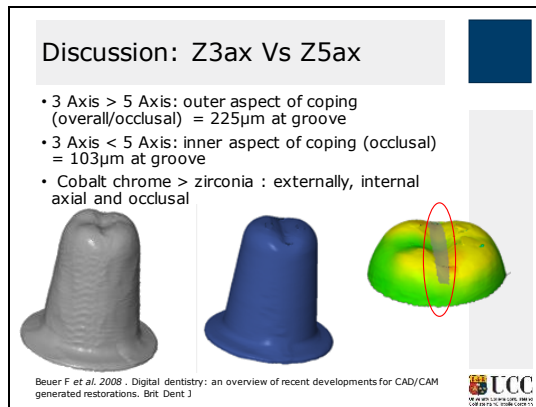
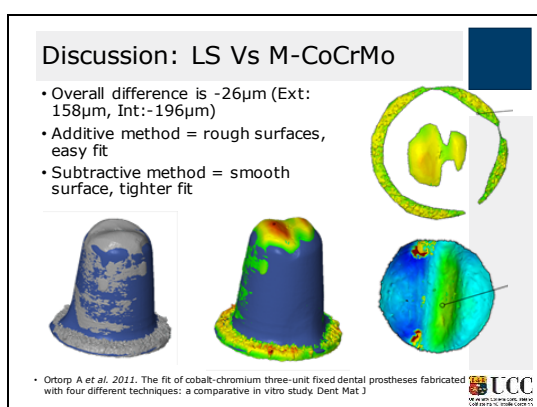




Localized Mean Deviations

Mean Deviations (SD), μm	LS	M	Z3ax	Z5ax
Internal	-32(36) ^{ab}	17(10) ^a	-45(42) ^b	-6(17) ^{ab}
External	-6(5) ^a	25(6) ^b	21(27) ^b	-7(19) ^a
Internal Occlusal	-52(20) ^a	54(9) ^b	136(29) ^c	-3(28) ^d
External occlusal	-26(16) ^a	-6(15) ^a	130(65) ^b	-30(31) ^a
Internal Axial	-14(6) ^a	37(15) ^b	-7(6) ^{ac}	7(5) ^c
External Axial	-30(6) ^a	39(6) ^b	-3(42) ^{ac}	10(7) ^{bc}
Internal Cervical	-46(47) ^a	-18(5) ^a	-44(66) ^a	-26(31) ^a
External Cervical	34(4) ^a	15(3) ^{ab}	21(10) ^a	-13(31) ^b

UCC logo



Calibration of Micro-CT for fabricated copings

Calibration rod VTX18CE000-013 was used to check the calibration of the system (Figure 87). Settings for the calibration are displayed on

Table **19**. The calibration rod is scanned and distance between the two centres of spheres is measured (actual). With known (nominal) measurement of the distance, measurement variables could be corrected.

$$(\text{Actual/nominal}) \times 100 = \text{Percentage difference}$$

Actual distance: 7.943417mm, Nominal distance: 7.8922mm \pm 0.001

$$(7.943417/7.8922) \times 100 = \underline{100.6\%}$$

Measured distance (actual) was found to be less than 1% greater than nominal distance. With this in mind, results of voxel resolution from scan conditions of dental copings cap were corrected.

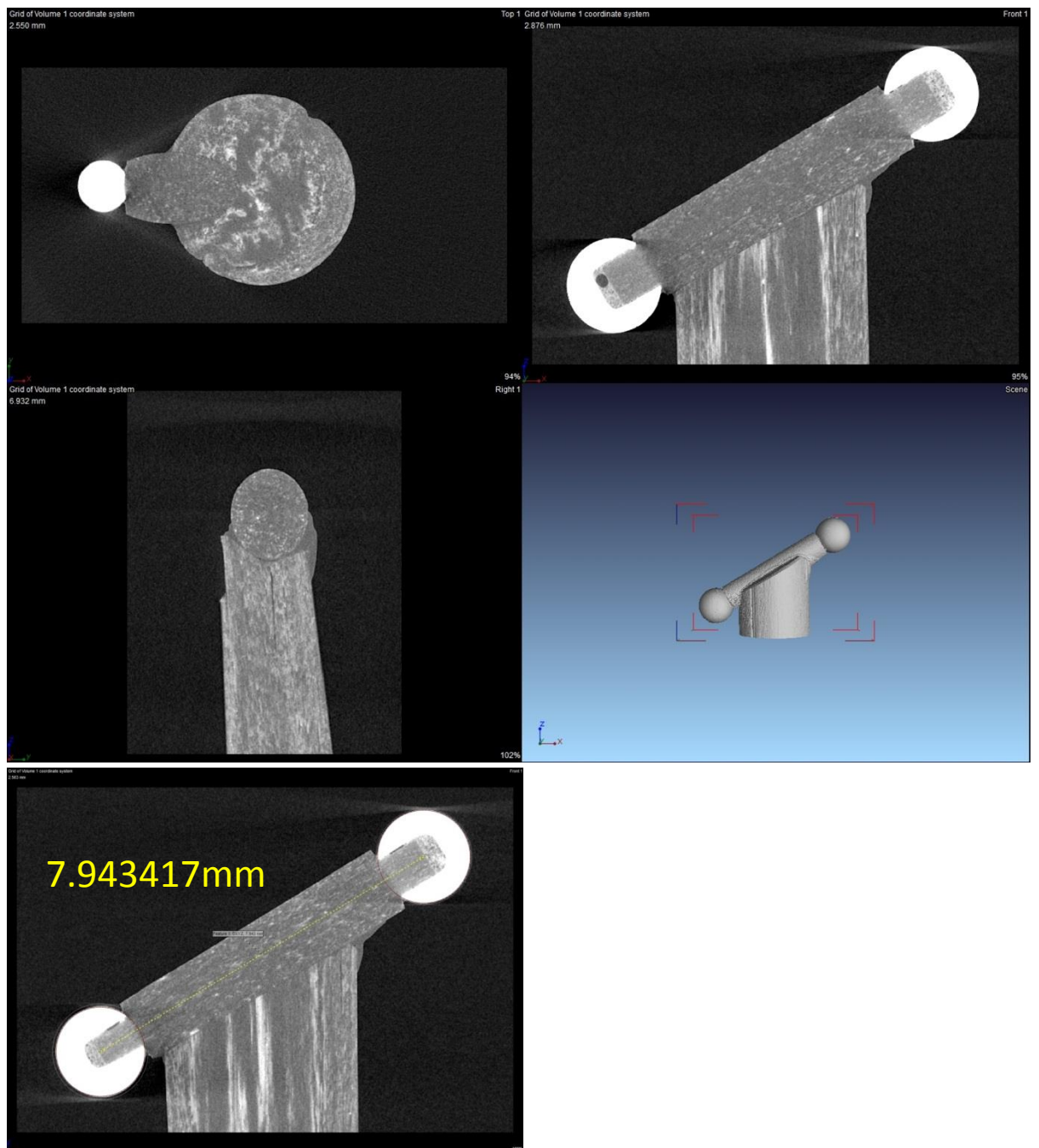


Figure 87 Micro-CT calibration Procedures

Table 19 Conditions for Calibration Rod VTX18CE000-013

Conditions	Parameters
Energy Source	80 keV
Current	60 μ A
Voxel Resolution	13.042809 μ m
Projections	7200

Calibration of Micro-CT for master aluminium model

A different calibration was performed for scanning the aluminium model due to difference in density and size (Table 20). Calibration rod VTX18CE000-012 was utilized for calibration purpose. The method for voxel resolution correction is the same as explained for CoCr scanning.

Table 20 Scan Conditions for Master Model and Calibration Rod VTX18CE000-013

Conditions	Master Model Scan	Calibration Rod VTX18CE000-013 Scan
	Parameters	
Energy Source	125 keV	90 keV
Current	60 μ A	120 μ A
Voxel Resolution	9.975831 μ m (Corrected)	9.999904 μ m
Projections	1440	2400

(Actual/nominal) x 100 = Percentage difference

Actual distance: 15.958615mm, Nominal distance: 15.9202mm \pm 0.001

$$(15.958615/15.9202) \times 100 = \underline{100.24\%}$$

Measured distance (actual) was found to be less than 0.5% greater than nominal distance. With this in mind, results of voxel resolution from scan conditions of master aluminium model were corrected. Scan of the master model was exported as STL files.

NPL reference standard dimensions for comparison with NPL CAD File

Table 21 Parameters of the NPL Reference Standard

Features	Parameter	Nominal /mm
Sphere 1	Diameter	5.0000
	x	0.0000
	y	0.0000
	z	0.0000
Sphere 2	Diameter	5.0000
	x	0.0000
	y	36.0000
	z	0.0000
Sphere 3	Diameter	5.0000
	x	36.0000
	y	36.0000
	z	0.0000
Sphere 4	Diameter	5.0000
	x	36.0000
	y	0.0000
	z	0.0000
Sphere 5	Diameter	21.2500
	x	11.7500
	y	24.2500
	z	10.0000
Sphere 6	Diameter	16.2500
	x	24.2500
	y	11.7500
	z	– 3.7500
Sphere 7	Diameter	5.0000
	x	11.7500
	y	9.2500
	z	0.8625
Cone 1*	Angle	60.0000°
	Diameter	4.7776
	x	11.7500
	y	9.2500
	z	0.0000
Torus 1	Diameter 1	12.5000
	Diameter 2	5.0000
	x	26.1250
	y	26.1250
	z	0.0000

